The palladium catalysed hydrogenation of multi-functional aromatic nitriles

Submitted for the Degree of Doctor of Philosophy

The University of Glasgow
School of Chemistry

Liam McMillan

October 2011

Abstract

A series of model compounds and a commercial Pd/C catalyst were used to study the issues relevant to the hydrogenation of aromatic nitrile molecules that are associated with an industrial agrichemicals process, where a primary amine is the target product.

Benzonitrile hydrogenation was found to be converted to high value benzylamine before an unexpected hydrogenolysis reaction led to the loss of ammonia to ultimately yield toluene as the final product. Indeed, gas phase infrared studies unambiguously showed the formation of ammonia for the first time. On closer investigation, the reaction was found to be a consecutive process where the order of reaction changed from first order for hydrogenation to zero order for hydrogenolysis. Co-adsorption studies proved that the two reactions occurred independently on two distinct Pd sites. The choice of catalyst and the use of an acid additive were shown to improve selectivity to benzylamine.

A dramatic change was noted when the aliphatic chain was extended. For benzyl cyanide hydrogenation, conversion was observed but, by way of a “spillover” process, the amine product was retained by the catalyst. Extending the chain further resulted in a complete loss in reactivity showing that electronic and structural factors had a major effect on activity and product distribution.

Mandelonitrile hydrogenation required an acid additive to facilitate conversion since a series of co-adsorption studies showed that under neutral conditions an intermediate hydroxyamine acted as a poison. Recycling of the catalyst showed that a cumulative poisoning effect was evident, but manipulation of Pd particle shape and size resulted in an extended lifetime and superior selectivity.

Introducing additional functionality to the aromatic ring meant that stabilised imine species were observed in the liquid phase. The nature of the substituent also affected product distribution and catalyst lifetime. MeO-, Me- and Cl-substituents all showed signs of reduced catalyst performance, but an OH-substituent exhibited greater durability, albeit with reduced selectivity to the primary amine. These systems also indicated the presence of a high energy site on the catalyst, which was responsible for the formation of secondary and tertiary amines.

Acknowledgments

I would like to thank everyone involved in this project and to those that have helped me throughout all my years at university and beyond.

Special thanks of course go to the *legend* that is Dr. David Lennon. I thank him for all his goodwill, good spirit and all his support and guidance over the years. Thank you for having faith in me, for all the good advice and for the intriguing conversations on the road, in the lab and in the pub.

Thanks to the following undergraduate project students: Justin Baker (University of Chicago), Ellen Keller (von Humboldt University), Stephen Howarth and Lauren Gilpin (University of Glasgow) who carried out work associated with this project throughout my time, adding insight and value to many of the results. Also thanks to Dr. David Lundie (Hiden Analytical) for his help in acquiring chemisorption and temperature programmes desorption data, Jim Gallacher for TEM analysis, Michael Beglan for carrying out atomic absorption measurements and Jim Tweedie for answering all my chromatography questions.

Thank you to my industrial sponsors Syngenta for providing an interesting and successful project, and for trusting and supporting me throughout the three years. Particular thanks go to my industrial supervisor Dr. Colin Brennan, for the informative meetings and for letting out some of Dave's secrets over dinner. I must also thank everyone at Jealott's Hill who made my time there informative, productive and enjoyable, including Dr. Martin Bowden, Michelle O'Mahoney and Rachel Donkor.

To Ian, Neil and June, thanks for making working in the Lennon group so enjoyable. Thanks to Andrew for the Mustang rides and drunken nights in California, for being a cracking mate and for never replying to text messages unless he's after something. Thanks especially to Clément and Robbie for "dragging" me to the pub, introducing me to Jaegerbombs and for letting me kip on their couches on countless occasions. I might not be any healthier, any richer or any more sensible, but it was worth it!

Finally to my Mum, Dad and sister – thank you for all your love, patience and support through the good and the (more often than not!) bad times.

To everyone else who helped in any way and in the words of the great David Lennon himself; “Cheers everybody, thank you, all the best!”.

For Mum

AUTHOR'S DECLARATION

I declare that, except where explicit reference is made to the contribution of others, that this thesis is the result of my own work and has not been submitted for any other degree at the University of Glasgow or any other institution.

Liam McMillan October 2011

Contents

List of Figures

List of reaction schemes

List of Tables

List of abbreviations (in order of use)

Ea	Activation energy
k	Rate coefficient
BPC	Buchi pressure controller
GC	Gas chromatography
FID	Flame ionization detector
HPLC	High performance liquid chromatography
DID	Diode array detector
NMR	Nuclear magnetic resonance
FTIR	Fourier transform infrared

BET	Brunauer Emmett Teller
AAS	Atomic absorption spectroscopy
TEM	Transmission electron microscopy
TPD	Temperature programmed desorption
K	Adsorption coefficient
DFT	Density functional theory
NBPEA	*N*-Benzyl-2-phenethylamine
BN	Benzonitrile
BI	Benzylimine
BA	Benzylamine
Tol	Toluene
FAB	Fast atom bombardment
BC	Benzyl cyanide
PEI	Phenethylimine
PEA	Phenethylamine
MN	Mandelonitrile
2-APE	2-Amino-1-phenylethanol
EELS	Electron energy loss spectroscopy
GCMS	Gas chromatography-mass spectroscopy
HBC	Hydroxybenzyl cyanide
HBI	Hydroxybenzylimine
TYR	Tyramine
LCMS	Liquid chromatography-mass spectroscopy

1 Background and Introduction

1.1 What is a catalyst?

A catalyst can be generally described as a substance that increases the rate at which a chemical reaction will reach equilibrium without itself being consumed in the process.[1] To achieve this, a catalyst provides an alternative reaction pathway that benefits from having a lower activation energy (Ea) and can be schematically described in the energy profile below (Figure 1). The primary advantage of using a catalyst therefore stems from the fact that its use (often) gives a higher reaction rate.

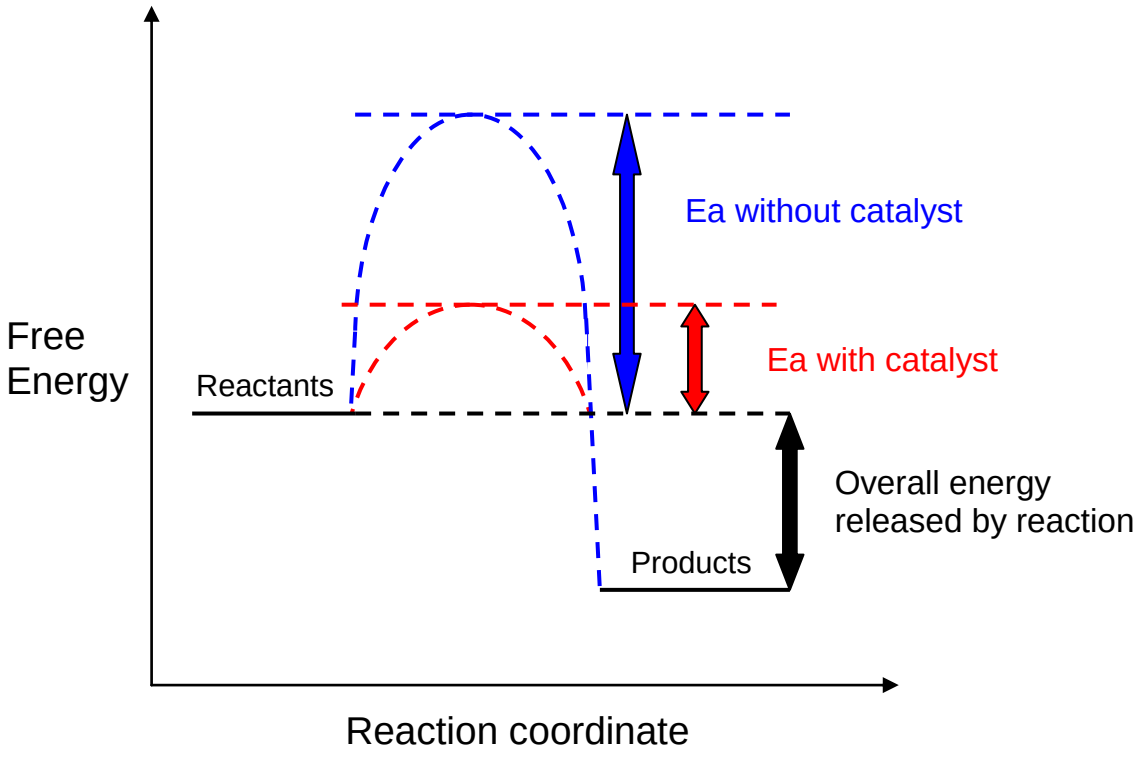

Figure 1. Diagram showing the energy profile of a non-catalysed (blue) and a catalysed reaction (red).[2]

Natural examples of catalysts can be found in the form of enzymes that act as highly selective catalysts for countless chemical reactions that take place within organisms. Industrially, it is reported that catalysts contribute to one-sixth of the value of all manufactured goods. Today over 90% of the chemical manufacturing processes employed worldwide utilise a catalyst in one form or another.[3]

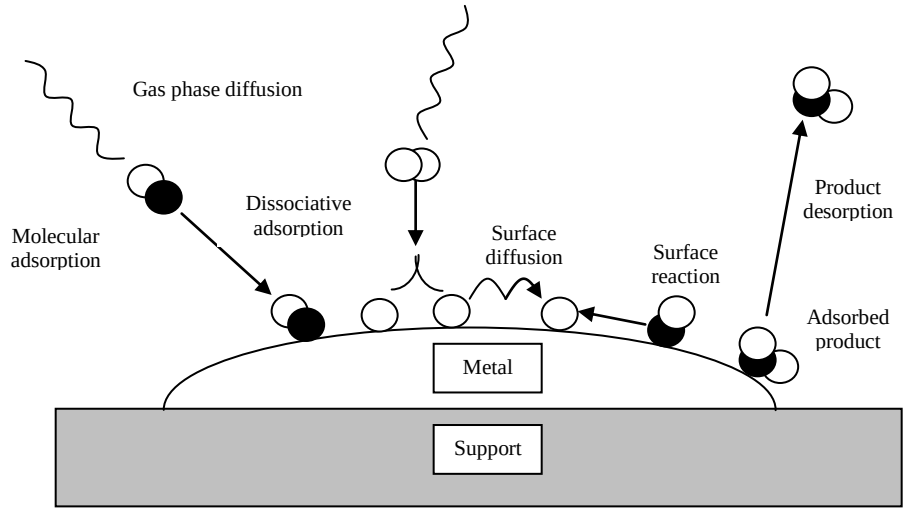

Figure 2. Surface interactions on a heterogeneous catalyst, typically a metal such as platinum or nickel.[4]

Catalysts offer alternative pathways for a reaction which may be complex but also more energetically favourable. The surface interactions associated with heterogeneous catalysts are summarised in Figure 2. One or more of the reactants strongly adsorb onto the catalyst surface via molecular or dissociative adsorption at the active sites of the catalyst. The catalyst interacts with the surface adsorbed species, which may just be a weakening of its bonds, before the molecules desorb.

Two main factors govern the choice of a particular catalyst for a specific reaction; the activity and the selectivity required.[5] The activity of a catalyst is a measure of the rate at which a substrate is converted to its corresponding product(s). Selectivity can be defined as the sum of the rate by which the desired product is produced divided by the rate by which all other products are produced. If a catalyst exhibits a high selectivity for a desired product then the rate at which it is formed is greater than the rate at which all other products are formed.

1.2 Heterogeneous catalysis

Heterogeneous catalysis is essential to the economic operation of a large number of industrial scale chemical processes, permitting large turnovers of reactant molecules at high selectivities. Also, because the catalysts are solids and the reactants and products are either in the gaseous or liquid phase, separation of the reagents from the (generally expensive) catalytic medium at the end of the reaction sequence presents no major problem.[4] This is not the case in homogeneous catalysis where separation of reagents and catalysts constitutes a major limitation in the successful exploitation of such reaction systems.[6]

Historically, interest at the University of Glasgow has focused on hydrogenation reactions over supported metal catalysts.[7-23] Traditionally, this has concentrated on reactions at the gas/solid interface, where relatively small molecular weight reactants in the gas phase are converted to gaseous products using a solid catalyst in the form of a powder. An example of such a reaction would be the hydrogenation of propyne to produce propane over supported platinum, palladium or gold catalysts.[7-12]

In line with shifts within the chemical industry towards higher molecular weight and higher value products, the catalysis/physical research laboratories in Glasgow have been active in operating liquid phase hydrogenation reactions. Examples of such reactions would be the hydrogenation of nitrobenzene over silica supported copper catalysts to produce aniline[13,14] and the stereoselective hydrogenation of 2-butyne-1,4-diol to produce *cis*-2-butene-1,4-diol over alumina supported palladium catalysts.[15-18] Recent experiences with hydrogenation and carbon-carbon bond forming reactions of substituted furans have also been informative.[18-23] These reactions are typically performed using a continuously stirred batch slurry reactor, in much the same way as the project discussed here (see Section 1.5).

In terms of fundamental information regarding adsorption complexes, reaction intermediates, reaction mechanisms, metal morphological effects, mass transport effects, *etc*., these 3-phase systems are substantially harder to understand than the relatively more straight forward gas/solid reactions.[24] Nevertheless, with the increased economic importance of fine chemicals to areas such as the

pharmaceutical and fragrance industries,[25] the demand for improved understanding and application in this area of research is indeed intense.

Initially, the research project was to concentrate on the selective hydrogenation of aromatic nitriles using a variety of supported metal catalysts. Despite the importance of this category of reaction in the fine chemicals business (pharmaceuticals and agrichemicals), relatively little is known about the nature of the active sites responsible for facilitating clean transformations at good reaction rates for extended lifetimes.[4] Currently, catalyst deactivation represents a serious drawback to the wide application of this technology and this project was intended to employ a number of chemical and spectroscopic techniques, developed to (i) define the active phase of the catalyst, (ii) develop reaction mechanisms and (iii) prepare catalysts that exhibit optimum yield for the target compounds.[4]

1.3 Economic, Industrial and Environmental Considerations

Approximately 80% of all products and materials produced by the highly successful chemical industry has at one time or another in their development, been through a process involving a catalyst.[26] As such, catalysis has a long history and wide reaching applications.

Traditionally, the fine chemicals industry has had a reputation for focusing solely on the yield of products but it is now widely accepted that there is a need for more environmentally acceptable processes.[27] In the drive towards cleaner and "greener" syntheses in the fine chemicals industry, the catalytic community is facing the challenges by using the three branches of catalysis – homogeneous, biological and heterogeneous. All three approaches have their own advantages. Homogeneous catalysis has wide applications in the bulk and fine chemicals industry,[28] biocatalysts have the advantage of being able to operate under mild conditions and with high selectivities[4] and heterogeneous catalysis has the advantages of ease of recovery and catalyst recycle and can be utilised in continuous processes.[29]

Indeed, heterogeneous catalysis has been widely used in the oil refining and the petrochemicals industry for some time,[30,31] providing the foundation for understanding their use in fine chemicals synthesis.[32] Moreover, in catalytic hydrogenation, bulk chemical processes have been scaled down to suit the fine chemicals market.[33]

1.4 Fine Chemicals

There is no universally accepted definition of the concept of “fine chemicals” – or for bulk or speciality chemicals for that matter. These classifications are not based on any intrinsic or chemical properties of the groups of chemicals in question. It is useful, however, to use the working definition of a fine chemical proposed by Sheldon *et al.*, whereby a fine chemical is one with a worldwide production volume of less than 10,000 tons per annum and one with a price in excess of $10US/kg.[27]

From a chemistry perspective, fine chemicals are generally multifunctional, complex molecules and as such are often volatile and have limited thermal stability. As a result, their synthesis is often carried out in the liquid phase, usually involving multiple steps and carried out in multifunctional equipment.[34]

Traditionally, heterogeneous catalysis has been associated with the bulk and petrochemicals industries, whereas fine chemicals proceed via predominantly non-catalysed organic synthesis routes.[35] While this is still broadly the case, there are a number of examples that show that heterogeneous catalysis can make a contribution to better production processes for complex agrochemicals and pharmaceuticals.[36]

The manufacture of such chemicals are typically characterised as being multi-step organic reactions in solution and on a rather small scale with varying amounts of (often toxic) by-products.[33] Catalysis can contribute on a number of levels. Firstly, by providing improved and cleaner production processes. Secondly, a catalyst can contribute by removing or helping to transform toxic or unwanted by-products.[36] Catalysis also allows a number of transformations to be made possible including (but not limited to) hydrogenation and dehydrogenation reactions; reductive

alkylation of amines; the metathesis of unfunctionalised olefins; oxidations and isomerisations.[37]

1.5 Hydrogenation Reactions

Catalytic hydrogenations are key reactions for organic synthesis on both a laboratory and industrial scale.[38] There are more hydrogenation catalysts available commercially than any other type, and for good reason. Hydrogenation is one of the most useful, versatile and environmentally acceptable reaction routes for organic synthesis, meaning that even today, hydrogenation research is still relevant, contemporary and beneficial.[39]

Hydrogenation is, therefore, a diverse topic and as such, this project will focus on some benchmark and model examples to show the basic principles of the molecular interconversion, including the choice of catalyst, mechanistic issues and its relevance to the fine chemicals industry.

1.6 Nitrile hydrogenation introduction

Primary amines are among the most important intermediates in the pharmaceutical, plastic and agrochemicals industries.[40] They can be synthesised in a number of different ways – *e.g.* reduction of nitro compounds[41], reduction of amides[42] or the reductive amination of oxo compounds[43] – but the most widely used process (in the pharmaceutical industry at least) is the heterogeneously catalysed hydrogenation of nitriles.[44] The selectivity of products is of vital importance, particularly for the production of primary amines. However, the literature has shown that condensation reactions between a highly reactive imine intermediate and the primary amine products will almost always lead to the formation of side products such as secondary and tertiary amines.[45] In addition to the choice of catalyst, the reaction conditions and starting nitrile are important factors to consider in achieving a high selectivity to the desired amine product.

For hydrogenation reactions generally, the choice of metal catalyst is dependent upon two factors – electronic factors and geometric structures of the active sites.[46] The adsorption of reactants onto metal surface sites requires vacancies within the

d-band of the surface metal which can accept electrons from the adsorbant. When there are a large number of vacancies within the d-band, as is the case in Groups 13 and 17, the gas is so strongly adsorbed to the surface that it is very difficult to remove and the reaction may not proceed. Equally, with metals in Group 11, the lack of d-band vacancies results in a weakly adsorbed state and, since reactivity is directly related to surface coverage,[33] the activity is also small (see Figure 3, below).

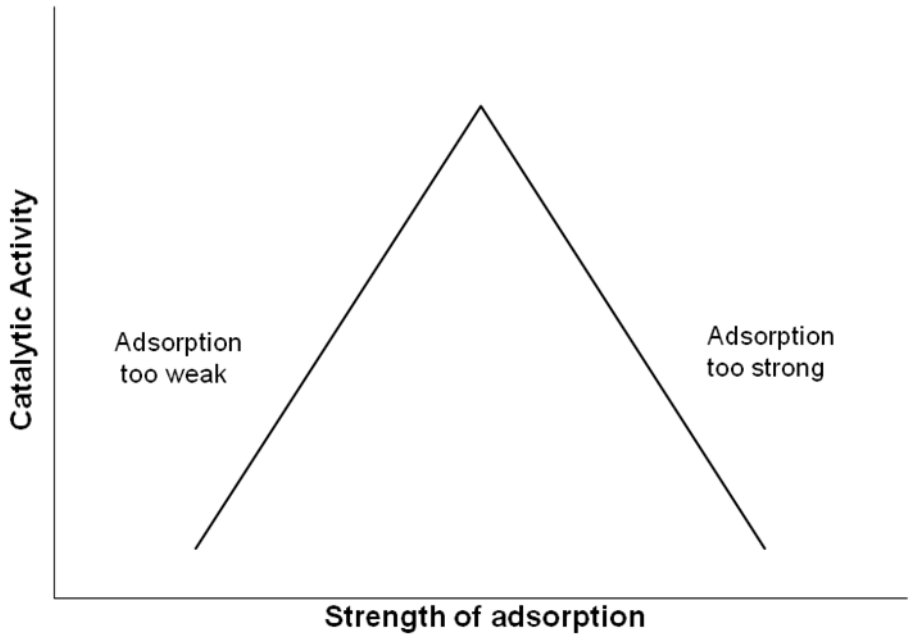

Figure 3. Diagrammatic representation of a "volcano" plot, showing the relationship between the strength of adsorption and catalytic activity.[47]

Maximum activity can be expected when the metal catalyst has the least number of vacant d-vacancies, the "electronic factor", which corresponds to the metals of Groups 8, 9 and 10 (closest to the peak of the 'volcano' plot in Figure 3). These groups of metals also give the optimum "geometric factor" associated with the active sites, *i.e.* the atoms of the metals are spaced such that the transition state complex formed during reaction is of the lowest possible energy.[27]

It would appear therefore, that there were numerous candidates. However, this list can be reduced by discounting metals that are not easily reduced from their oxides *e.g.* Ti, V, Cr, Zr *etc*. Additionally, Ag and Au have been shown to have low

hydrogenation activity.[45,46] In the example of acetylene (C_2H_2) hydrogenation activity, the following trend is reported:

$$Pd > Pt > Ni, Rh > Co > Fe > Cu > Ir > Ru > Os > Au$$ [47,48]

On balance, palladium tends to be the best generic candidate and has become the basis of many commercial hydrogenation processes due to its balance of selectivity and activity and at a viable cost. Palladium is normally used as a supported heterogeneous catalyst and because of its inherently high activity and low cost, these catalysts typically contain 0.5% w/w of metal to maintain selectivity.[27]

However, despite palladium's dominance in the reaction, other catalyst formulations may be suitable. These include nickel, cobalt and copper borides to improve selectivity[52] and a copper promoted Raney nickel catalyst.[53]

A review of the literature identified a number of different catalysts that were active in the hydrogenation of nitriles. These included the typical hydrogenation catalysts nickel, palladium, platinum, rhodium and ruthenium (which may give a good selectivity to primary amine[51,52] but may also deactivate quickly[54]). Other catalysts identified included cobalt, borane, metal boron hydride and lithium aluminium hydride[56]. Other various bimetallic catalysts of the general nature M-Cu/NaY and M-Ni/NaY have also been identified (where M=Pd, Pt, Rh, Ru).[57]

The activity of the hydrogenation catalysts was found to be greatly dependant on the type of support used,[40] while the selectivity to primary amines remains high on most supports studied. In a study of different supports, alumina was found to be the best candidate over silica, silica-alumina and titania. Selectivity was also found to follow the same trend with respect to choice of catalyst support.[40]

It was found that the formation of by-products is usually caused by the reaction of primary amine products with an intermediate imine species to give a secondary or tertiary amine. This may be overcome, for example, by the formation of salts with mild acids such as NaH_2PO_4 in which the amine salt formed is kept in the aqueous phase of a water/DCM solvent mixture[44] or with the addition of one or two molar

equivalents of HCl or H_2SO_4.[55-58] Evidence of the presence of an imine species has also been identified.[52,59]

As with many catalytic reactions, reaction conditions, *i.e.* temperature and pressure, play an important role. It was found that an increase in pressure was coupled with an increase in selectivity and activity to the primary amine product. However, while increasing temperature gives an increase in initial reaction rate, selectivity to primary amine decreased significantly.[27]

In summary, it is clear that heterogeneous catalysis has shown much scope in the hydrogenation of nitriles, because of its many advantages over conventional 'quantitative' methods of synthesis.[32] These include 'greener' synthesis routes, fewer waste products, and milder reaction conditions. As there is currently an increasing demand for high-value, more complex chemicals, research into specific, highly selective and active catalyst systems has become increasingly desirable. This stems from the fact that the chemistry underlying these reactions is by no means fully understood nor straightforward.

1.6.1 Assumed mechanism for the hydrogenation of nitriles

Von Braun *et al.* posited in 1923 the idea of an imine species being formed during nitrile reduction (Scheme 1).[62] The presence of imines has been repeatedly established[52,60,61] and this mechanism is now almost universally accepted.

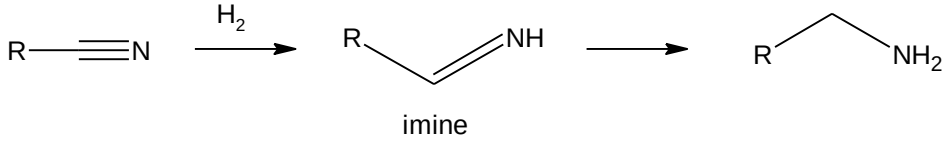

Scheme 1. The assumed reaction scheme for nitrile hydrogenation via an imine intermediate to yield a primary amine.[62]

Selectivity is of great importance and priority in this method of reduction, due to the often-high purity requirements and the multiple possibilities of side reactions.[63] Below is a scheme showing possible unwanted side reactions that can occur when

the primary amine is the target product (Scheme 2).[64] This mechanism shows the addition of the primary amine to the intermediate imine to form a dialkylimine intermediate, followed by subsequent hydrogenolysis. However, an equally valid pathway could be the elimination of ammonia to give a Schiff base which is then hydrogenated to the final secondary amine.[65] The exact mechanisms followed in reality are still under debate, however, it has been shown that these further steps do take place on the surface of the catalyst/support system.[55] Further research, using *in situ* infrared and mass spectrometric techniques, is required to systematically confirm these postulations.

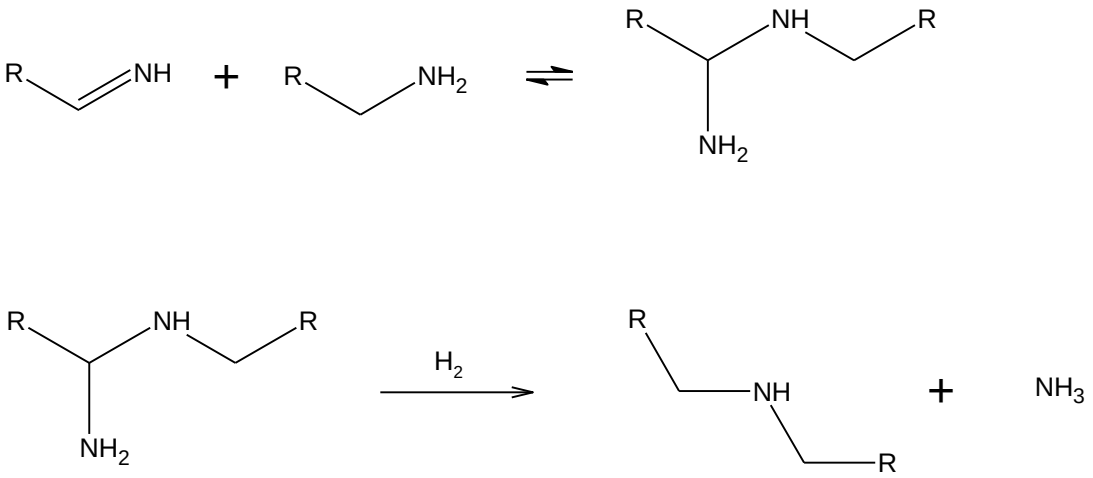

Scheme 2. Possible side reactions in the reduction of amines and/or nitriles.[64]

In some of the most recent and detailed mechanistic studies, Huang and Sachtler put forward the suggestion that the catalytic hydrogenation of a nitrile is not simply the addition of adsorbed hydrogen to the nitrile moiety.[64] Using deuterium substitution the following mechanism was proposed (Scheme 3):

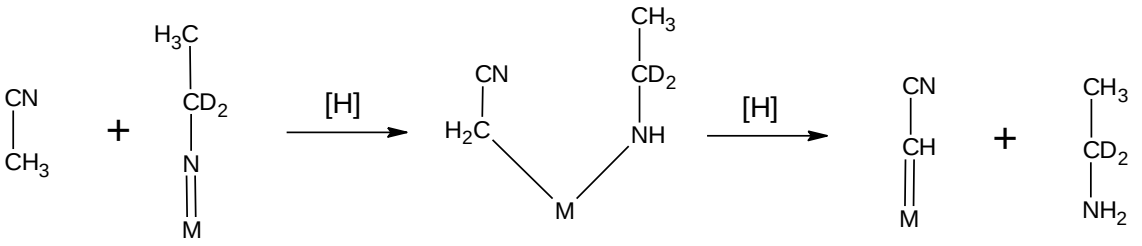

Scheme 3. Reaction scheme showing how Huang and Sachtler postulate that nitrile reduction involves a more complex relationship between reactants and the metal.[54]

The work suggests a relationship between the ability of a metal to form double bonds and the selectivity of that metal. However controversial the mechanism of nitrile hydrogenation may still be, there is a general consensus that enables the formation of a global reaction scheme as detailed in Scheme 4 below.

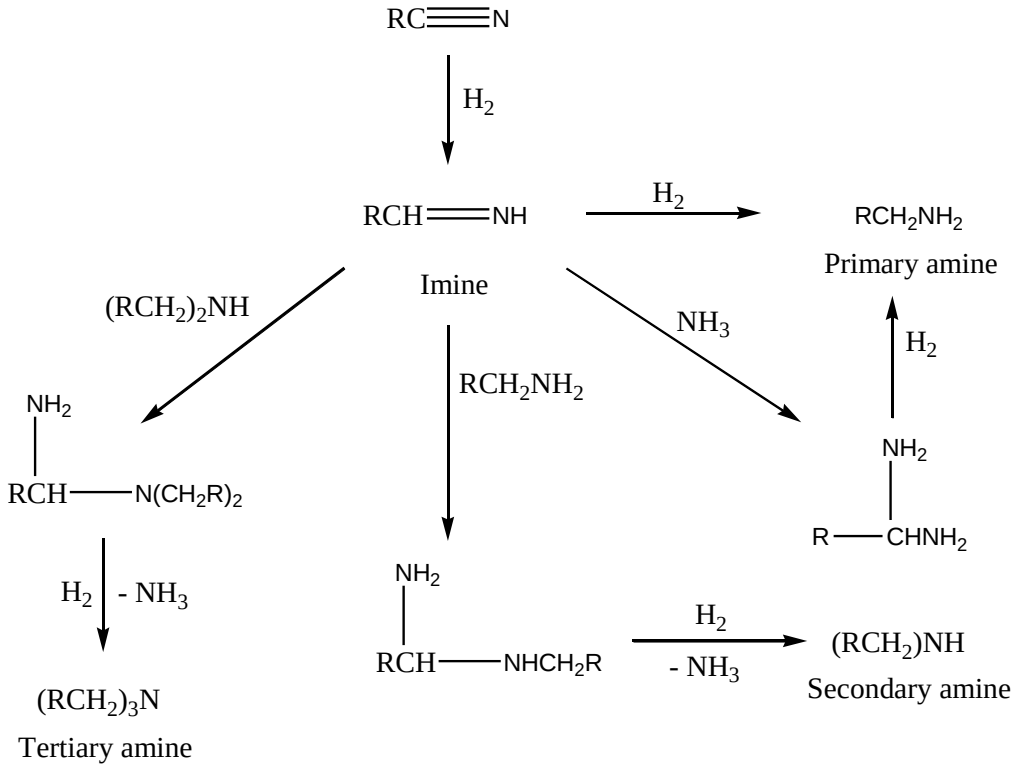

Scheme 4. Proposed reaction pathway to primary, secondary and tertiary amines via the reaction of intermediate imine species.[32]

The crucial issue with nitrile hydrogenations is thought to be the equilibrium that represents the partitioning of the imine intermediate between the reaction solvent and the catalyst surface. It is suspected that the residence time of this entity on the metal crystallites critically affects the selectivity of the system.[66] Specifically, catalyst formulations that retain the imine at the catalyst surface will facilitate its subsequent hydrogenation to the primary amine. Conversely, catalysts that favour the rapid desorption of the imine into the liquid phase will make the imine more available for condensation with other species, which will lead to the formation of secondary and tertiary amines, amongst others.[45] Thus, it is anticipated that correlation between solvated imine concentrations and product distributions can provide considerable insight into the origins of the selectivity patterns observed.

1.7 The industrial process and application of model compounds

This project was undertaken in collaboration with Syngenta, a company specialising in crop protection measures.[67] One of their processes involves the hydrogenation of a ring-substituted aromatic cyanohydrin (general formula X-,Y-C_6H_3-CH(OH)CN, where X and Y represent two unidentified substituent groups) and represents a multi-variate reaction system that forms part of a herbicide production chain (Scheme 5, below).

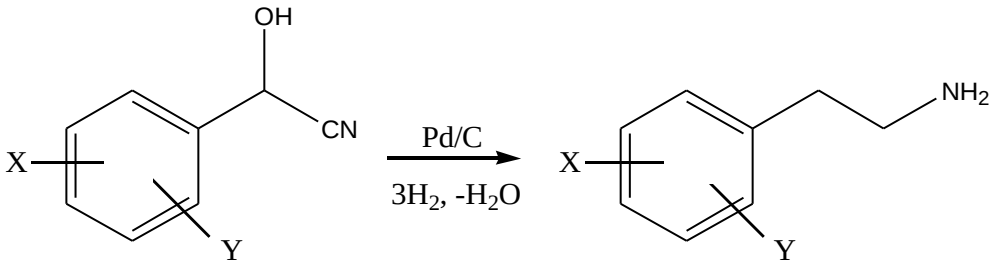

Scheme 5. Generalised reaction scheme for the industrial process.

As with the hydrogenation of all cyanohydrins and with reference to Scheme 6, two possible reaction routes may be considered. Firstly, in the “preferred” reaction route, a condensation reaction is followed by the hydrogenation of the nitrile moiety to yield a *di*-substituted aromatic primary amine (X-,Y-$C_6H_3CH_2CH_2NH_2$). However, the second, alternate route shows that nitrile hydrogenation can occur first to yield a hydroxyamine intermediate. Such an intermediate may then (i) react with the process solvent to yield a methoxy-adduct as shown, (ii) react with the primary amine product to yield secondary and ultimately tertiary amines or (iii) lose water to yield the final desired product.

Although relatively simple in appearance, the process is complicated by the fact that the “preferred” reaction route is found to be disfavoured, primarily due to the higher strength of adsorption of the nitrile group on the active catalyst. An additional complication is observed in that many of the intermediates and products of the favoured reaction route (the hydroxyamine intermediate, methoxy-by-product and secondary and tertiary amines) are known catalyst poisons. The industrial hydrogenation process may therefore be considered as being a “self-poisoning” reaction.

The use of a relatively “mild” catalyst such as Pd/C is interesting in itself. As was discussed previously (Section 1.6), many other metal catalysts, but particularly the Raney-type catalysts of Ni and Co would be particularly active in such a system.[68] However, given the numerous functional groups that must be retained in the final product, such highly active, “harsh” catalysts may result in the loss of this valuable functionality, given the fine chemicals context.[68]

The aim of this project was, therefore, to investigate all such issues relevant to the hydrogenation of aromatic nitriles. However, given the complex nature of product distribution and poisoning effects, together with the fact that many of the reactants and products are Schedule 1 classed drugs (or drug precursors), it was deemed beneficial to use model compounds. One of the benefits of using model compounds is that, given the relatively sparse amount of literature available concerning the study of aromatic nitrile hydrogenation over platinum group metals, investigations can focus on simpler systems and conclusions may then be applied to more complex situations.

In that vein, it was decided that the best model system to start with would be benzonitrile, given that it is the simplest of all aromatic nitriles. From such a starting point, information regarding reaction mechanism, deactivation or poisoning issues, reaction conditions, catalyst choice and product distribution could be studied without the additional complexity envisaged with any further functionality inherent in the system.

The information obtained in this system could then be used to direct the various parameters (*i.e.* reaction conditions) for more complex model systems and, eventually, lead on to benefit the industrial system.

The industrial system is undefined in this study and no results are presented on the reaction. Rather, the data presented here represents a fundamental investigation of issues relevant to the hydrogenation of aromatic cyanohydrins and is inherently generic in nature. The final results section of the thesis (Section 3.7) describes work carried out at the industrial centre that compares reactions undertaken on these generic substrates (benzonitrile, mandelonitrile, *etc*.) but using an industrial catalyst and an industrial test reactor.

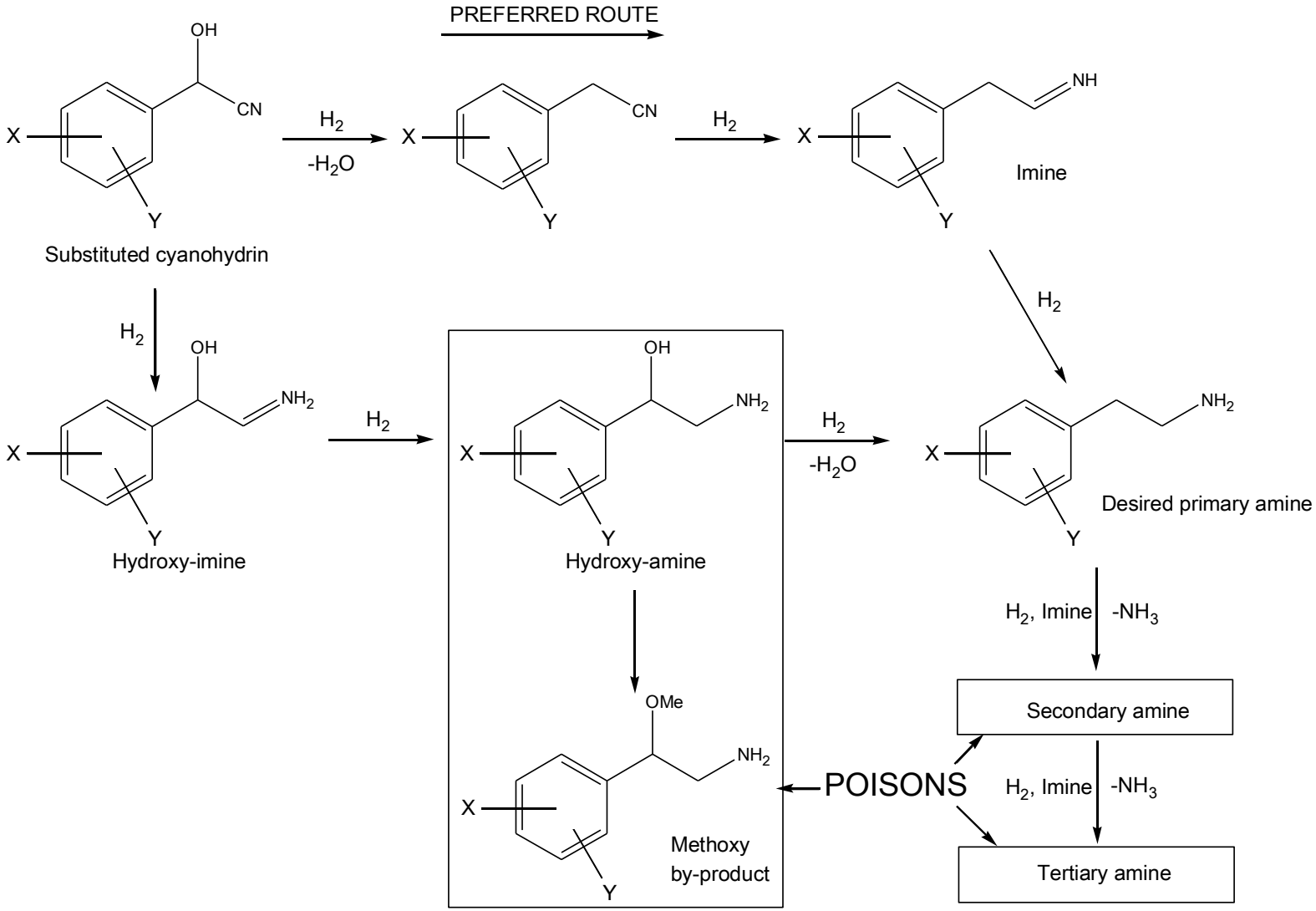

Scheme 6. Generalised reaction scheme for the industrial hydrogenation process.

1.8 Reaction kinetics and activation energy

Liquid-phase reaction kinetics involves the development and application of rate laws, which describe the relationship between concentration and rate of reaction. Kinetic studies can provide valuable insight into the reaction mechanism and also informs us of the temperature dependence of the rate of reaction.

Manipulation of kinetic data can give information about the rate-limiting step of some reaction processes; modification of the experimental conditions can then be made to allow optimisation of the system.[69]

For heterogeneous systems, catalyst activity is strongly dependent on the transport of molecules to the catalyst surface; their ability to adsorb to the surface; how easy it is to establish the maximum (or optimum) surface coverage of both hydrocarbon and hydrogen and how efficiently and quickly products are desorbed and transported away from the active sites.[27] This represents the "mass transfer limitations" of the reaction and can have an overriding effect on both catalyst activity and selectivity in hydrogenation.[27]

The transport of reactants to and from the catalyst surface describes mass transport or diffusion processes. When these steps are slower than the others listed, the reaction is said to be under diffusion control. If any of the other steps are slow, *i.e.* they are the rate-determining step, then the reaction is said to be under kinetic control.

Reactions can be classified as being under diffusion or kinetic control upon inspection of the rate data and calculation of the activation energy of the particular reaction. Put simply, a reaction with activation energy in excess of *ca.* 20 kJ mol^{-1} describes a reaction that is under kinetic control. A reaction with activation energy of less than *ca.* 20 kJ mol^{-1} is defined as a reaction under diffusion control.[70]

1.8.1 Calculation of rate coefficient, activation energy and order of reaction

The rate coefficient, k, of a chemical reaction is the coefficient that precedes reactant concentrations in a simple rate equation. For example;

$$Rate = k[A]^x[B]^y[C]^z \quad (1)$$

where [A], [B], [C] = concentration of reagents A, B and C respectively,

x, y, z = order of reaction with respect to said reagents.

The rate coefficient includes all factors that affect reaction rate, with the exception of concentration, which is accounted for in the equation itself. It is therefore, by its definition, not a constant and is affected by temperature as described by the Arrhenius equation, (3) below, but also by surface area of adsorbent (*i.e.* catalyst surface) and ionic strength among others. In the present work, rate coefficients for reactions were calculated using graphical methods by application of the integrated form of the first order rate law, below (the reactions studied are assumed to follow first order kinetics).

$$\ln\left[\frac{A_0}{A}\right] = kt \quad (2)$$

where $[A_0]$ = initial concentration, mol L^{-1}

[A] = concentration at time, t

t = time, s

k = rate coefficient, s^{-1}

The apparent activation energy (Ea) of a reaction is the minimum kinetic energy that the reactants must possess in order for the reaction to proceed in the direction of products. The rate coefficient of most reactions increases as the temperature is increased and the dependence of the rate coefficient, k, on the temperature of the system is described by the Arrhenius equation;

$$k = Ae^{-\frac{Ea}{RT}} \quad (3)$$

where k = rate coefficient, s^{-1} for first order reactions,

A = the pre-exponential constant, s^{-1} for first order reactions,

R = the gas constant, 8.314 J K^{-1} mol^{-1},

T = the absolute temperature of the reaction medium, K,

Ea = the apparent activation energy of the reaction, J mol^{-1}.

Manipulation of the Arrhenius equation to a more useful form allows calculation of the activation energy, Ea, via graphical methods:

$$\ln k = \ln A - \frac{Ea}{RT} \quad (4)$$

Thus, plotting ln k versus reciprocal temperature in degrees Kelvin, yields a straight line of gradient –Ea/R. Application of the molar gas constant gives the activation energy, Ea.

2 Experimental

2.1 Reactors

The reactors used throughout the project can be described as 3-phase batch slurry reactors. H_2 gas and product vapour make up the gaseous phase; the solvent and starting material are in the liquid phase and the catalyst is the solid phase. All three phases are mixed together to give, ideally, a fine suspension. In terms of fundamental information regarding adsorption complexes, reaction intermediates, reaction mechanisms, metal morphological effects, mass transport effects, *etc.*, these 3-phase systems are substantially harder to understand than the relatively more straight forward gas/solid reactions. However, from an industrial point of view, liquid-phase reactions are more common due to the ease of handling of liquids and the fact that semi-hydrogenated products are accessible.[20]

2.1.1 Buchi batch autoclave

The Buchi batch autoclave system is described as a well-mixed batch reactor[18] and is shown schematically in Figure 4. Reagents are charged to the system and left to react on the catalyst, with a constant pressure of hydrogen being maintained. Since the laboratory in which the reactor was housed is not designed as a high-pressure laboratory, the autoclave was only used to a maximum pressure of 5 bar of hydrogen, instead of its maximum capacity of 12 bar. The Buchi autoclave is specially designed for laboratory-scale hydrogenation reactions and comprises of four, separate, interconnecting systems:

- The Buchi autoclave;
- The Buchi press-flow gas controller;
- The autoclave motor-speed controller, and;
- The Julabo refrigerated and heating circulator.

The autoclave was based on a tripod design for strength and support and the reactor vessel has a volume of 0.5 litres and is constructed of glass. All piping of gases was done through 0.25 inch stainless steel Swagelok® piping and all

connections on the reactor were also stainless steel.

For safety reasons, a rupture element was installed adjacent to the reactor pressure gauge and is designed to burst if the pressure rises above a specified safe level. In addition to the rupture element, the reactor was not operated without the presence of the Perspex shielding, in case of explosion.

A motor connected to a toothed belt drove the autoclave stirrer shaft, via a magnetic drive, which allowed continuously variable speed transmission. To limit any leaks during high-pressure operation, the magnetic drive was installed so that the rotating shaft could be driven with no need for mechanical seals. The rotational velocity of the stirrer shaft was controlled by means of the autoclave motor-speed controller. The cover plate for the autoclave contained five ports which all allowed access to the reactor vessel. Each port was used respectively for:

- Gas supply to the reacting solution within the vessel;
- Scavenge port for waste gases;
- Sample taking and reagent injection;
- Internal thermocouple;
- Catalyst and solvent charging to the reactor (pre-reaction)

2.1.1.1 Buchi Pressure Flow Gas Controller (BPC)

The BPC 1202 system consisted of a gas controller and a control box. The gas controller allowed two gases, inert (nitrogen) and active (hydrogen or deuterium for hydrogenations or oxygen for oxidation reactions) to be supplied directly to the reactor via a gas reservoir. The gas controller monitored the active gas pressure before the reservoir (regulated pressure) and after the reservoir (delivery pressure). The regulated pressure could be adjusted via a regulator tap (controlled manually). The delivery pressure gave a representation of the pressure within the vessel, assuming there were no gas leaks. The larger the difference between the regulated pressure and the delivery pressure, the larger the volume of gas was supplied to the reactor.

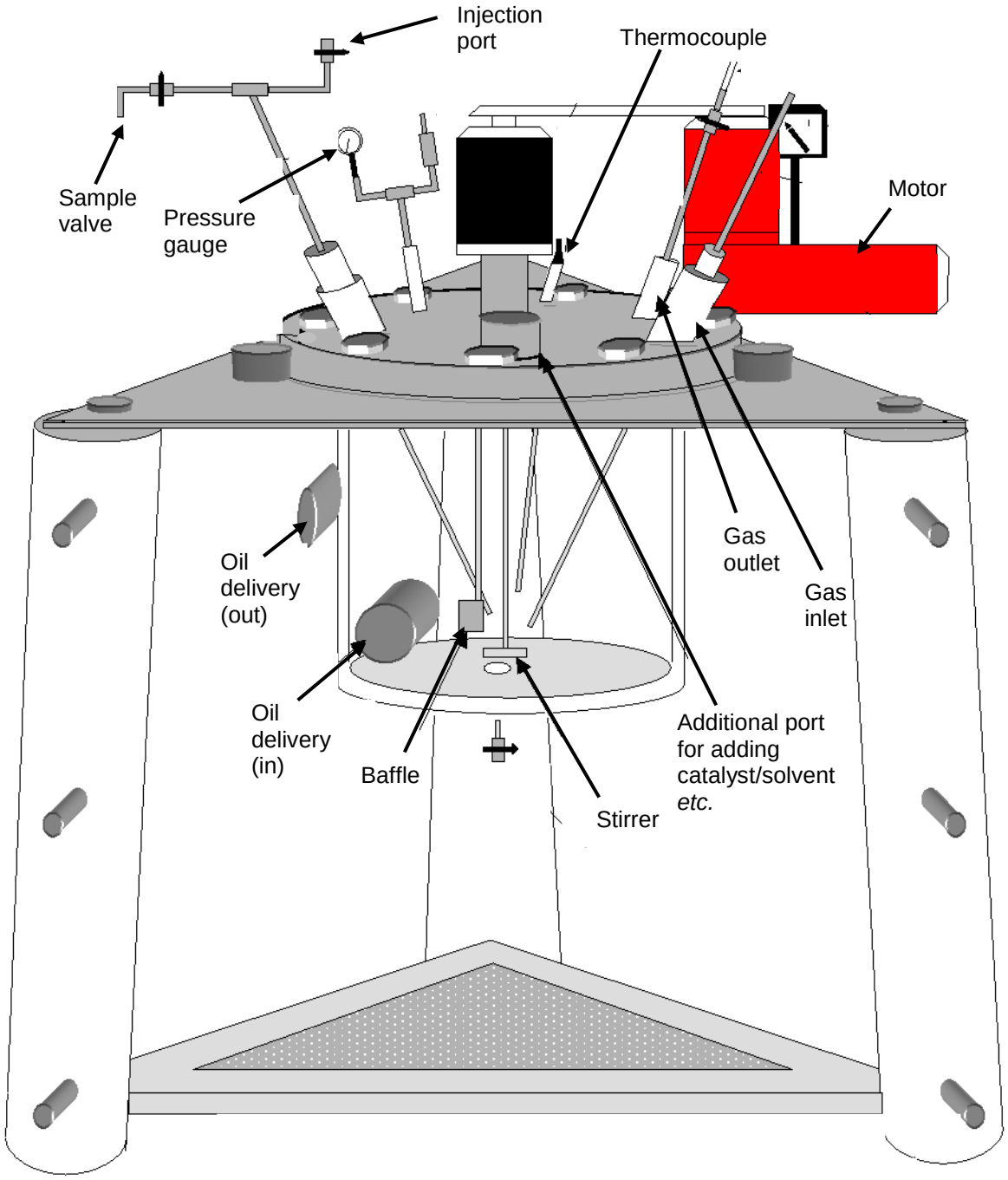

Figure 4. Schematic diagram of the Buchi batch autoclave used in the majority of studies presented here.

The maximum reactor pressure used was 5 bar (although 6 bar was permissible). The maximum regulated pressure used was 5.5 bar. This was controlled via the control box, which was connected directly to the gas controller, and also monitored active gas consumption.

2.1.1.2 The Autoclave Motor-Speed Controller

The SM 94 autoclave motor-speed controller was connected to the magnetic drive of the stirrer shaft. This tachometer measured the speed of the rotating shaft within the reactor vessel and also included functions for controlling the stirrer motor.

2.1.1.3 The Julabo Refrigerated and Heating Circulator

This system pumped Julabo Thermal M oil (temperature range 50 – 170 ^{o}C) to the reactor vessel, which contained two jackets. The oil was pumped via the pressure pump into the bottom port of the 0.5 litre vessel and was subsequently circulated back to the bath via a suction pump connected to the top port of the vessel. Temperature could be monitored internally (*i.e*. within the oil bath) or externally (*i.e.* within the vessel via the thermocouple). For best results, the heater was operated in the external mode so that a precise reaction temperature (typically 60^{o}C) could be maintained.

2.1.1.4 Experimental Procedure

Approximately 0.5 g of catalyst was wetted with 1-2 mL of water (particularly with carbon supported catalysts, since they can be pyrophoric) and the resultant slurry added to the reactor together with 300 mL of solvent (methanol). The Julabo heater/refrigerator was switched on and the temperature set. The scavenge tap was opened so that a constant flow of hydrogen could be added to the vessel to initiate reduction. The motor was then switched on and set to 300 rpm and the system left for 30 minutes to allow activation of the catalyst.

During catalyst reduction, approximately 15-20 mmoles of reactant was dissolved

in 50 mL of the same solvent used in the reactor (to make a total of 350 mL). Helium was used to degas the reactant solution for at least 15 minutes.

The stirrer motor and the gas flow were stopped and the scavenge tap closed. The 50 mL solution of reactant/solvent was injected into the reactor via the injection port. The closed system was then purged with hydrogen until the delivery pressure reached 4 bar. The motor speed was increased to 800 r.p.m. to start the reaction. This pressure was maintained throughout the reaction.

The reaction mixture was sampled regularly throughout the course of reaction, with more samples taken in the initial stages in order to garner rate data from reaction profiles. When taking a sample, the stirrer motor speed was decreased to zero and the sample taken via the sample port. The motor speed was then increased back up to 800 rpm. During sampling the hydrogen uptake was noted before and after the sample was taken. The sample was then filtered through a 0.2 μm syringe filter and analysed offline.

2.1.2 Ambient pressure reactor

The ambient pressure apparatus shown in Figure 5 was centred on a 100 mL 3-necked round-bottomed flask. In the first port a glass sparge was connected for the use of hydrogen introduction. The sparge was modified to contain a glass frit in order to achieve more efficient bubbling of hydrogen gas that aided solvation. The second port was fitted with a water cooled coil-condenser designed to keep the reactants in the liquid phase. Initial studies showed that solvent evaporation was found to be a problem despite the water cooling. As such, glass rashig rings were added to the core of the condenser to achieve turbulent flow and increase residence time of solvent/reactants in the cooled part of the condenser. The final port was equipped with a septum, used for the addition of reactant solution and withdrawal of samples with a syringe.

A Cole-Palmer gas flow meter was used to regulate hydrogen flow, thus maintaining a constant hydrogen concentration in solution. A constant temperature was maintained by submerging the system in a stirred silicon oil bath, the

temperature of which was controlled using an IKA magnetic stirrer hotplate system fitted with a 'Fuzzy Logic' temperature controller. The reaction medium was agitated by use of a 2 cm cross-shaped magnetic stirrer bar.

Whilst the Buchi batch autoclave may be considered as the "work-horse" reactor, for later reaction systems involving either high value starting materials or products, the ambient pressure reactor offered a scale-down option that enabled reactions to be carried out in smaller volumes as the larger, Buchi reactor, but allowed for similar concentrations to ensure accurate sample analysis.

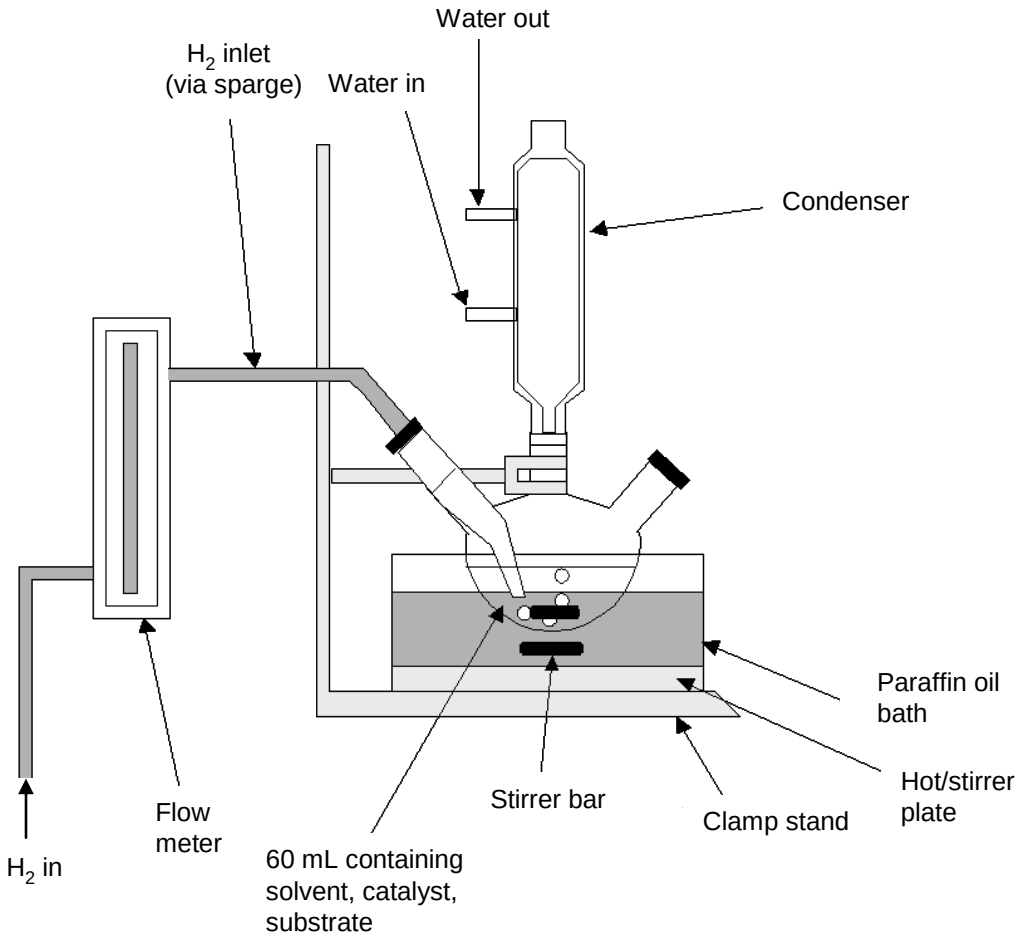

Figure 5. Schematic representation of the ambient pressure reactor, used in reactions where elevated hydrogen pressure was not required.

2.1.2.1 Experimental Procedure

Approximately 0.18 g of catalyst was wetted with a few drops of water to prevent any spontaneous combustion of the carbon supported catalyst, and the resultant slurry added via an open neck of the reactor together with 50 mL of solvent (methanol) and a cross shaped magnetic stirrer bar. The glass sparge was connected to a side-arm, the condenser to the central opening and a rubber stopper to the other side arm to create a “closed” system. High pressure, cold water was allowed to flow through the condenser and the reactor system was lowered into the oil bath such that the level of liquid in the reactor was below that of the silicone oil in the bath. Hydrogen gas was introduced at 60 mL min^{-1} via the sparge such that it bubbled through the catalyst/solvent slurry mixture, stirring was initiated and the system was then left for 30 minutes to allow activation of the catalyst.

Following catalyst reduction, a charge of reactant was dissolved in 10 mL of the methanol (reaction solvent). Helium was used to degas the reactant solution for at least 15 minutes. Stirring was stopped and the 10 mL solution of reactant/solvent was injected into the reactor through the rubber stopper.

The reaction mixture was sampled regularly throughout the course of reaction, with more samples taken in the initial stages in order to garner rate data from reaction profiles. A 1 mL glass syringe with an attached needle was used to sample the reaction and the sample was then filtered through a 0.2 μm syringe filter and analysed offline.

2.1.3 Gas phase batch reactor

The apparatus comprises a modified Graseby-Specac 5660 heated gas cell (shown in Figure 6 and Figure 7) connected to the catalyst characterisation facility (see Section 2.3.2) enabling the flow of a variety of gases. The cell is fitted with isolation valves and is housed within a dry-air purged Nicolet Avatar 360 FT-IR spectrometer. An injection septum within the cell enables reagents to be added to the reaction system.

For the gas phase studies presented here, the catalyst was mounted within a glass sample holder that locates within the base of the cell, such that the catalyst was not in the path of the infrared beam. In this way, all spectra presented arise from the composition of the gaseous phase, with no contribution from the catalyst or the catalyst surface in order to simplify the analysis.

2.1.3.1 Experimental procedure

The catalyst mass, quantity of reagent and pressure of hydrogen were selected to yield a full hydrogenation profile in a time that was sufficiently long (*ca.* 30 min) so that infrared spectra of sufficient signal/noise ratio could be repeatedly recorded during that interval, in order to define a representative reaction profile. In this manner, 1 part of the 1% Pd/Al_2O_3 catalyst was diluted with 100 parts of the support material (γ-alumina) and ground in a pestle and mortar, then *ca.* 500 mg of this mixture was pressed into a thin disc using a 13 mm die (Specac) pressurised at 10 tonnes by a hydraulic press (PerkinElmer). The catalyst disc was reduced under a flow of 10% H_2/He at a temperature of 100 ^oC. The hydrogen composition was increased to yield an equimolar mixture of hydrogen and helium at the same flow rate and, after 10 minutes, the reactor was isolated at a pressure of 1.2 bar. A liquid chromatography syringe (Hamilton Bonaduz) was used to inject a 10.0 μL aliquot of nitrile reagent into the cell via the septum. Thus, the infrared cell is acting as a batch reactor under conditions where reasonable conversions represent multiple turnovers, unhindered by the availability of hydrogen.[71]

Scanning of the infrared spectrum commenced as soon as the injection of the nitrile was complete. Infrared spectra were recorded at a resolution of 4 cm^{-1}, co-adding eight scans and requiring an acquisition time of *ca*. 10 s. The reaction temperature was maintained at an appropriate level to ensure that all the reagents remained in the gaseous phase (80 ^oC for benzonitrile hydrogenations). Given the relative simplicity of the experimental arrangement, the reacting gases obey the Beer–Lambert law, thereby permitting calibration curves to be readily produced. In this way, the number of moles of the majority of reagents could be reliably determined from the integrated infrared intensity for a particular vibrational feature.

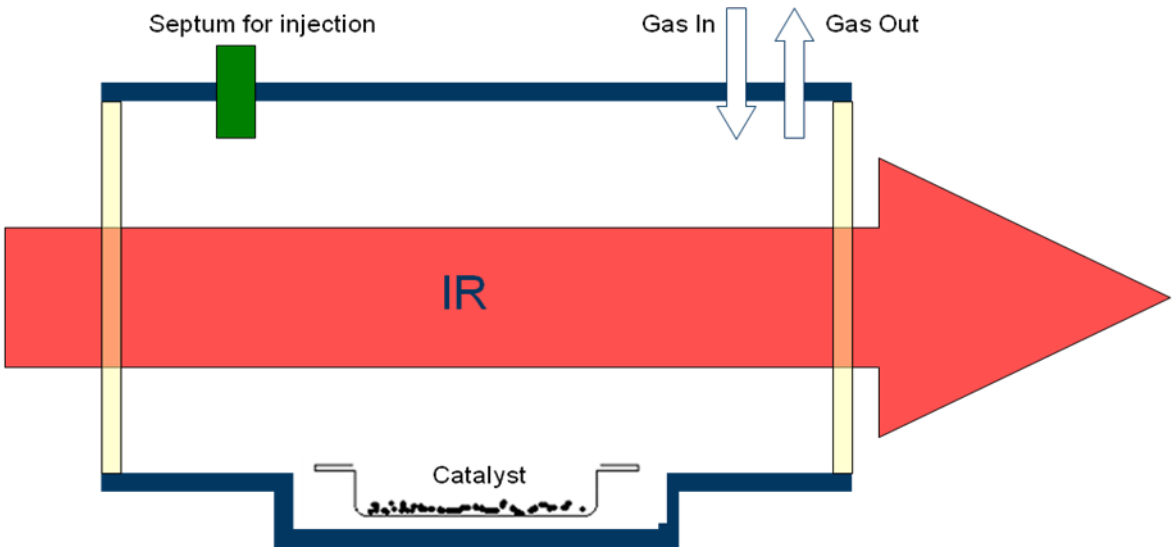

Figure 6. Schematic cross sectional diagram of the Graesby-Specac modified gas cell used in gas phase hydrogenation reactions. Note that the catalyst is placed such that it lies outwith the path of the beam so that only species in the gas phase were analysed.

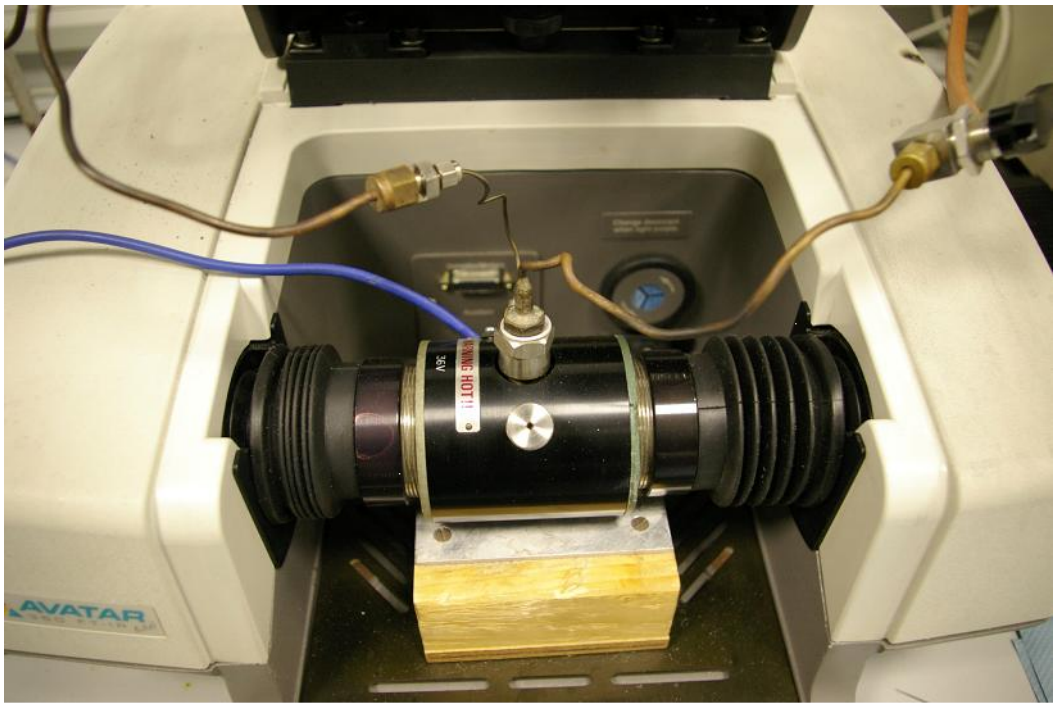

Figure 7. Photograph of the Graesby-Specac modified gas cell housed within a Nicolet Avatar infrared spectrometer.

2.1.4 Syngenta Parr reactor

The system used at the industrial centre centred on a Parr batch autoclave reactor, capable of containing a liquid volume of 100 mL, as shown in Figure 8. Pressurised gases (nitrogen as a purge and hydrogen as a reactant gas) could be added quickly through a port at the top of the reactor via a mass flow controller, thus meaning that reaction pressure could be attained almost instantly. Whereas all reactions performed in this study were considered as batch reactions (*i.e.* all reactants were added and the reactor sealed), the Parr system benefits from the addition of a high-pressure HPLC pump for substrate addition so that it could also operate as a fed-batch system. The reactor system could be submerged in a silicone-oil bath for reactions at elevated temperature. However, reactions were typically carried out at ambient temperature. Control of gas flow, temperature, stirring speed and (in the case of fed-batch reactions) substrate addition rate was automated by the use of Atlas software.

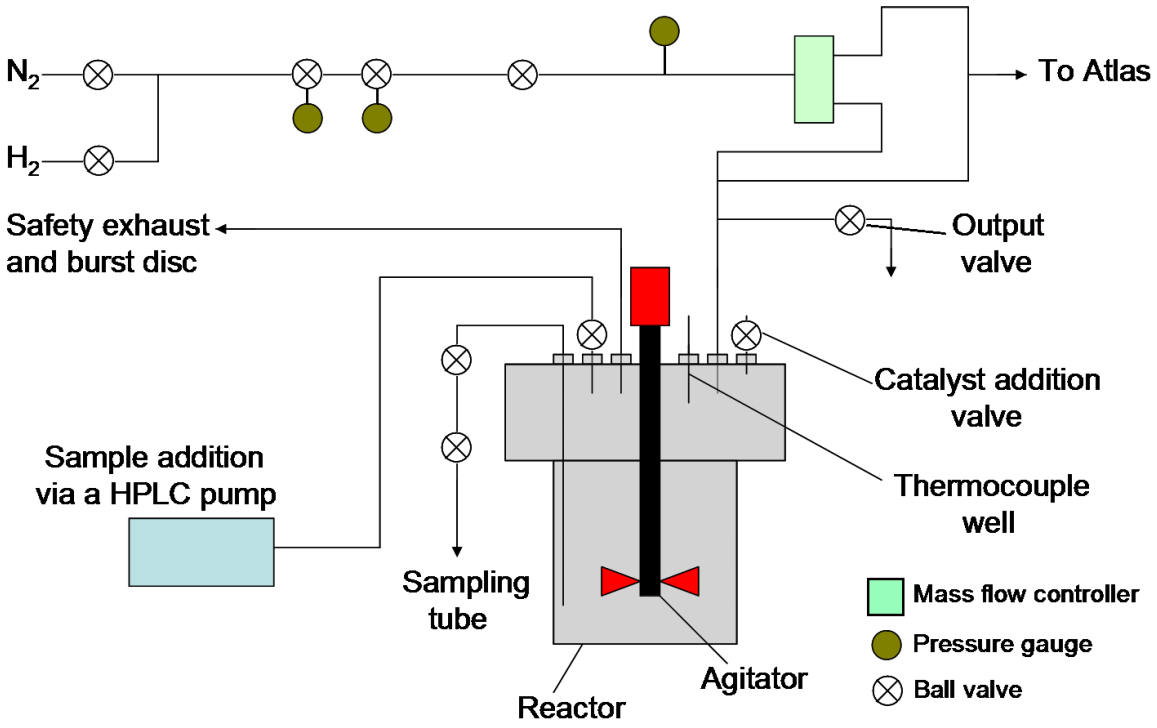

Figure 8. Schematic diagram of the Parr system used for hydrogenation reactions at the industrial centre.

2.1.4.1 Experimental procedure

Approximately 0.5 g of catalyst was wetted with a few drops of water to prevent any spontaneous combustion of the carbon supported catalyst, and the resultant slurry injected into to the reactor along with 50 mL of solvent (methanol), through the catalyst addition valve. The reactor was then sealed and purged with nitrogen before the catalyst was reduced under flowing hydrogen at the reaction temperature for 1 hour and under agitation.

Following catalyst reduction, a charge of reactant was dissolved in 20 mL of the same solvent used in the reactor. Helium was used to degas the reactant solution for at least 15 minutes. Stirring was stopped and the 20 mL solution of reactant/solvent was injected into the reactor through the same addition valve.

The reactor was then pressurised quickly to the desired reaction pressure (6 bar) before stirring was resumed. The reaction mixture was sampled regularly throughout the course of reaction, with more samples taken in the initial stages in order to garner rate data from reaction profiles. A 1-2 mL aliquot sample was taken and then filtered through a 0.2 μm syringe filter and analysed offline.

2.2 Analytical techniques

2.2.1 Gas-Liquid Chromatography

Gas-liquid chromatography is one of the most common methods of sample separation and identification in analytical chemistry[72]. The gas chromatograph (GC) flows a sample through a capillary column using a carrier gas (the mobile phase, usually helium). The rate at which different components exit the column is dependent on a number of variables including the column packing (the stationary phase) which separates the components based on a variety of chemical and physical properties and their interaction with the stationary phase, but also the carrier gas flow rate, column length and column temperature. As the gaseous constituent components of the sample exit the column they individually enter the detector, resulting in an electrical response that can be recorded by a number of methods.

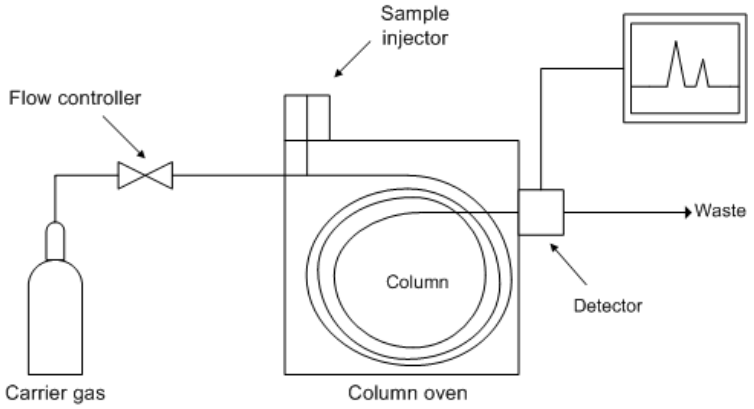

Figure 9. Diagrammatic representation of a gas-liquid chromatograph.[73]

2.2.1.1 Flame Ionisation Detector

The flame ionisation detector is sometimes regarded as a universal detection method in gas-chromatographic techniques and is shown in Figure 10. When the vaporised sample leaves the column it is mixed with hydrogen gas and air and ignited. Combusted hydrocarbons produce ions that are detectable by the collector electrode. A high voltage is applied at the tip of the burner and the collector electrode situated just above the flame detects the change in potential produced by the ions.

FID detectors are popular due to their robustness and ease of use among many other advantages including:

- high sensitivity to a vast array of organic molecules
- little or no response to water, atmospheric gases or carrier gas
- the response is generally not affected by fluctuations in temperature, flow rates or pressure
- there is excellent linear response to analytes over a wide concentration range, ensuring easy calibration for quantitative analysis.[74]

The main drawback to using an FID is the fact that samples are destroyed in the process of analysis.[75]

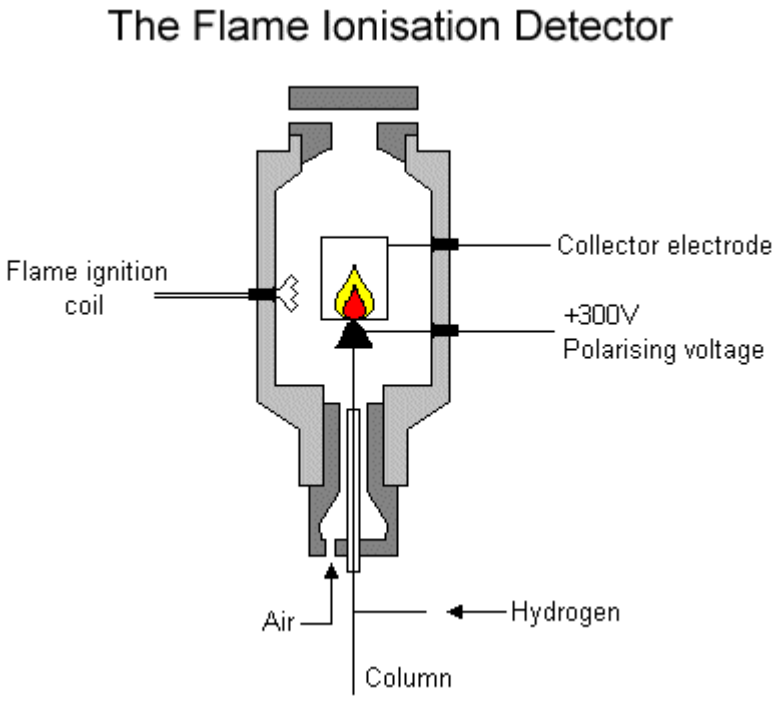

Figure 10. Diagrammatic representation of a flame ionisation detector.[76]

Gas chromatography analysis was carried out on a Perkin-Elmer 8500 Series Gas Chromatograph fitted with a Varian Chrompack CP-Sil 8 CB column (30 m x 0.20 mm ID, 0.33 µm film).

2.2.2 High performance liquid chromatography

High-performance liquid chromatography (HPLC) is an analytical technique widely used in biological and analytical chemistry to identify, quantify and purify the components of an often complex mixture.[77] HPLC differs from gas chromatography in that it utilises a liquid mobile phase rather than a carrier gas to separate the components of a solvated liquid, and then pumped through a column at high pressure. Resolution (*i.e.* separation) is determined by the interaction between the solute components and the stationary phase (the packing material of the column). The interaction of the solute with mobile and stationary phases can be tailored through the choice of solvents (mobile phase) and column (stationary

phase). As a result, HPLC has a somewhat higher degree of versatility over other chromatographic systems.[78]

The hardware required for HPLC includes a pump, injector, column, detector and some form of data recorder (typically an integrator or a computer with the necessary software for data analysis). Separation occurs at the column and, since the stationary phase is composed of micrometre size porous particles, a high pressure pump is required to ensure a flow of mobile phase through the column.

Optical detectors are the most common type used in HPLC systems. These detectors pass a beam of light through the flowing column effluent as it passes through a low volume flow cell.[79] The variations in light intensity caused by UV absorption, fluorescence emission or change in refractive index from the sample components passing through the cell, lead to changes in the output voltage, which gives a quantitative response that is diagnostic of a particular component. The most common type of detector is the UV/VIS photodiode array detector (DAD), which allow simultaneous collection of chromatograms over a range of wavelengths.[79]

HPLC analysis was carried out in this project on a Hewlett Packard 1050 Series HPLC with a Thermo Hypersil C18 base deactivated column, and the data was collected on a Hewlett Packard 3396 Series III integrator.

2.2.3 Nuclear magnetic resonance spectroscopy

Some nuclei have a non-zero nuclear spin quantum number (I) and in the presence of a magnetic field they can have 2I + 1 orientations. Protons have a spin of I = ½ which gives them two possible orientations, one of low energy which is aligned with the magnetic field and one of high energy which is opposed to the field.[80] At thermal equilibrium there is a slight excess of those in the lower energy orientation, this is called the bulk magnetization (M) parallel to the applied magnetic field (B_0).[80] When a radiofrequency signal (rf) is applied to the system, the distribution of spin orientations is changed if the signal matches the Larmor frequency, the resonance frequency of the spins,[81] *i.e.* it will tip the spins away

from B_0. As soon as M is tilted away from the z-axis, it will start to precess about B_0 (Figure 11).[81]

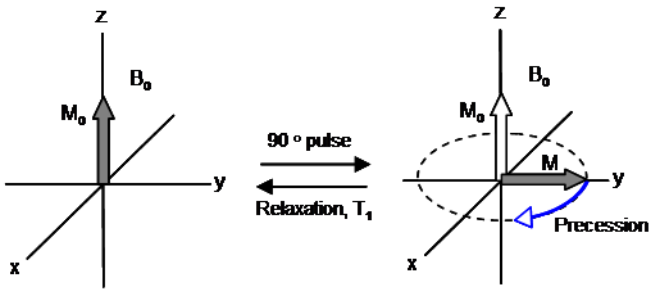

Figure 11. Effect of a 90 ° pulse on the magnetic field.

A receiver coil measures the signal oriented along the y-axis, and so measures positive, then zero and then negative signal as the spins precess from y to x and then to –y. The frequency of this oscillating signal is the difference between the frequency of the spins and the excitation frequency.[80] The magnetization, M, decays back to thermal equilibrium, M_0, exponentially. The components of M which are parallel and perpendicular to M_0 decay through different process, *spin-lattice* and *spin-spin* relaxation. The spin-lattice (or longitudinal) relaxation occurs by energy transfer from the nuclear spin to the other spins in the system, caused by fluctuating magnetic fields in the sample.[81] Spin-spin relaxation occurs through transfer of spin between excited nuclei.[82]

The oscillating signal is, therefore, gradually decaying, and is represented by a cosine-type function that experiences exponential decay.[80] This signal is called the free induction decay (fid) which is Fourier transformed into the frequency domain and a spectrum is produced. The chemical shift of a proton is the difference in frequency of the proton resonance to that of an internal standard, usually tetramethyl silane (TMS).

The investigation of species present at low concentration in solution by ^{1}H NMR spectroscopy is a common problem. Here, the signal intensity of the reaction solvent is typically much greater than the intensity of the species present in a reaction sample. Suppression of the solvent signal was therefore required. Recent developments in the pre-saturation pulse sequence technique have enabled the suppression of two solvents, for use on LC-NMR samples.[83] This technique is

known as the WET sequence, Water suppression Enhanced through T_1 effects,[84] and can reduce the water signal in biological samples. Modification of this pulse sequence has been previously developed and optimised and was applied here to study reaction samples of low concentration in isopropanol or methanol (the reaction solvents used here).

^{1}H NMR spectra were recorded on a Bruker Avance 400 MHz spectrometer fitted with a Quattro Nucleus Probe (QNP) able to investigate four nuclei; ^{1}H, ^{19}F, ^{31}P and ^{13}C. A Wilmad NMR capillary tube containing the deuterated solvent (Figure 12) was used to analyse the reaction samples, allowing the deuterated solution to remain separated from the sample solutions, and thus enabling quantitative concentration data to be obtained. Any deuterated solvent mixing with the reaction sample would otherwise affect the concentration of that sample. The deuterated solvent used in all experiments was methanol-d_4, since its signal would not interfere with those of the species being investigated, and would be “hidden” by the large peaks of the reaction solvent.

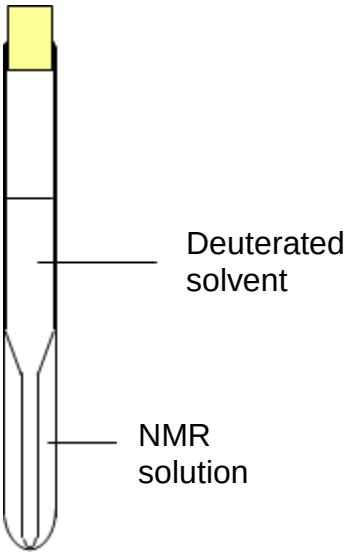

Figure 12. Deuterated solvent NMR capillary tube.

2.2.4 Infrared spectroscopy

FTIR spectroscopy has been used in this project to study the gas phase hydrogenation of benzonitrile. Two major advances of infrared spectroscopy were the introduction of the Michelson interferometer in 1891, and the application of the Fourier Transform in 1966, which allowed much faster recording of spectra.[85]

Infrared spectroscopy measures molecular vibrations, which cause a change in the electric dipole moment of the molecule.[86] A non-linear molecule will have 3N degrees of freedom, where N is the number of atoms in the molecule. Three of these are translational modes and three are rotation, leaving 3N-6 vibrational modes.[87] However, not all of these will be infrared active, and some may be degenerate. There are different types of vibrational modes: stretches (ν), bends (δ), rocks (ρ), torsions (τ) and wags (ω). Such modes enable identification of molecules, but in this study, analytical standards were used for identification purposes.

In the present study, infrared spectroscopy was used to study the gas phase hydrogenation of benzonitrile in modified batch reactor housed within a Nicolet Avatar 360 FT-IR spectrometer (as discussed in Section 2.1.3).

2.3 Catalyst preparation and characterisation

2.3.1 Catalyst preparation for 1% Pd/Al_2O_3

395.00 g of γ-alumina extrudates (BASF Q332, BET surface area of 186 $m^2\ g^{-1}$) were covered with deionised water and stirred with a motorised stirrer. A solution of 9.76 g $Pd(NO_3)_2.xH_2O$ (Aldrich, 205761) was added and the mixture was stirred for 48 hours.

The solvent was removed by means of a rotary evaporator at 80 ºC. The product was calcined in air overnight at 200 ºC. A fraction of the resulting extrudates was ground and sieved to a size of 250-500 μm. The calculated Pd content was 0.98 wt. %.

All other catalysts used herein (5% Pd/C, Aldrich, 205680 and PtO_2, Aldrich, 206032) were commercially supplied by Sigma Aldrich, with the exception of the industrial catalyst (5% Pd/C), which was supplied by Syngenta.

2.3.2 Catalyst characterisation facility

The catalyst characterisation and test facility used for gas-phase experiments and catalyst characterisation is shown in Figure 13. The line can be split into two general regions, a vacuum line and an ambient pressure line. The vacuum line operated at a base pressure of approximately 1 x 10^{-6} Torr and was able to operate in either pulsed or continuous flow mode, with the pulses being introduced via a sample loop, with a calibrated volume 4.71 cm^3. A storage bulb or cold finger (allowing gases to be freeze pump thawed) could be used for the containment of reactant or adsorbate gases. The two pressure gauges were Baratron capacitance manometers, one that was accurate to 1 Torr and therefore used for measuring low pressures and the other to 1000 Torr, which was used to measure pressures up to atmospheric.

For adsorption isotherm reactions, the catalyst was added to a “U-tube” quartz reactor fitted with a glass sinter, such that it operated as a plug flow reactor and had a downward flow of reactant gases. A Watlow furnace was raised around the reactor and the reactor was then plugged with quartz “super” wool to prevent heat-loss and ensure a controlled temperature ramp. The furnace temperature and ramp rate was controlled using an 818P Eurotherm Temperature controller. Effluent gases could be quantitatively monitored and analysed by gas chromatography (with a thermal conductivity detector) or by mass spectrometry.

For gas phase hydrogenation reactions, a Specac gas cell fitted with KBr or CaF_2 windows could be used as a batch reactor, and analysed by *in situ* infrared spectroscopy. Although not discussed here, a variety of different infrared cells could be used to analyse gases or to probe their interactions with the surface of catalysts. Given such a configuration, the facility was capable of carrying out a variety of distinct experimental measurements, namely:

1. TPR (Temperature Programmed Reduction)
2. TPD (Temperature Programmed Desorption)
3. TPO (Temperature Programmed Oxidation)
4. Volumetric adsorption isotherms
5. Pulsed mode adsorption isotherms
6. Gas phase catalytic reactions
7. Catalytic characterisation.

2.3.2.1 Line Volume Calibration

For all pulsed experiments, a sample loop was used to introduce the gas into the system. The sample loop consisted of three POR/6 Youngs Taps. In order to determine the volume of the sample loop, a vessel of *known* volume was used (typically an evacuated 1 L bulb). The bulb could be attached to the vacuum section of the line and back filled with helium. The helium was then expanded into the line and any pressure difference noted. This was repeated several times using different pressures of helium, and the ideal gas law used to calculate the sample loop volume (the calibration could also be confirmed by gravimetric measurements of the helium filled bulb).

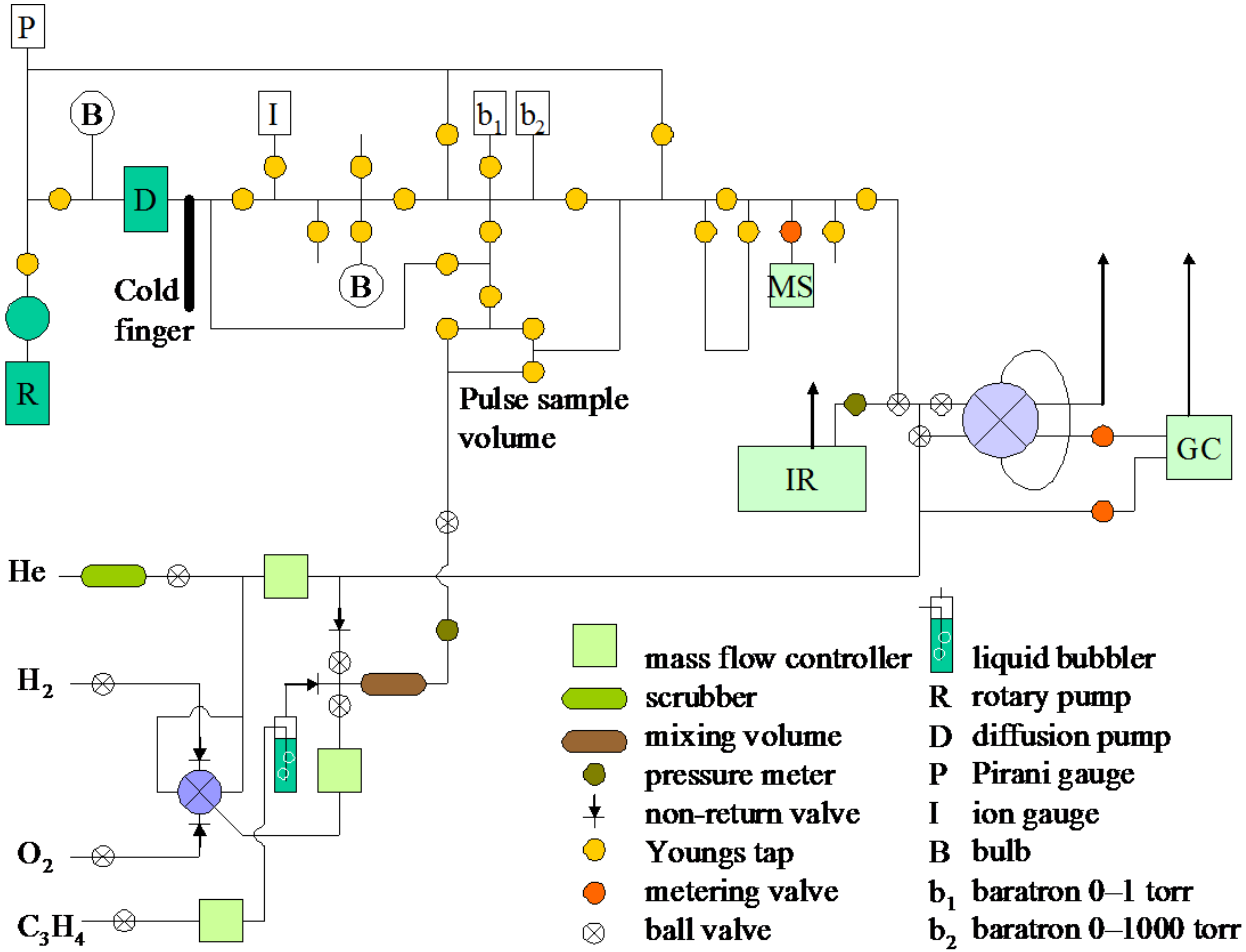

Figure 13. Schematic of the catalyst characterisation line.

2.3.3 Atomic Absorption Spectroscopy

Atomic absorption spectroscopy (AAS) is an analytical technique used to determine the concentration of a particular metal in a sample. The technique typically uses a flame or graphite furnace to atomise the sample upon which a beam of light (from a hollow cathode lamp made from the element to be determined) is shone through and absorbance measured via a detector.[88] Here, AAS was carried out on a Perkin Elmer 1100 Atomic Absorption Spectrometer at 247.6 nm with an acetylene flame to determine the concentration of palladium within the various palladium catalysts.

A stock solution containing 100 ppm of palladium in 10 % hydrochloric acid was prepared from a 1000 ppm standard (Sigma-Aldrich) by mixing 10 mL of stock solution with 90 mL of 10 % hydrochloric acid in a volumetric flask. From this solution, 2, 4, 6, 8 and 10 mL portions were decanted into separate volumetric flasks and made up to 100 mL using 10 % (aqueous) hydrochloric acid. These solutions were the standards, which were used to calibrate the system.

A sample of the catalyst being tested was then weighed out to make approximately a 5 ppm solution, for example, to make 100 mL of a 5 ppm solution from a 5 wt % catalyst, 10 mg of catalyst would be required. The samples were then left for an hour in 10 mL of concentrated hydrochloric acid at 393 K to let the metal leach from the substrate, after which, the samples were left to cool and were filtered into 100 mL volumetric flasks, which were made up to the mark, using distilled water.

2.3.4 Transmission Electron Microscopy

Transmission electron microscopy (TEM) is a microscopy technique whereby a beam of electrons is transmitted through an ultra thin specimen, interacting with the specimen as it passes through. An image is formed from the electrons transmitted through, magnified and focused by an objective lens and appears on an imaging screen, such as a fluorescent screen in more modern TEMs, or to be

detected by a sensor such as a CCD camera or in this case onto a layer of photographic film.[89]

2.3.5 CO chemisorption

The process of chemisorption can be used in a quantitative manner to calculate the total amount of metal that is available for reaction, assuming that a monolayer of the adsorbate is formed. This is known as the dispersion of the catalyst and is normally expressed as a percentage of the total metal atoms. In the case of a supported metal catalyst, the dispersion is the total number of surface metal atoms; the equation for which is shown below.

$$Dispersion\ \ \% = \frac{Number\ of\ \ Surface\ \ Atoms}{Total\ \ Number\ of\ \ Atoms} \times 100 \qquad (5)$$

When using supported metal catalysts, there are several molecules selected to use for adsorbates. These include carbon monoxide, oxygen, hydrogen and nitric oxide. In all these cases, it is important to know:

- What is the metal to adsorbate stoichiometry?
- Does the molecule dissociatively adsorb?
- Does the support play any part in the adsorption, *i.e.* is there spillover, or does the support play an active role in adsorption?

The two most popular ways of performing chemisorption experiments are volumetric chemisorption[90] and pulsed chemisorptions.[91] In the case of palladium, it is well documented that upon hydrogen adsorption, not only does the hydrogen dissociate, but it can also absorb into the bulk of the metal.[92] This complicates measurement of the dispersion of palladium catalysts using hydrogen. It is believed that carbon monoxide chemisorbs onto the surface of palladium with little or no dissociation so this makes it an ideal molecule to use for chemisorption measurements. However, the literature on the Pd/CO system reports Pd:CO ratios of 1:1[93] and 1:2.[94] This discrepancy requires justification; therefore care

must be taken when carrying out chemisorption studies as to the conditions and the stoichiometry being used.

Pulsed chemisorption[82,83] studies were performed by placing a known mass of catalyst (*ca.* 250mg) into the reactor and reducing it in a flowing 5% H_2/He mix for 1 hour at 373 K. Pulses of a known volume of CO were passed over the catalyst using helium as a carrier gas. The point of saturation was monitored using a thermal conductivity detector (HP 5890 Chromatograph fitted with a Varian 17% Sebaconitrile chromosorb PAW 80-100 mesh TCD column). Saturation point was determined when three peaks of equal area were observed on the integrator. Since the volume and pressure of gas passed over were known, it was possible to calculate the dispersion of the catalyst assuming a 1:2 ratio of CO:Pd.[85,86]

The dispersion of a catalyst can be used to estimate particle size, provided certain assumptions are made, namely that the particles are all of the same size and are spherical.[87,88] From these assumptions, dispersion may be expressed as:

$$D = \frac{6A}{\rho S_a N_a d} \times 100 \qquad (6)$$

Where: D = Dispersion

A = Atomic weight (106.42 g mol^{-1})

ρ = Density of metal (12.02 x 10^{-21} g nm^{-3})

S_a = Average surface area occupied by one active atom (0.0806 nm^2)

N_a = Avogadro's number

d = Average particle diameter

Therefore, in the case of palladium, average particle diameter can be calculated by:

$$d = \frac{109}{D} \qquad (7)$$

2.3.6 CO Temperature programmed desorption

Temperature programmed desorption (TPD) can be a useful tool to probe the adsorption energy of a catalyst for a particular adsorbate, and it can also give an indication of any surface reactions occurring on the catalyst.[97] Typical probe molecules used for this are H_2, CO and NO.[97] TPD experiments are performed as follows: a known mass of catalyst is loaded into a reactor and reduced. Once reduced, the gas being used for the analysis is pulsed onto the catalyst until saturation, using an inert carrier gas such as He or N_2. Once saturated, a linear ramp is used to heat the sample to temperatures up to 1000 K. The effluent gas is passed through a mass spectrometer, which analyses the gas with respect to mass, thus giving a plot of the gas pressure with respect to temperature. In this way, the nature of binding sites on the catalyst's surface can be analysed.

3 Results and discussion

3.1 Catalyst characterisation

3.1.1 Atomic absorption spectroscopy

In performing atomic absorption spectroscopy, the calibration curve shown in Figure 14 was used to calculate the palladium content for each of the catalysts used in the present study. The results are summarised in Table 1, below. Such measurements revealed that the metal loading for the synthesised Pd/Al_2O_3 was found to be 1.00% in agreement with the calculated palladium content. However, at 3.63%, the metal content of the commercially supplied Pd/C was found to be much lower than the quoted 5%. However, it is believed that this may be due to the fact that not all of the palladium had leached out of the sample during preparation. To ensure full dissolution of metal, the preparation experiment could be repeated at higher temperature or with a stronger leaching agent (*e.g. aqua regia*).

Table 1. % Metal loading of the supported metal catalysts used in this study as calculated by atomic absorption spectroscopy.

Catalyst	Absorbance (a.u.)	Concentration (ppm)	Mass of Pd in sample (mg)	% Loading of Pd in catalyst
5% Pd/C	0.092	4.53	0.450	**3.63**
1% Pd/Al_2O_3	0.102	5.02	0.502	**1.00**

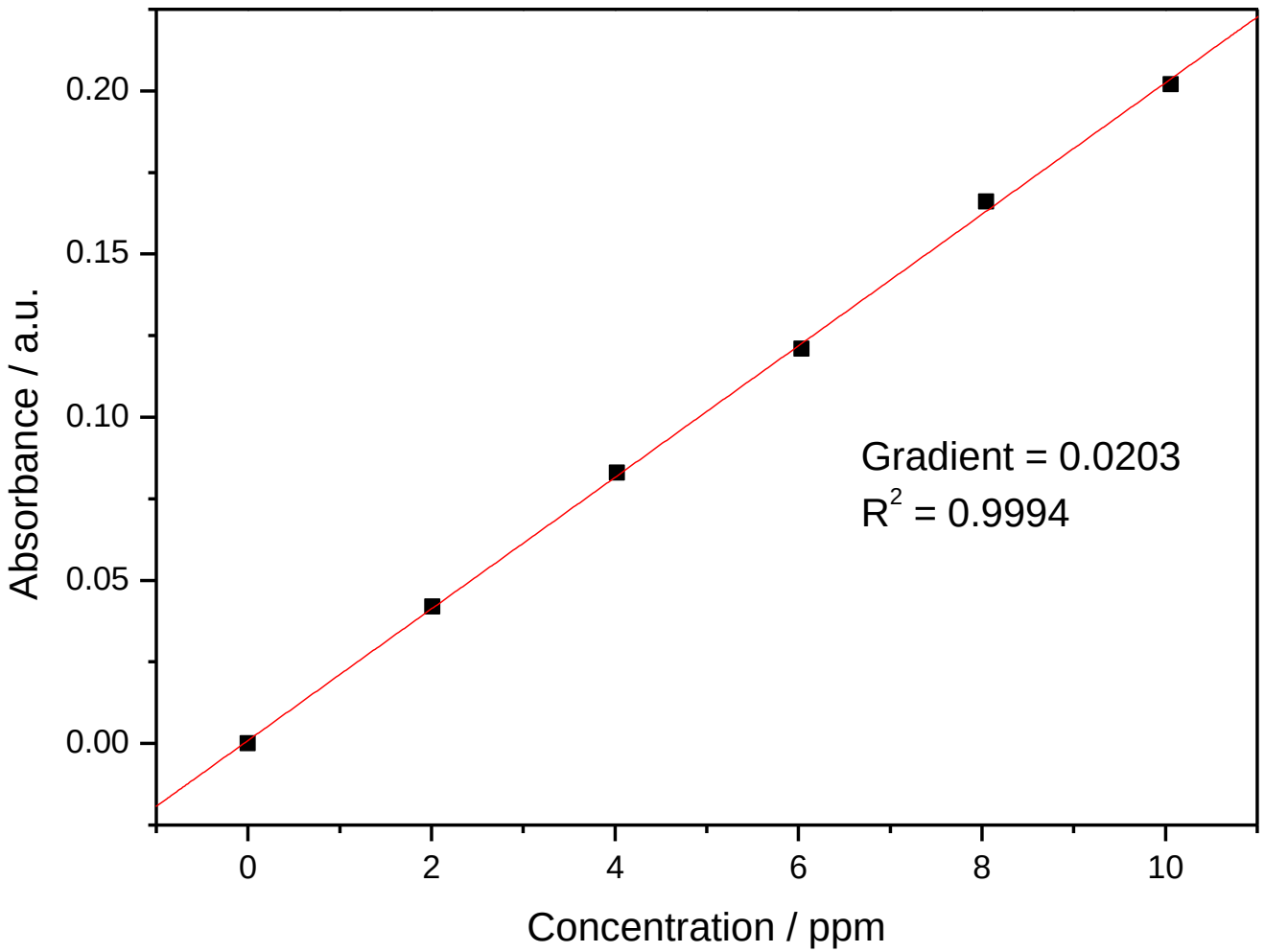

Figure 14. Atomic absorption spectroscopy calibration curve for Pd content carried out on a Perkin Elmer 1100 Atomic Absorption Spectrometer at 247.6 nm with an acetylene flame.

3.1.2 Transmission electron microscopy

Although TEM is a useful tool in giving a clear and reasonably accurate idea of the size, shape and type of particles present in the sample, it is only efficient if metal particles exhibit sufficient contrast with the support. Figure 15 shows the TEM images obtained for Pd/C (Figure 15(a) and (b)) and Pd/Al_2O_3 (Figure 15 (c) and (d)) Unfortunately, for Pd/Al_2O_3, sufficient contrast could not be found and, coupled with relatively low resolution, no informed estimation of particle shape can be proposed at this time for either catalyst sample. Fortunately, atomic absorption spectroscopy confirms that Pd metal is present and all catalysts exhibit distinct reactivity, uniquely attributed to the Pd.

Nevertheless, particle size distribution histograms were produced and are shown in Figure 16 and Figure 17. It can clearly be seen that there exists a narrow particle size distribution of *ca.* 2.0 $\pm$ 0.5 nm for Pd/C (Figure 16), as one might expect for a commercially sourced catalyst. On the other hand, Figure 17 shows a skewed Gaussian distribution for Pd/Al_2O_3 with a much larger particle size and wider distribution of *ca.* 7.0 $\pm$ 2.0 nm, *i.e*. in the range 5.0-9.0 nm.

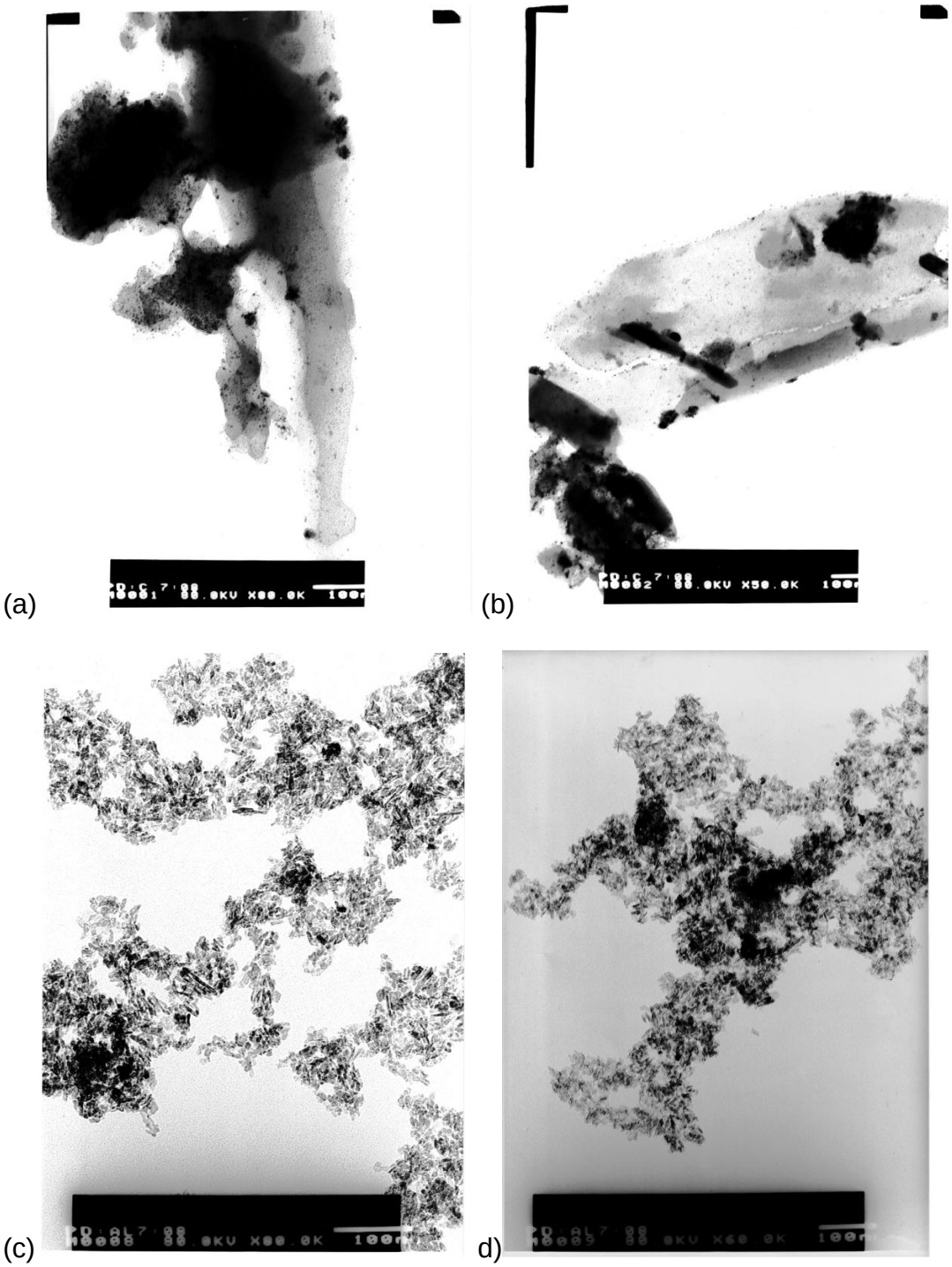

Figure 15. TEM images for 5% Pd/C (a) and (b) and 1% Pd/Al_2O_3 (c) and (d).

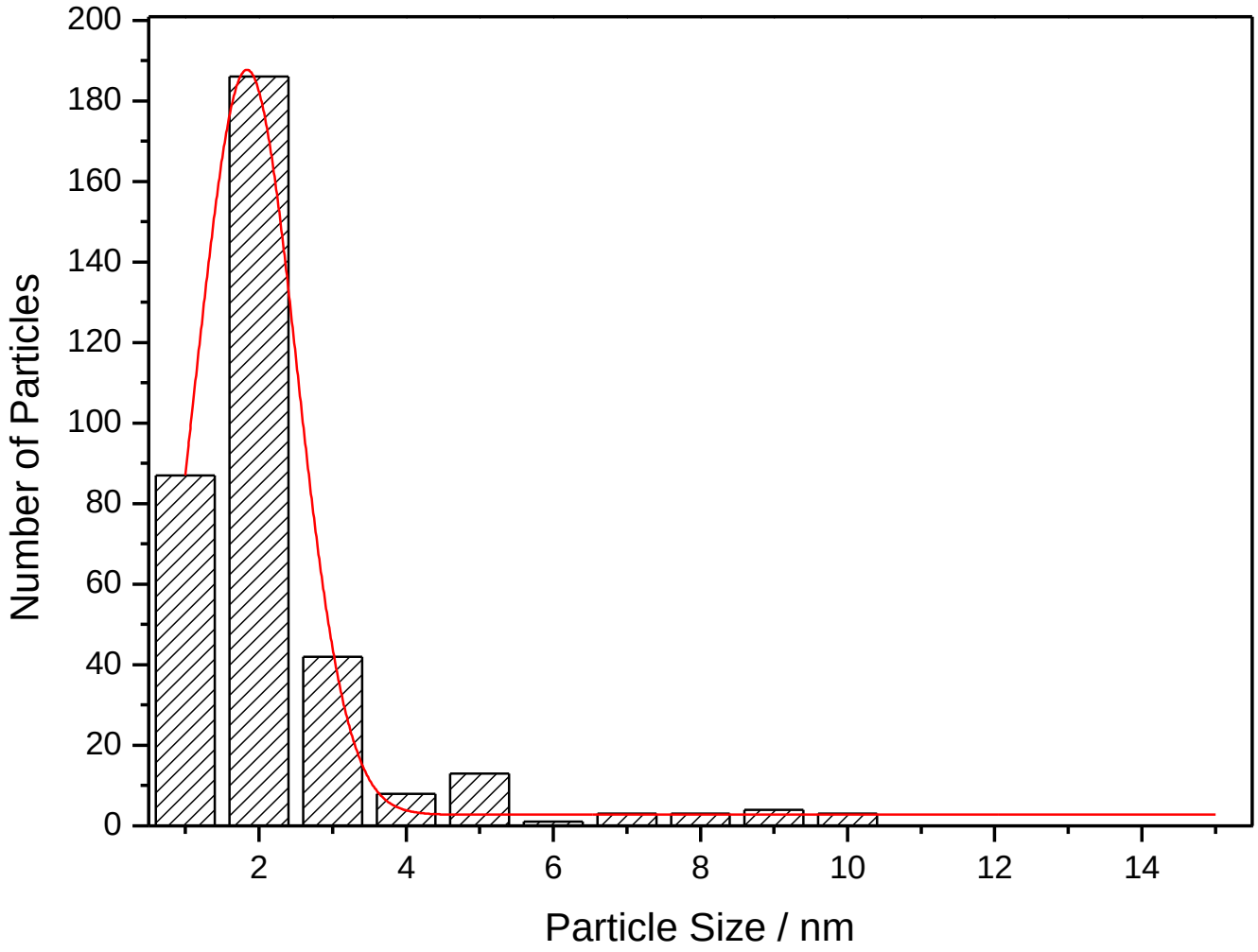

Figure 16. Particle size distribution histogram for 5% Pd/C, as determined by a particle size count of TEM images.

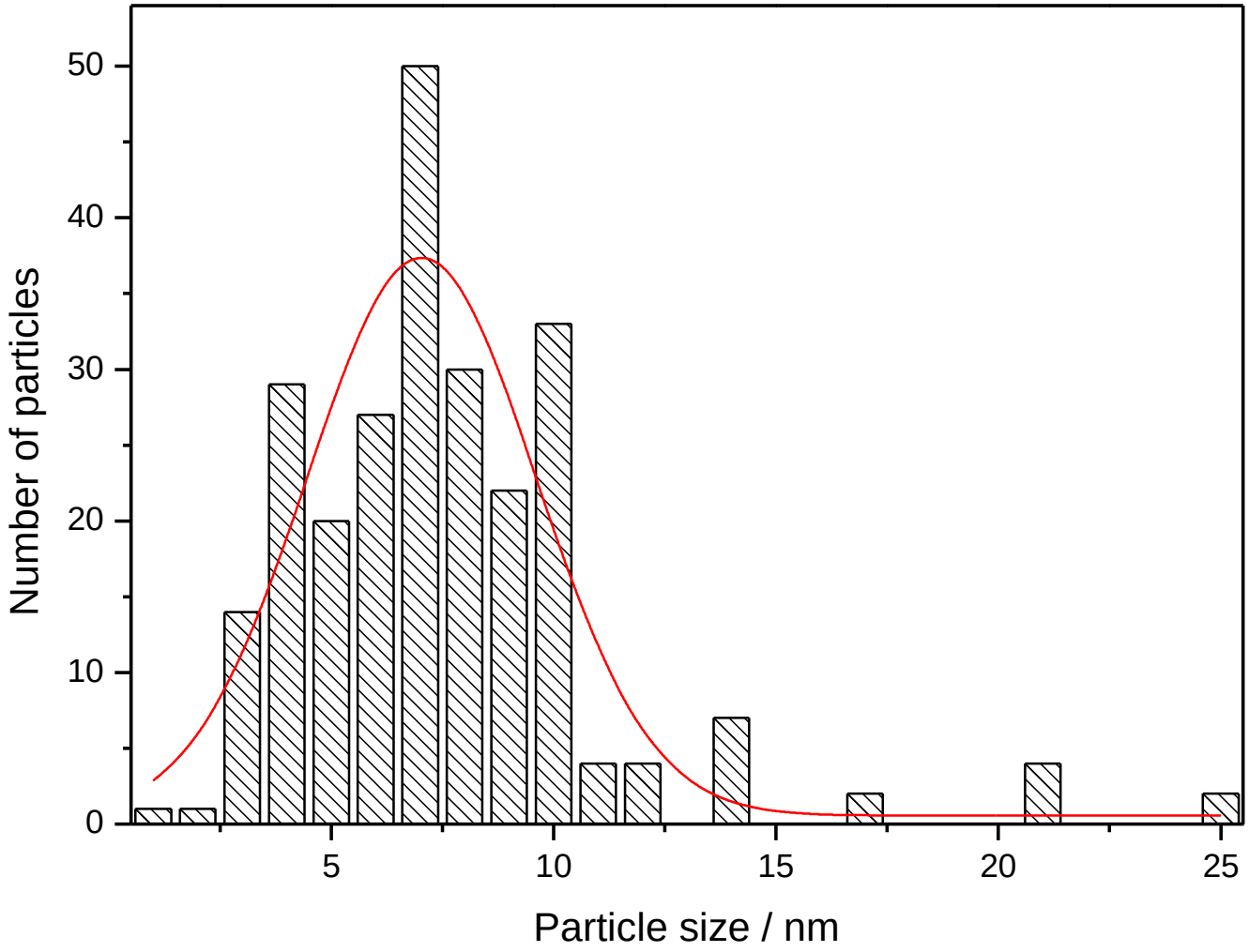

Figure 17. Particle size distribution histogram for 1% Pd/Al_2O_3, as determined by a particle size count of TEM images

3.1.3 CO adsorption isotherms

CO adsorption isotherm data for 5% Pd/C and 1% Pd/Al_2O_3 are summarised in Table 2, below. For 5% Pd/C, the adsorption isotherm is shown in Figure 18 and a maximum CO capacity of 9.24 x 10^{-6} moles $CO/g_{catalyst}$ was obtained. Assuming a $CO:Pd_{(s)}$ ratio of 1:2[97] this equates to 2.78 x 10^{18} $Pd_{(s)}$ $atoms/g_{catalyst}$, which, according to (7) corresponds to a Pd dispersion of 54 % and a mean particle size of 2.0 nm. For 1% Pd/Al_2O_3, the adsorption isotherm is shown in Figure 19 and the maximum CO capacity was found to be 6.30 x 10^{-5} moles $CO/g_{catalyst}$, corresponding to 1.89 x 10^{19} $Pd_{(s)}$ $atoms/g_{catalyst}$. Using (7) again, this corresponds to Pd dispersion of 13.4 %, considerably lower than that for Pd/C. The average particle diameter was found to be 8.1 nm. Both average particle diameters were found to be in broad agreement with the particle size distribution histograms obtained for the two catalysts.

Table 2. Summary of CO adsorption isotherm results and calculations.

Catalyst	CO uptake ($moles/g_{cat}$)	Dispersion (%)	Average particle diameter (nm)
5% Pd/C	9.24 x 10^{-5}	54.0	2.0
1% Pd/Al_2O_3	6.30 x 10^{-6}	13.4	8.1

Figure 20 shows the CO temperature programmed desorption profile for 5% Pd/C and shows three features centred around 475, 640 and 850K. The lower CO bands were assigned to CO chemisorption on Pd crystallites, with the higher temperature CO band attributed to (partial) decomposition of carboxy species present on the carbon support material.[98]

The CO temperature programmed desorption profile for 1% Pd/Al_2O_3 is presented in Figure 21 and shows 2-shouldered features centred around *ca.* 550 and 650 K. The lower temperature CO band at 550 K is assigned to CO chemisorption on Pd crystallites and the higher temperature bands are attributed to (partial) decomposition of carboxy species present on the carbon support material.[98] The signal for CO_2 loosely follows that for CO, apart from a signal at *ca*. 450 K, which is attributed to oxidised species as a result of contaminant oxygen in the flow gas.

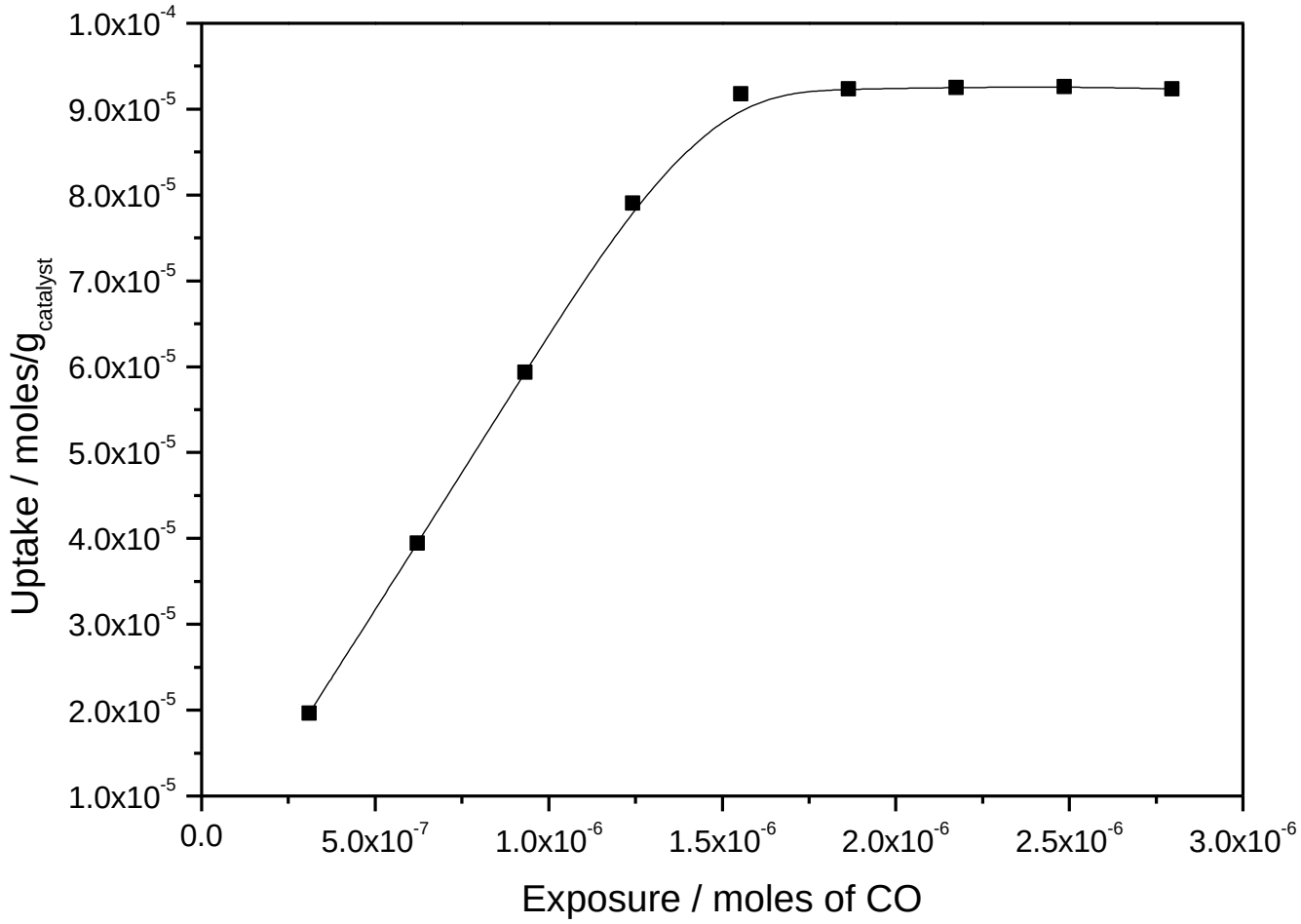

Figure 18. The CO adsorption isotherm for 5% Pd/C at 40^{o}C.

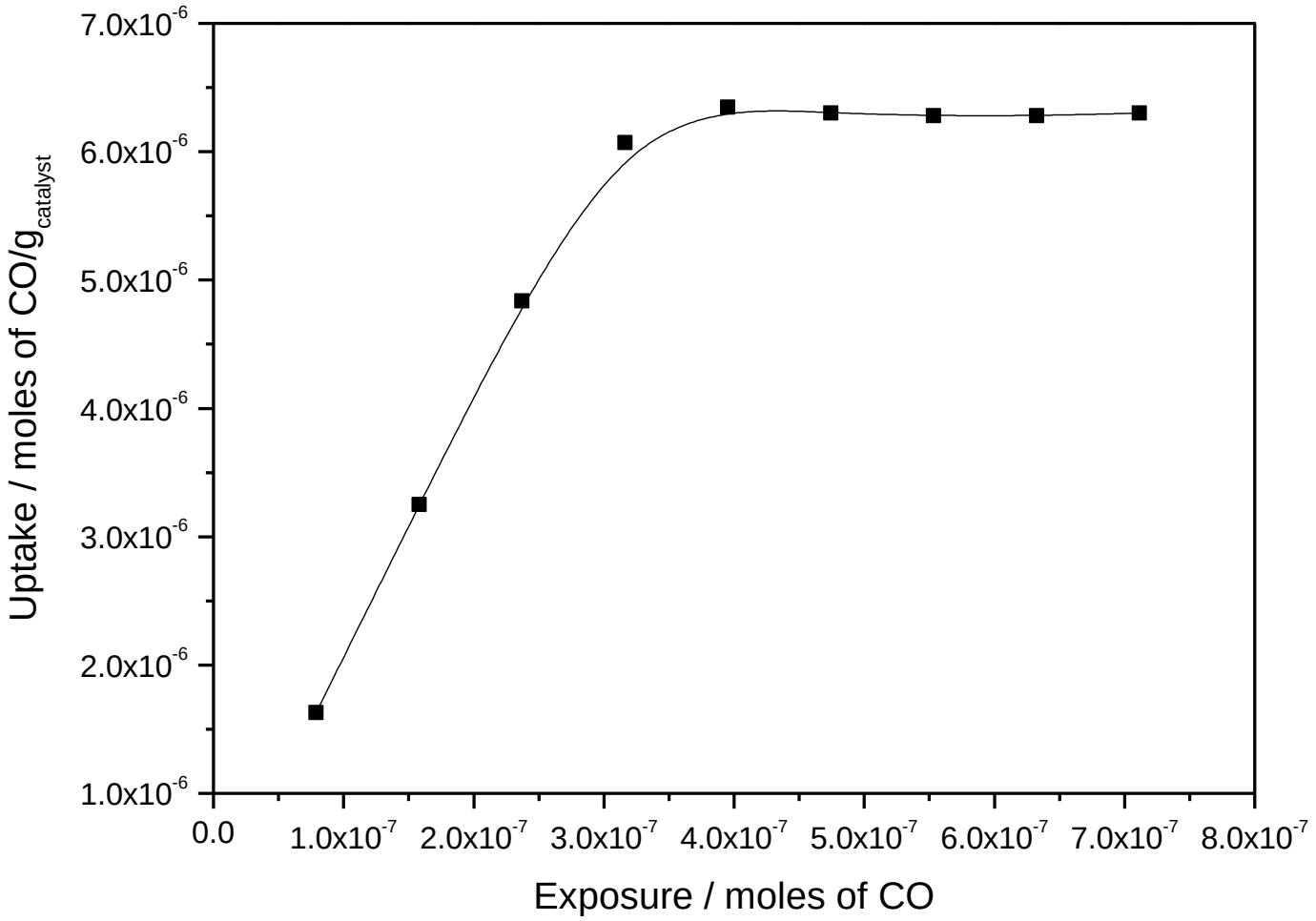

Figure 19. CO adsorption isotherm of 1% Pd/Al_2O_3 at 40^{o}C.

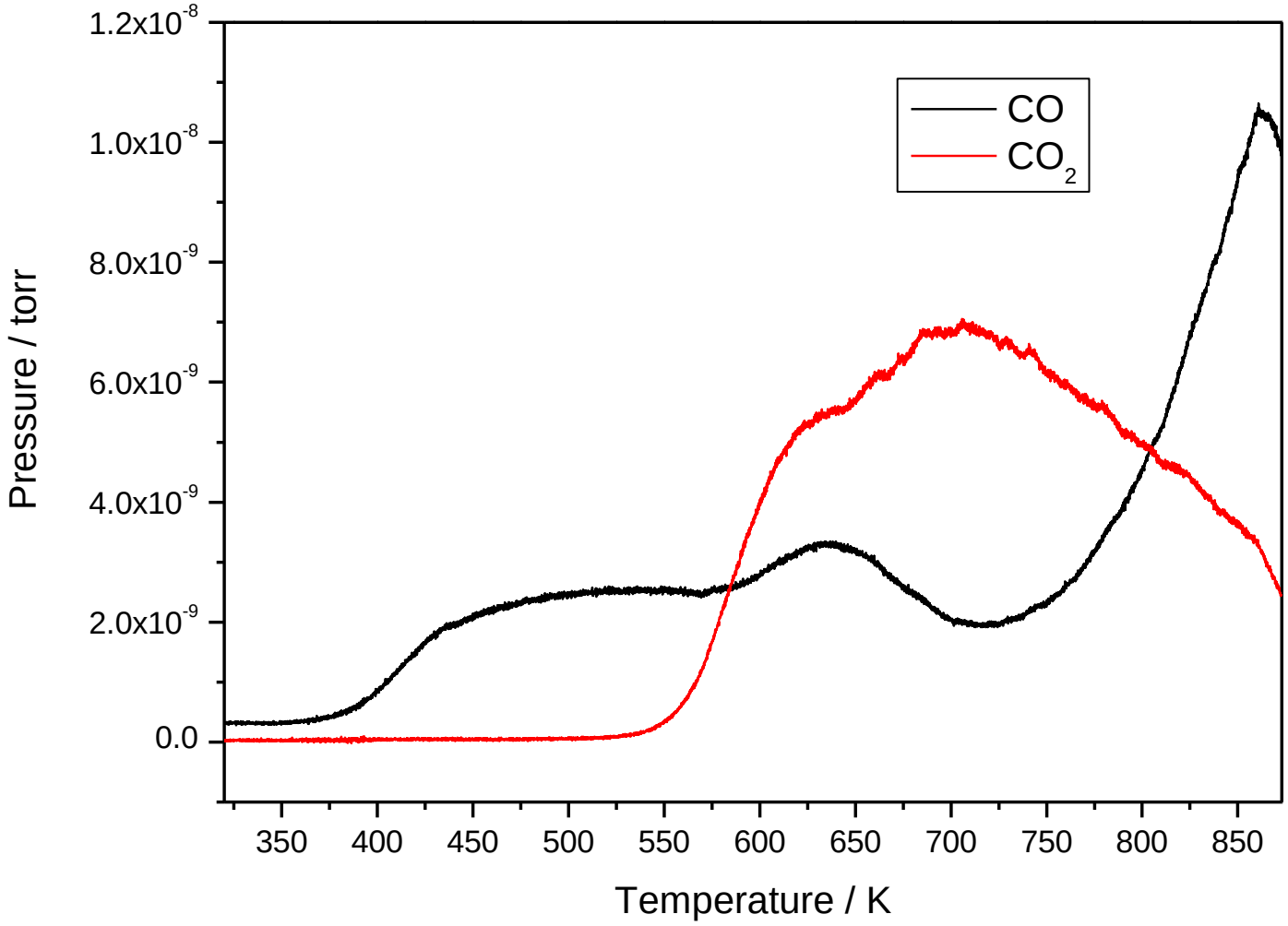

Figure 20. CO temperature programmed desorption for a saturation dose of CO on 5% Pd/C.

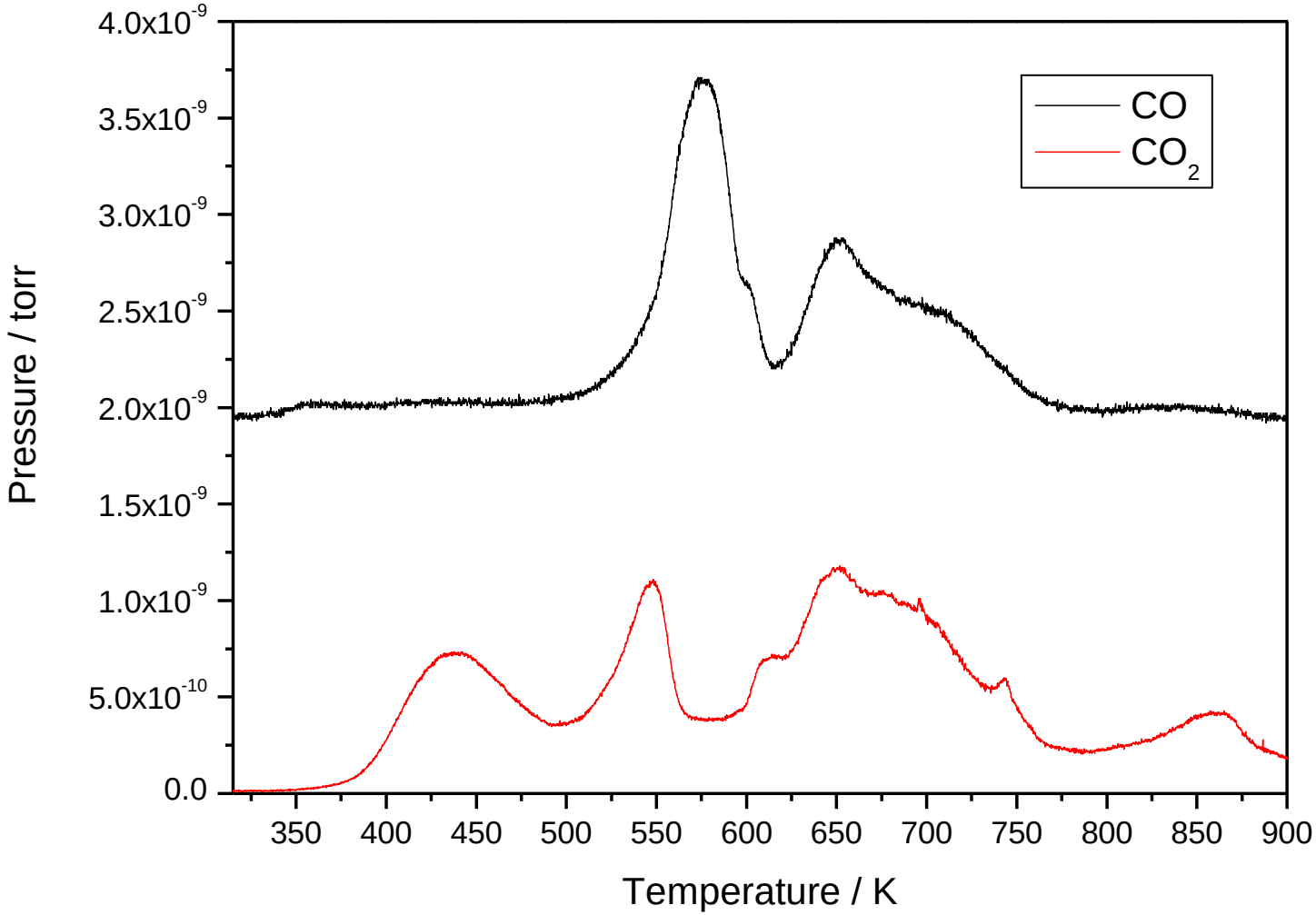

Figure 21. CO temperature programmed desorption for a saturation dose of CO on 1% Pd/Al_2O_3.

3.2 Benchmarking reactions

3.2.1 Hydrogenation of benzaldehyde (C_6H_5CO)

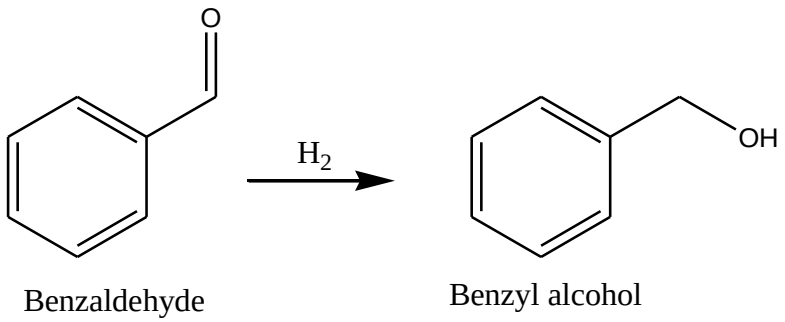

Scheme 7. Reaction scheme for the hydrogenation of benzaldehyde.

The hydrogenation of benzaldehyde (Scheme 7) was used as a benchmark reaction to ensure that the catalyst/reactor configuration was functioning correctly. Benzaldehyde is known to be susceptible to hydrogenation over a variety of catalysts and conditions.[99] The commercially available 5% Pd/C proved to be too severe to allow reasonable sampling since the reaction was found to reach completion in less than 20 minutes. Therefore, the 1% Pd/Al_2O_3 (which together with a lower metal content, was found to have a lower dispersion and larger average particle size), was chosen in the benchmark reaction.

The reaction profile in Figure 22 shows that benzaldehyde hydrogenation proceeded to completion in approximately 100 minutes. Benzyl alcohol ($C_6H_5CH_2OH$) was found to be the only product of the reaction. A reasonable mass balance plot was obtained that showed no inconsistencies. Repeat results at both atmospheric and elevated pressures gave similar results. Therefore, the consistent results ensure that this benchmark reaction showed that the reaction system operates well for hydrogenation reactions and that the catalysts used are suitable.

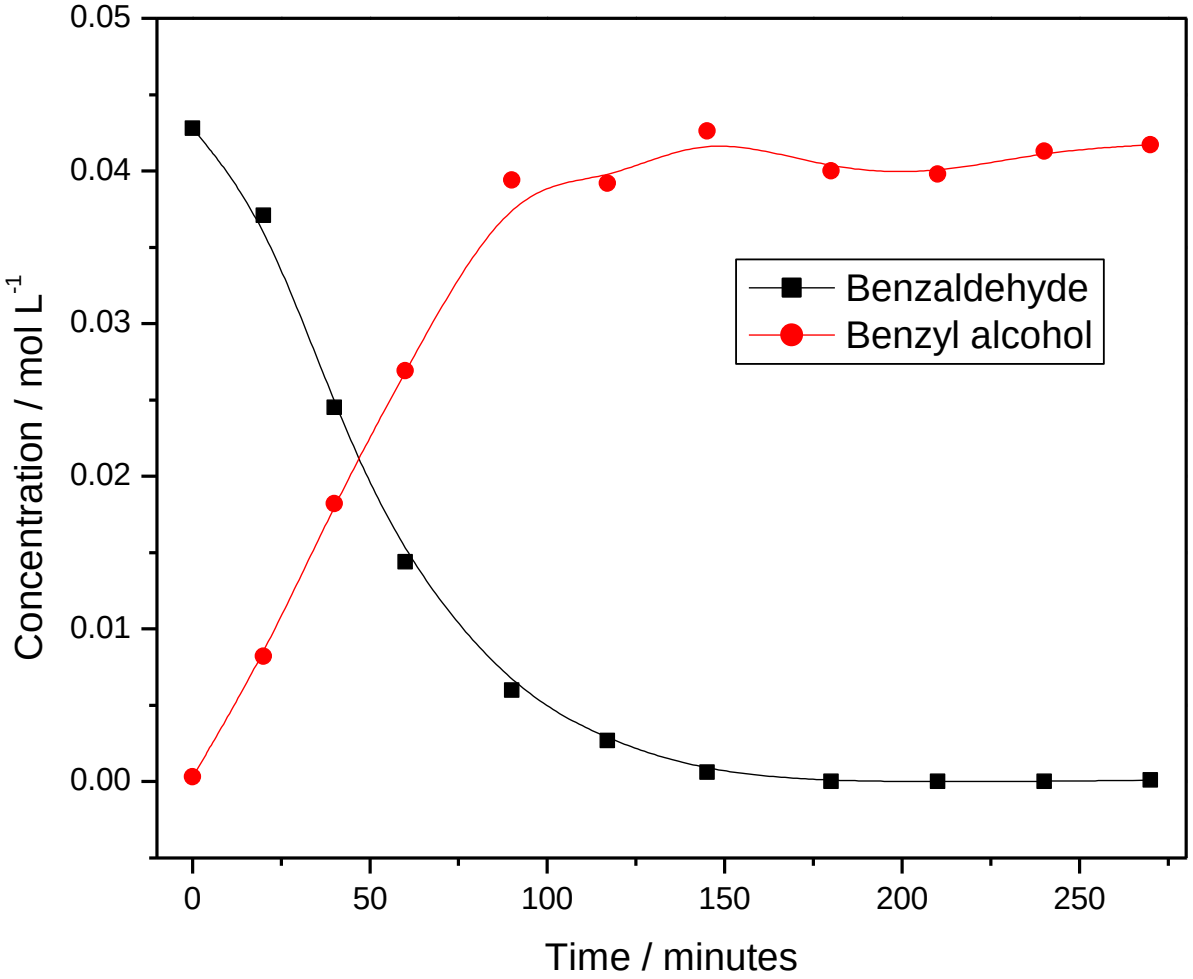

Figure 22. Reaction profile for the hydrogenation of benzaldehyde versus time on stream over 0.5 g 1% Pd/Al_2O_3, at 60 ^oC, 4.0 bar, *ca.* 0.0175 moles of benzaldehyde.

3.3 Issues relevant to the hydrogenation of benzonitrile (C_6H_5CN)

3.3.1 Benzonitrile hydrogenation

Benzonitrile hydrogenation was considered as the first model compound since it is the simplest of all aromatic nitriles. The molecule consists essentially of an aromatic ring and the nitrile functionality. Benzonitrile hydrogenation to benzylamine was originally expected to be a relatively simple reaction, with the addition of two molar equivalents of molecular hydrogen across the CN triple bond facilitating the transformation. However, the reaction proved rather more complex in terms of the progression of reaction and in terms of kinetics and rate law.

Figure 23 shows the concentration *vs.* time plot for the liquid phase hydrogenation of benzonitrile over 5% Pd/C at 60 ^{o}C. Benzonitrile was consumed quickly and returned a full mass balance after the completion of the reaction, which occurred at around 75 minutes (as was evidenced by hydrogen uptake ceasing). The reaction profile appeared to show a consecutive reaction[100] whereby significant amounts of benzylamine ($C_6H_5CH_2NH_2$) were formed (31% selectivity at 50% conversion), before surprisingly being consumed by the reaction to form the undesired toluene ($C_6H_5CH_3$) with 100% selectivity at 100% conversion of benzonitrile, as in Scheme 8.

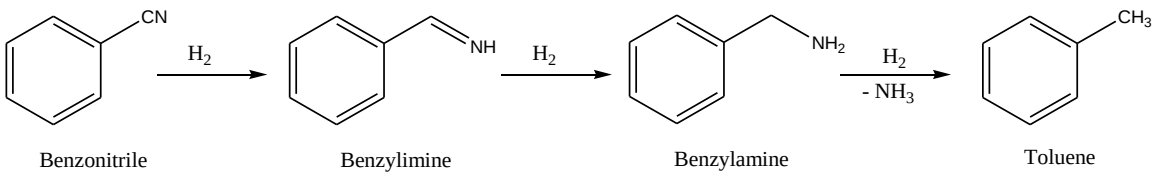

Scheme 8. Proposed reaction scheme for the hydrogenation of benzonitrile to benzylamine and subsequent hydrogenolysis to toluene over Pd/C.

This hydrogenolytic reaction has been reported previously,[44] but does not feature prominently in the heterogeneous catalysis literature, although it is well established in the organic literature,[93] Recently, researchers at Delft applied spectroscopic techniques to propose a reaction cycle that suggests toluene can be

formed by two distinct processes over a Pd/Al_2O_3 catalyst: (i) hydrogenolysis of benzylamine, or (ii) direct hydrogenolysis of benzonitrile.[103]

Repeat results at lower temperature and atmospheric pressure using the ambient pressure reactor also showed significant amounts of toluene in the product distribution, by the route suggested in Scheme 8. No secondary or tertiary amines were formed, in contrast to the generally accepted product distribution of hydrogenation of nitriles over Pd.[40,96,97] Indeed, the complete mass balance provides evidence that hydrogenation of benzonitrile was not complicated by a contribution from coupling reactions. No imine intermediate was observed since it may be considered as a high-energy intermediate that only exists on the catalyst surface[103]. As such it could not be detected by the down-stream chromatographic methods used here.

The initial mass imbalance observed (from around 0 to 60 minutes) was in large excess to the number of available Pd sites, as determined by CO adsorption isotherm (missing mass : Pd(s) = 88 : 1), and so must have been retained by the carbon support. This “spill-over” effect is well established and the mass balance was found to recover following the formation and subsequent desorption of toluene, implying that adsorption of the intermediate benzylamine (and possibly the surface imine) was the cause of the loss of mass.

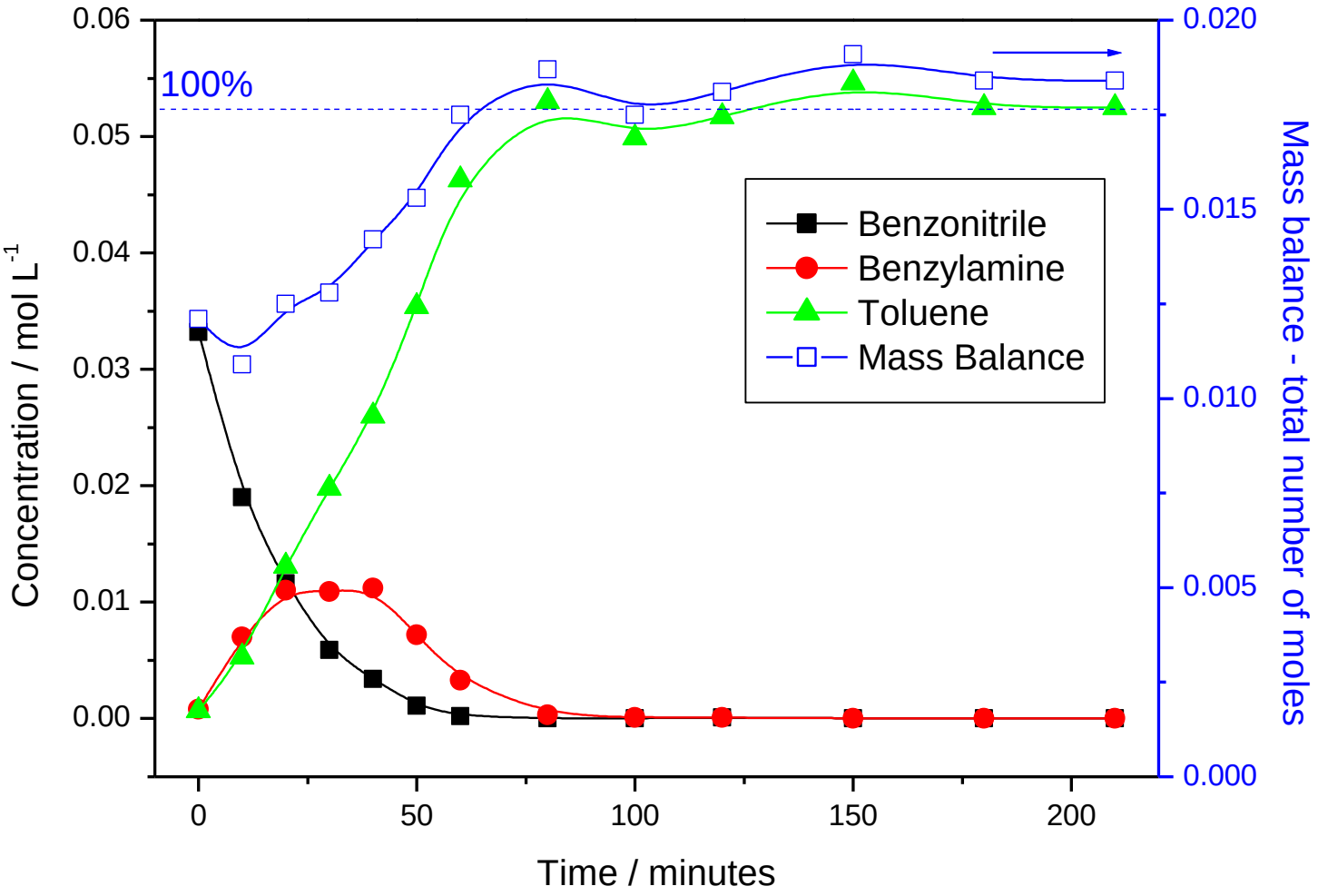

Figure 23. Reaction profile and mass balance for the hydrogenation of benzonitrile over 0.5 g 5% Pd/C, at 60 ^{o}C, 4.0 bar, *ca.* 0.0175 moles of benzonitrile. The dashed line represents the incident concentration of benzonitrile.

3.3.1.1 Rate law and kinetics of benzonitrile hydrogenation

Benzonitrile concentration was varied from 0.012 to 0.096 mol L^{-1} to show the effect that concentration of starting material has upon the hydrogenation reaction. Figure 24 shows a van't Hoff plot for the reaction parameters that were varied in order to determine reaction order and a rate law for benzonitrile hydrogenation. In the case of benzonitrile concentration, it is evident that the initial rate of reaction remains effectively constant upon variation in concentration. Therefore, it was concluded that the reaction had an order of zero with respect to nitrile concentration. If one considers the relative adsorption coefficients (K) of reactants, then a zero order dependence upon benzonitrile concentration suggests that $K_{Benzonitrile} >> K_{Hydrogen}$.

On varying the partial pressure of hydrogen form 2.0 to 5.0 bar, an increase in initial reaction rate is evident. The order of reaction from the van't Hoff plot (Figure 24) indicated a non-integer order of *ca.* 0.3. This is in conflict with previous studies where results indicated first order dependence on the initial rate with respect to hydrogen partial pressure[40].

Finally, catalyst (5% Pd/C) mass was varied from 0.15 to 1.02 g in an attempt to investigate its effect upon the hydrogenation rate of benzonitrile. The initial rate was found to increase linearly with increasing catalyst mass. This result indicated first order dependence of the initial rate with respect to catalyst mass and indeed, the van't Hoff plot (Figure 24) confirmed first order. However, since it can be assumed that the amount of catalyst remains constant throughout the duration of the reaction, the first order dependence upon catalyst mass may be neglected from the rate law and that the reaction is governed by a pseudo order regime instead.

Therefore, in this case, the rate law may be defined as:

$$Rate = \frac{-d[BN]}{dt} = k[BN]^{0}[H_2]^{0.3}[Pd_{(s)}]^{1} \qquad (8)$$

and simplified to give:

$$Rate = \frac{-d[BN]}{dt} = k[H_2]^{0.3} \quad (9)$$

The fact that the order of reaction appears to be non-integer, implies some inherent complexity within the reaction mechanism.[106]

A first order plot was constructed (Figure 25) and indicates that benzonitrile hydrogenation has an overall reaction order of 1. The order of 0.3 obtained from the van't Hoff plot is therefore in conflict with the overall situation. A possible explanation for this complexity is thought to be due to how the analysis was performed and what components in the reaction were measured. Starting material (benzonitrile), intermediate (benzylamine) and final product (toluene) could all be observed in the liquid phase and as such, could be calibrated and measured. However, the reaction profile does not include any measurement of the imine intermediate (benzylimine, $C_6H_5CH{=}NH$), since it is neither observed in the liquid phase, nor can it be calibrated. It is assumed that benzylimine exists only as a highly reactive, surface bound intermediate. It is believed that the absence of this important elementary reaction in the reaction profile leads to the non-integer order of reaction with respect to hydrogen pressure.

The non-conformity of the experimental rate law indicates a degree of complexity within the reaction system. Rather than a simple A → B transformation, here we are only measuring the conversion of A (*i.e.* benzonitrile). The fact that the reaction is found not to be first order with respect to hydrogen pressure, indicates a possible limitation of hydrogen supply. Another possible source of the rate law complexity may be explained if one considers that an order of 0.3 could be considered as similar to 0.5. A reaction order of 0.5 for hydrogen may be consistent with a Langmuir-Hinshelwood mechanism for hydrogen dissociation, similar to that suggested by Joly-Vuillemin *et al.* for Raney Nickel catalysts.[106] Further work is required to tie down the exact nature of the inconsistency in the rate law. Indeed, modelling of this reaction (and other systems) is currently underway at the industrial centre.

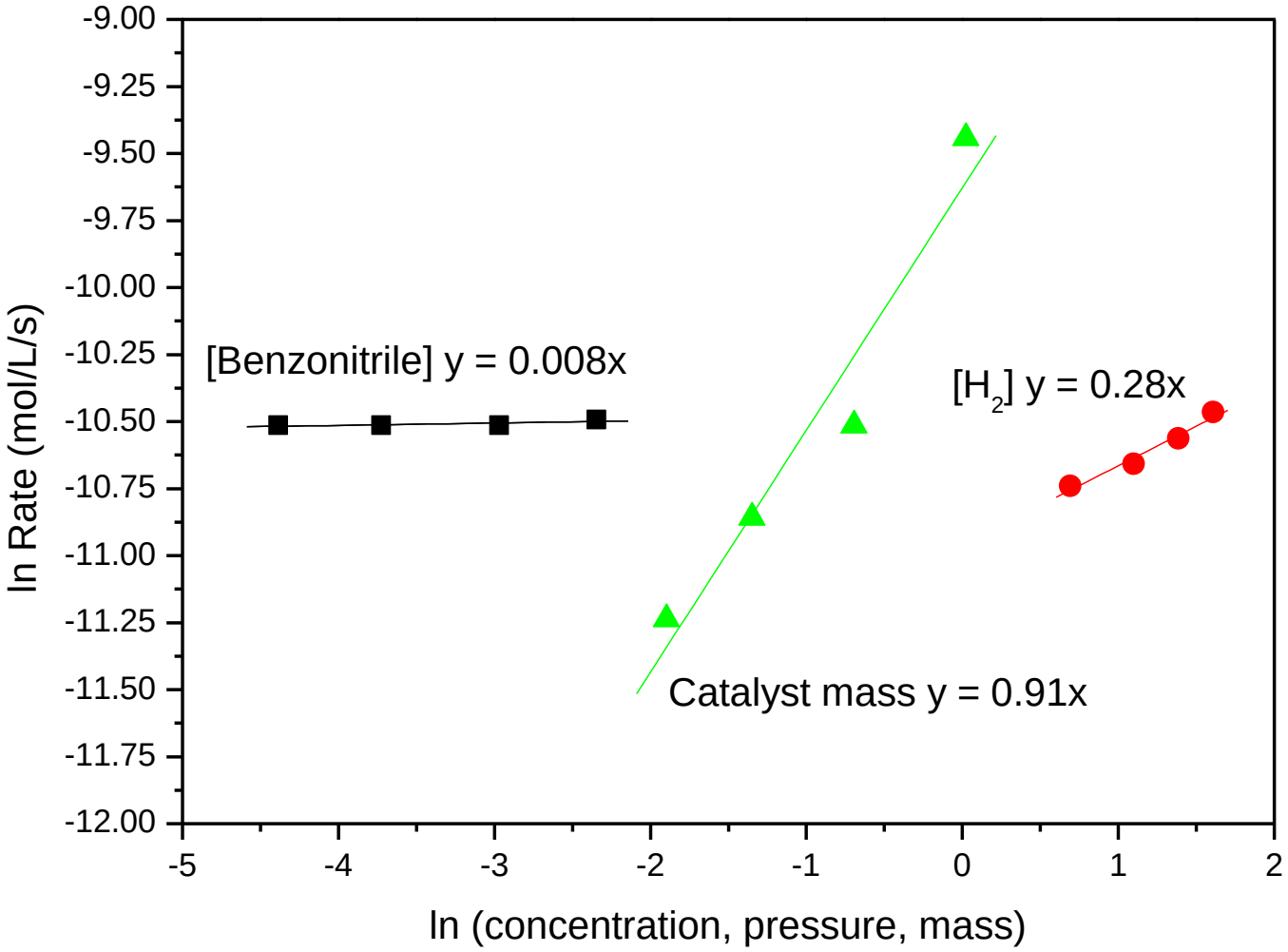

Figure 24. The van't Hoff plots constructed for the reaction variables of benzonitrile hydrogenation, *i.e.* benzonitrile concentration, hydrogen pressure and catalyst mass.

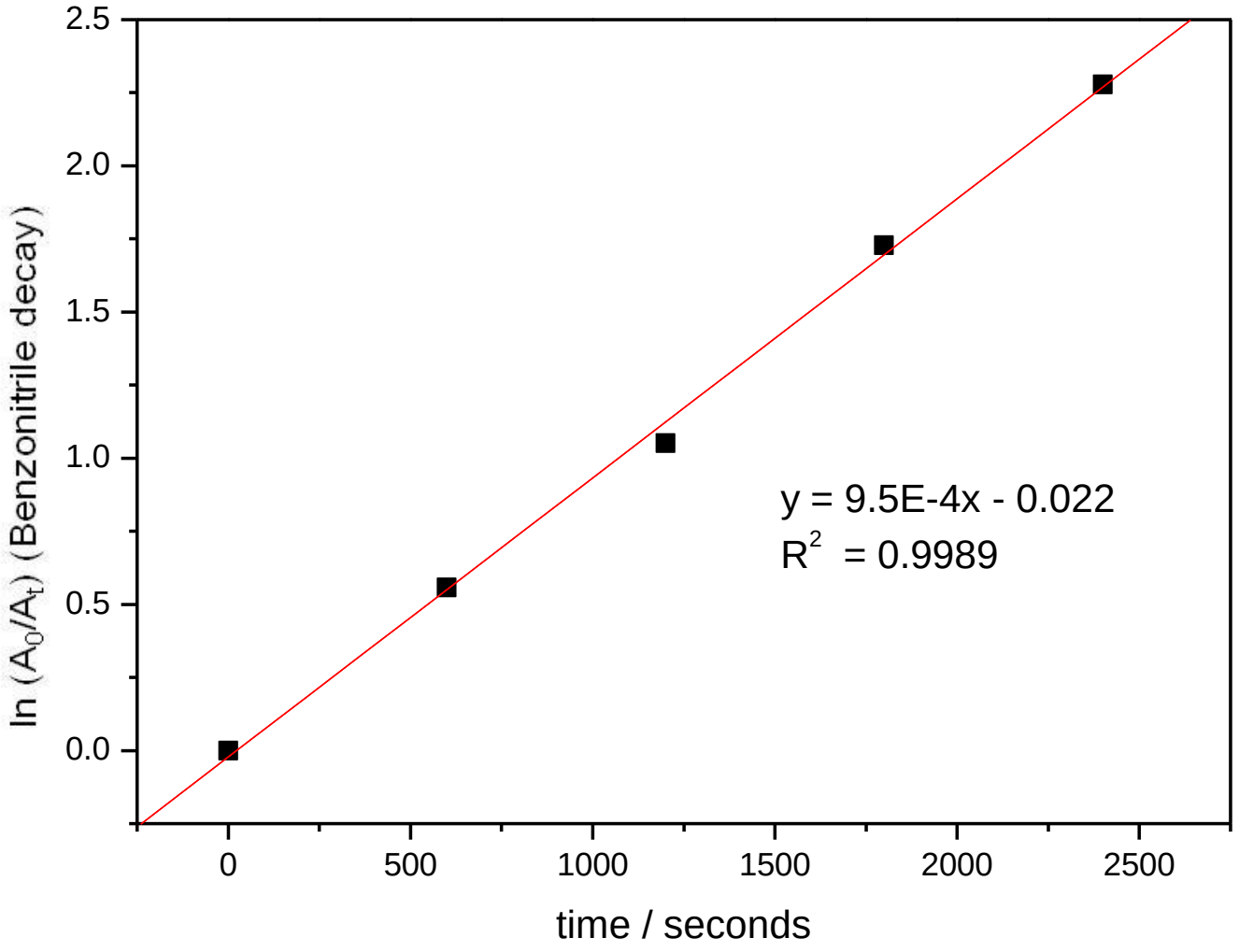

Figure 25. A first order data fit (ln (A_o/A_t) vs. time) for benzonitrile hydrogenation over Pd/C at 60 ^{o}C.

Reaction temperature in the hydrogenation of benzonitrile was varied from 30-60 ^{o}C in the Buchi batch autoclave at 4 bar and was found to have a great effect upon the reaction. For each reaction, a plot of ln ($^{[Ao]}/_{[A]}$) *vs.* time was constructed and used to determine the rate coefficients (k), which are presented in Table 3.

Table 3. Rate data at various temperatures for benzonitrile hydrogenation. This data was used to construct an Arrhenius plot (Figure 26).

Temp. (^{o}C)	Temp. (K)	1/T (x 10^{-3} K^{-1})	k (x10^{-4} s^{-1})	ln k
30	303	3.30	2.43	-8.322
40	313	3.19	4.11	-7.797
50	323	3.10	4.90	-7.621
60	333	3.00	6.76	-7.299

An Arrhenius plot for benzonitrile hydrogenation was, therefore, constructed (Figure 26), from which a slope of -3399.11 K^{-1} was obtained and used to calculate an activation energy by manipulation of the Arrhenius equation. The activation energy was calculated as:

$$-{Ea}/{R} = -3388.11K^{-1}$$

$$Ea = 3388.11K^{-1} \times 8.3145JK^{-1}mol^{-1}$$

$$Ea = 28170.4Jmol^{-1}$$

$$\underline{Ea = 28.17kJmol^{-1}}$$

An activation energy of 28.17 kJ mol^{-1} was considered a surprisingly low figure for a well stirred batch hydrogenation reaction. It is understood that an activation energy below *ca.* 20 kJ mol^{-1} represents a reaction under diffusion control.[4] Therefore, an activation energy of 28.17 kJ mol^{-1} suggests that the hydrogenation of benzonitrile operates under kinetic control, *i.e.* the rate determining step will include reagent ability to adsorb to the catalyst surface; how easy it is to establish the maximum (or optimum) surface coverage of both nitrile and hydrogen or how efficiently and quickly products are desorbed from the surface. Mass transport effects *i.e.* the transport of reactants to and from the catalyst surface, can be concluded as being negligible under such a regime.

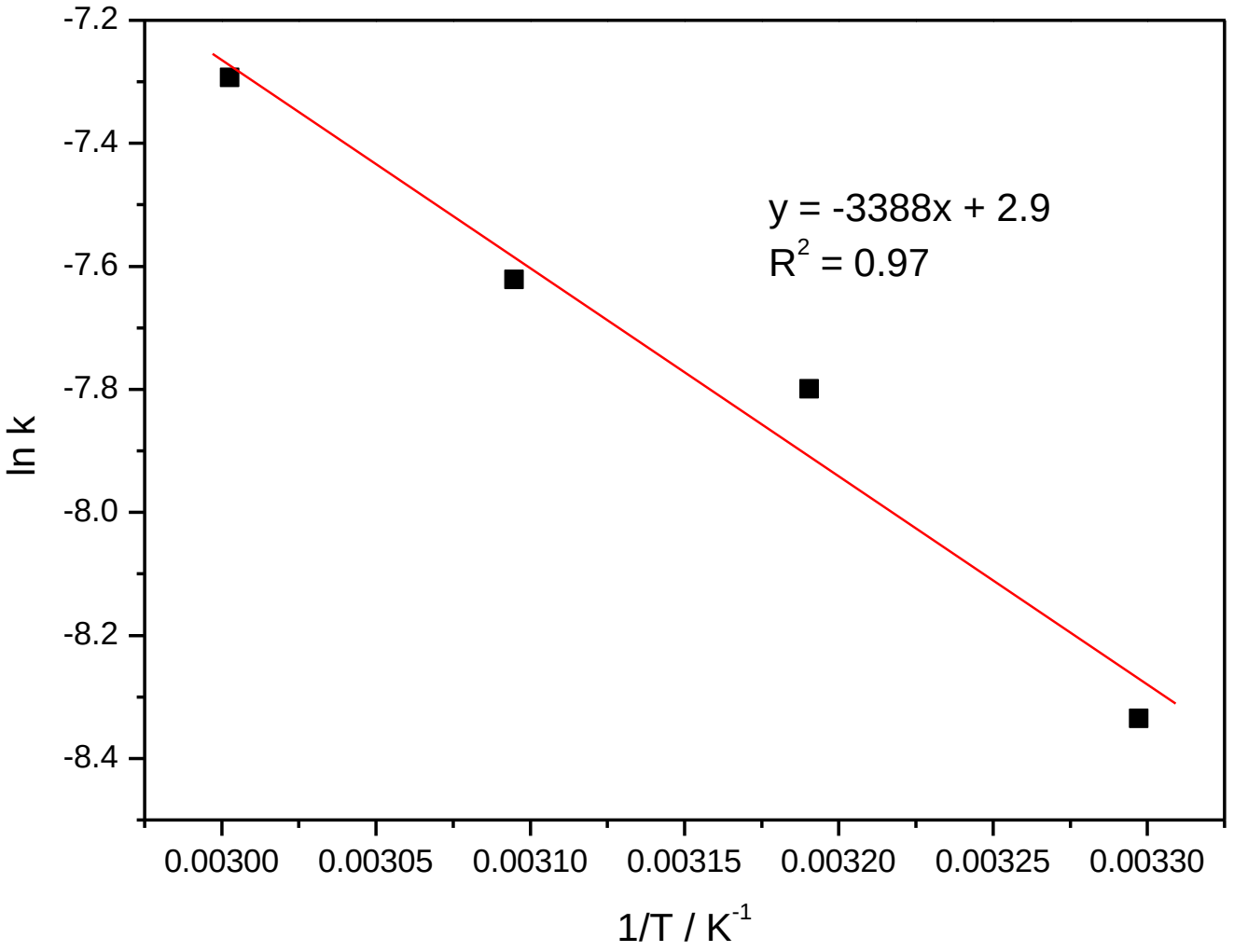

Figure 26. Arrhenius plot for the hydrogenation of benzonitrile over a temperature range of 30-60 ^{o}C.

3.3.2 Hydrogenolysis of benzylamine ($C_6H_5CH_2NH_2$)

To fully understand the nature of the consecutive reaction, the hydrogenolysis of benzylamine – the intermediate in the hydrogenation of benzonitrile – was studied in detail. Benzylamine was converted with 100% selectivity to toluene (as in Scheme 9, below), by the same hydrogenolysis reaction as was observed in benzonitrile hydrogenation. However, in the absence of benzonitrile, benzylamine decay, toluene production appeared, on inspection of the reaction profile (Figure 27), to follow zero order kinetics, given the observed linear increase in toluene concentration.

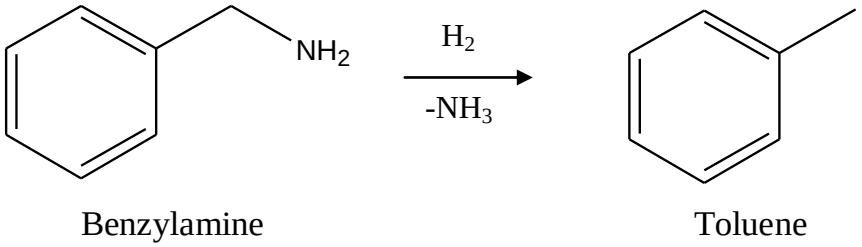

Benzylamine Toluene

Scheme 9. The hydrogenolysis of benzylamine to toluene over Pd/C.

The initial mass imbalance observed was in agreement with benzonitrile hydrogenation, but perhaps indicates that the amine is more strongly bound to the catalyst support rather than benzonitrile or an undetectable intermediate.

This hydrogenolytic reaction is not discussed in any great detail within the heterogeneous catalysis literature,[41,95] but is widely known in the synthetic organic literature[102] where it is used as a method of removing the benzyl protecting group from amine functionality (and generally a benzyl group attached to any heteroatom, but particularly oxygenates). A postulated reaction mechanism for how such a reaction occurs has been developed from a model proposed by Kocienski and is shown in Scheme 10.[107]

For benzylamine in the generic mechanism, -XR is representative of an amine group ($-NH_2$) and –R' donates a hydrogen atom. In the mechanism, it is observed that for cleavage of the C-N bond to occur, the amine must orientate itself and bind

with a particular dual-adsorption mode. In this way, it is suggested that adsorption of both the amine group and the aromatic ring are necessary to facilitate hydrogenolysis. It is believed that this particular geometry and the distance between the functional groups defines hydrogenolysis specificity (further discussion of such an issue will take place later for other model systems in Section 3.5). Once bound, a weakening of the C-N bond results in the loss of ammonia (in the particular case of benzylamine). However, strictly speaking and from an organic synthesis perspective, the benzyl group (or toluene) should be considered as the leaving group, since the R-group in the generic scheme may represent a larger extended network in itself.

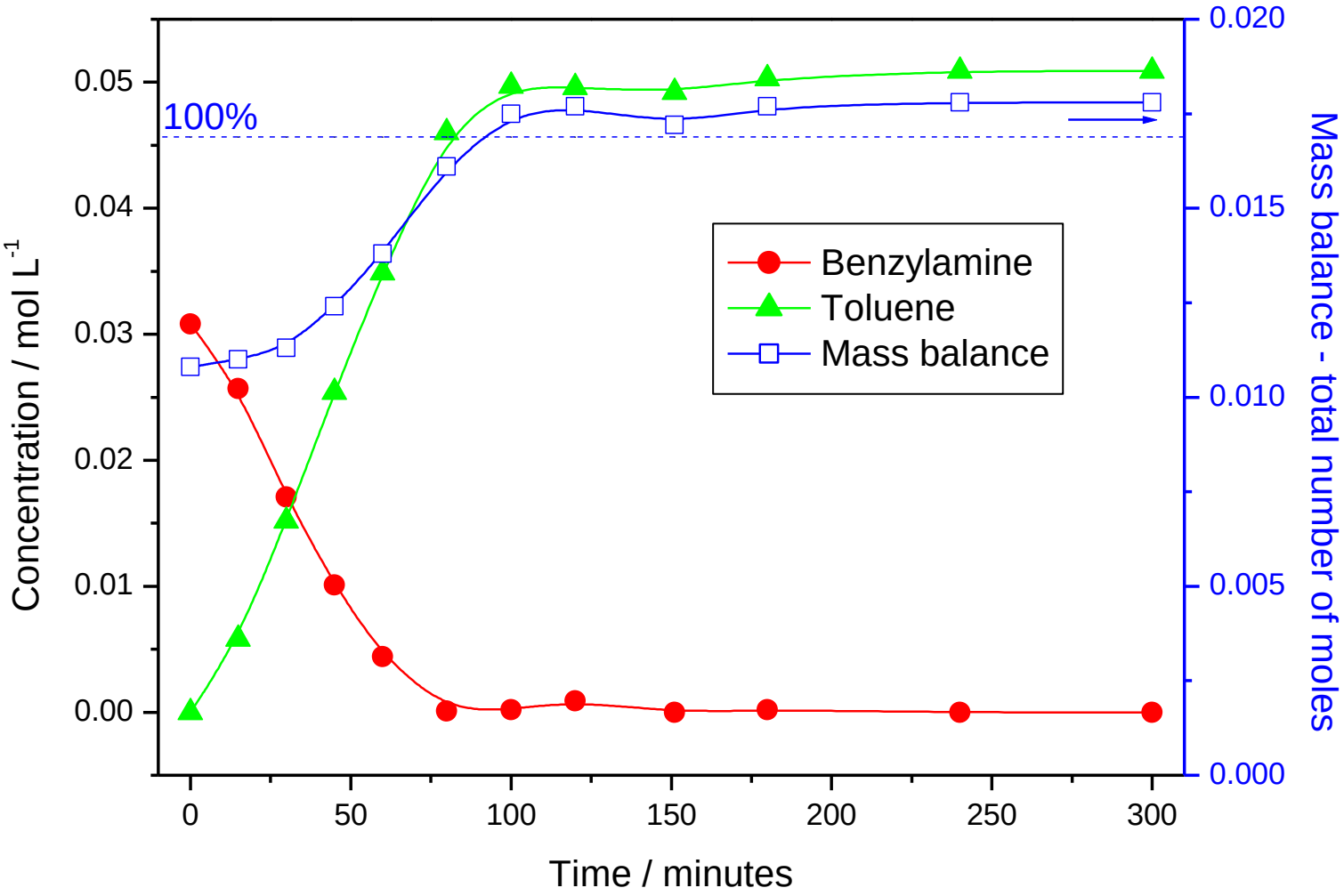

Figure 27. Reaction profile and mass balance for the hydrogenolysis of benzylamine over 0.5 g 5% Pd/C, at 333 K, 4.0 bar, *ca.* 0.0175 moles of benzylamine. The dashed line represents the incident concentration of benzylamine.

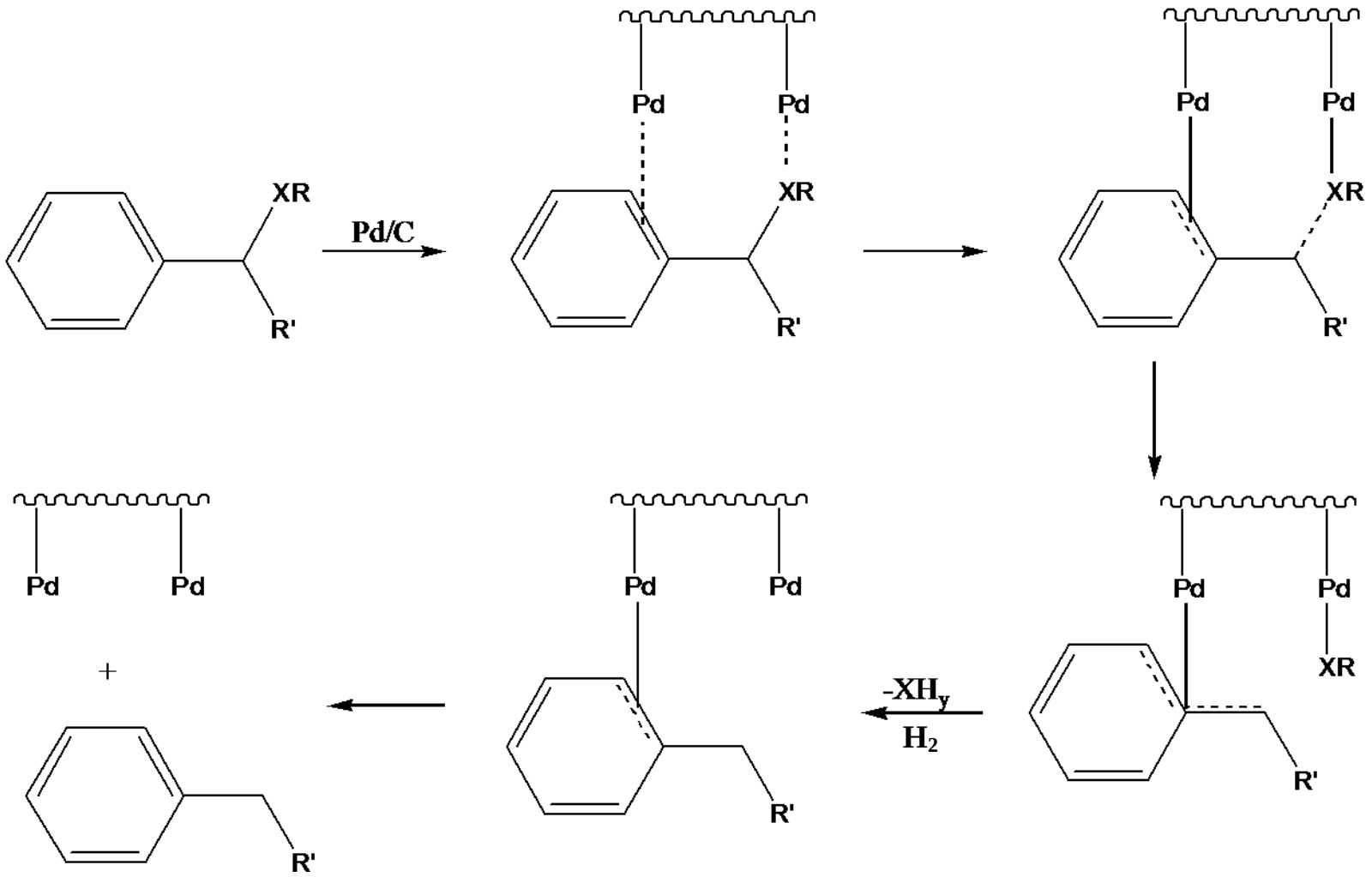

Scheme 10. Proposed reaction mechanism for hydrogenolysis resulting in the removal of a benzyl group, as developed by a model proposed by Kocienski *et al.* For the particular case of benzylamine, XR represents an amine group and R' a hydrogen atom.[107]

3.3.2.1 Rate law and kinetics of benzylamine hydrogenolysis

Van't Hoff plots were obtained to determine the reaction order with respect to benzylamine concentration, hydrogen pressure and catalyst mass, and are shown in Figure 28. Once again, the mass of catalyst can be assumed as being pseudo first order for the same reasons as outlined in Section 3.3.1.1. As with benzonitrile hydrogenation, the concentration of starting material was zero order, but in contrast to the nitrile reaction, hydrogen pressure was also found to be zero order. This data allows one to describe the hydrogenolysis of benzylamine by the rate law below:

$$Rate = \frac{-d[BA]}{dt} = k[BA]^0[H_2]^0[Pd_{(s)}]^1 \quad (10)$$

Therefore,

$$Rate = \frac{-d[BA]}{dt} = k \quad (11)$$

Together with the increased strength of adsorption of the amine over the nitrile, the zero order nature of amine reduction appears to mask the true first order nature of the first reaction step. The overall order of the hydrogenolysis reaction was confirmed by fitting the data in a zero order plot, as shown in (Figure 29).

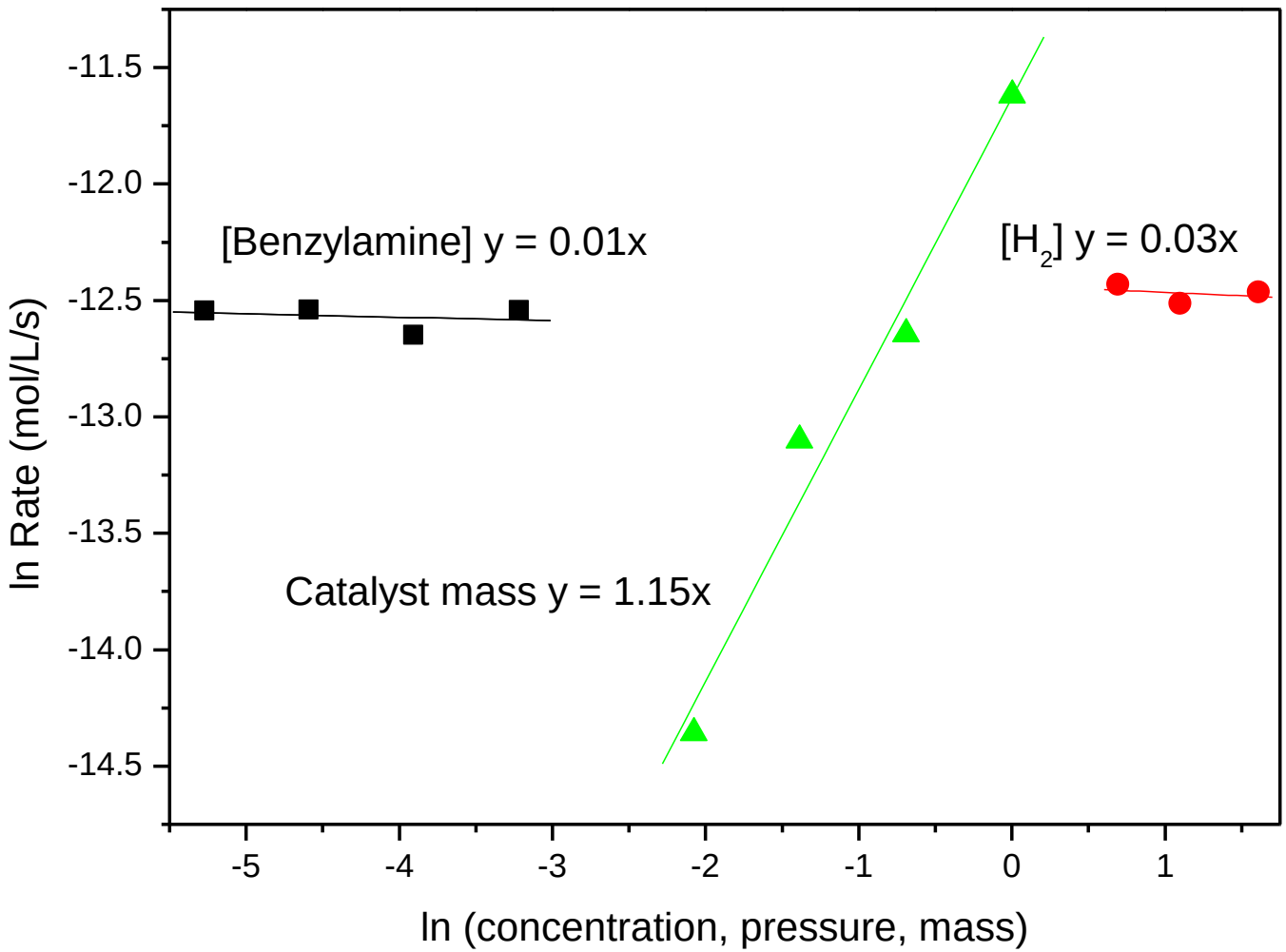

Figure 28. The van't Hoff plots constructed for the reaction variables in the hydrogenolysis of benzylamine, including benzylamine concentration, hydrogen pressure and catalyst (Pd/C) mass.

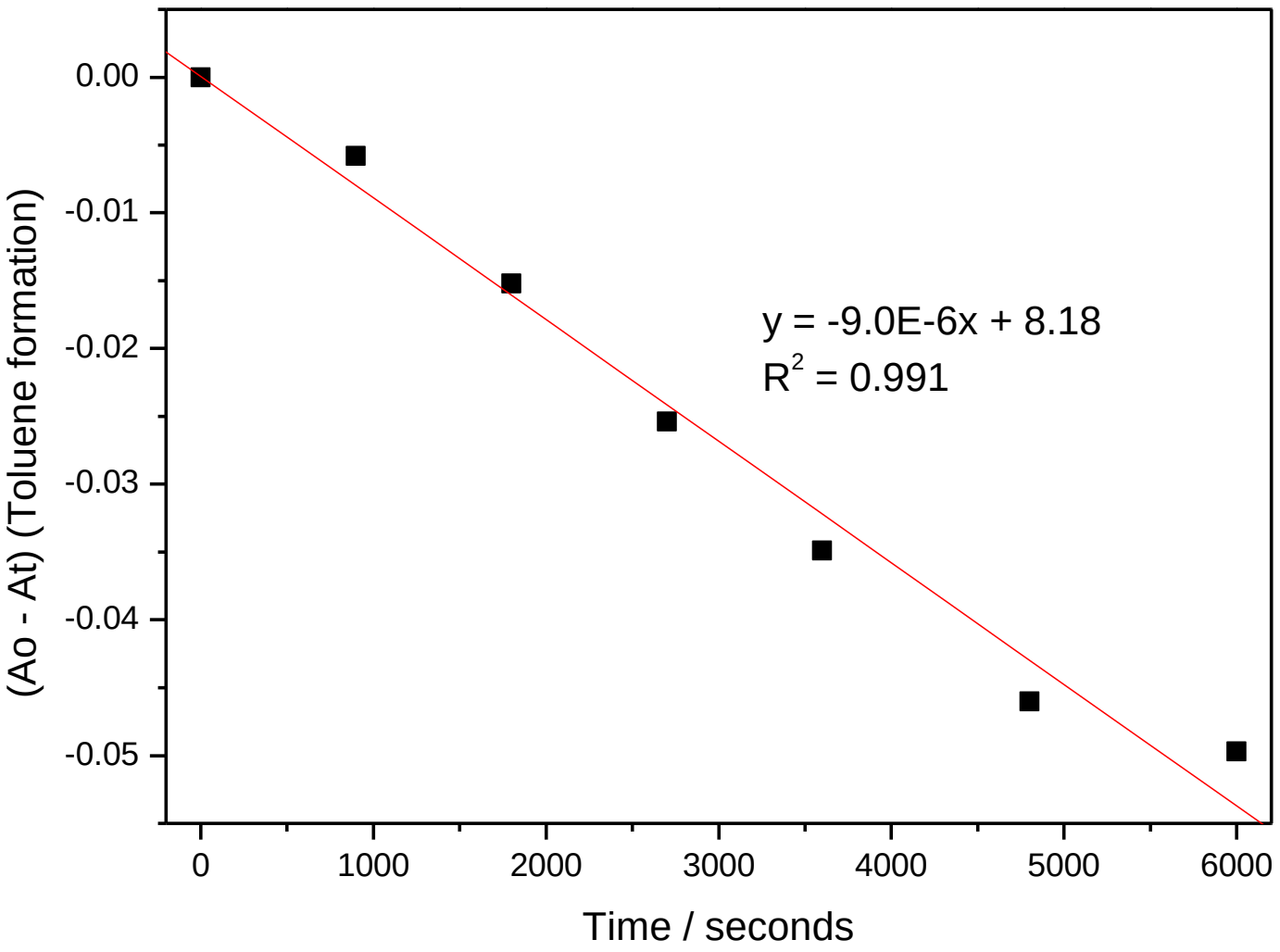

Figure 29. A zero order plot ((A_o-A_t) vs. time) for benzylamine hydrogenolysis over Pd/C at 60 ^{o}C.

Reaction temperature in the hydrogenolysis of benzylamine was varied from 303-333K in the Buchi batch autoclave at 4 bar and was found to have a great effect upon the reaction. For each reaction, a plot of ($A_0 - A_t$) *vs.* time was constructed and used to determine the rate coefficients (k), which are presented Table 4.

Table 4. Rate coefficients at various temperatures for benzylamine hydrogenolysis. These data were used to construct the Arrhenius plot in Figure 30.

Temp. (^oC)	Temp. (K)	1/T (x 10^{-3} K^{-1})	k (x10^{-4} mol L^{-1} s^{-1})	ln k
30	303	3.30	6.8	-7.29
40	313	3.19	4.9	-7.62
50	323	3.10	4.1	-7.80
60	333	3.00	2.4	-8.33

The Arrhenius plot (Figure 30) obtained for benzylamine hydrogenolysis gave a slope of -9633 K^{-1} and was used to calculate an activation energy by manipulation of the Arrhenius equation. The activation energy was calculated as:

$$-Ea/R = -9633K^{-1}$$
$$Ea = 9633K^{-1} \times 8.3145JK^{-1}mol^{-1}$$
$$Ea = 80093Jmol^{-1}$$
$$\underline{Ea = 80.09kJmol^{-1}}$$

The activation energy of 80.09 kJ mol^{-1} for benzylamine hydrogenolysis was much larger activation than the activation energy of 28.17 kJ mol^{-1} obtained for benzonitrile hydrogenation. As well as confirming the kinetic regime of the reaction[4], the higher figure confirms that the mass imbalance observed in the initial stages of both reactions was as a result of the higher strength of adsorption of the amine as compared to the nitrile.

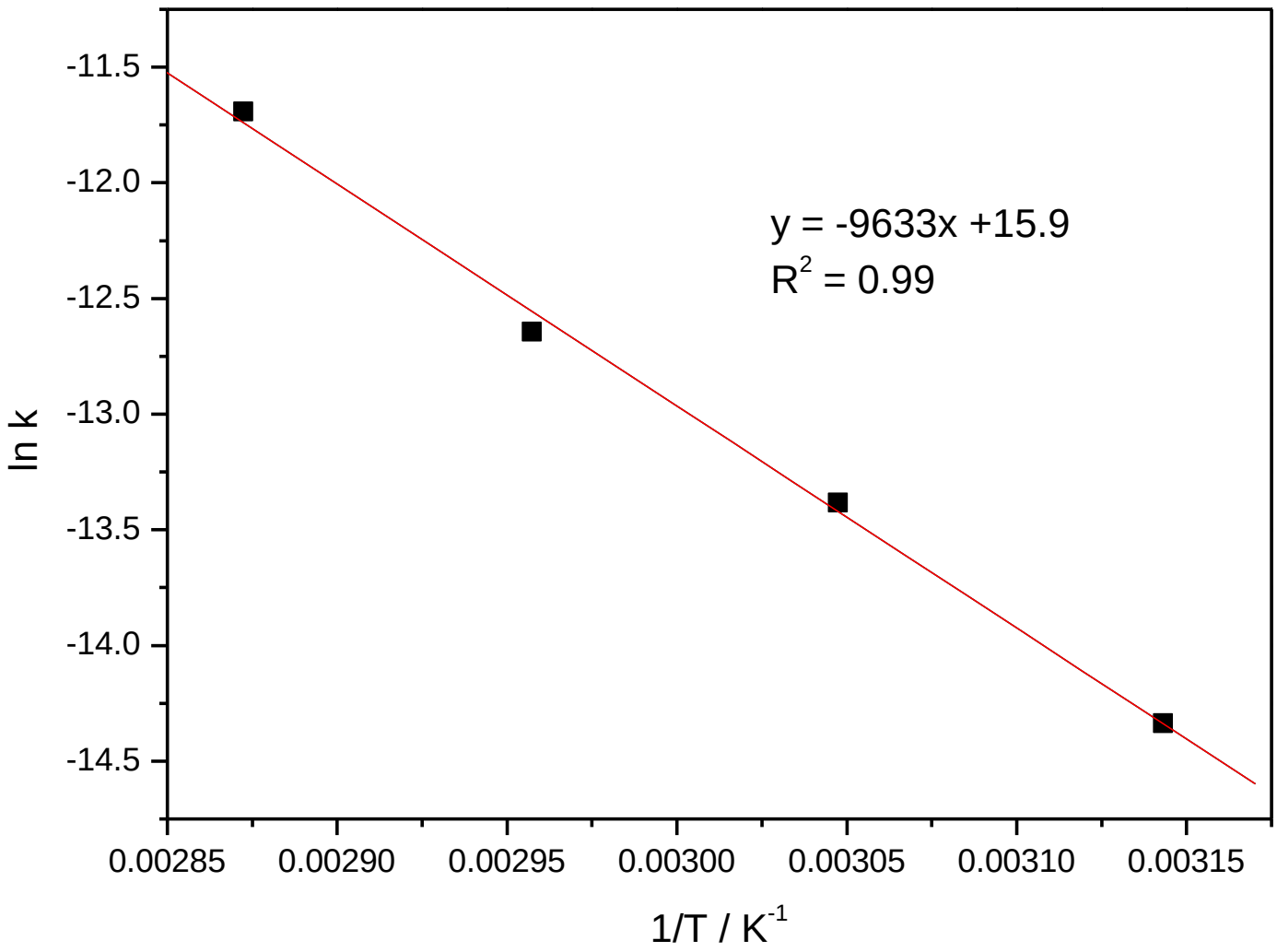

Figure 30. Arrhenius plot for the hydrogenolysis of benzylamine over a temperature range of 30-60 ^{o}C.

3.3.3 Mechanistic studies

In tandem with the model studies, experiments were carried out to try and obtain a more complete understanding of the reaction mechanism, particularly that of hydrogenolysis. Historically, the mechanism of hydrogenolysis within the context of aromatic nitrile hydrogenations has been overlooked in the literature, and in the particular case of benzylamine hydrogenolysis, no experimental data has been published to show the presence of ammonia (see Scheme 8).

As such, some gas phase reactions were carried out and analysed by FTIR spectroscopy. A known amount of benzonitrile was added to a gas cell with KBr windows containing an appropriate mass of reduced catalyst and the reaction followed over time. Initial studies using Pd/C were found to be much too fast to obtain any useful spectra, so the synthesised 1% Pd/Al_2O_3 (as described in Section 2.3.1, and diluted 1:100 in alumina) was used. This less active catalyst ensured reasonable sampling time. Assignment tables for reactants and products are included in Appendix 1.

Figure 31 shows the decay of the diagnostic CN stretch for benzonitrile (2238 cm^{-1}) *vs.* reaction time. The loss of such a feature suggests benzonitrile conversion to be relatively fast and complete. Coupled with the loss of nitrile functionality, a growth of the CH bend (aromatic) of toluene (729 cm^{-1}) is observed over a comparable sampling time (Figure 32). No nitrile or amine functionality was observed at the end of reaction.

Figure 33 shows the final FTIR spectrum recorded for the reaction and indicated full conversion of the nitrile moiety since no CN stretch is visible at 2238 cm^{-1}. The formation of toluene is confirmed by the presence of the diagnostic aromatic CH bend at 729 cm^{-1} and for the first time by direct methods, ammonia is confirmed by its three characteristic bands at 3444, 1631 and 950 cm^{-1} [108]. This is interpreted as confirming the existence of the hydrogenolysis reaction. To the best knowledge of the author, this is the first time that the production of ammonia has been unambiguously established for this reaction.

Figure 34 shows the reaction profile obtained for gas phase benzonitrile hydrogenation. Unfortunately, due to the overlap of diagnostic bands for benzylamine with toluene and ammonia (*e.g.* the aromatic and aliphatic C-H stretch region of toluene and benzylamine were observed at similar energies, and no N-H stretch was observed in the gas phase in reference spectra for benzylamine), no quantitative or qualitative data could be obtained for the intermediate. Similarly, ammonia was not quantified.

In addition, during the optimisation of reaction conditions, it was found that at temperatures above *ca.* 90 ^{o}C, a breakdown of benzonitrile was observed. Therefore, reactions were limited to 80 ^{o}C, but at this lower temperature, it proved difficult to ensure all benzonitrile was present in the gas phase. Figure 34 shows that over the first 5 minutes of reaction, benzonitrile concentration increased. This anomaly was attributed to liquid benzonitrile entering the gas phase over time. However, a more useful benzonitrile decay curve was obtained when one considered the initial, calculated concentration of benzonitrile (Ao), based upon the amount of benzonitrile injected in to the closed system. Including this figure as the time = 0 minutes sample ensured a complete profile for benzonitrile decay could be constructed. As such, the conversion fits well to a first order exponential decay, suggesting that the kinetics of the reaction were not affected in the gas phase (since overall first order dependency was retained as in the liquid phase reactions). The mass imbalance observed may be attributed to loss of material to the catalyst (and support). It is also noted that, as configured, the IR arrangement used samples only in the gas phase.

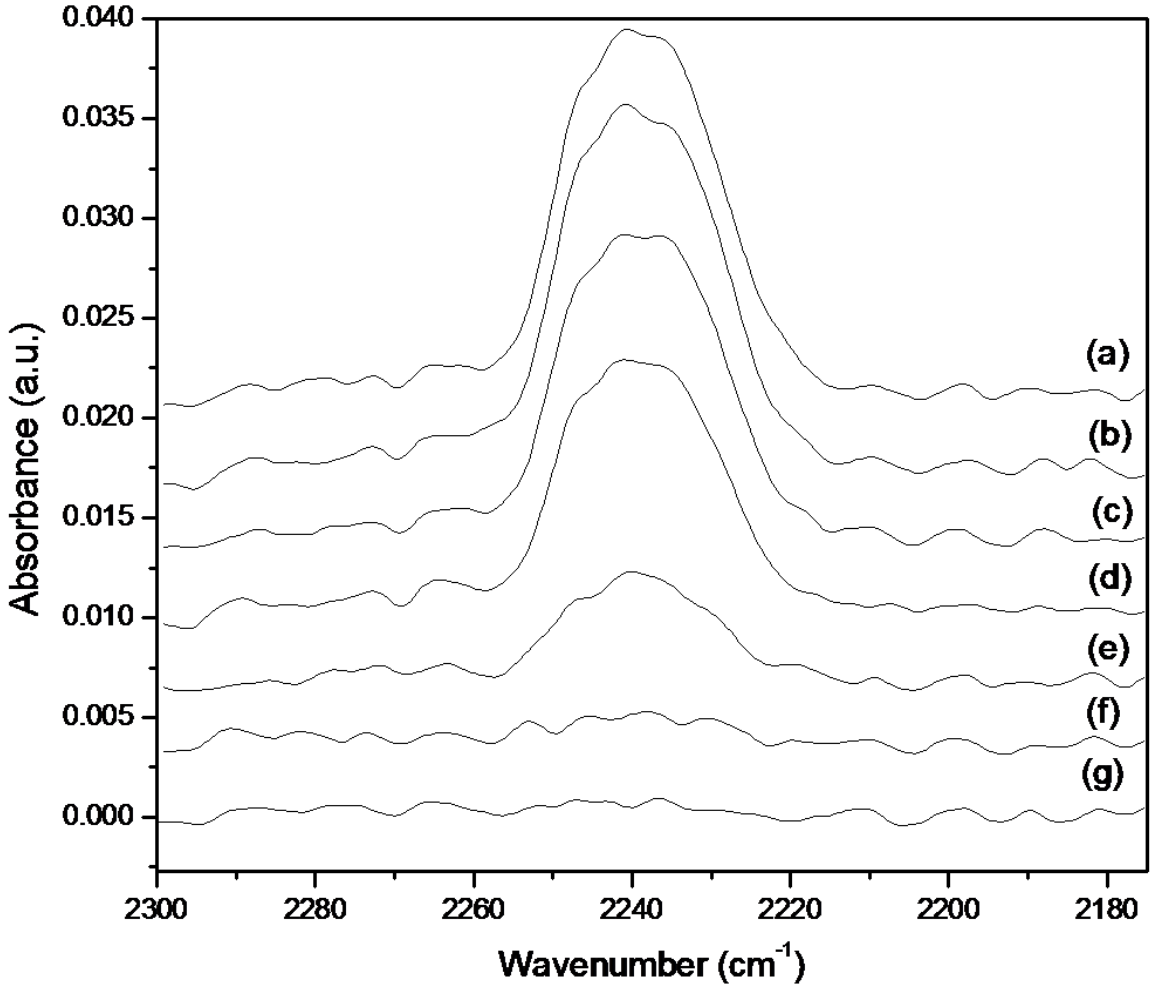

Figure 31. Decay in CN infrared stretching intensity (2238 cm^{-1}) over time in the gas phase hydrogenation of benzonitrile over Pd/Al_2O_3. (a) 3, (b) 5, (c) 7, (d) 9, (e) 15, (f) 25 and (g) 30 minutes sample time.

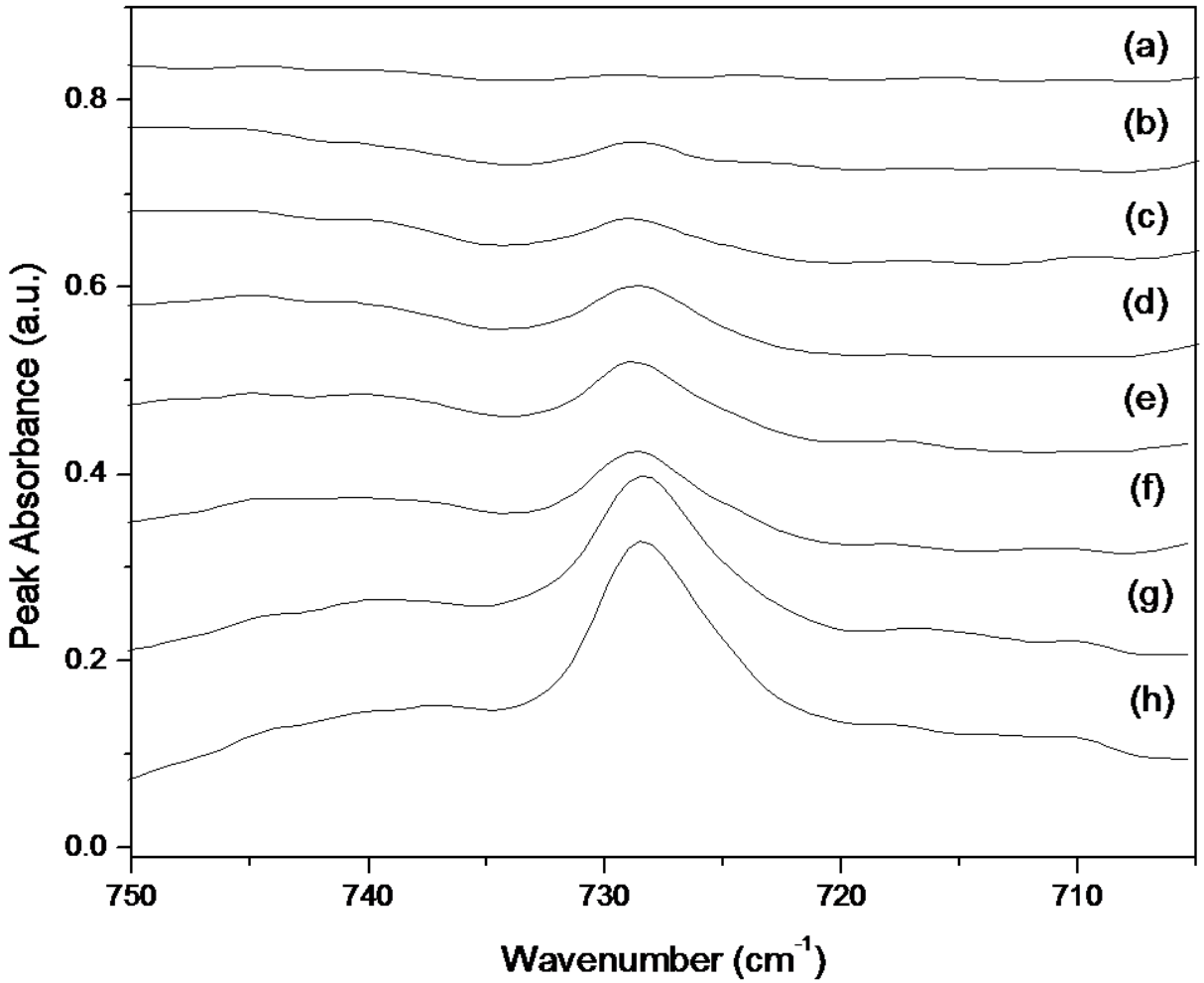

Figure 32. Increase in aromatic CH (729 cm^{-1}) infrared bending intensity of toluene over time in the gas phase hydrogenation of benzonitrile over Pd/Al_2O_3. (a) 0, (b) 2, (c) 4, (d) 6, (e) 8, (f) 10, (g) 20 and (h) 30 minutes sampling time.

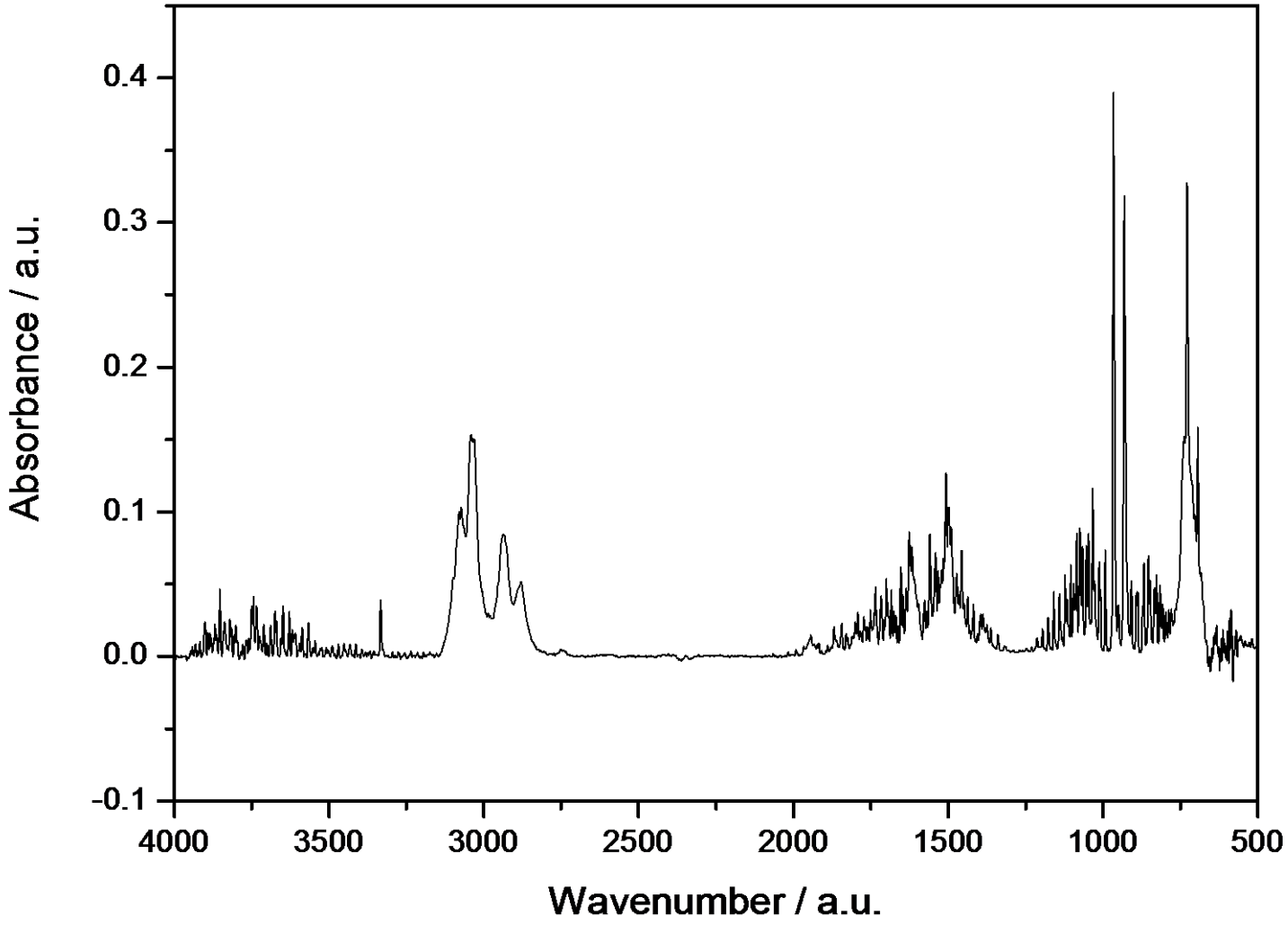

Figure 33. Final FTIR spectrum in the gas phase hydrogenation of benzonitrile over 5% Pd/Al_2O_3 at 30 minutes.

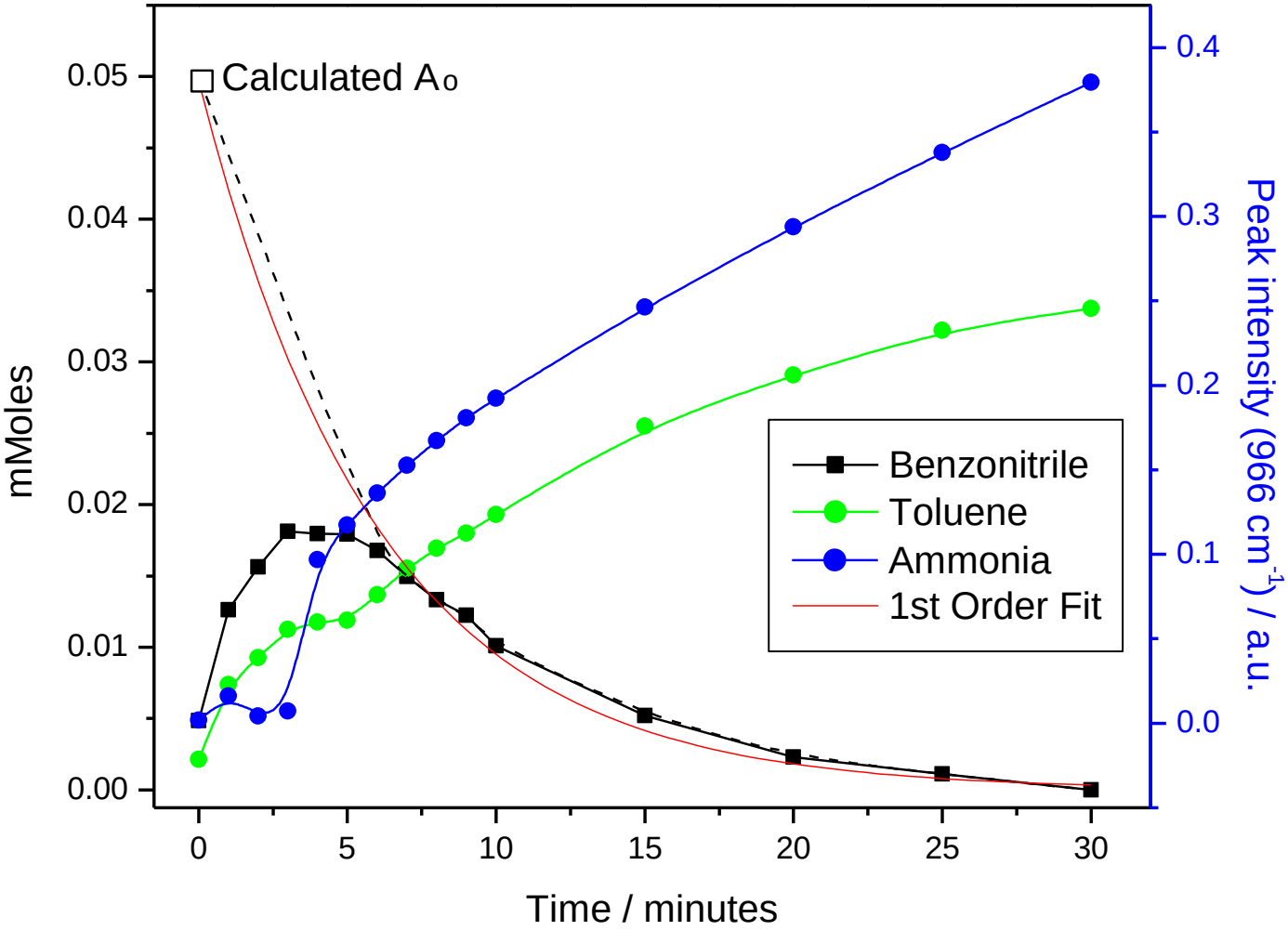

Figure 34. Reaction profile for the gas phase hydrogenation of benzonitrile over Pd/C, 80 ^{o}C, 2 bar H_2.

The hydrogenation of benzylamine followed a similar trend, where ammonia production was observed to coincide with toluene formation. Thus, the hydrogenolysis reaction can be unambiguously associated with the loss of selectivity of benzylamine from the hydrogenation of benzonitrile.

Deuterium studies were performed on the hydrogenation of benzonitrile and hydrogenolysis of benzylamine in an attempt to decouple the diagnostic bands for all reaction components, in order to obtain more complete reaction profiles. Density Functional Theory (DFT) calculations performed elsewhere[109] confirm the vibrational assignments for the deuterated and partially deuterated products. Figure 35 shows the final IR spectrum recorded in the deuteration of benzonitrile and indicates the formation of toluene-d_3 and ND_3 (note highlighted region A showing the shifted band for the C-D aliphatic stretch of toluene at around 2138 cm^{-1}, as compared to the C-H stretch region in Figure 33 at 2912 cm^{-1}). Deutero-benzylamine ($C_6H_5CD_2ND_2$) must also be formed as an intermediate when one considers Scheme 11 (a). This indicates hydrogen addition occurs at the unsaturated centres external to the ring. The aromaticity of the ring remained intact throughout the series of hydrogenation steps.

The deuterium hydrogenolysis of benzylamine (whose final IR spectrum is shown in Figure 36) produced entirely expected results. Namely, upon completion, toluene-d_1 ($C_6H_5CH_2D$) was observed and not toluene-d_3 ($C_6H_5CD_3$) as was observed for benzonitrile hydrogenation in deuterium (Figure 35). This is observed when one considers the highlighted regions A and B for toluene, which show the presence of both aliphatic C-H (2912 cm^{-1}) and C-D (2138 cm^{-1}) stretches respectively.

Despite this, ammonia was observed as fully deuterated (ND_3). These observations suggest that the final ammonia formation process was somehow decoupled from the addition of deuterium to the benzylamine. If $C_6H_5CH_2D$ forms, it would be expected that NH_2D would result from hydrogenolysis (Scheme 11 (b)).However, it is thought that the $NH_2 + D_2 \Leftrightarrow ND_3 + H_2$ exchange reaction is fast (catalysed by Pd) and effectively makes the ammonia production *unselective* in this case. Originally, it had been hoped that ammonia isotopomers (distinguishable by IR) would be diagnostic for the adsorption geometry linked with

the benzylamine hydrogenation process. However, that was not accessible in this case due to the fast H/D exchange.

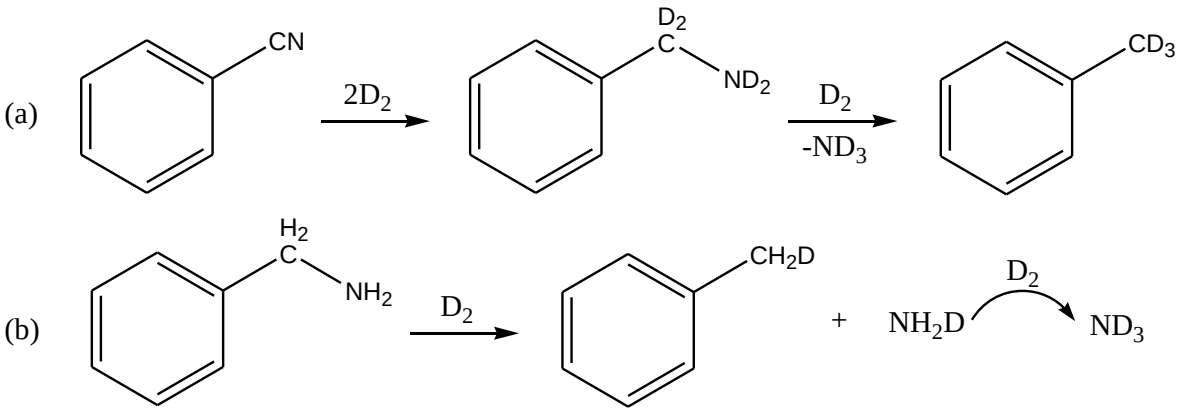

Scheme 11. (a) The deuterium hydrogenation of benzonitrile showing the formation of toluene-d_3 as final product and; (b) the deuterium hydrogenolysis of benzylamine resulting in the formation of toluene-d_1 and the H/D exchanged ammonia-d_3.

That toluene-d_1 appears to undergo no H/D exchange once formed, indicates that the H/D distribution is selective and is indicative of the adsorption geometry during the hydrogenolysis process. This realisation enables one to formulate a global reaction scheme that can account for the benzonitrile/benzylamine, H_2/D_2 results. Such a scheme is presented in Figure 37.

Thus, the unambiguous detection of evolved ammonia confirms the feasibility of the hydrogenolysis reaction in the benzonitrile system over a supported Pd catalyst. Indeed, the reaction profile for the reaction confirms hydrogenolysis to be the cause of a dramatic loss in selectivity to benzylamine. Moreover, deuterium experiments provide new information on how this reaction occurs at the catalyst surface.

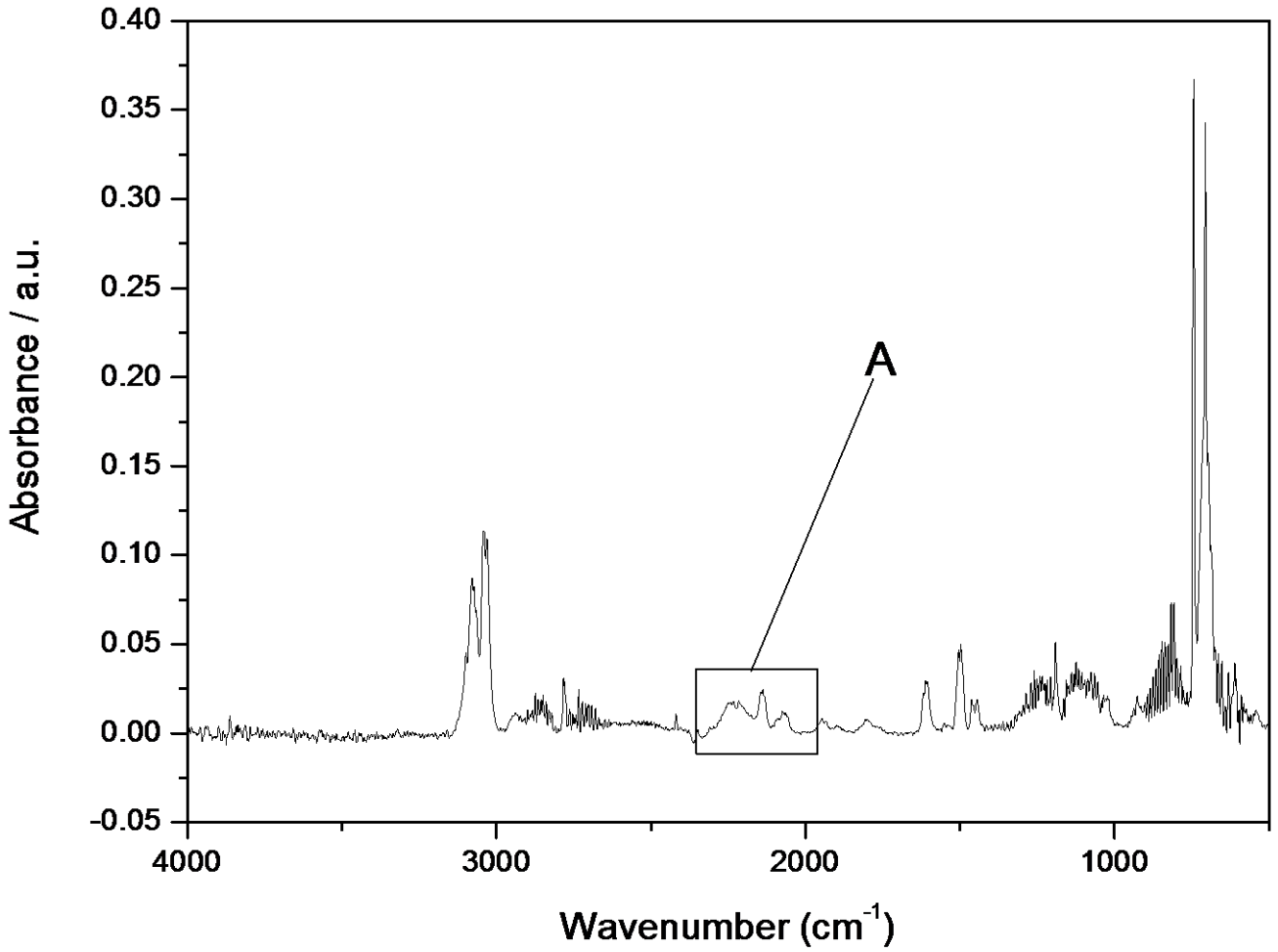

Figure 35. Final IR spectrum recorded (30 minutes) in the gas phase deuterium hydrogenation of benzonitrile over Pd/Al_2O_3. The highlighted region A corresponds to the C-D aliphatic stretch of toluene (2138 cm^{-1}).

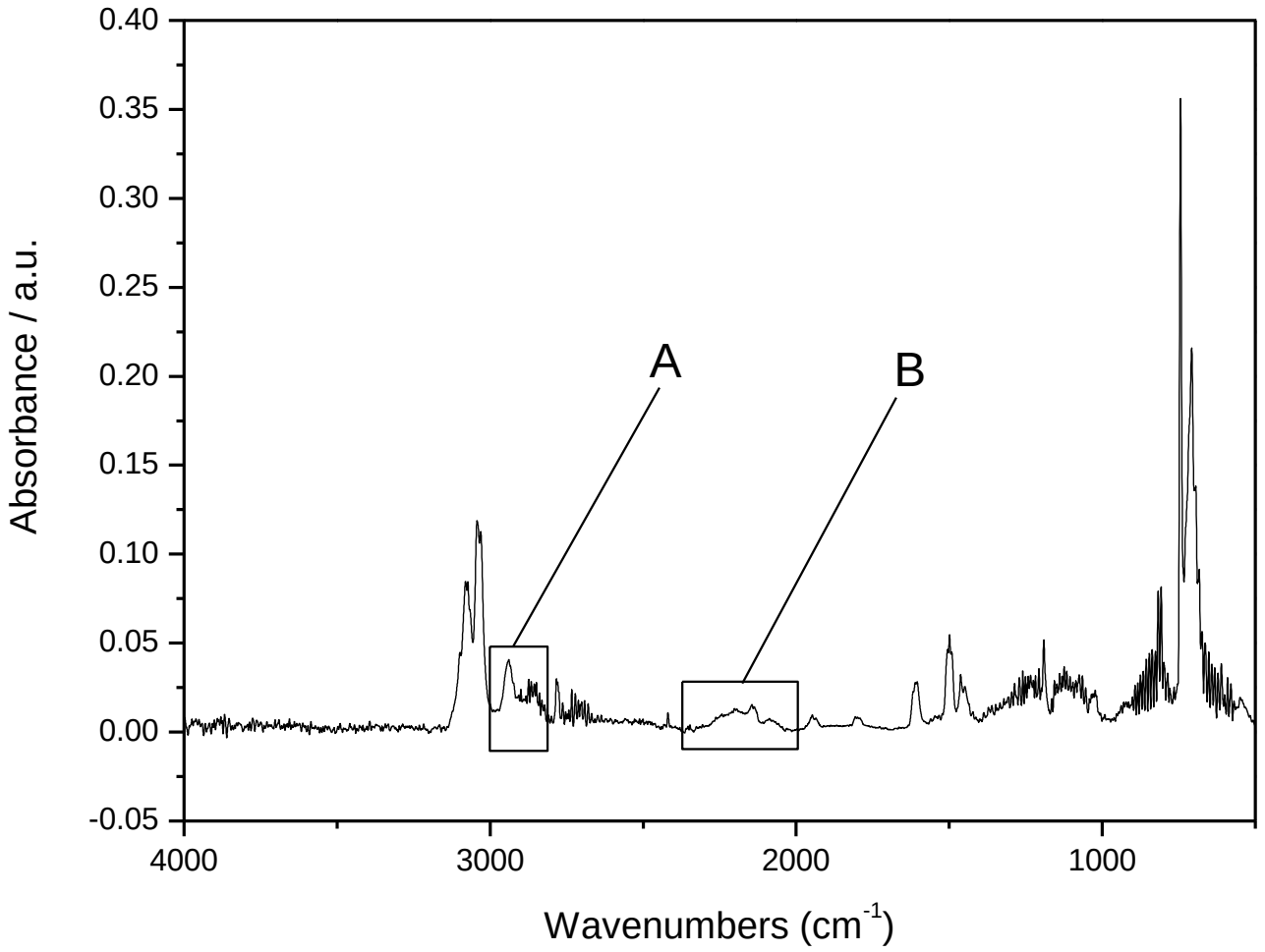

Figure 36. Final IR spectrum recorded (30 minutes) in the gas phase deuterium hydrogenolysis of benzylamine over Pd/Al_2O_3. The highlighted regions A and B correspond to the aliphatic C-H stretch (2912 cm^{-1}) and aliphatic C-D stretch (2138 cm^{-1}) of toluene-d_1 ($C_6H_5CH_2D$) respectively.

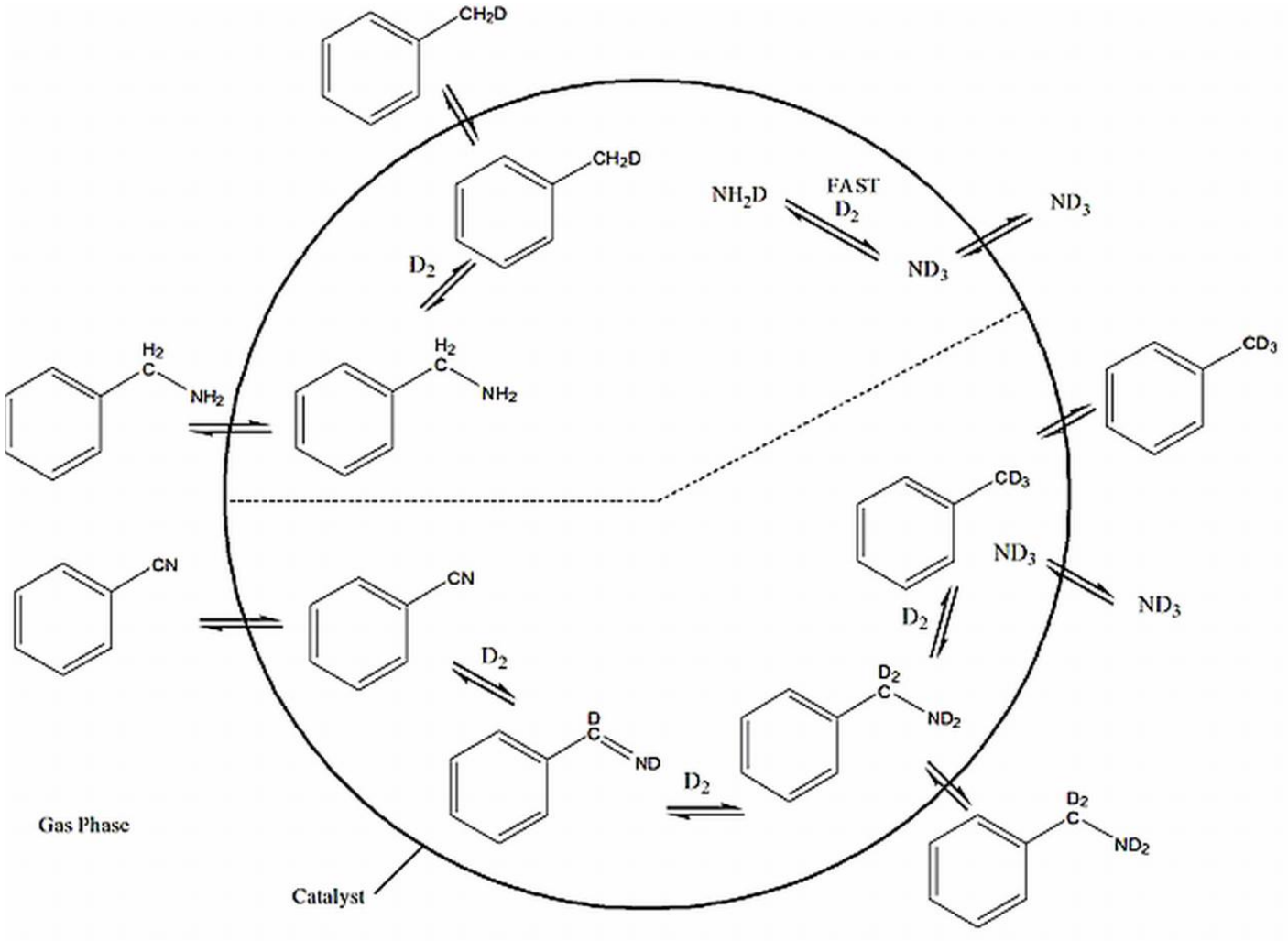

Figure 37. Global reaction scheme for the deuteration of benzonitrile and benzylamine. Note that species within the catalyst area are surface species not measured in the gas phase. Those outside the catalyst area may be measured experimentally in the gas phase by IR. The dashed line is only intended to separate the reaction schemes and intermediates of the deuteration reactions and does not represent any interface or physical separation on the catalyst surface.

3.3.4 Co-adsorption studies

To explore the consecutive nature of benzonitrile hydrogenation, equimolar amounts of both benzonitrile and benzylamine were studied. These experiments were undertaken in order to determine how the hydrogenation step (benzonitrile $\rightarrow$ benzylamine) might influence the hydrogenolysis step (benzylamine $\rightarrow$ toluene). It was assumed that the shapes of their formation/decay would confirm understanding of the reaction. The resulting reaction profile is presented in Figure 38 and quite definitively shows benzonitrile hydrogenation to be independent of benzylamine hydrogenolysis. The former conforms to a single exponential decay curve (first order process) with a rate coefficient comparable to reactions without addition of benzylamine. On the other hand, toluene formation commences from the onset of reaction at a rate that is independent of time/concentration up to a saturation value that represents full conversion. The zero order profile indicates that the hydrogenolysis reaction is occurring independently of the hydrogenation process.

This situation is indicative of site-selective chemistry and can be explained within the confines of a 3-site model. Firstly, all processes require a steady supply of hydrogen so Site I is attributed to Pd sites which support dissociative adsorption of dissolved dihydrogen. Thence, Site II is responsible for the hydrogenation step whilst the hydrogenolysis reaction takes place at Site III. This arrangement would permit hydrogenation and hydrogenolysis to occur simultaneously, as is seen in Figure 38. Additionally, given that the loss of mass observed in the reaction of benzonitrile and benzylamine was attributed to adsorption on the carbon support, the special site (ad)* is included to signify that transport of materials can be mediated through the support. Such a spillover effect has been shown to occur on other carbon supports.[110]

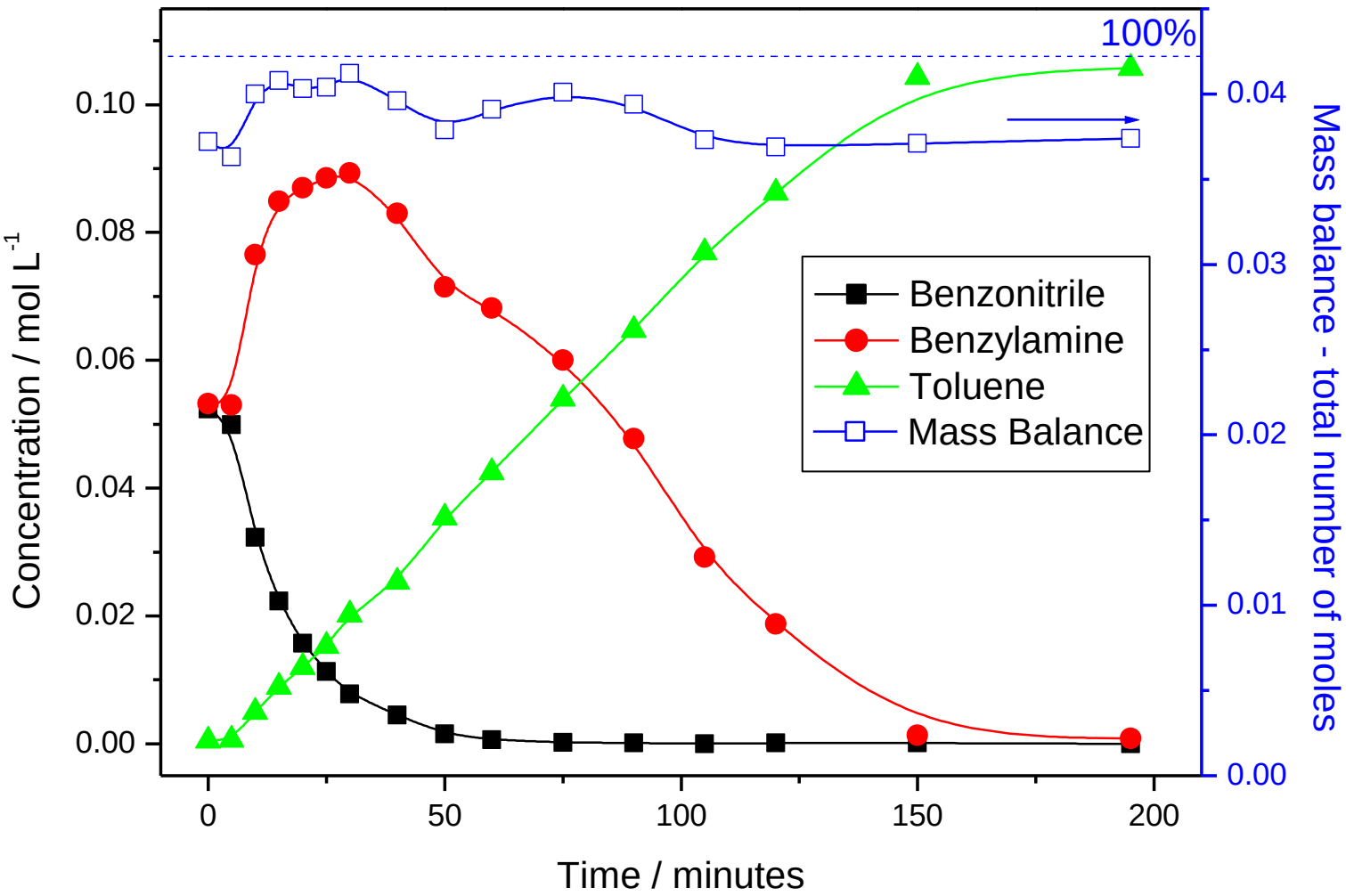

Figure 38. The co-hydrogenation of benzonitrile and benzylamine over 0.5 g 5% Pd/C, 333 K, 4.0 bar, ca. 0.017 moles of benzonitrile and benzylamine. The dashed line represents the incident combined concentration of benzonitrile and benzylamine.

Scheme 12 attempts to demonstrate how the molecules participating in the benzonitrile hydrogenation process are partitioned between the catalyst surface and the liquid phase. k_1 and k_2 are rate coefficients associated with the hydrogenation and hydrogenolysis steps respectively. K_1, K_2, K_4 and K_5 represent adsorption coefficients, with K_2 strongly favouring the adsorbed state whilst K_5 favours the presence of toluene in the liquid phase. K_3 represents the equilibrium between the imine and the enamine.

In order to define the more global nature of this reaction system, Scheme 12 needs to include a description for material spilling over on to the carbon support. Figure 39 schematically links the concepts of the 3 site model with the interchange of molecules between the liquid phase, Pd crystallites and the carbon support. It is defined within the confines of the benzonitrile reaction profile (Figure 23) but is intended to be universal in that it potentially describes the elementary process associated with the hydrogenation of aromatic nitriles over a Pd/C catalyst.

The initial mass imbalance observed in the hydrogenation of benzonitrile (Figure 23) is also consistent with the proposed schemes if one acknowledges that mass transport of reactants and products can be mediated through the carbon support. Retention of reactants/products on the support, where no further reaction is thought to occur, would thus render that molecule undetectable in the liquid phase. Thus, in the case of benzonitrile hydrogenation at least, this pathway is thought to be the origin of the low mass balance in the initial stages of that reaction, given that catalyst fouling is not observed.

When the relative strengths of adsorption are considered, it is possible to explain the role each reactant molecule has to play in the reactions involved. The partition between liquid phase and adsorbed phase seems to play the most important role. From the experimental results, it can be assumed that K_4 (adsorption/desorption of benzylamine) is much stronger than K_1 (benzonitrile). Also, since intermediate imine/enamine species are not observed in the liquid phase, one can assume that K_2 (and especially K_3) is zero. Finally K_5 (toluene adsorption/desorption) approaches infinity, *i.e.* when toluene is formed, it cannot re-adsorb to reduce any further, which is shown by the complete mass balance after reaction.

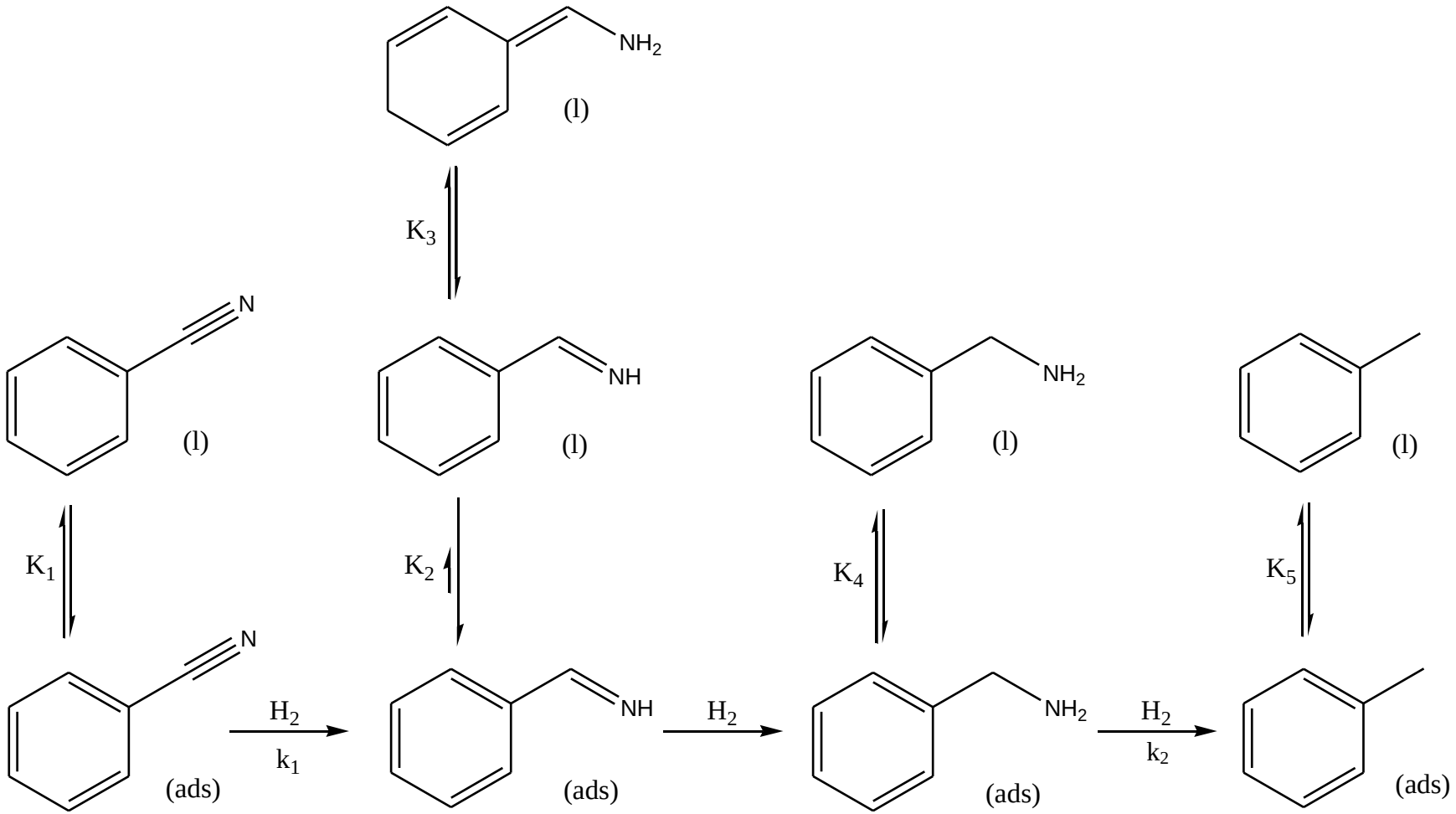

Scheme 12. Partitioning of adsorbed (ad) and liquid phase (l) species in the hydrogenation of benzonitrile of Pd/C. k_1 and k_2 are rate coefficients associated with the hydrogenation and hydrogenolysis steps respectively. K_1, K_2, K_4 and K_5 are adsorption coefficients, K_3 is an equilibrium constant. See text for definition of active sites.

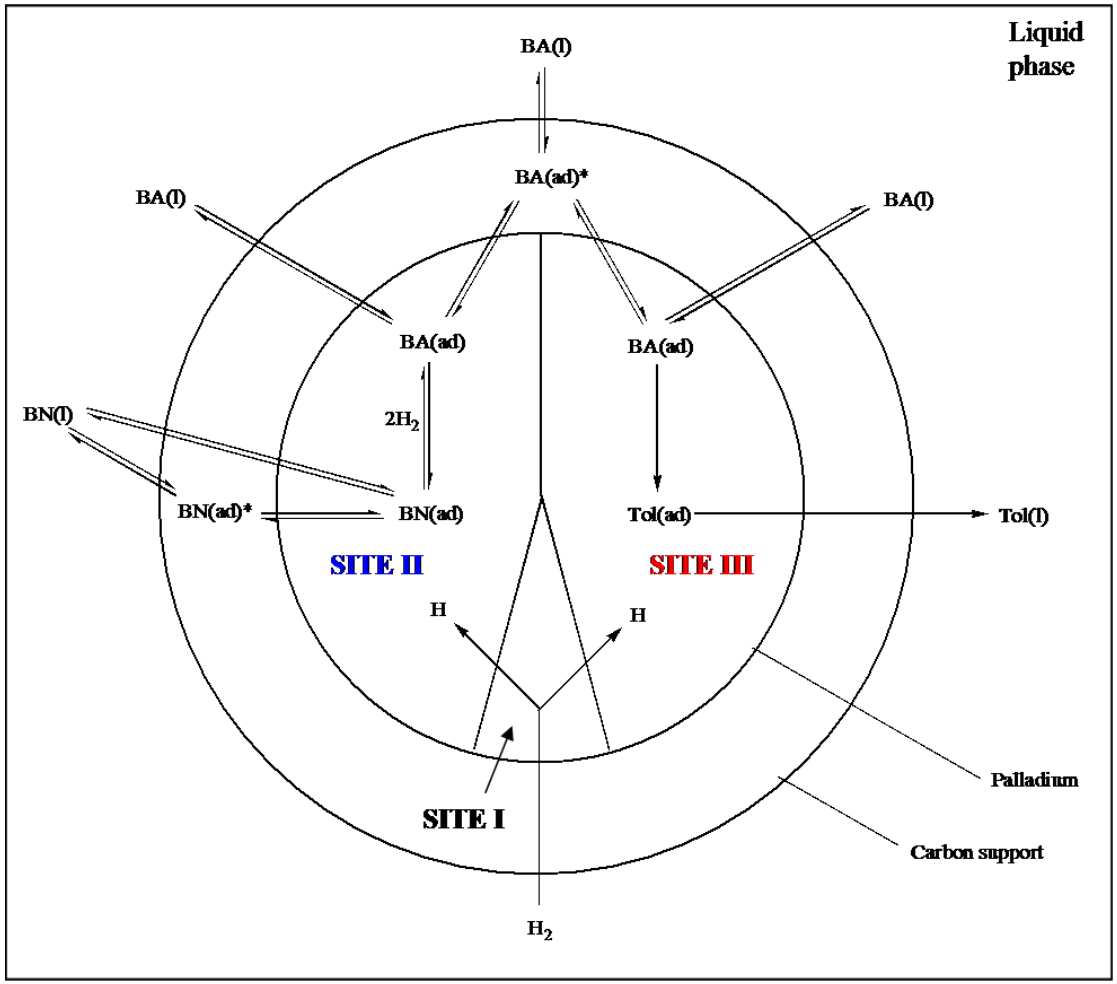

Figure 39. Suggested catalyst model for 5% Pd/C in the hydrogenation of benzonitrile and hydrogenolysis of benzylamine, showing schematically that hydrogen dissociation (Site I), hydrogenation (Site II) and hydrogenolysis (Site III) occur on distinct sites. (BN-Benzonitrile, BA-Benzylamine, Tol-Toluene)

3.3.5 Kinetics of consecutive reactions, first order (hydrogenation) to zero order (hydrogenolysis) fit

To further investigate the nature of the orders of reactions for benzonitrile hydrogenation and benzylamine hydrogenolysis, one can consider comparing the experimentally gained data with a data fit to kinetic expressions governing a consecutive reaction with a change from first to zero order.[111]

$$Benzonitrile \xrightarrow{k_1} Benzylamine \xrightarrow{k_2} Toluene \quad (12)$$

To do this, one must consider a kinetic scheme for the reaction in (12). In such a case, the differential forms for the rates of change of each reactant/product are:

$$\frac{d[BN]}{dt} = -k_1[BN]_t \quad (13)$$

$$\frac{d[BA]}{dt} = k_1[BN]_t - k_2 \quad (14)$$

$$\frac{d[T]}{dt} = k_2 \quad (15)$$

where [BN], [BA] and [T] represents the concentration of benzonitrile, benzylamine and toluene respectively. With some manipulation, (13) and (14) can be integrated to give:

$$[BN]_t = [BN]_0 e^{-k_1 t} \quad (16)$$

$$[BA]_t = [BN]_0 - [BN]_0 e^{-k_1 t} - k_2 t \quad (17)$$

and since via the mass balance relationship all reactants/products must equal $[BN]_0$, *i.e.*:

$$[BN]_t + [BA]_t + [T]_t = [BN]_0 \quad (18)$$

then:

$$[T]_t = k_2 t \quad (19)$$

The final equation to describe toluene change over time requires careful consideration, since it implies that concentration increases without limit. In reality, and has been shown in the reaction profiles for benzonitrile hydrogenation and benzylamine hydrogenolysis, this cannot happen since the original concentration of benzonitrile is finite. However, one must consider that whilst modelling this reaction, initial rates have been used for all calculations. Over time, the individual reaction steps do not follow their initial rate and reagent concentrations are ultimately determined by thermodynamics.

That said, Figure 40 shows that the experimental data (obs) fits well with the modelled kinetics (calc). At least to a first approximation, the reaction was confirmed as a two-stage consecutive process, where the first reaction (hydrogenation) follows first order, and the second reaction (hydrogenolysis) follows zero order kinetics.

It can be seen that the modelled data for toluene formation follows a linear increase at extended times, whereupon it begins to deviate from the experimentally observed profile. However, as has been stated previously, the modelled data fits well when considering the initial rate of formation. The main difference between the two data sets is that the maximum concentration of benzylamine appears low when compared to the kinetic data. However, this can be explained by benzylamine adsorption on the carbon support, as has been described previously (Section 3.3.1.1). Similarly, the model takes no account of the elementary reaction step of imine formation, which cannot be accounted for experimentally in this system (since no imine was experimentally observed).

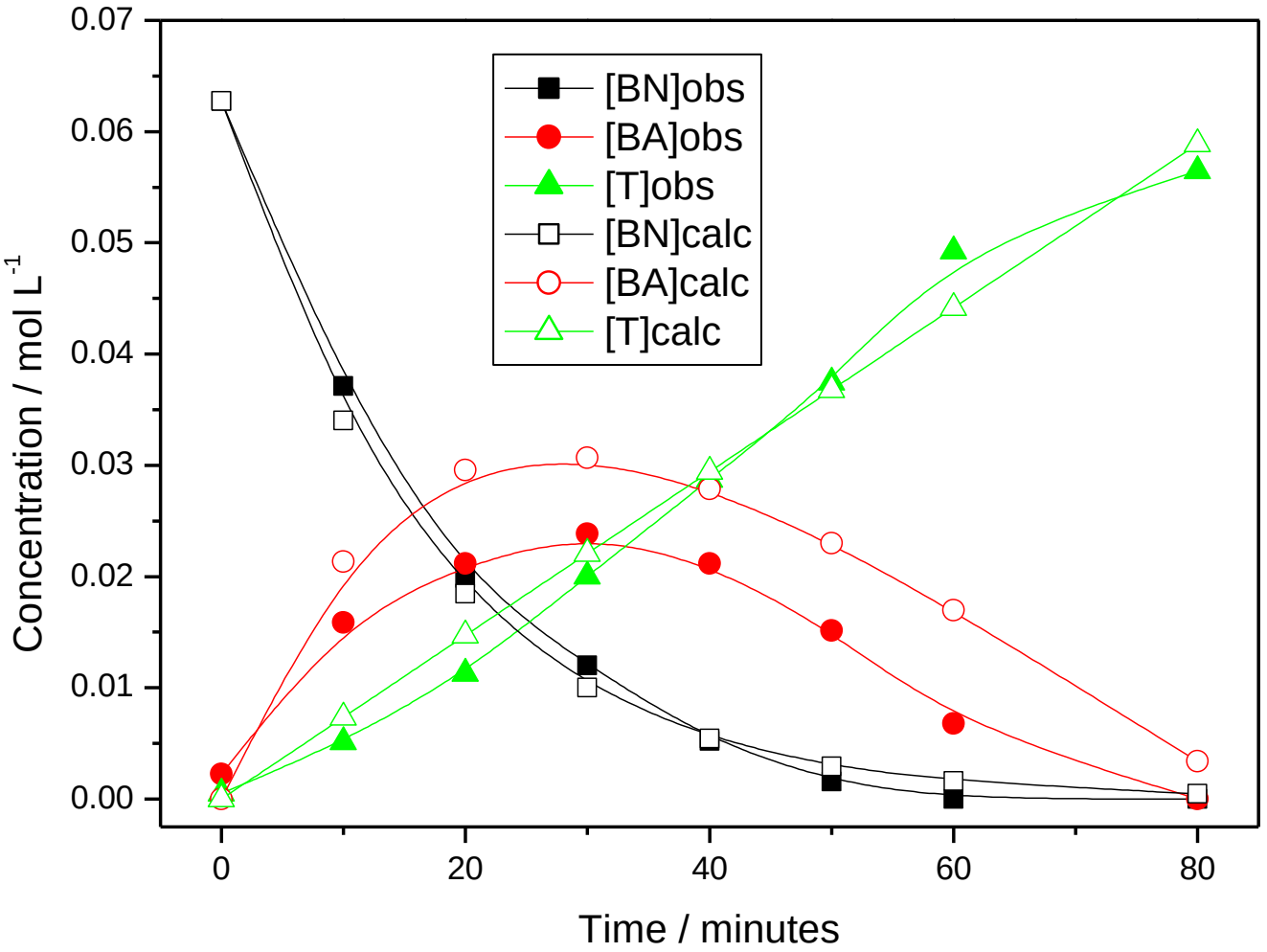

Figure 40. A comparison of the reaction profiles for benzonitrile hydrogenation by experimental means (obs, closed shapes) and by calculation of the kinetic expressions governing a consecutive 1st to 0th order process (calc, open shapes), where [BN], [BA] and [T] represent the concentrations of benzonitrile, benzylamine and toluene respectively.

3.3.6 Controlling selectivity to benzylamine

Two possible solutions were envisaged to control the selectivity to benzylamine – (i) the choice of catalyst and (ii) the use of additives. In terms of the choice of catalyst, the project was limited, since the more common Raney-type catalysts used for nitrile hydrogenations[68] were thought to be much too active for the more functionalised substrates that would be used later in the project. As such, the different catalysts used were limited to supported precious metals similar to that already used.

3.3.6.1 The choice of catalyst to control selectivity

3.3.6.1.1 Benzonitrile hydrogenation over Pd/Al_2O_3

Hydrogenation of benzonitrile was repeated using an in-house 1% Pd/Al_2O_3 catalyst. Figure 41 shows reduced activity of the catalyst as compared to the commercial 5% Pd/C catalyst. Toluene was produced in lower but still significant quantities over time, with selectivity still relatively high at 37% at the end of sampling time. However, at 50% conversion of benzonitrile, there appeared to be little benefit in selectivity to benzylamine over the preferred 5% Pd/C catalyst (Table 5), with selectivity falling from 38% for Pd/C to 31% for Pd/Al_2O_3. Complete conversion of benzonitrile was not observed over an extended reaction time and with the formation of benzylamine, there came a small decrease in mass balance. The loss of mass may be similarly attributed to that for benzonitrile and benzylamine reactions.

3.3.6.1.2 Benzonitrile hydrogenation over PtO_2

When reducing nitro compounds to amines, PtO_2 (Adam's catalyst) has been shown to be useful in minimising reduction of amine functionalities[32,102] and was used in this instance to reduce selectivity to toluene by minimising conversion of benzylamine. Figure 42 shows that a higher selectivity to primary amine (86%) and a lower selectivity to toluene (7%) were observed and from Table 5 it can be seen that at 50% conversion, selectivity to benzylamine is significantly higher than for the palladium catalysts (71%). For the course of reaction time, the concentration of

toluene appears to remain effectively constant. Again, with the formation of benzylamine, mass balance decreased. Nevertheless, the reaction did proceed to completion with the observed uptake of hydrogen ceasing at around 300 minutes. The use of PtO_2 in the hydrogenation of benzonitrile therefore proved to be a useful method for controlling conversion to toluene.

However, despite the narrow range of catalysts used, it appears that the control of selectivity to primary amines may not be best served by the choice of catalyst. Indeed, even over the best performing catalyst (PtO_2), the reaction was slow and selectivity was only marginally improved (as compared to Pd/C). Therefore, chemical methods were thought to be the easiest, and most effective way to control selectivity to the desired primary amine.

Table 5. Comparison of the selectivity to benzylamine in the hydrogenation of benzonitrile at 50% conversion of reagent.

Catalyst	Selectivity to benzylamine (%)
5% Pd/C	38
1% Pd/Al_2O_3	31
PtO_2	71

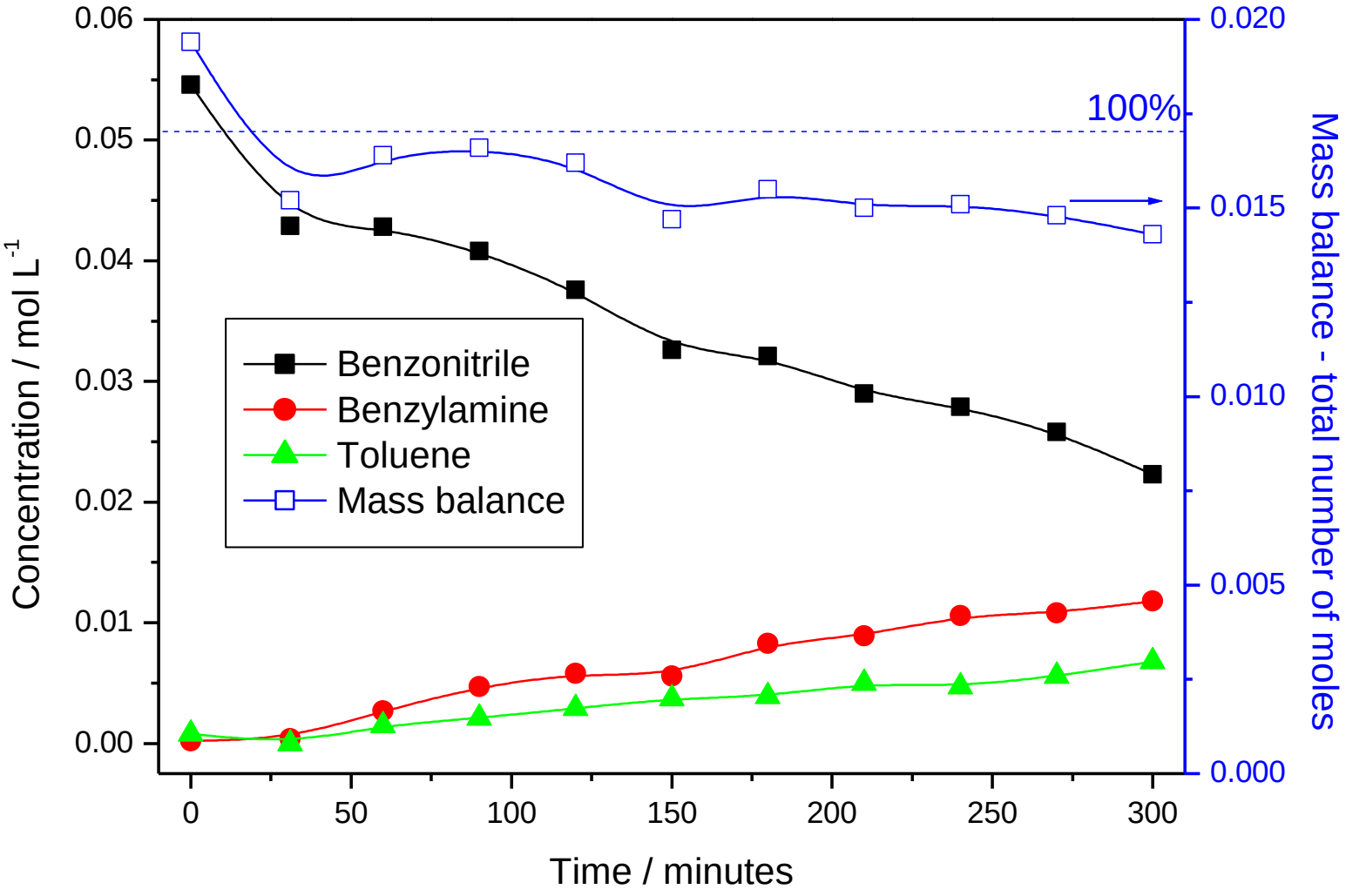

Figure 41. The hydrogenation profile of benzonitrile over 0.5 g 1% Pd/Al_2O_3, 333 K, 4.0 bar, ca. 0.017 moles of benzonitrile. The dashed line represents the incident combined concentration of benzonitrile and benzylamine.

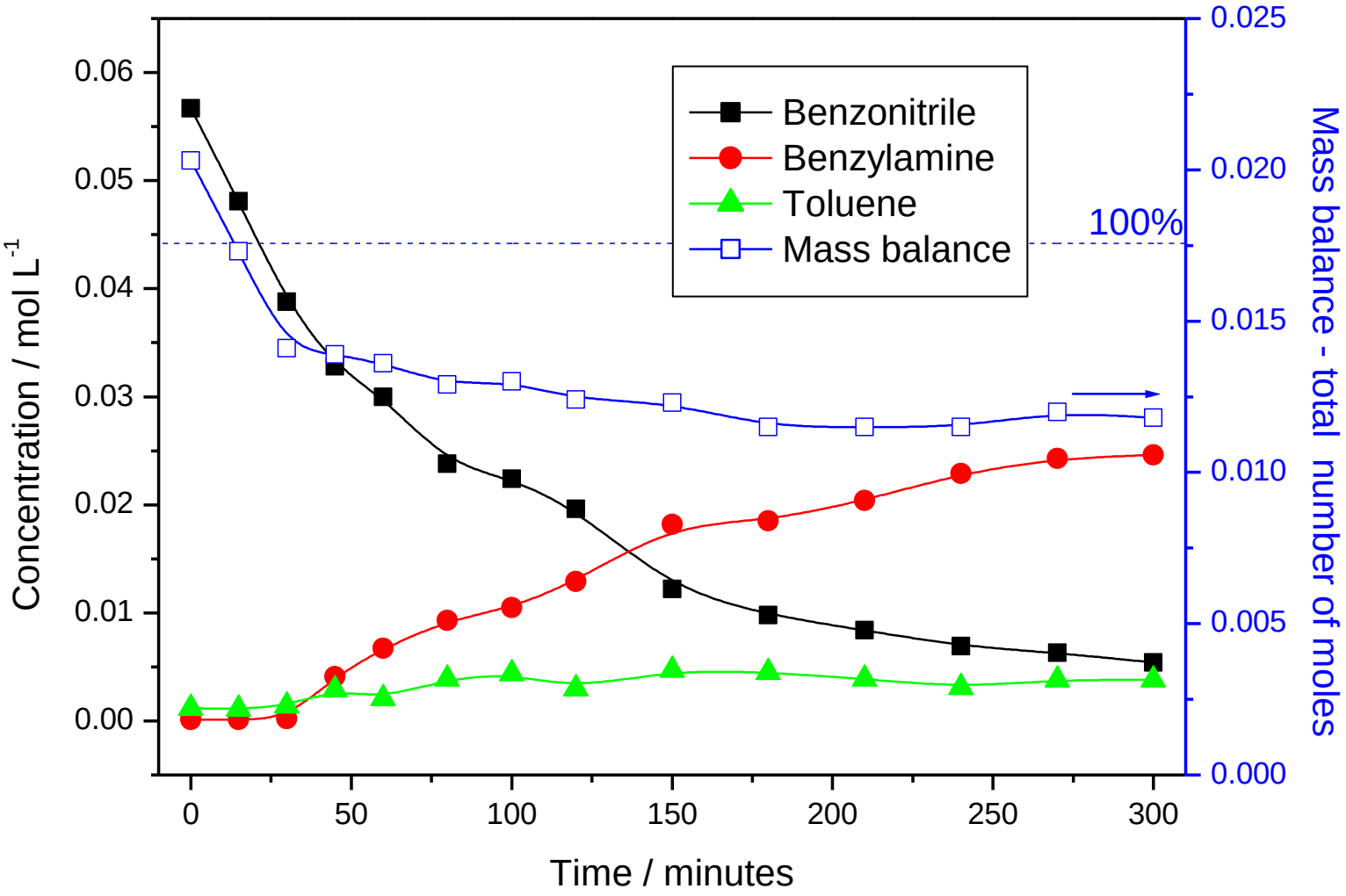

Figure 42. The hydrogenation profile of benzonitrile over 0.5 g 5% PtO_2, 333 K, 4.0 bar, ca. 0.017 moles of benzonitrile. The dashed line represents the incident combined concentration of benzonitrile and benzylamine.

3.3.6.2 Effect of acidic additive (H_2SO_4)

The ideal candidate for an additive to prevent hydrogenolysis would be the basic ammonia, which affects the equilibrium between benzylamine and toluene, and is the usual method in organic reactions.[113] However, since the chemistry in this project is concerned with cyanohydrins, a basic additive could not be used.

Under basic conditions, the equilibrium of the cyanohydrin molecule can be affected to such an extent that it would cause the breakdown of the molecule to ultimately yield HCN (Scheme 13 below). Of course for benzonitrile hydrogenation, one need not consider such safety implications since there is no cyanohydrin functionality. However, due to these safety concerns and for comparable results with more functionalised systems, no bases were used.

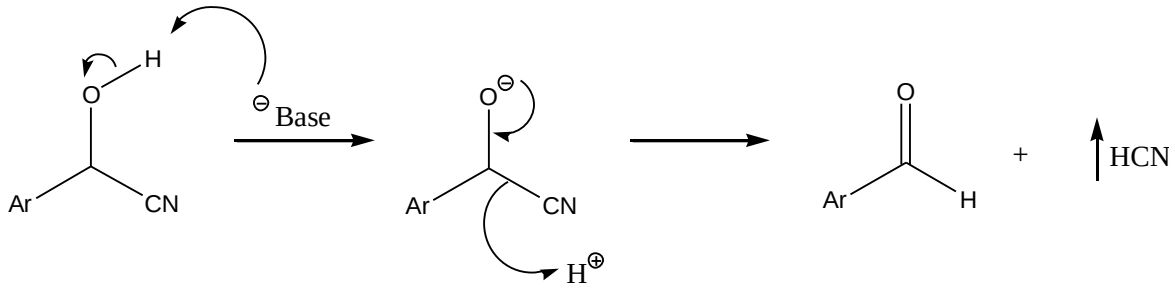

Scheme 13. Cyanohydrin breakdown under basic conditions.

Instead, an acid additive (H_2SO_4) was considered as the best alternative. Nitrile hydrogenation to primary amines is sometimes coupled with the formation of secondary or tertiary amines. As has been observed in the present work, hydrogenolysis may also occur. Previous studies have shown that with the addition of an equivalent amount or more of acid, selectivity to the primary amine product can be increased.[58-60] An acid is used in the relevant Syngenta industrial process for just such a reason. It is thought to function by forming a salt with the primary product and thus, prevent the formation of higher amines. In the case of benzonitrile hydrogenation, it was hoped that it would eliminate the formation of toluene, by preventing re-adsorption of the amine.

Figure 43 shows that a decrease in benzonitrile concentration (with a comparable rate to reactions in the absence of an acidic additive) was observed over time. Hydrogen uptake ceased at a time approximating to the full conversion of benzonitrile, suggesting that further conversion to toluene did not occur. However, no other reagents were observed in the liquid phase by GC analytical methods. Nevertheless, a white solid product was isolated from the reaction mixture following removal of the catalyst by vacuum filtration and the solvent by rotary evaporation. Once isolated, the solid was subjected to various analyses in an attempt to identify it. Its melting point was found to be in the range 270-275 ^{o}C and compared well with that for an as synthesised benzylamine-hydrogen sulfate salt (by mixing equimolar amounts of benzylamine and concentrated sulphuric acid, summarised in Table 6).

Mass spectrometry (fast atom bombardment, FAB) gave further evidence that the white solid was the expected benzylamine-hydrogen sulfate salt. Figure 44 and Figure 45 below compare the mass spectrum obtained for both the synthesised salt and the unknown solid respectively, and shows that the MH^+ ion is common between the two (*m/z* 108 (MH^+, 100% for both).

NMR spectra for the two salts were recorded by dissolving in methanol-d_4 and Figure 46 shows the spectra to be remarkably similar. Three peaks for each were identified with the same chemical shifts and the same proton integrations (δ_H (400 MHz; methanol-d_4) 3.8 (2H, s, NH_2), 4.5 (2H, s, CH_2) and 7.1 (5H, m, Ph)).

Table 6. The melting points of benzylamine-hydrogen sulfate salt and the product of benzonitrile hydrogenation under acidic conditions.

	Melting Point (^{o}C)
Benzylamine-hydrogen sulfate	273-275
Benzonitrile hydrogenation product	270-275

Such a range of analytical techniques proves that the product of benzonitrile hydrogenation with an acid additive was a benzylamine-hydrogen sulfate salt, and was found with a 92% yield. The results indicate zero formation of toluene and an increase in the selectivity to the desired primary amine product. A basic work-up of the salt in NaOH solution yielded, after filtration, the isolated primary amine product in a 46% yield.

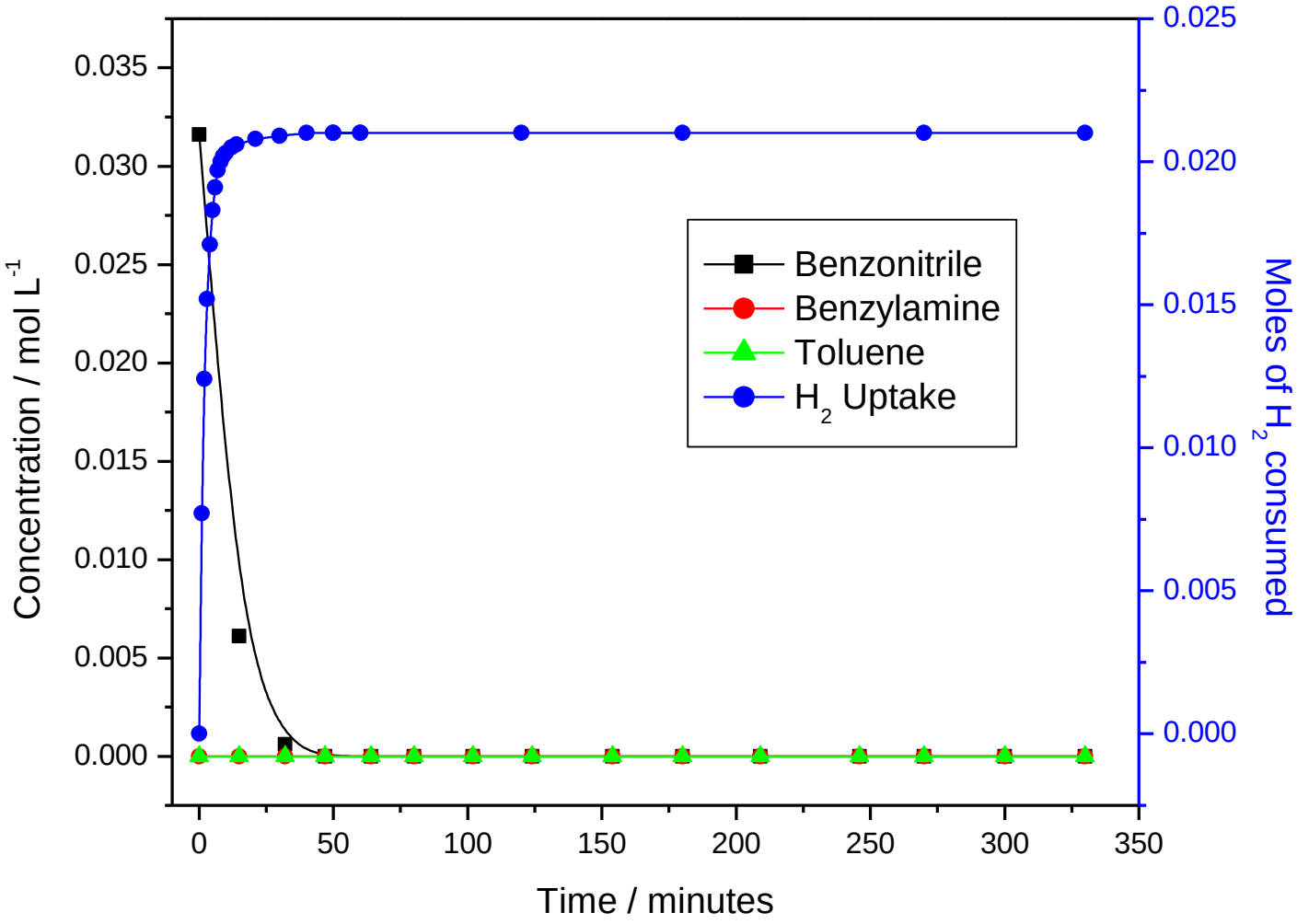

Figure 43. The reaction profile and hydrogen uptake for the hydrogenation of benzonitrile over 0.5 g 5% Pd/C, 333 K, 4.0 bar, ca. 0.017 moles of benzonitrile and equimolar amount of H_2SO_4.

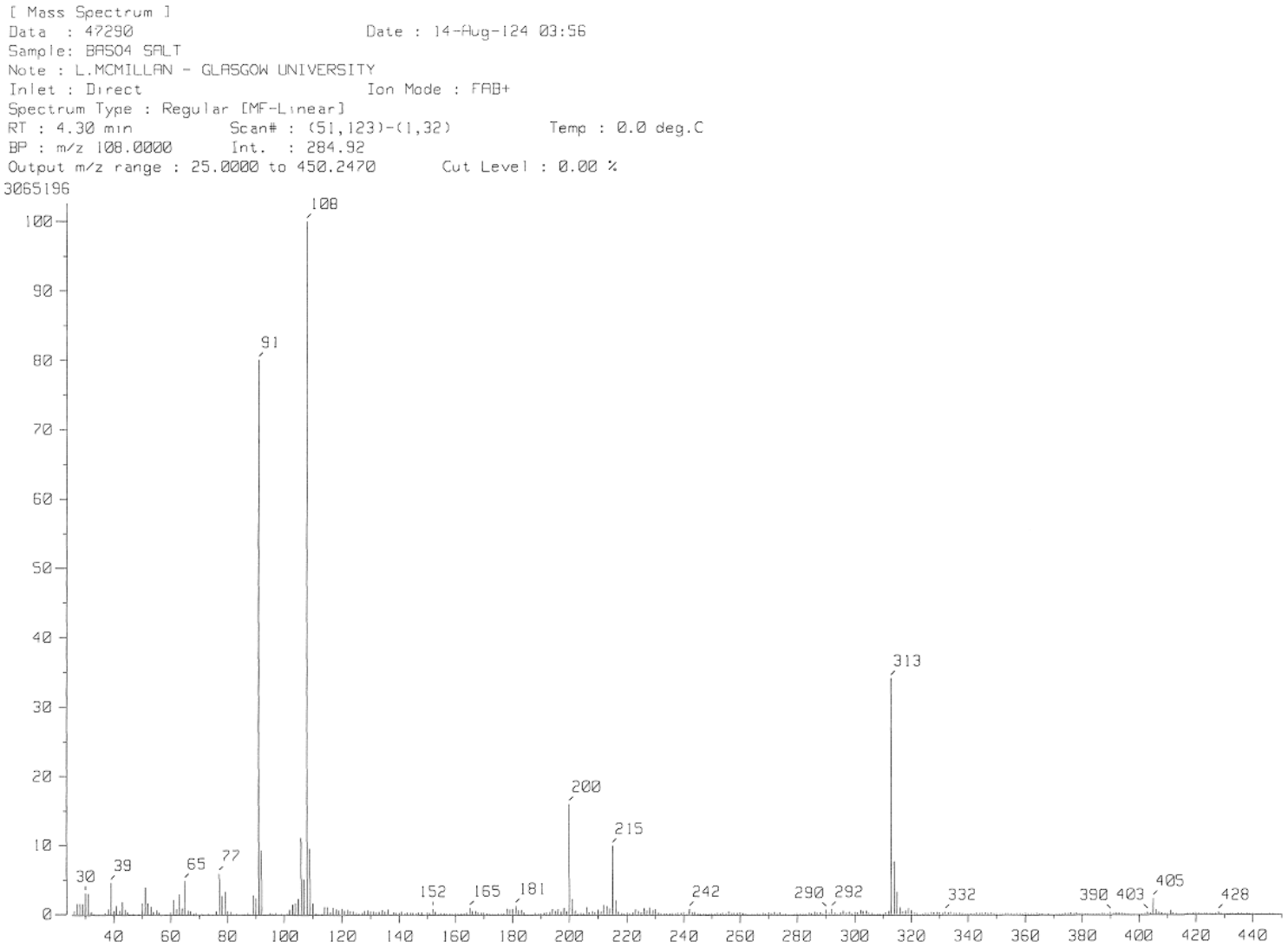

Figure 44. The mass spectrum of an as-synthesised sample of benzylamine hydrogen sulfate salt.

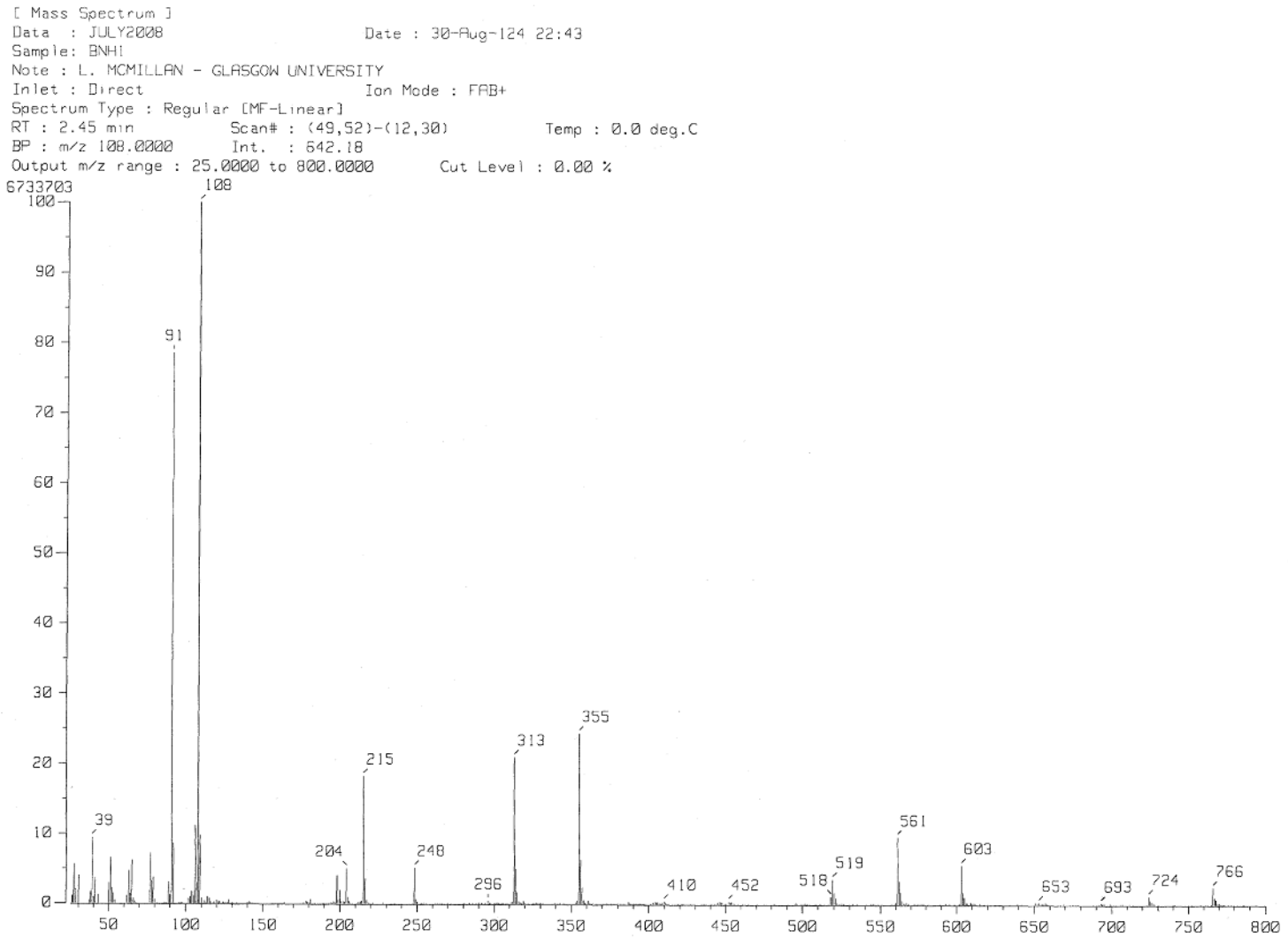

Figure 45. The mass spectrum of the solid product obtained from the hydrogenation of benzonitrile under acidic conditions.

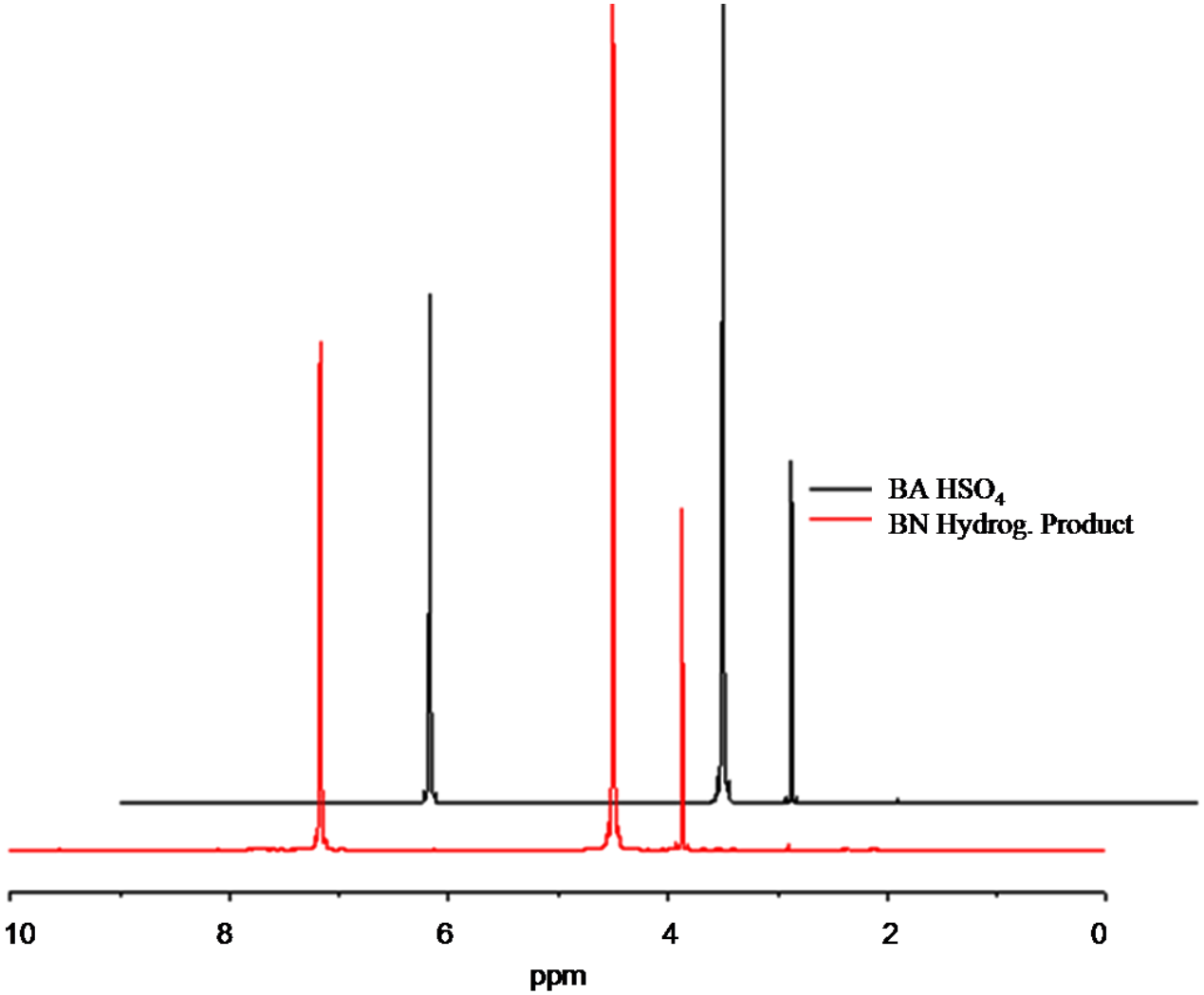

Figure 46. Comparison of the nmr spectra of benzylamine-hydrogen sulfate salt (BA HSO_4) and the isolated product of benzonitrile hydrogenation carried out under acidic conditions (BN Hydrog. Product).

3.3.7 Conclusions

- The liquid phase hydrogenation of benzonitrile over supported Pd catalysts proved to be more complex than was originally believed. Rather than selective hydrogenation to benzylamine, an unforeseen hydrogenolytic step occurred whereby the complete conversion of benzylamine to toluene was observed.

- It was found that the benzonitrile hydrogenation reaction was overall pseudo first order with respect to the amount of catalyst, zero order with respect to nitrile concentration. In contrast to other investigations,[40] the order of the reaction with respect to hydrogen was found to be a non-integer order of *ca.* 0.3. The activation energy for the catalytic hydrogenation of benzonitrile was found to be 28.2 kJ mol^{-1}, describing a reaction under kinetic control.

- The hydrogenolysis of benzylamine was found to have an activation energy of 80.1 kJ mol^{-1}. It was also found that the rate law differed from that of benzonitrile, and that there was an overall zero order dependence.

- Co-hydrogenation studies on a mixture of benzonitrile and benzylamine show the hydrogenation and hydrogenolysis reactions to be occurring simultaneously and independently. This behaviour in interpreted in terms of a 3 site model: dissociative hydrogen adsorption takes place at Site I, hydrogenation takes place at Site II and Site III is associated with the hydrogenolysis reaction.

- Greater selectivity to primary amine can be achieved with the choice of catalyst, where PtO_2 offered significant improvement over Pd catalysts and hydrogenolysis can be eliminated completely by the use of acidic additive.

3.4 Extending the aliphatic chain

3.4.1 The hydrogenation of benzyl cyanide ($C_6H_5CH_2CN$)

It was anticipated that benzyl cyanide would be readily hydrogenated to its corresponding primary amine in much the same way as benzonitrile, yielding phenethylamine ($C_6H_5CH_2CH_2NH_2$) as the final product (as shown in Scheme 14). However, as can be seen in Figure 47, below, no conversion of benzyl cyanide was observed. Indeed, the expected amine product was absent, and only a very small amount of hydrogen was consumed in the initial stages of the reaction.

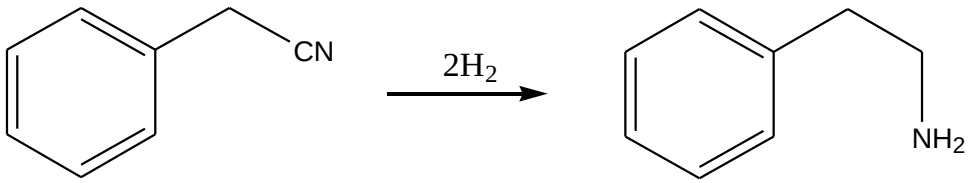

Benzyl cyanide Phenethylamine

Scheme 14. Benzyl cyanide hydrogenation.

It therefore appears that the addition of a single $–CH_2–$ group is coupled with a dramatic loss in conversion from 100% for benzonitrile hydrogenation, to 0% for benzyl cyanide.

3.4.1.1 Repeatability problems with different batches of catalyst

It was during this period of research in the project that a replacement batch of 5% Pd/C was required from the suppliers (Aldrich). However, no catalyst from the previously used batch was available. Therefore a new batch was acquired and benchmarked against the hydrogenation of benzonitrile. Whilst the repeatability between both batches was acceptable, upon re-examining the hydrogenation of benzyl cyanide, a vastly different reaction profile was obtained.

This time, conversion of benzyl cyanide occurred, as was determined by the reaction profile in Figure 48. It was, therefore, decided that a larger supply (50 g) of this batch of Pd/C should be purchased and used for the duration of the project, to prevent any varying results for other systems to be tested. Whilst the exact

nature of the difference between this and the previous batch could not be ascertained, it was suggested that a difference in the carbon support (its source, its acidity *etc*.) may have been the cause of any differences. However, it should be noted that the new batch of catalyst was tested against all other substrates presented here, with only benzyl cyanide hydrogenation showing any change in activity. As such, the reaction shown in Figure 47 (older batch of catalyst) should be neglected and only the profile shown in Figure 48 should be used in discussions.

The above two paragraphs have been included for completeness and show a degree of variability between batches of the Pd/C used in these studies. Indeed, the benzyl cyanide reaction seems to indicate a change in performance over time. These are issues sometimes encountered in heterogeneous catalysis. Nevertheless, it is noted that with the exception of Figure 47, all of the profiles shown in this thesis are reproducible with the updated batch of Pd/C. Thus, the work presented here is internally consistent and reproducible. However, batch to batch variability and temporal consistency of the commercial catalyst needs confirming should any scale up options be considered at the industrial centre.

From comparison with the initial mass imbalance for benzonitrile hydrogenation (Section 3.3.1 and Figure 23), it is believed that phenethylamine was retained (via strong adsorption of the amine) by the carbon support, since it too is in large excess compared with the available Pd surface sites ($phenethylamine_{(missing)}$: Pd(s) = 365 : 1).

In considering Figure 48, no products were observed in the liquid phase. The hydrogen uptake curve shows that a stoichiometric amount of hydrogen was consumed by the reaction, *i.e*. sufficient to facilitate complete conversion of benzyl cyanide to phenethylamine. Previous work has highlighted the relevance of the nitrile unit being in conjugation with the aromatic ring.[114] Although conjugation is absent with benzyl cyanide, the substrate has obtained 100 % conversion (albeit with the absence of any detectable products), so it appears that the nitrile group can be reduced with this catalyst despite no conjugation within the π network (overlap of p orbitals associated with the nitrile functional group and the aromatic ring). To further test this hypothesis, an extended aliphatic ‘spacer’ unit was examined, Section 3.4.2.

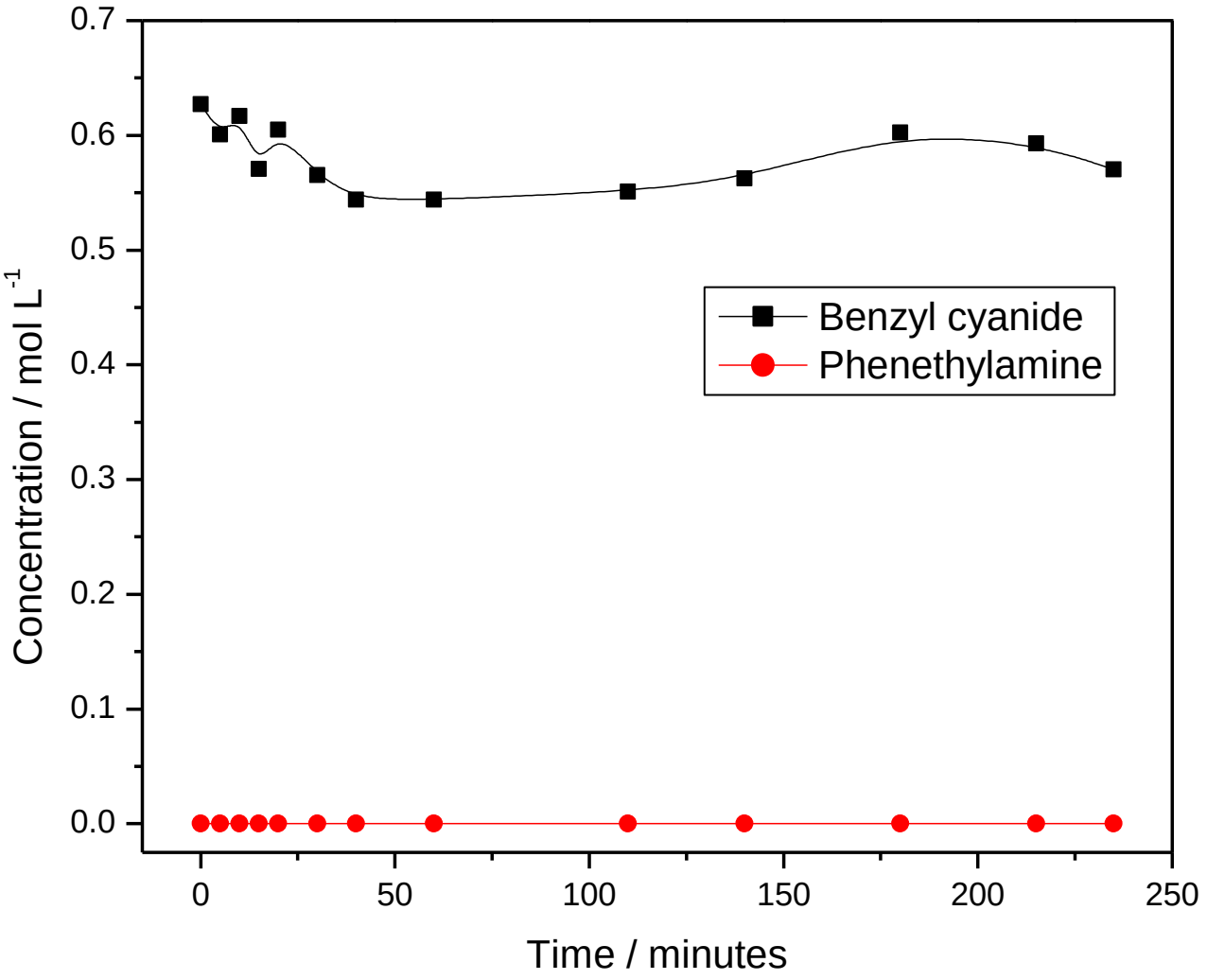

Figure 47. The hydrogenation profile of benzyl cyanide over 0.5 g 5% Pd/C (old batch), 333 K, 4.0 bar, ca. 0.017 moles of benzyl cyanide.

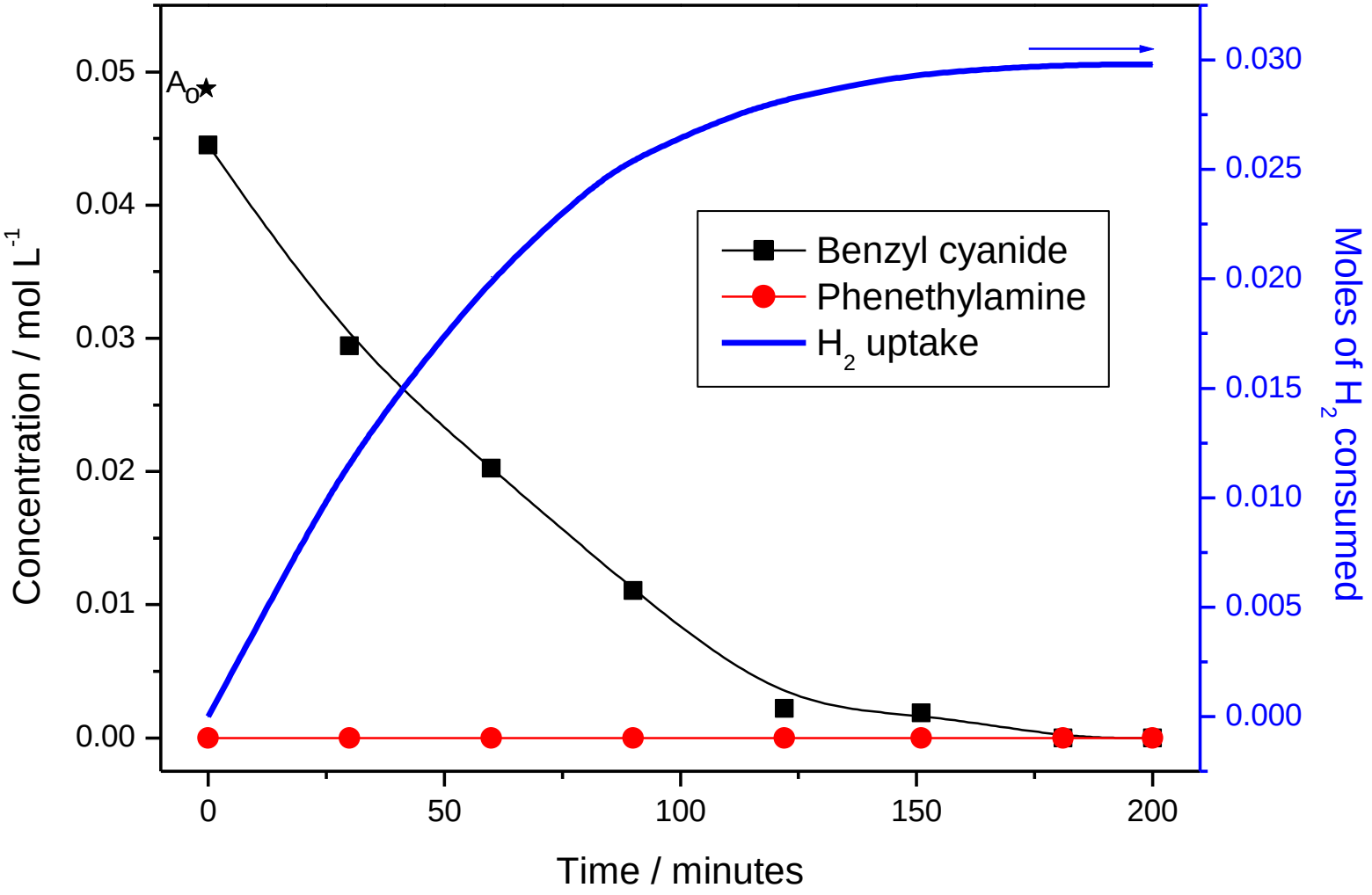

Figure 48. The reaction profile and hydrogen uptake curve for the hydrogenation of benzyl cyanide over 0.5 g 5% Pd/C (new batch), 333 K, 4.0 bar, ca. 0.017 moles of benzyl cyanide.

3.4.2 The hydrogenation of 3-phenylpropionitrile ($C_6H_5CH_2CH_2CN$)

The reaction profile for the hydrogenation of 3-phenylpropionitrile (Scheme 15) is seen in Figure 49 where, in stark contrast to benzonitrile hydrogenation (Figure 23) but somewhat consistent with benzyl cyanide hydrogenation (Figure 48), no products are observed in the liquid phase. In contrast to both of those reaction profiles, however, was the observation that very little conversion was observed. This gave an indication that the length of aliphatic chain has some effect of the facility for hydrogenation over this Pd/C catalyst. Interestingly, the reaction does not produce a complete mass balance, suggesting some degree of substrate/product retention by the catalyst. The quantity of 'missing' material ($moles_{(missing)} : Pd_{(s)} = 76 : 1$) again indicates retention by the carbon support. With little perceived conversion of nitrile and minimal hydrogen uptake (*ca.* 0.005 moles consumed; full conversion to primary amine equates to a hydrogen uptake of *ca*. 0.0335 moles), it is suggested that the 3-phenylpropionitrile is more strongly adsorbed to the catalyst surface than benzonitrile or benzyl cyanide. Further, the mass imbalance evident at short reaction times is thought to indicate an initial activity, which is then somehow quenched.

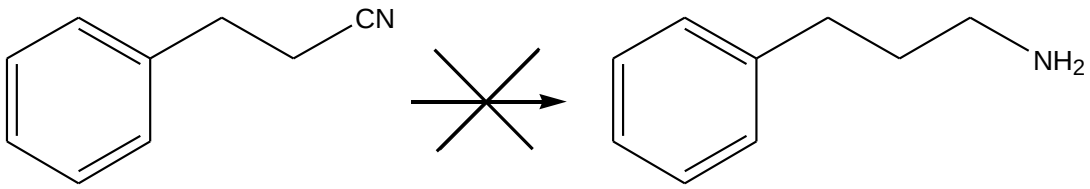

3-Phenylpropionitrile 3-Phenylpropylamine

Scheme 15. 3-Phenylpropionitrile hydrogenation.

Arai *et al*. have shown that catalyst deactivation in the initial stages of reaction could be attributed to strongly adsorbed amines blocking active sites.[115] Here, since a small amount of hydrogen was consumed by the reaction, some degree of conversion of 3-phenylpropionitrile is inferred. Thus, small amounts of amine product adsorbed on the catalyst (Pd) could be strongly adsorbed and consequently 'poison' subsequent hydrogenation activity. Since the substrate concentration is in large excess compared to the surface Pd sites, only a fraction of the mass imbalance would be required to poison such sites.

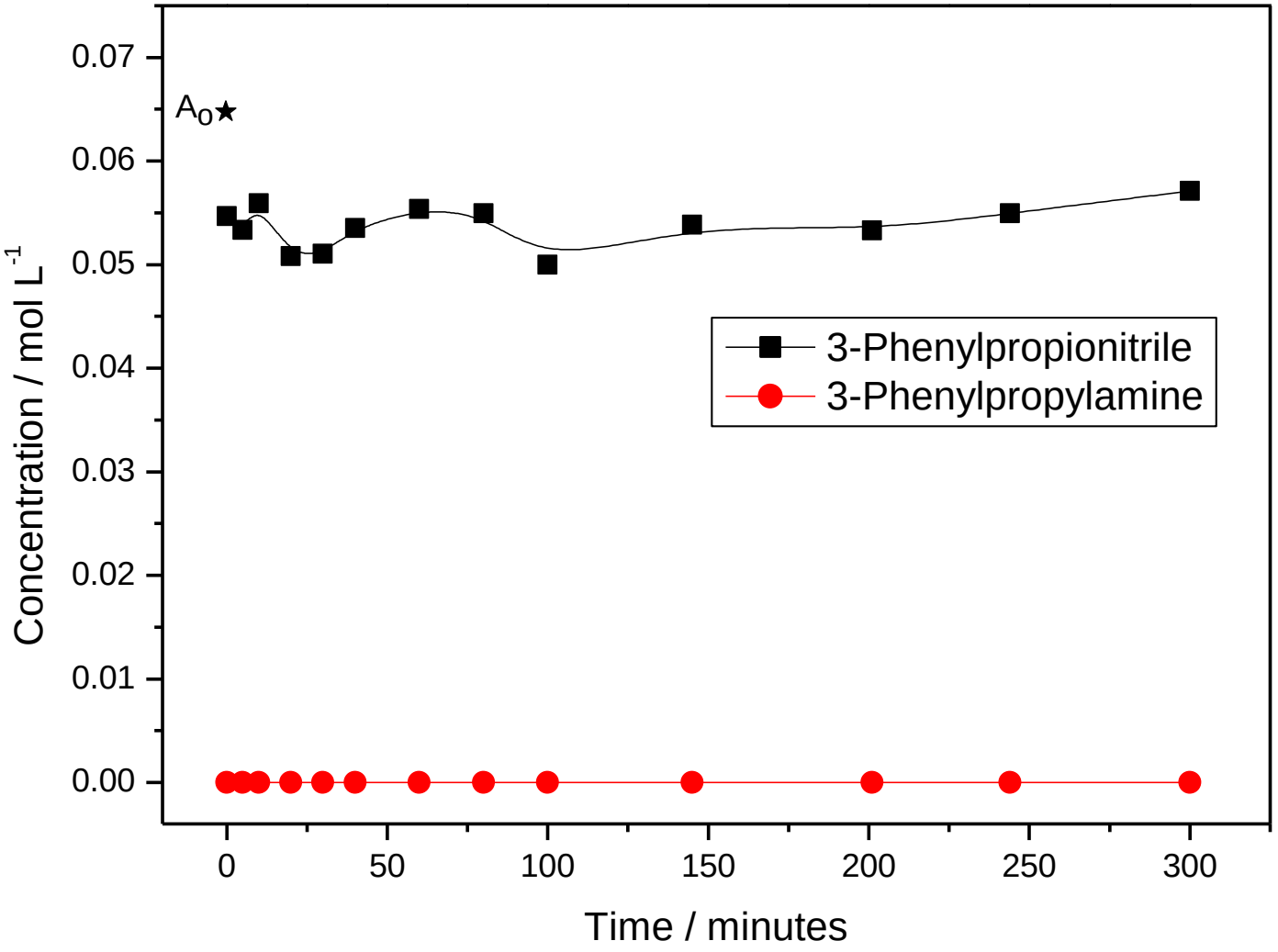

Figure 49. The hydrogenation profile of 3-phenylpropionitrile over 0.5 g 5% Pd/C, 333 K, 4.0 bar, ca. 0.017 moles of 3-phenylpropionitrile, showing the non-facile nature of nitrile reduction. Ao indicated the incident concentration of nitrile.

3.4.3 The hydrogenation of cinnamonitrile ($C_6H_5CH=CHCN$)

The above section demonstrates problems in hydrogenating 3-phenylpropionitrile. As previous reports have noted, conjugation of the nitrile group can assist reduction of that unit,[114] so it was deemed useful to consider the case of cinnamonitrile. Could the presence of the double bond and conjugation between the nitrile group and the aromatic ring be used to induce hydrogenation of the nitrile group? If yes, then this would be a viable route to 3-phenylpropylamine ($C_6H_5CH_2CH_2CH_2NH_2$). The reaction profile is shown in Figure 50 and shows hydrogenation of the double bond to yield 3-phenylpropionitrile to be rapid and comprehensive. Interestingly however, no further reduction takes place thereafter, with the nitrile functional unit remaining intact and the system returning a complete mass balance, as shown in Scheme 16. Thermodynamically, in systems without ammonia, the C=C bond has been shown to preferentially adsorb and be reduced over the CN group.[114] This is entirely consistent with Figure 50, where only reduction of the olefinic unit is seen; no 3-phenylpropylamine is detectable over the full reaction coordinate.

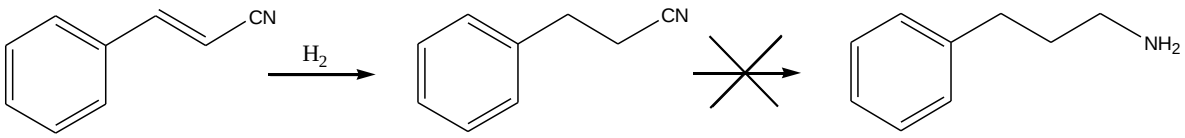

Cinnamonitrile 3-Phenylpropionitrile 3-Phenylpropylamine

Scheme 16. The hydrogenation of cinnamonitrile to phenylpropionitrile. Reduction of the nitrile functionality was found not to be facile under the conditions used here.

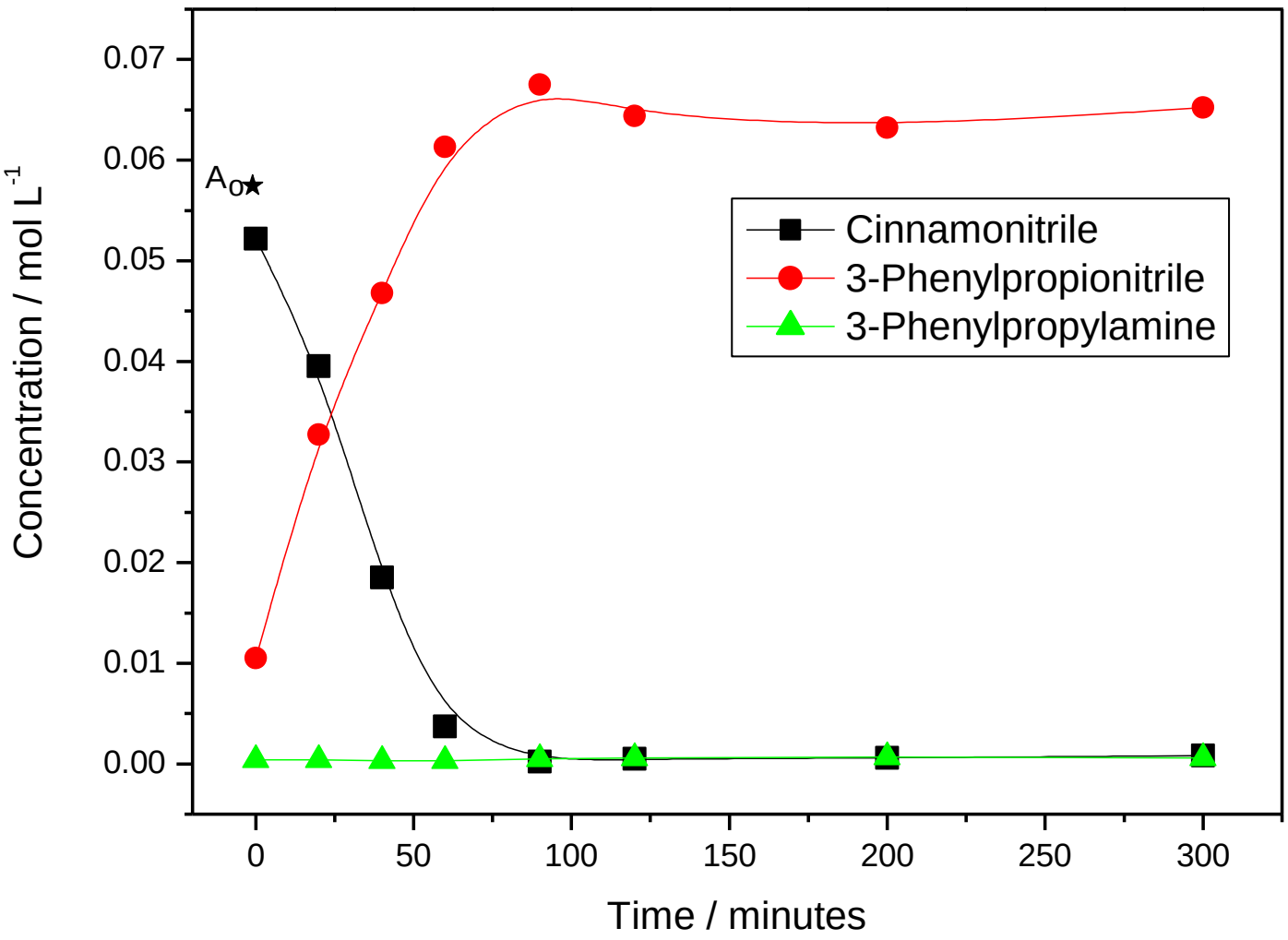

Figure 50. The hydrogenation profile of cinnamonitrile over 0.5 g 5% Pd/C, 333 K, 4.0 bar, ca. 0.017 moles of cinnamonitrile, showing that olefin hydrogenation was fast, but reduction of the nitrile functionality was not observed. Ao indicated the incident concentration of nitrile.

3.4.4 The co-adsorption of benzonitrile and benzyl cyanide

In an attempt to further understand the connection between different amines and hydrogenation lability, the hydrogenation of equimolar amounts of benzonitrile and benzyl cyanide were investigated. Figure 51 below shows the resulting reaction profile. In line with their individual profiles (Figure 23 and Figure 48 respectively), both reagents are fully converted, although at a slower rate than seen previously. This is thought to reflect competition for hydrogenation sites (Site II).

Hydrogen consumption corresponds to a smooth growth curve and stops once no reagents remain. Concentrating first on benzonitrile, a similar profile to Figure 23 is discernible, with benzylamine displaying an intermediate profile and toluene identified as the final product. However, the profile connected with benzyl cyanide conversion is different to that seen in Figure 48, because significant quantities of phenethylamine are seen in Figure 51. Previously (Section 3.4.1), the absence of this product was attributed to retention by the carbon support. Its presence in the liquid phase in Figure 51 (below) suggests there to be a degree of competition for adsorption sites on the carbon under co-adsorption conditions. Moreover, the fact it is observable in this case gives some credibility to the assumption that phenethylamine is actually produced though not seen when only benzyl cyanide and hydrogen are added as reagents (Figure 48).

A further point worth noting in Figure 51 is an incomplete mass balance of 57% (of the incident concentration of reagents) at the end of sampling time. This mass loss is accounted for by formation of the secondary amine *N*-benzyl-2-phenethylamine ($C_6H_5CH_2CH_2$-NH-$CH_2C_6H_5$, or NBPEA) via the cross-coupling of intermediate benzylimine ($C_6H_5CH{=}NH$) with phenethylamine, or possibly of phenethylimine ($C_6H_5CH_2CH{=}NH$) with benzylamine, as referenced against analytical standards. No products were observed corresponding to the symmetrical secondary amines that one would expect from the coupling of (i) phenethylimine with phenethylamine or (ii) benzylimine with benzylamine. The remaining mass imbalance (small) can be accounted for by residual phenethylamine on the carbon support.

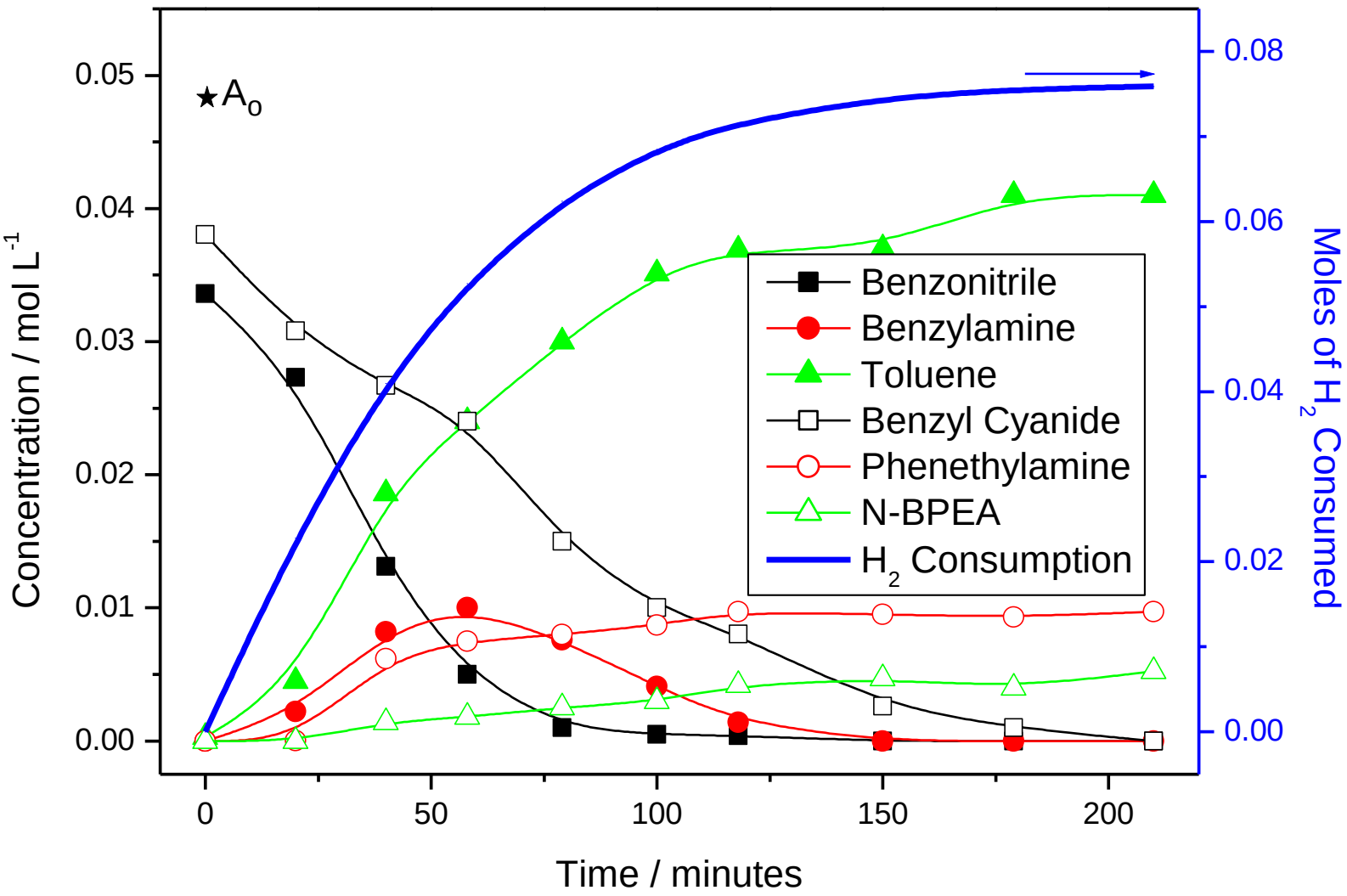

Figure 51. The co-hydrogenation of benzonitrile and benzyl cyanide over 0.5 g 5% Pd/C, 333 K, 4.0 bar, ca. 0.017 moles of benzonitrile and benzyl cyanide. Ao indicates the incident concentration of each nitrile.

Clearly, the co-adsorption of benzonitrile and benzyl cyanide leads to a series of competing interactions which perturb the reaction profiles seen in the single hydrogenation reactions. Not least, this includes competition for adsorption sites on the carbon support by the benzyl cyanide derived amine (phenethylamine) as well as formation of secondary amines (*N*-benzyl-2-phenethylamine).

Scheme 17 attempts to illustrate the various sets of interdependencies, whilst additionally recognising the site-selective nature of the Pd crystallites as defined in the catalyst model in Figure 39. Further, since neither benzylimine nor phenethylimine are observed in the liquid phase, it is believed that the coupling reactions that lead to formation of the secondary amine must be catalyst mediated.

Scheme 12 can also be used to describe outcomes seen for nitriles other than benzonitrile. For benzyl cyanide and 3-phenylprionitrile, no amine is seen in the liquid phase in either case. Concentrating on benzyl cyanide first, which exhibits full conversion with associated hydrogen uptake within 200 minutes, it is assumed that the absence of phenethylamine indicates that this material is bound to the catalyst surface. However, as the quantity of amine vastly exceeds the surface Pd density (365 : 1) then this capacity can only be accommodated by the carbon support material. Assuming that hydrogenation only occurs on the metal, one needs to invoke a spillover process where the amine is actually bound to the carbon. In this situation K_4 must disfavour partitioning from the metal to the liquid phase and the rate of spillover must be a relatively facile process under the conditions examined here.

The situation is different with 3-phenylpropionitrile as, in contrast to benzyl cyanide, only a finite degree of conversion (*ca.* 15%) is seen. Thus, with reference to Scheme 12, it is thought that K_4 strongly favours retention of amine at the metal surface which effectively poisons the catalyst and prevents any further hydrogenation activity. The fact that the degree of retained molecules exceeds the surface Pd density (76 : 1) indicates that spillover is occurring as well.

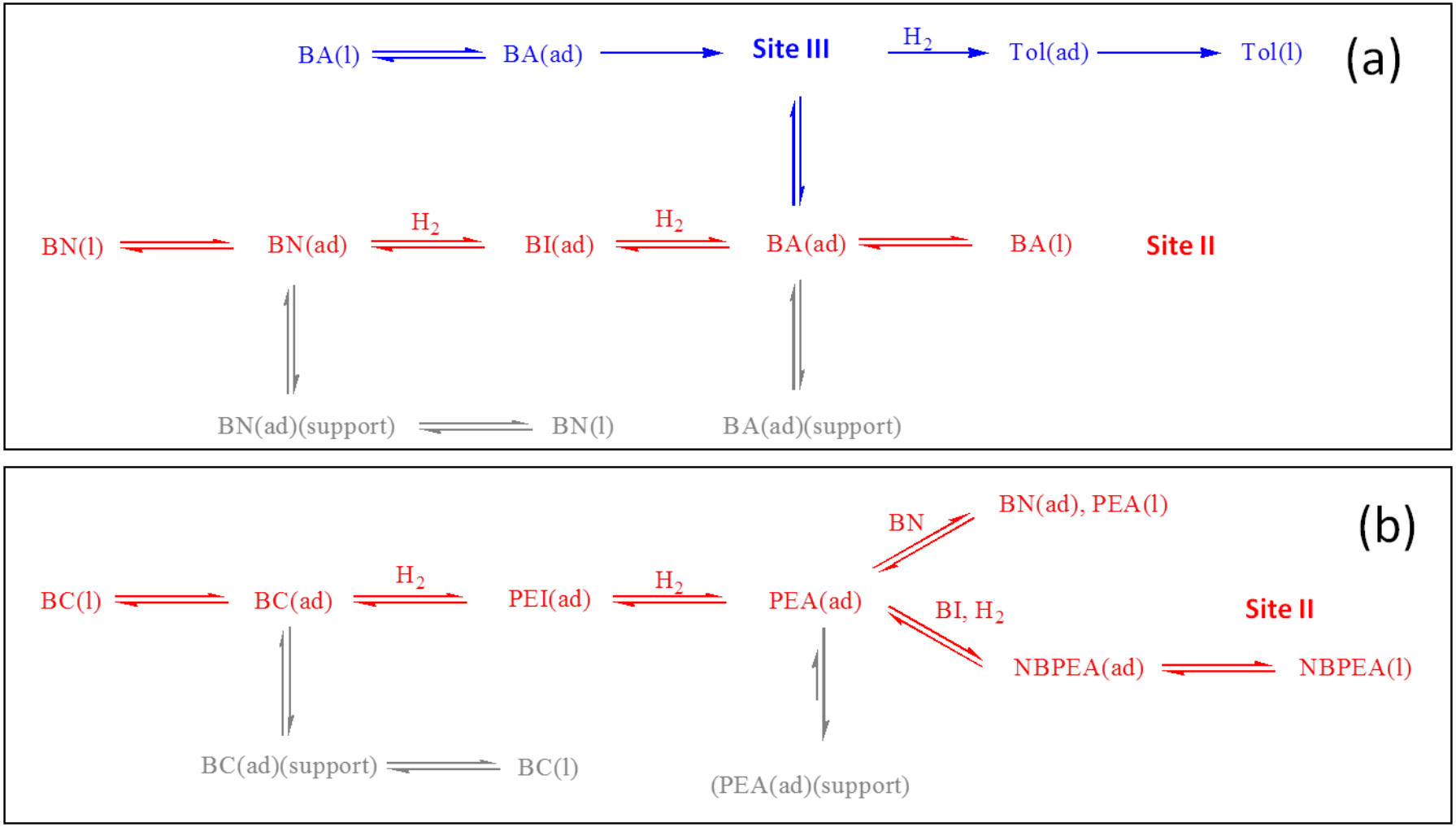

Scheme 17. Proposed reaction schemes for the co-hydrogenation of (a) benzonitrile and (b) benzyl cyanide, showing the role of hydrogenation site (red, Site II), hydrogenolysis site (blue, Site III) and the support (grey), and the need for addition of an additional species in order to observe reaction products.

3.4.5 Conclusions

The liquid phase hydrogenation of benzyl cyanide, 3-phenyl propionitrile and cinnamonitrile over a 5% Pd/C catalyst was investigated in isopropyl alcohol at 4 bar and 333 K. The following observations can be made.

- Benzyl cyanide and 3-phenylpropionitrile hydrogenation result in no product formation in the liquid phase. In the case of 3-phenylpropionitrile loss of activity is attributed to amine product poisoning Pd sites. For benzyl cyanide, converted product is believed to partition on to the carbon support.

- 3-Phenylpropionitrile is the only product in the hydrogenation of cinnamonitrile. The carbon-carbon double bond is selectively reduced with respect to the carbon-nitrogen triple bond. The conjugation between the nitrile group and the aromatic ring did not assist nitrile reduction in this case.

- Hydrogenation of a mixture of benzonitrile and benzyl cyanide indicates the competitive nature of the reaction system, which induces the presence of phenethylamine (source = benzyl cyanide hydrogenation) in to the liquid phase. This coincides with the formation of the secondary amine *N*-benzyl-2-phenethylamine which, due to the absence of imines in the reaction mixture, is thought to form at the catalyst (Pd) surface.

3.5 Issues relevant to the hydrogenation of mandelonitrile ($C_6H_5CH(OH)CN$)

In a move towards more complex nitrile model compounds, mandelonitrile was considered as an ideal candidate to probe the nature of cyanohydrin hydrogenation activity over Pd/C. As with the hydrogenation of all cyanohydrins, two possible reaction routes were envisaged and are summarised in Scheme 18, below. Firstly, if k_3 was favoured, then a loss of water would lead to benzyl cyanide as a reaction intermediate, before being converted to the desired primary amine product, phenethylamine ($C_6H_5CH_2CH_2NH_2$). Secondly, were k_1 to be favoured, then nitrile hydrogenation would occur first giving the hydroxylamine, 2-amino-1-phenylethanol ($C_6H_5CH(OH)CH_2NH_2$), as an intermediate. Subsequent conversion leads to the same primary amine (phenethylamine) as the final product.

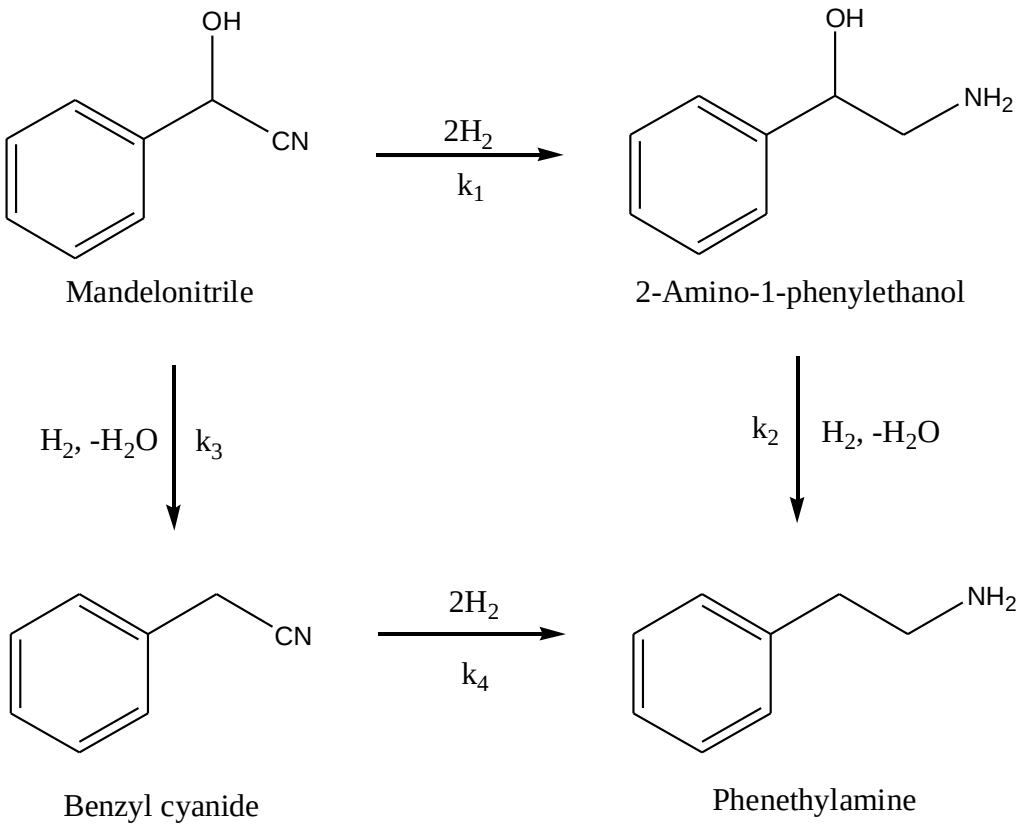

Scheme 18. The 2 possible routes for mandelonitrile reduction to phenethylamine.

The initial thoughts regarding the reaction mechanism for mandelonitrile was that the loss of hydroxyl group occurred via a conventional dehydration reaction. However, with the knowledge gained from the hydrogenolysis of benzylamine, it is proposed that the loss of water in mandelonitrile is facilitated by a hydrogenolytic

mechanism. It is known that in organic synthesis strategies, benzyl groups can be used as protection for alcohols by the same mechanism as outlined in Scheme 10.[107] For mandelonitrile and the intermediate 2-amino-1-phenylethanol, the same "dual" binding geometry can be attained (*i.e.* adsorption of the aromatic ring and the hydroxyl group) that would lead to the loss of water. In such a case, and with reference to Scheme 10, the -XR group may be attributed to the alcohol functionality, whereas the –R' group is characterised as either CN (for mandelonitrile) or as $–CH_2NH_2$ (for 2-amino-1-phenylethanol). Given the high activity associated with benzonitrile hydrogenation and benzylamine hydrogenolysis, the multi-step hydrogenation of mandelonitrile was predicted to be facile over a Pd/C catalyst.

3.5.1 Mandelonitrile hydrogenation

Surprisingly, under the conditions used here, mandelonitrile proved difficult to hydrogenate. Figure 52 shows that only very small concentrations of intermediate 2-amino-1-phenylethanol were formed in the early stages of reaction, reaching a maximum at around 20 minutes, and remaining constant thereafter. Interestingly, hydrogen uptake ceased at a time approximating to maximum 2-amino-1-phenylethanol concentration. As a result of the poor conversion of mandelonitrile, only very small amounts of phenethylamine were observed in the liquid phase and only in the early stages of reaction. However, after reaching a maximum concentration at around 12 minutes, any phenethylamine formed was lost to the reaction system (presumably to the catalyst or carbon support). Despite the poor progress of reaction, it was observed that no benzyl cyanide was formed, even in the very early "active" stages of the reaction. This suggested that k_1 was strongly favoured, and that k_3 was strongly disfavoured.

From the reaction profile, it appears that any initial conversion of mandelonitrile ceased upon formation of intermediate 2-amino-1-phenylethanol. Such an observation may be consistent with a self-poisoning reaction whereby 2-amino-1-phenylethanol may be much more strongly adsorbed onto the catalyst than mandelonitrile, resulting in the blocking of available Pd sites and the cessation of reaction. Further investigations into to such a scenario will be discussed later.

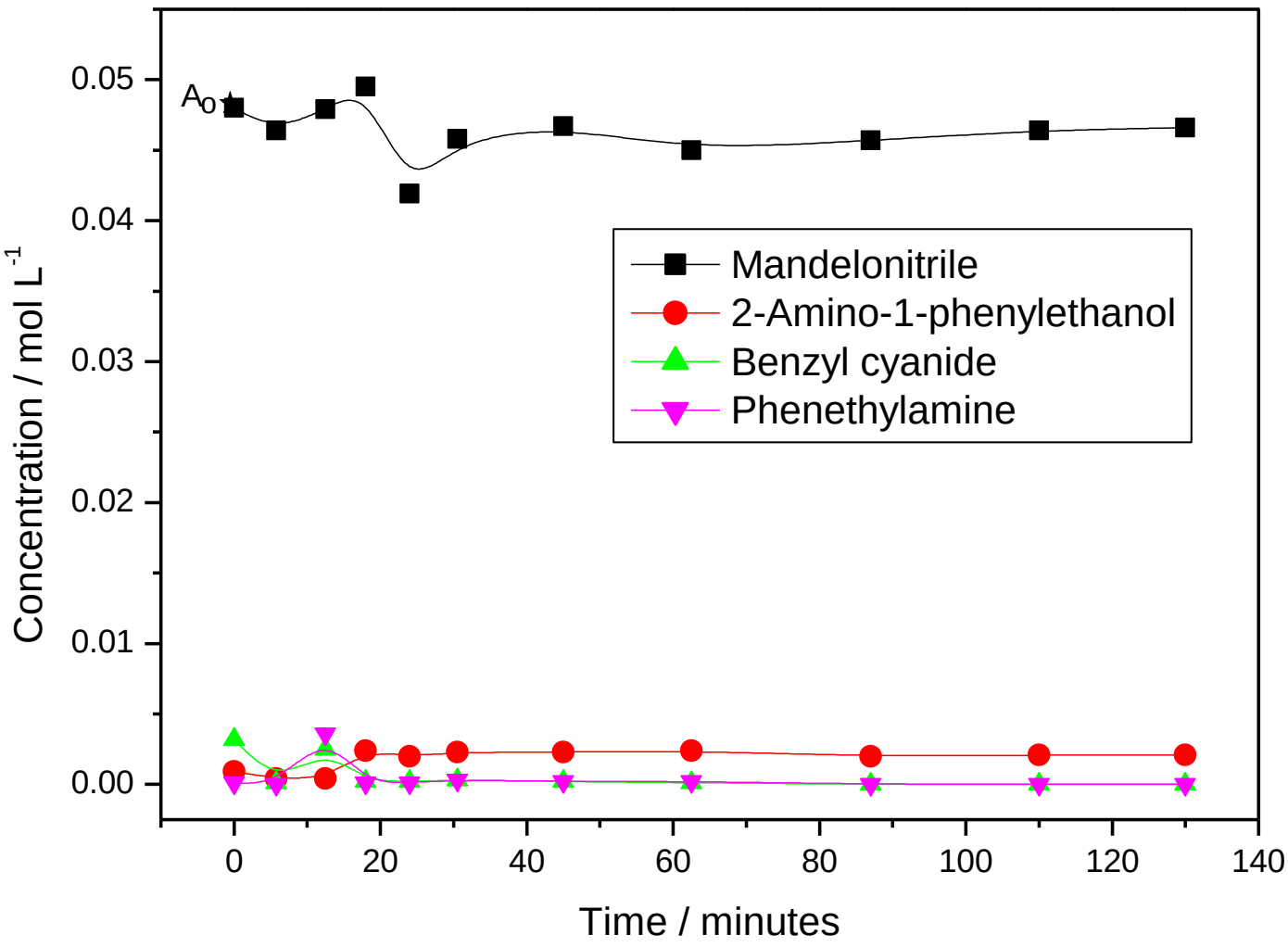

Figure 52. The hydrogenation profile of mandelonitrile over 0.5 g 5% Pd/C, 333 K, 4.0 bar, ca. 0.017 moles of mandelonitrile, showing the non-facile nature of nitrile reduction. Ao indicated the incident concentration of nitrile.

3.5.2 2-Amino-1-phenylethanol hydrogenolysis

Given that since small concentrations of 2-amino-1-phenylethanol were observed in the liquid phase for mandelonitrile hydrogenation over Pd/C, its conversion to phenethylamine was considered to try and understanding what effect (if any) the hydroxyamine has upon catalyst activity. Interestingly, despite no observable conversion in the reaction profile (Figure 53), as determined by a very small hydrogen uptake, a large amount of 2-amino-1-phenylethanol was retained by the catalyst/support (2-amino-1-phenylethanol$_{(missing)}$: Pd$_{(s)}$ = 228 : 1).

Two possible reasons for the poor activity of the Pd/C in such a hydrogenolysis reaction were envisaged. Firstly, the catalyst is simply inactive for such a transformation. This would appear to be unlikely given the highly active hydrogenolysis reactions observed in the benzonitrile studies in both liquid and gas phases. Also, it is widely regarded in the organic literature that the breaking of a C-O bond in hydrogenolysis deprotection methods, is much easier than the breaking of a C-N bond.[94,99] Again, when one considers the ease of C-N breaking in the benzonitrile studies, inactivity of the catalyst for such a transformation seems improbable.

Secondly, when one considers that a hydroxyamine intermediate is a known poison in the industrial process (see Section 1.7), it is possible that 2-amino-1-phenylethanol may also be a poison over Pd/C. Given the differing concentrations of 2-amino-1-phenylethanol and mandelonitrile observable in the liquid phase*, i.e*. mandelonitrile was not retained by the catalyst in Figure 52, but 2-amino-1-phenylethanol was in Figure 53, this further suggests that 2-amino-1-phenylethanol was more strongly adsorbed. Since some conversion occurs in mandelonitrile hydrogenation up to the point of maximum 2-amino-1-phenylethanol concentration, evidence for the poisoning effect of the hydroxyamine is further alluded to.

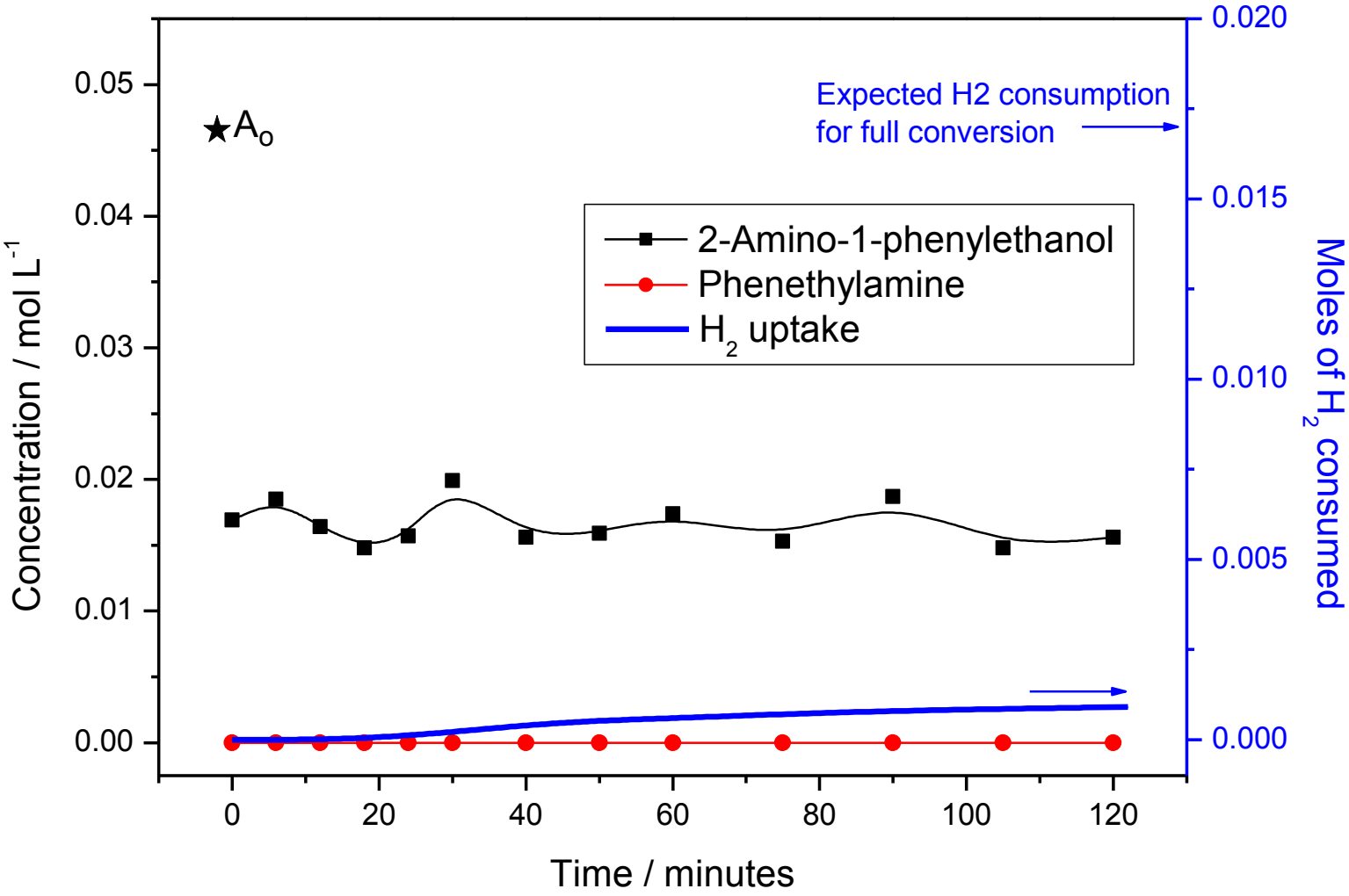

Figure 53. The reaction profile and hydrogen uptake for the hydrogenolysis of 2-amino-1-phenylethanol over 0.5 g 5% Pd/C, 333 K, 4.0 bar, ca. 0.017 moles of 2-amino-1-phenylethanol, showing the non-facile nature of nitrile reduction. Ao indicated the incident concentration of nitrile.

3.5.3 Co-adsorption studies

3.5.3.1 Mandelonitrile and benzonitrile co-adsorption

To test the hypothesis of mandelonitrile being a self-poisoning reaction, the facile and well understood benzonitrile was used as a probe reaction. Previous work found benzonitrile to be facile to hydrogenation under the same conditions used here, and with a relatively fast reaction rate (Section 3.3). To investigate the nature of adsorption of the species involved in mandelonitrile hydrogenation, it was used as a “probe reaction”. The degree to which benzonitrile underwent conversion can therefore act as a measure of how the mandelonitrile reaction poisons the Pd/C catalyst.

Equimolar amounts of mandelonitrile and benzonitrile were added together and the reaction carried out as before. Figure 54 shows that some mandelonitrile was lost from the liquid phase, but no products for that reaction were observed at all. However, the concentration of benzonitrile remained effectively constant for the duration of sampling time and retained a relatively complete mass balance. No products of the benzonitrile reaction were observed, and there had been no issue relating to their retention in previous studies. Only a small amount of hydrogen was consumed by the reaction, indicating that little conversion of mandelonitrile or benzonitrile had taken place and that the mandelonitrile reaction was poisoning the catalyst.

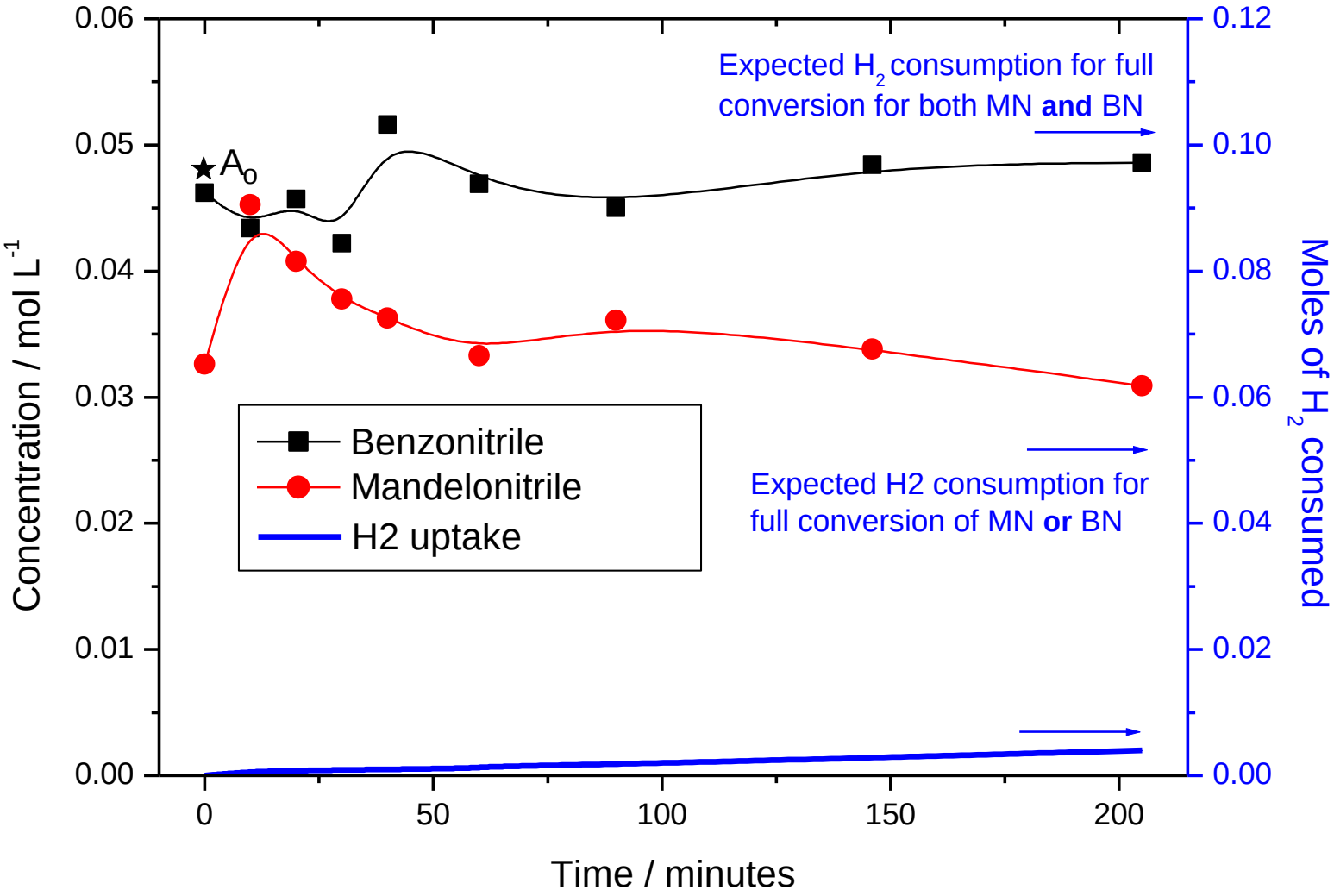

Figure 54. The co-hydrogenation of benzonitrile and mandelonitrile over 0.5 g 5% Pd/C, 333 K, 4.0 bar, ca. 0.017 moles of benzonitrile and mandelonitrile. Ao indicates the incident concentration of each nitrile.

3.5.3.2 2-Amino-1-phenylethanol and benzonitrile co-adsorption

When a similar experiment was carried out using equimolar amounts of 2-amino-1-phenylethanol and benzonitrile, no conversion of either substrate was observed (Figure 55). Benzonitrile concentration remained constant with no products observed and no hydrogen was consumed by the reaction. Here, 2-amino-1-phenylethanol was observed in larger concentrations in the initial stages than it was in the single reaction (Figure 53), but tailed off to reach a similarly low level. The profile is indicative of 2-amino-1-phenylethanol approaching its equilibrium value, but the kinetics of this process are retarded by competitive adsorption between benzonitrile and 2-amino-1-phenylethanol for Pd sites. However, 2-amino-1-phenylethanol exhibits the higher adsorption coefficient. The early high levels of 2-amino-1-phenylethanol is assumed to be due to competition for palladium/support sites with benzonitrile. Any loss of 2-amino-1-phenylethanol from the liquid phase must primarily be as a result of retention on the catalyst support ($2\text{-amino-1-phenylethanol}_{(missing)}$: $Pd_{(s)}$ = 213 : 1). However, any adsorption of 2-amino-1-phenylethanol on Pd has a high enough strength of adsorption to block the site, and confirm that 2-amino-1-phenylethanol acts as a poison.

3.5.3.3 Mandelonitrile and benzylamine co-adsorption

A similar co-adsorption study could not be obtained for mandelonitrile and benzylamine hydrogenations due to safety concerns. There is a risk that when cyanohydrins are under basic conditions (with benzylamine being a base), that they may break down to form HCN as shown in Scheme 13 (Section 3.3 cyanohydrin breakdown). Therefore, the reaction was not considered in this study.

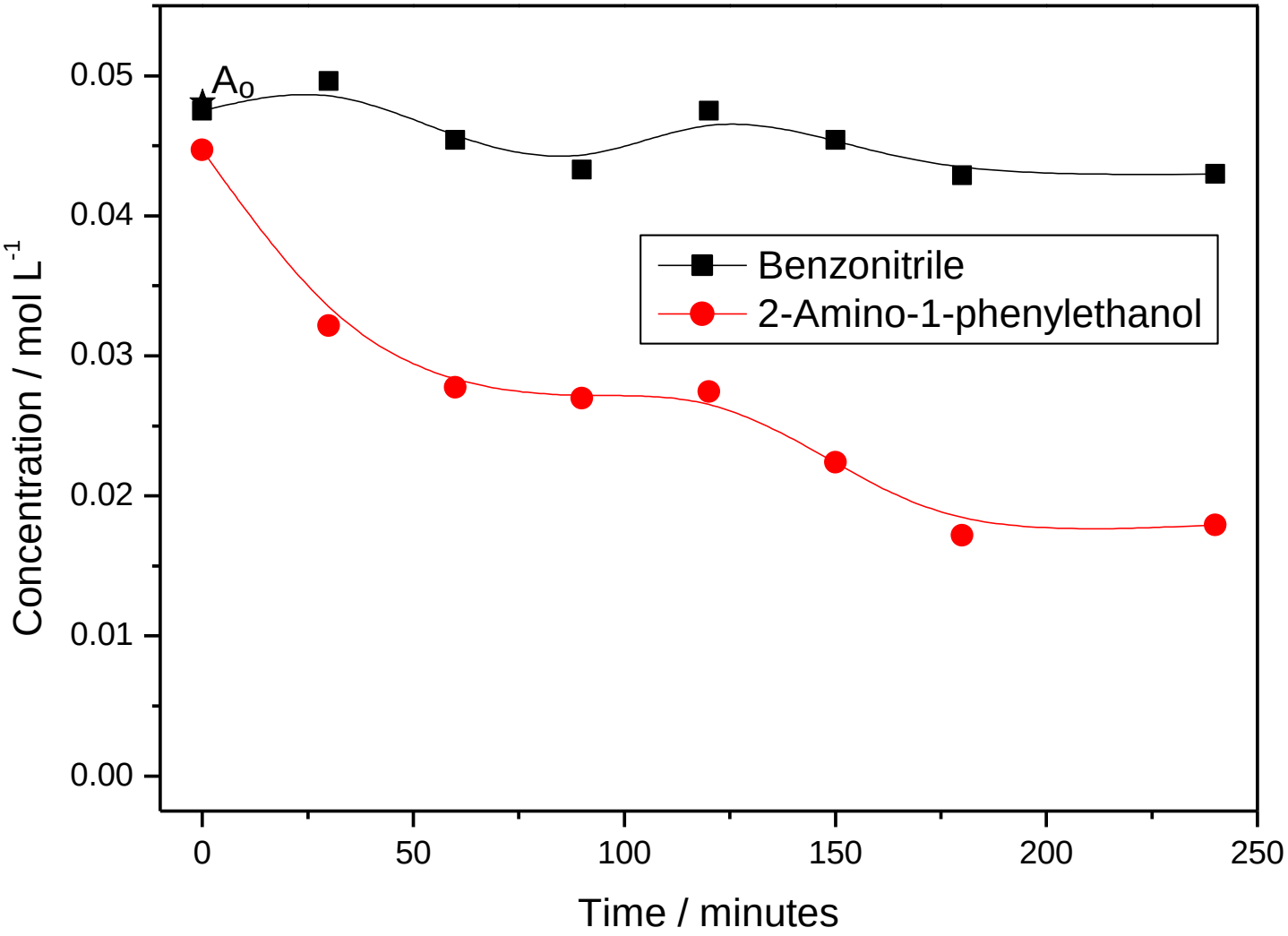

Figure 55. The co-hydrogenation of benzonitrile and 2-amino-1-phenylethanol over 0.5 g 5% Pd/C, 333 K, 4.0 bar, ca. 0.017 moles of benzonitrile and 2-amino-1-phenylethanol. Ao indicates the incident concentration of each nitrile.

3.5.4 Mandelonitrile hydrogenation with an acid additive (sulphuric acid)

Similar to the hydrogenation of benzonitrile discussed previously (Section 3.3.6.2), H_2SO_4 was used as an acidic additive in the hydrogenation of mandelonitrile. Acid additives have been shown to be useful in controlling selectivity to primary amines in other nitrile hydrogenation reactions.[56,57] The acid functions by forming a hydrogen sulfate ($[HSO_4]^-$) salt with amine products (Scheme 19), and thus preventing them from reacting to produce secondary and tertiary amines. Here, it was hoped that the acid would protonate amine products and thus prevent them from having the necessary amine 'anchor' believed to be the cause of their retention on the catalyst/support system.

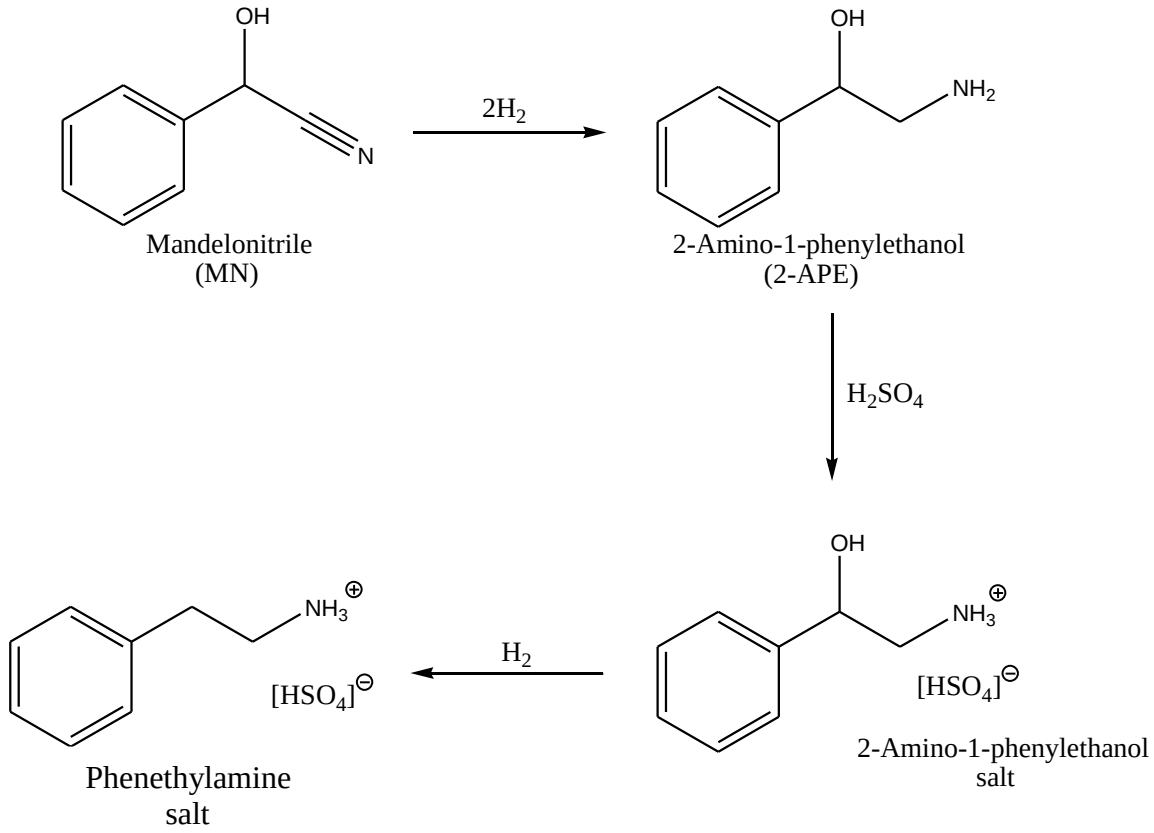

Scheme 19. Mandelonitrile hydrogenation under acidic conditions to yield phenethylamine salt.

As a test case, the reaction was first performed at atmospheric pressure in the ambient pressure glass reactor. In such a reactor, complete conversion of mandelonitrile occurred within approximately 1 hour (Figure 56). The reduced concentration of mandelonitrile at time zero was coupled with phenethylamine salt

forming from the onset of reaction, resulting in a complete initial mass balance. 2-Amino-1-phenylethanol (salt) is formed as an intermediate with maximum concentration observed at around 20 minutes, before it is converted to phenethylamine (salt). Only a very small concentration of benzyl cyanide is observed in the initial stages, showing that mandelonitrile hydrogenation proceeds almost exclusively via 2-amino-1-phenylethanol salt. The profile is suggestive of a 2-step consecutive process in much the same way as benzonitrile conversion to toluene was. Such a dramatic change in activity as compared to reactions under neutral conditions was surprising, given that conversion could be increased from around 0% to 100% with merely the addition of an acid.

For a direct comparison with the previous mandelonitrile hydrogenation studies, the reaction was repeated at elevated pressure in the Buchi batch autoclave. At increased pressure (4 bar), the hydrogenation of mandelonitrile occurred in a similar manner, but with a much faster rate (Figure 57) than at atmospheric pressure. Here, 2-amino-1-phenylethanol and phenethylamine salts were both observed in the liquid phase in the initial stages of reaction. 2-Amino-1-phenylethanol salt is again the predominant intermediate species present, confirming that the reaction proceeds via the hydroxyamine. Hydrogen consumption ceases at around 20 minutes, indicating complete reaction and the hydrogen uptake equates to that expected for complete conversion of mandelonitrile to phenethylamine salt.

Under neutral conditions, it is believed that 2-amino-1-phenylethanol binds strongly (possibly irreversibly) to the site responsible for hydrogenation (Site II) as is shown in Scheme 20. It is known that some amine products from aliphatic nitrile hydrogenation reactions, can bind irreversibly to the catalyst, reducing catalyst lifetime and eventually leading to total retardation of activity.[115] Such a binding geometry prevents hydrogenolysis since the geometry required as outlined in Scheme 10, cannot be attained.

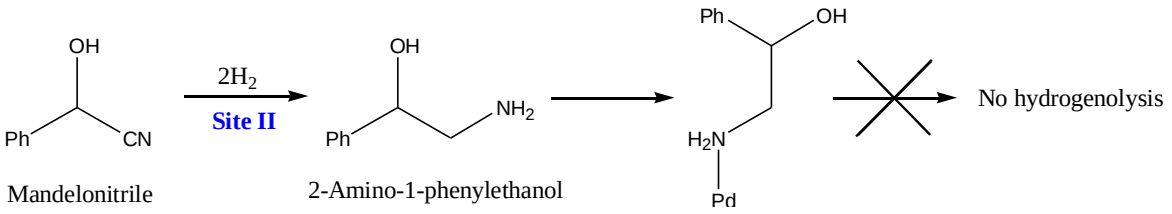

Scheme 20. Mandelonitrile hydrogenation self-poisoning mechanism whereby the intermediate 2-amino-1-phenylethanol adsorbs irreversibly at the nitrogen lone pair and thus preventing the correct binding orientation for hydrogenolysis.

In the presence of acid however, the formation of R-NH_3^+ prevents the amine group from binding to the catalyst surface, thus enabling the intermediate hydroxyamine to bind in the correct geometry to facilitate hydrogenolysis, *i.e.* adsorption of the aromatic centre and the hydroxyl group (Scheme 21).

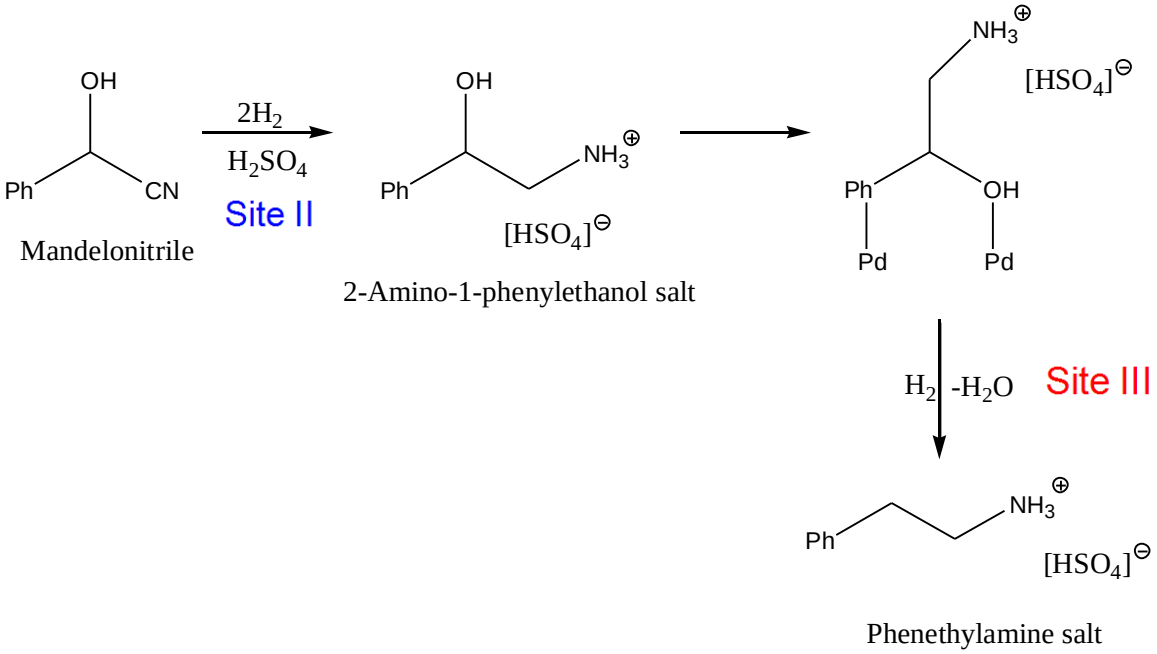

Scheme 21. Mandelonitrile hydrogenation with an acid additive, showing that protonation of the amine groups prevents adsorption at the nitrogen load pair. Thus, the correct binding orientation to facilitate hydrogenolysis is favoured and the reaction can proceed to yield phenethylamine (salt).

Therefore, it has been shown that with the addition of equimolar (or higher) amounts of acid, the poisoning effect of mandelonitrile hydrogenation can be prevented. In doing so, conversion can be increased from an extremely low amount to 100%, and selectivity to the salt of the desired primary amine can be increased to near 100%. As with the benzylamine salt in previous acid studies (Section 3.3.6.2), phenethylamine can be isolated by the reaction of its hydrogen sulfate salt by treatment with sodium hydroxide.

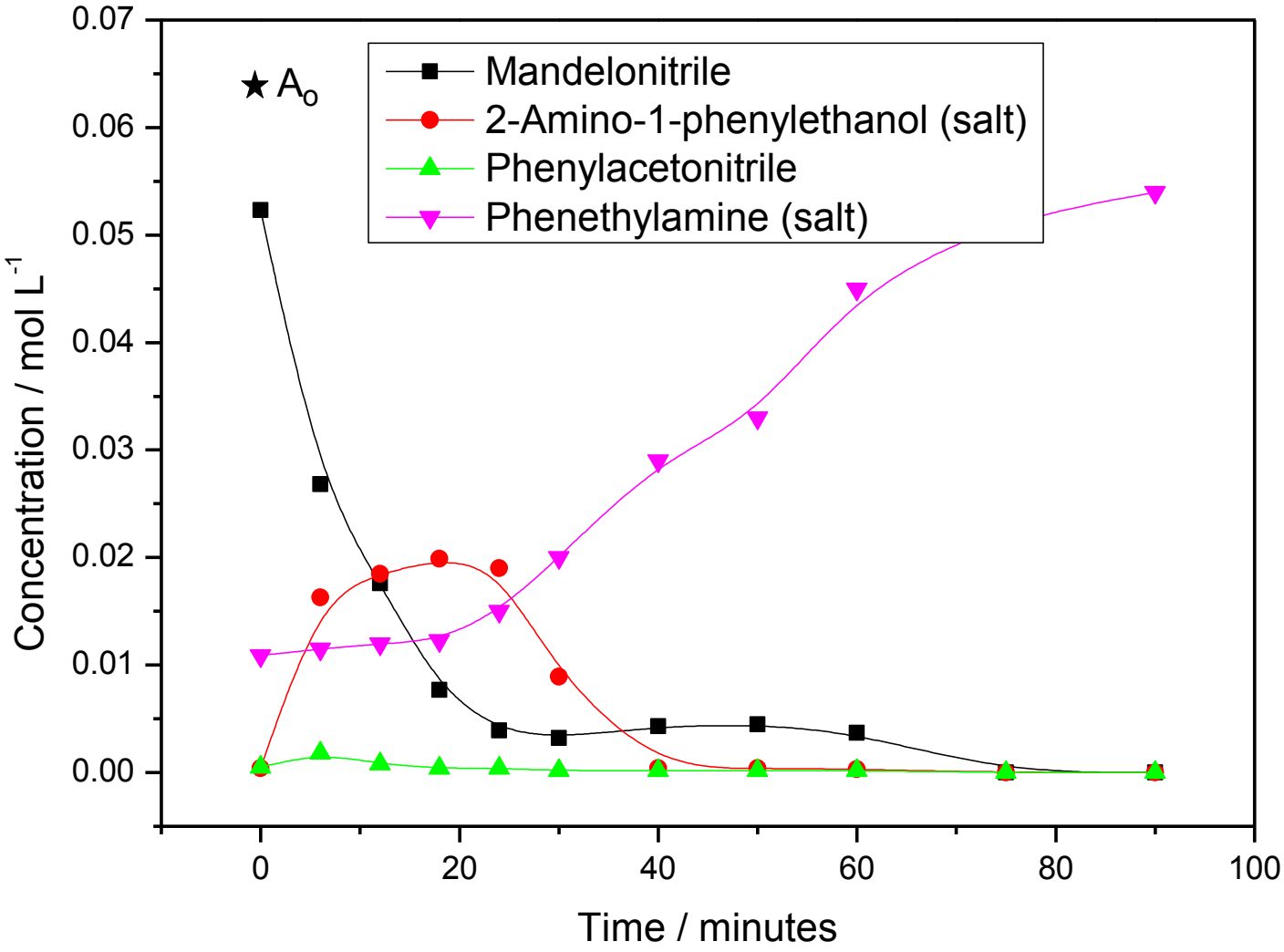

Figure 56. Reaction profile for the hydrogenation of mandelonitrile over 0.5 g 5% Pd/C, 60°C, ambient pressure reactor, ca. 0.003 moles of mandelonitrile, equimolar H_2SO_4. Ao indicates the incident concentration of nitrile.

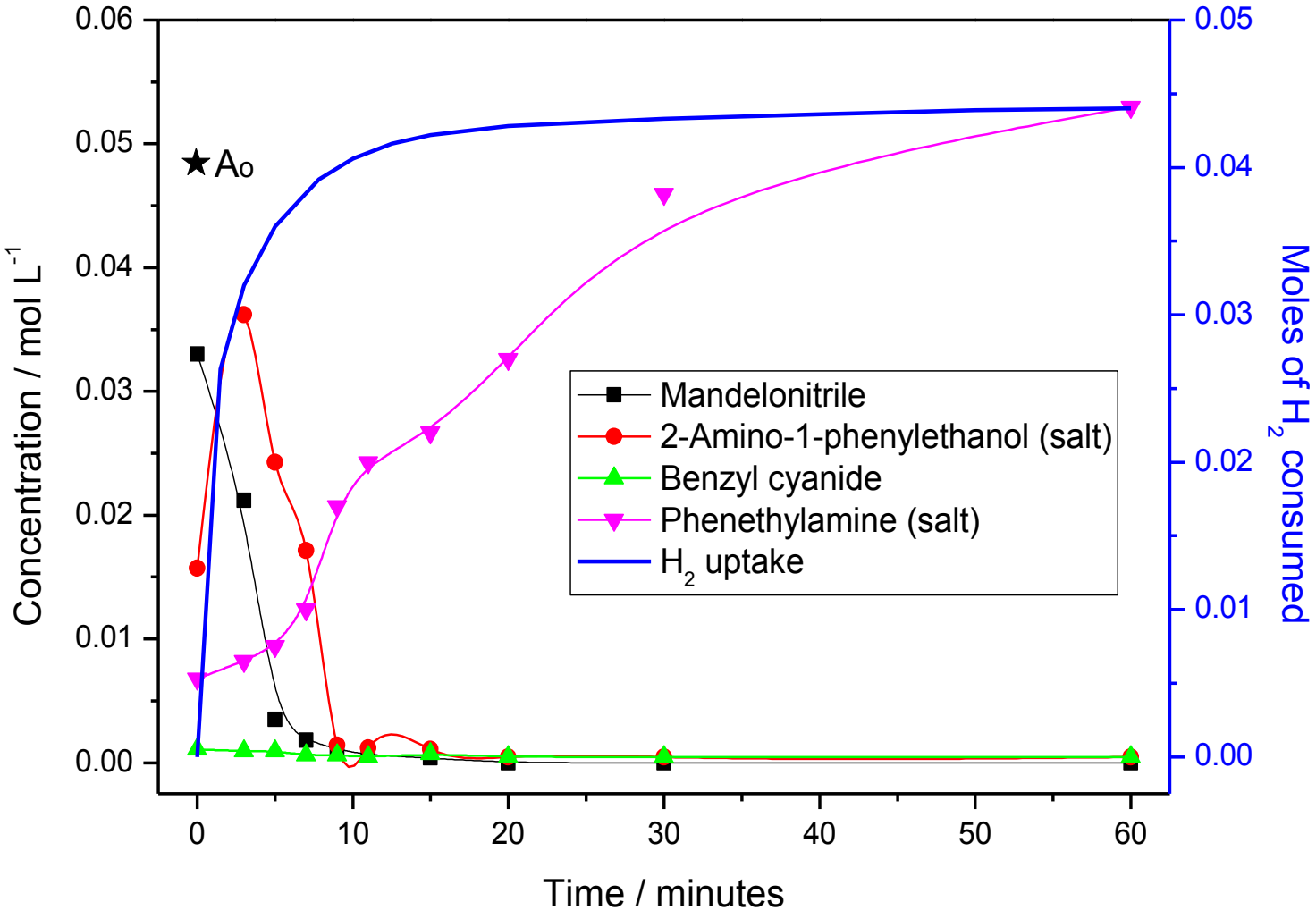

Figure 57. Reaction profile for the hydrogenation of mandelonitrile over 0.5 g 5% Pd/C, 60°C, 4 bar hydrogen, ca. 0.017 moles of mandelonitrile, equimolar H_2SO_4. Ao indicates the incident concentration of nitrile.

3.5.5 Replicating the fed-batch system of the industrial centre with multiple mandelonitrile additions

As was discussed in the introductory remarks, the industrial process uses a fed-batch reactor and suffers from catalyst deactivation over time. However, under acidic conditions, no deactivation issues were observed for any model systems tested thus far. Therefore, in an attempt to replicate the fed-batch nature of the industrial reactor, repeat additions of reactants was performed.

Mandelonitrile and sulphuric acid were added in equimolar amounts to the ambient pressure reactor and allowed to react as has been previously discussed. Then, a second aliquot of reactants (both mandelonitrile and acid) was added and given a similar length of time for reaction with no sampling. Once a sufficient period of time had passed (typically 90 minutes), a reaction sample was analysed and a significant amount of unreacted mandelonitrile was observed. This process was repeated a further twice, *i.e.* 4 additions of mandelonitrile /acid in total. After each addition and subsequent reaction time, a larger amount of mandelonitrile remained in the liquid phase until the 4^{th} addition when no conversion of mandelonitrile occurred (Figure 58). Conversion of mandelonitrile fell from close to 100% for the initial addition, to 0% for the 4^{th} addition. Hence, despite the addition of acid, which had been shown to prevent poisoning of the catalyst, the catalyst loses activity with each charge of the reactor. Eventually, upon the 4^{th} addition, all hydrogenation activity was lost.

This shows that there is an additional source of catalyst deactivation not directly encountered up to now. Given that for the first run (effectively) complete conversion of mandelonitrile is observed, it would seem that an initially minority process is simultaneously underway which on increased cycling comes to dominate the process.

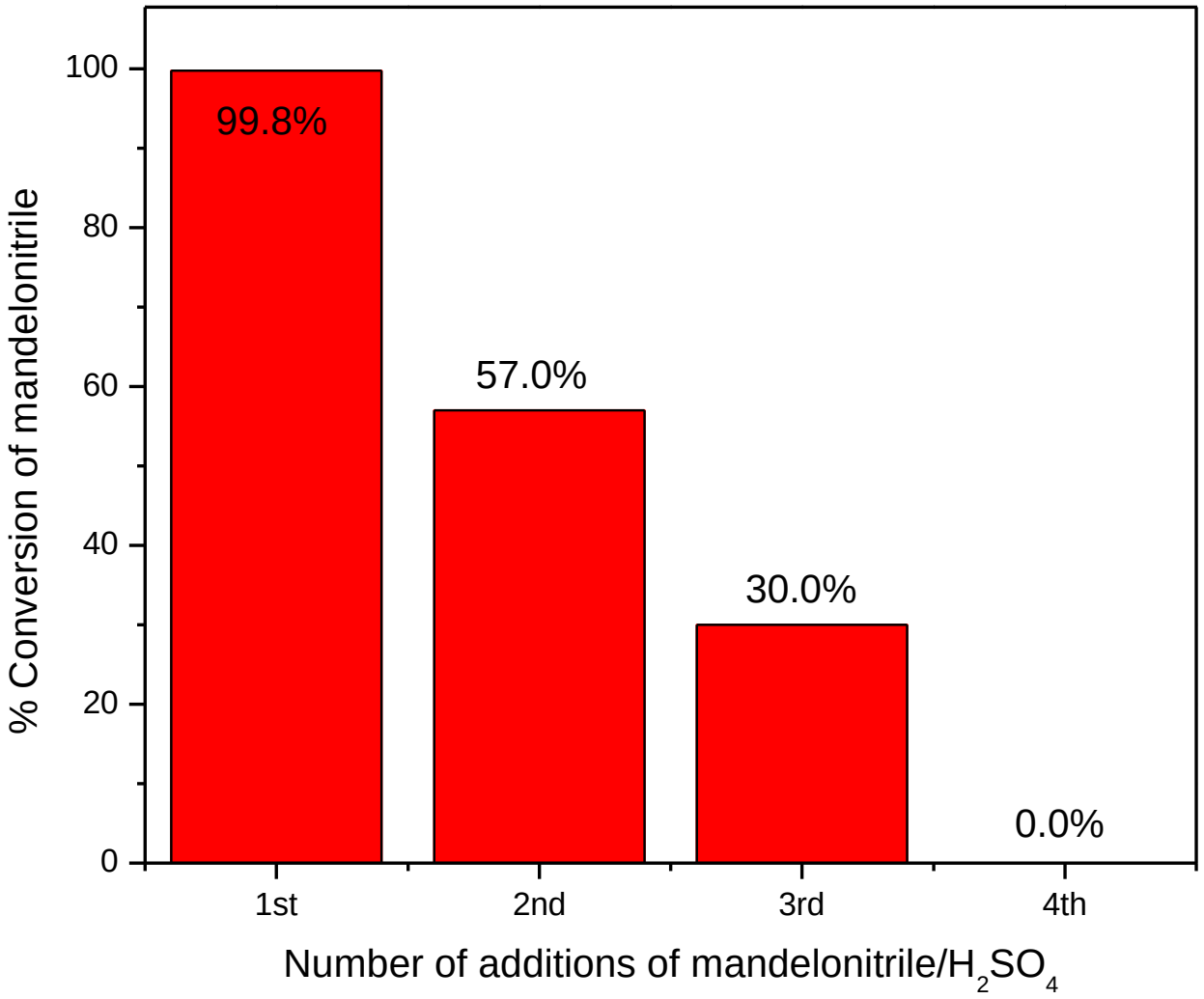

Figure 58. The change in conversion after repeat additions in the hydrogenation of mandelonitrile over Pd/C.

This cumulative poisoning effect was attributed to a build up of species on active sites. One possibility is through the deposition of a carbonaceous over-layer by the breakdown of reagents/products. Secondly, it is believed that residual imine intermediate can lead to secondary and tertiary amines that may be responsible for the poisoning. It was proposed that both weakly and strongly bound imine species were present. When weakly bound, the imine was free to continue conversion to hydroxyamine and further to the desired primary amine product. However, when strongly bound to higher energy catalytic sites (possibly “edge sites”), an alternative route can be opened whereby coupling of imine and amine leads to higher amines, as is shown in Scheme 22. The surface area taken up by strongly adsorbed secondary and tertiary amines leads to a sudden and increasing loss of activity. Since no imines or higher amines were observed in the liquid phase it was assumed that this process must be limited to the catalyst surface. However, spectroscopic surface studies have yet to be performed on this system, so the true nature of the poisoning is unclear.

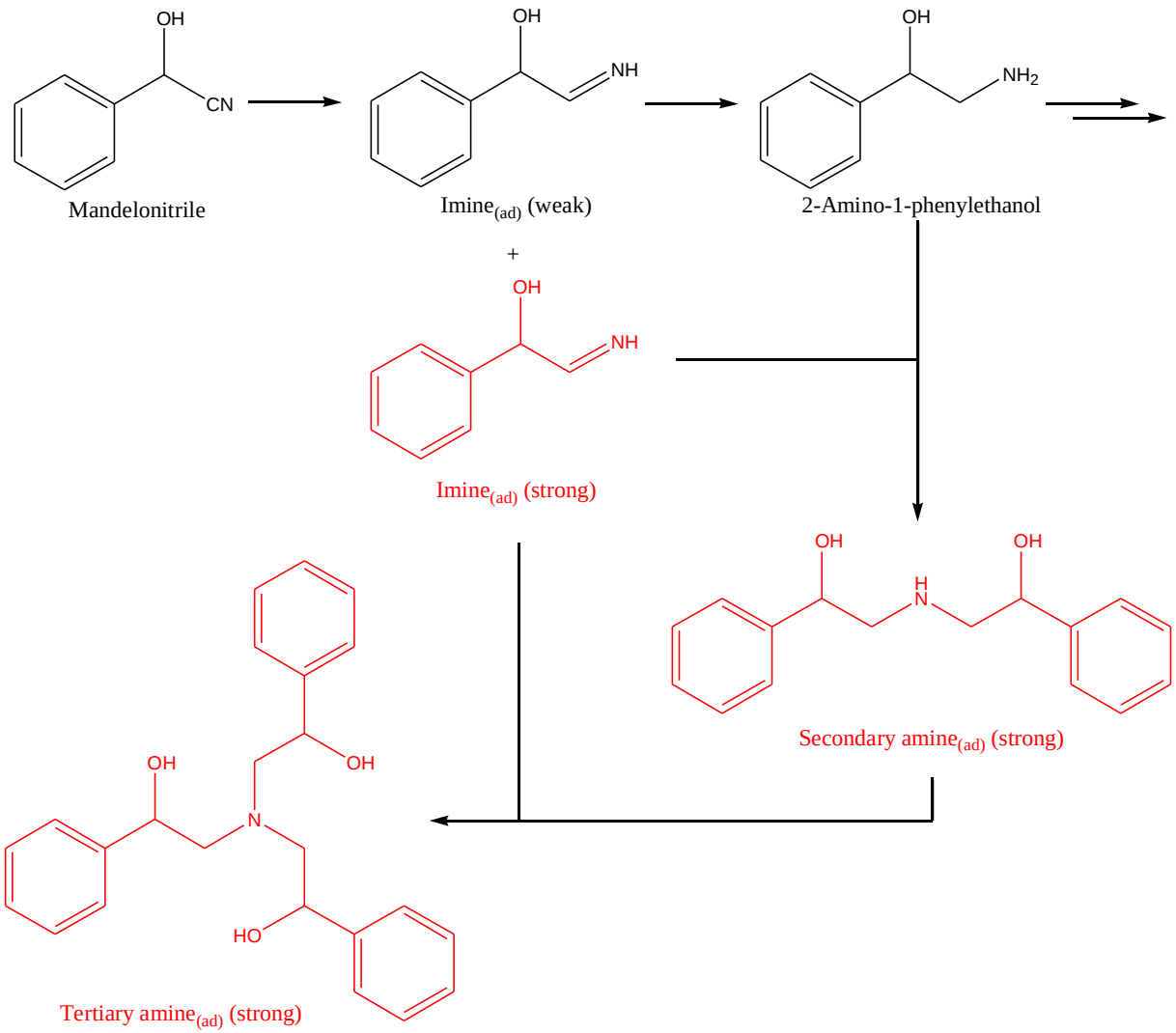

Scheme 22. Reaction scheme showing the presence of both weakly and strongly bound imine intermediates. When weakly bound, the reaction can proceed. When strongly bound, coupling reactions and strong adsorption of higher amines leads to deactivation.

3.5.6 Tailoring catalytic morphology to enhance the lifetime of Pd/C in the hydrogenation of cyanohydrins systems

The hypothesis suggested for mandelonitrile hydrogenation that a loss in activity is mediated by so called “high energy edge sites”, may be useful if one is to develop a strategy to increase catalyst lifetime and selectivity. In attempting to maximise catalyst surface area and metal dispersion, degradation of particle shape can occur whereby the number of atoms within the particle is too few to satisfy the formation of well defined sphere-like structures. The result may be an increase in corner and edge sites. Therefore, reducing the number of these sites may improve selectivity and catalyst lifetime in cyanohydrin hydrogenations.

It has been shown previously that manipulation of particle shape and size is possible,[116] and heating a catalyst in an inert environment, can in some cases alter the catalytic properties.[117] Annealing at high temperatures (up to 900 °C) has been shown to facilitate agglomeration of metal particles on the support, and leads to larger particles of a more spherical nature, as represented schematically in Figure 59. Post-treatment analysis of such catalysts suggests domination of planar sites with much fewer corner and edge sites.[116,117]

Therefore, the 5% Pd/C was subjected to a high temperature treatment (400 ^{o}C) under flowing helium for 1 hour (on the catalyst characterisation line) in an attempt to induce agglomeration of Pd particles and possibly increase catalyst lifetime. The reduction in high energy corner and edge sites via annealing was expected to cohere with a prolonged activity of the catalyst, contrary to the characteristic catalytic death as shown by the unannealed material. The following is included to show the potential of tailoring the morphology of the catalyst to achieve greater lifetime, but the results presented should be noted as being only a preliminary study.

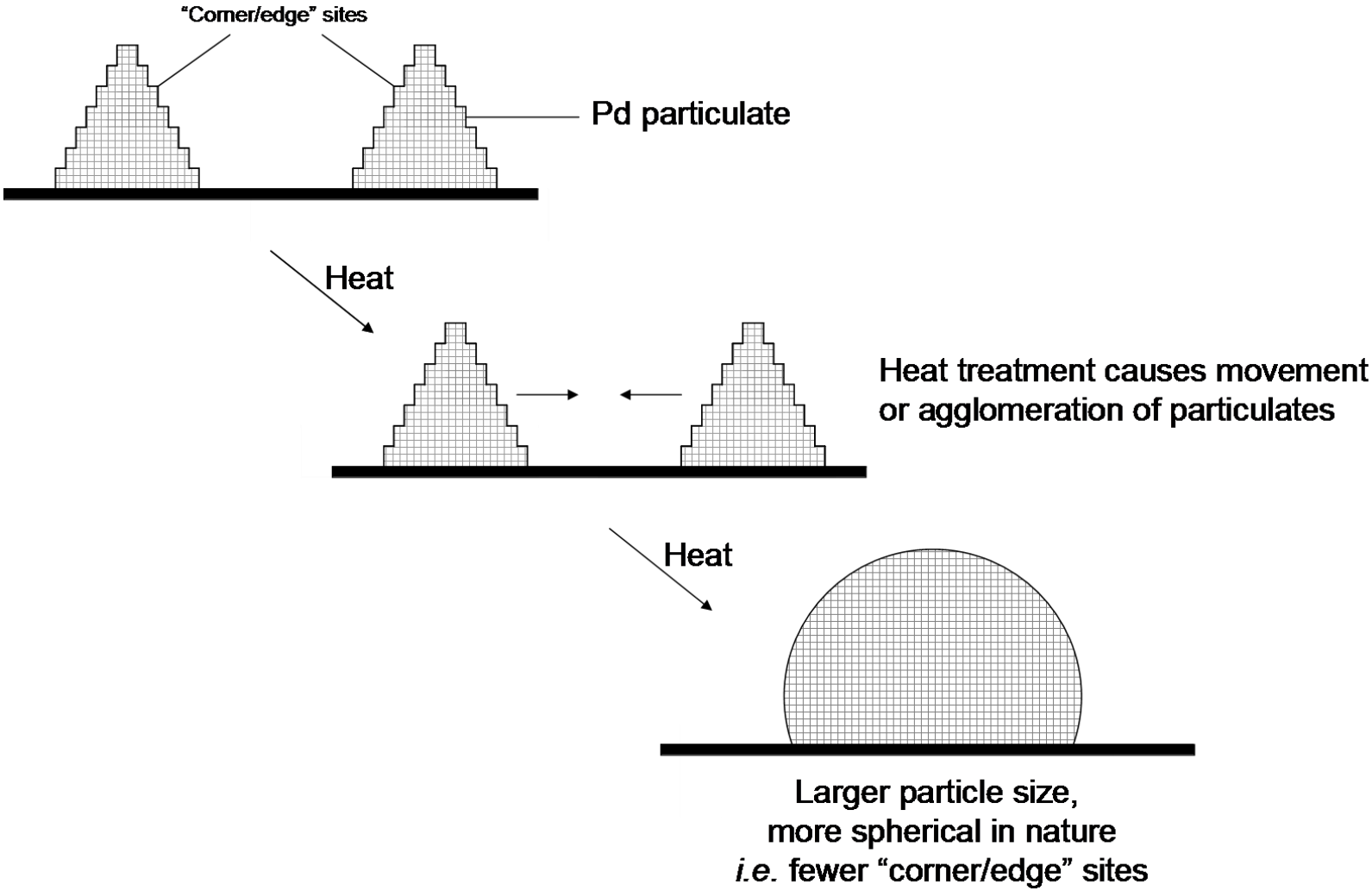

Figure 59. Schematic showing how heat treatment (or annealing) causes movement and agglomeration of Pd particulates, resulting in the formation of larger particle size with fewer corner/edge sites associated with deactivation.

3.5.6.1 Characterisation

Table 7 shows that the surface area and average pore diameter of the annealed Pd/C sample was not affected to any great degree by the treatment, suggesting the process had not affected the carbon support. The marginal increases in surface area and pore diameter may be attributed to a probable decrease in Pd dispersion.

Table 7. The BET surface area and average pore diameter of both untreated and annealed 5% Pd/C.

	BET Surface Area ($m^2 g^{-1}$)	Average Pore Diameter (Å)
Annealed	823.3	25.5
Unannealed	806.8	24.8

TEM images (Figure 60) reveal there to be a much larger particle size for the annealed catalyst as compared to the average particle size of 2.0 nm for the unannealed. Electron energy loss spectroscopy (EELS) aided the identification of Pd particles. The contrast between carbon and palladium was found to be poor due to overlap of their respective EELS spectra. However**,** Figure 60 clearly shows a single, large, oval shaped Pd particle (with an approximate vertical diameter of 100 nm). Therefore, the annealing treatment would appear to have been successful in terms of facilitating agglomeration of Pd particles. It was therefore hoped that such a process would have decreased the concentration of high energy edge sites, and be useful in increasing catalyst lifetime.

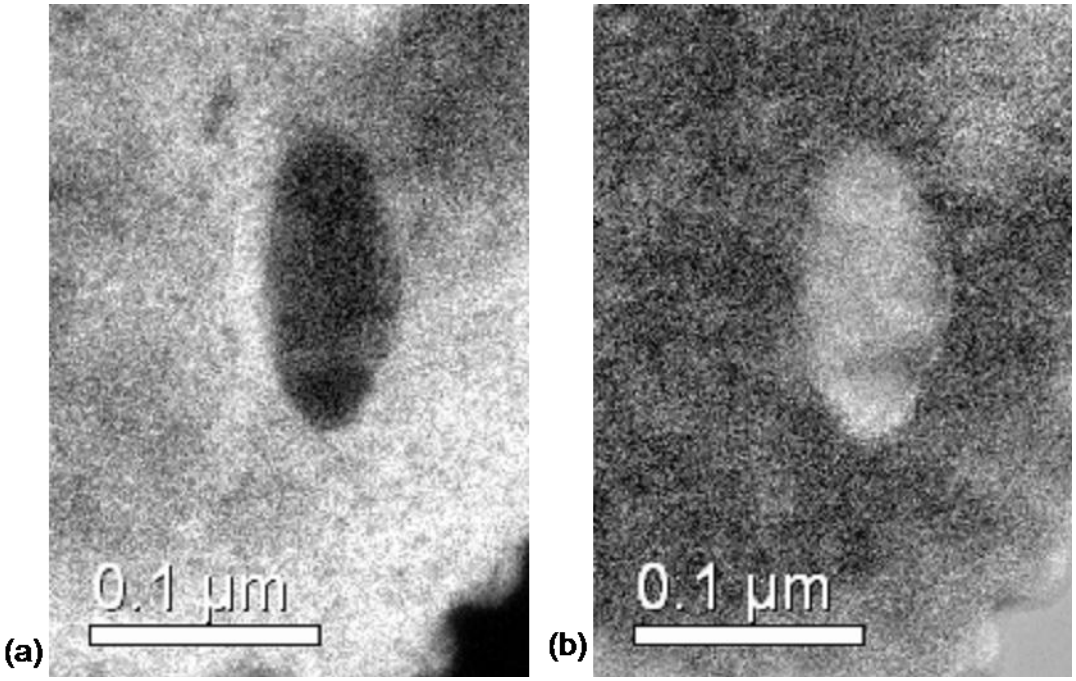

Figure 60. TEM images of the annealed catalyst where a) is carbon mapped and b) is palladium mapped. Despite the poor contrast the palladium particle appears to be over 100nm vertically.

3.5.6.2 Mandelonitrile hydrogenation over the annealed Pd/C catalyst (acidic conditions)

Figure 61 shows the reaction profile obtained for mandelonitrile hydrogenation with an acid additive over the annealed Pd/C catalyst. The profile appears similar to that obtained for mandelonitrile over the unannealed catalyst. Both reactions display the loss of nitrile functionality from the onset of reaction, indicating the annealed catalyst to be active, despite the heat treatment. As before, 2-amino-1-phenylethanol salt was observed as the intermediate in the process. However, it was observed in much larger concentrations than over the unannealed catalyst, reaching a maximum at around 10 minutes, corresponding to a time equating to 100% conversion of the nitrile. Interestingly, no phenethylamine salt was observed in the initial stages, and only observed after full conversion of mandelonitrile. Such an observation suggests a competition for sites, with the nitrile dominating the catalyst surface in the early stages. Only when all of the nitrile has been consumed, do catalytic site become available for the hydrogenolysis reaction to follow in the consecutive process. This suggests that the number of available Pd sites has been reduced by the annealing treatment.

Another difference between the profile for the annealed catalyst and that in Figure 57 is that the hydrogenolysis reaction was observed as being much slower. Whereas Figure 57 showed hydrogenolysis to be fast, over the annealed catalyst, 2-amino-1-phenylethanol salt decay is observed as a slow process. Once again, this is indicative of a loss in the number of available active sites over the catalyst. Indeed, when one compares the rate of mandelonitrile hydrogenation over both catalysts (Figure 62), it can be seen that the unannealed catalyst has an inherently faster reaction rate. One can assume that the increased particle size of palladium in the annealed catalyst to be responsible.

The near complete mass balance confirms activity, but also suggests that retention of reactants or products is disfavoured. From these initial studies, it is proposed that the annealed catalyst is dominated by lower energy planar sites which do not facilitate the formation of secondary or tertiary amines. The analysis also suggests that for the annealed catalyst, the nitrile is binding to hydrogenation sites (Site II). It is possible however, that the exchange dynamics as to how the reagents bind to different sites could be different for the annealed catalyst as compared to the standard commercial catalyst.

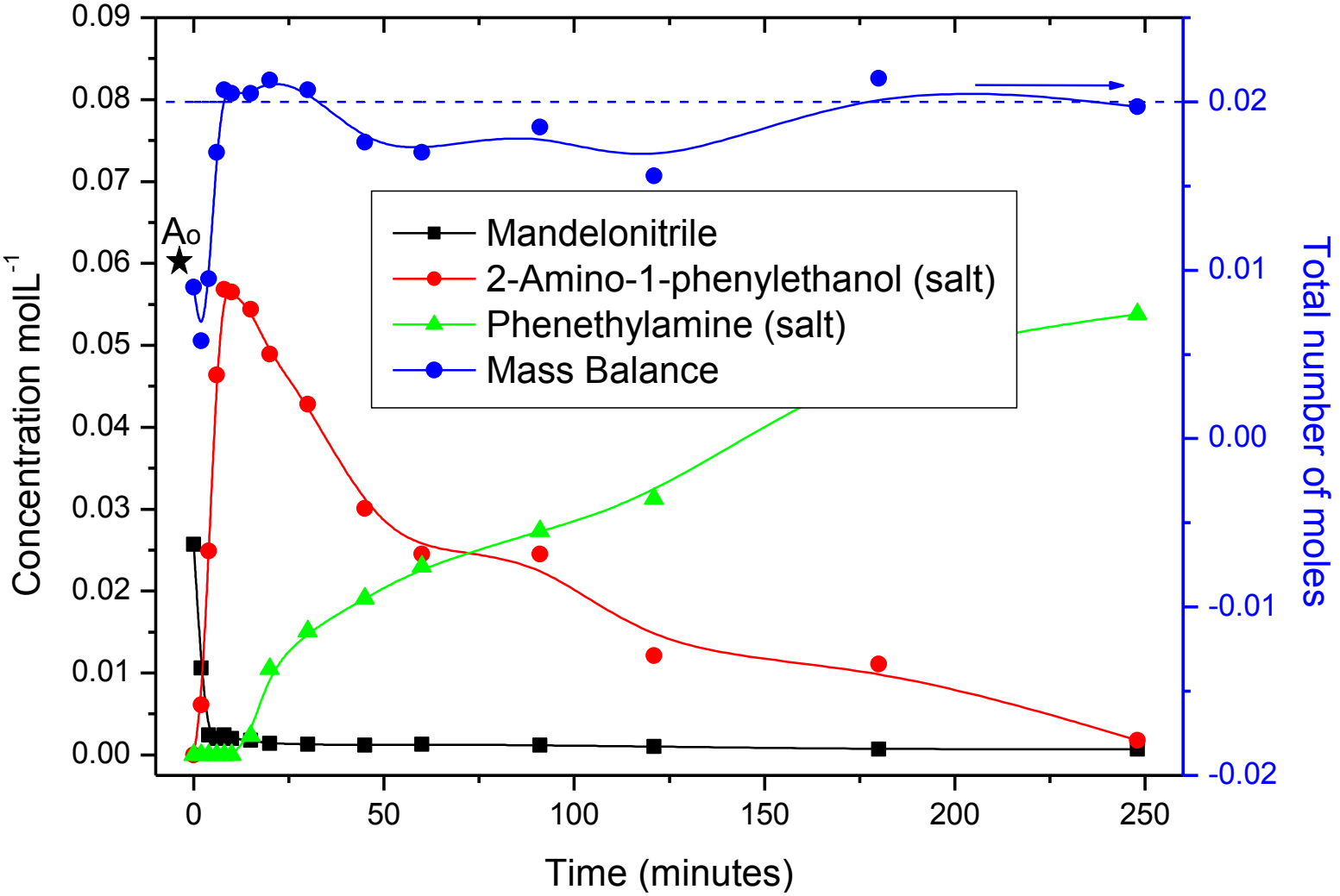

Figure 61. Reaction profile for the hydrogenation of mandelonitrile over the annealed 5% Pd/C, *ca.* 0.02 moles of mandelonitrile, equimolar H_2SO_4, 4 bar H_2, 60 ^oC.

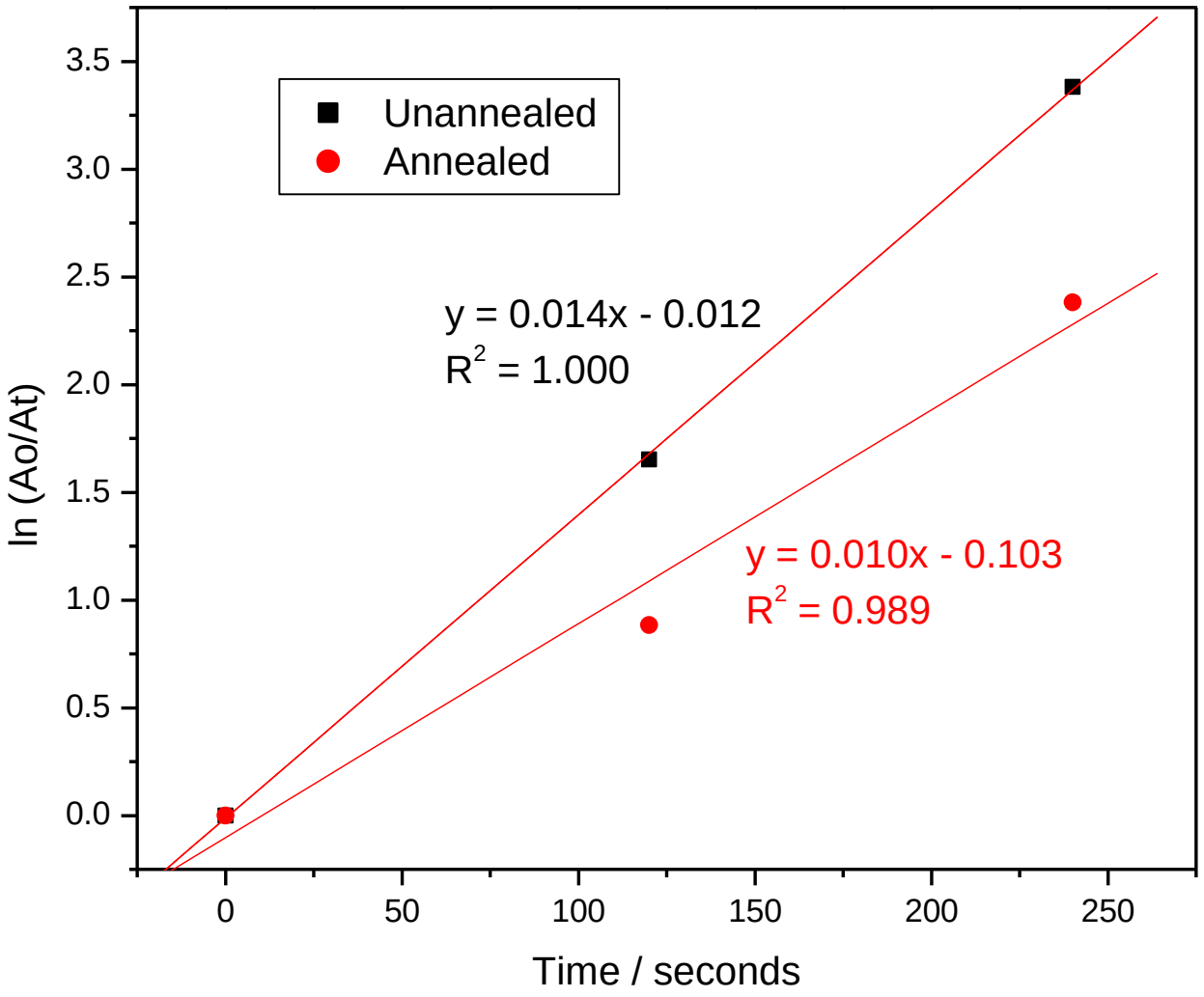

Figure 62. Comparison of the initial rate of reaction in the hydrogenation of mandelonitrile over the unannealed and annealed Pd/C catalysts.

3.5.6.3 Repeat additions of mandelonitrile over the annealed Pd/C catalyst

Replicating the repeat additions experiment in Section 3.5.5 (performed in order to replicate the fed-batch process at the industrial centre), was the obvious next step to determine what effect, if any, the annealing treatment had on catalyst lifetime. Therefore, the annealed catalysts susceptibility towards deactivation was probed by repeatedly charging aliquots of mandelonitrile and sulphuric acid, whilst allowing an appropriate reaction time for each charge.

With the unannealed catalyst, complete catalytic deactivation occurred following the fourth addition. However, Figure 63 shows that over the annealed catalyst, the hydrogenation of mandelonitrile was revealed to be a much more efficient process, whereby a reduction of only 7% conversion occurred between the first and last additions. This loss of activity can be considered as a vast improvement on the complete deactivation exhibited by the unannealed catalyst. Figure 63 therefore supports the suggestion that the annealing process does indeed reduce the number of high energy edge sites that were thought to be the cause of reduced catalytic performance over the unannealed catalyst.

A repeated test, with a greater number of additions is required to fully test the hypothesis and investigate how far the trend continues. However, this favourable aspect was deemed to be beyond the scope of these academic studies. Instead, a sample of the modified catalyst has been dispatched to the industrial centre in order to investigate its performance in the hydrogenation of the process substrate.

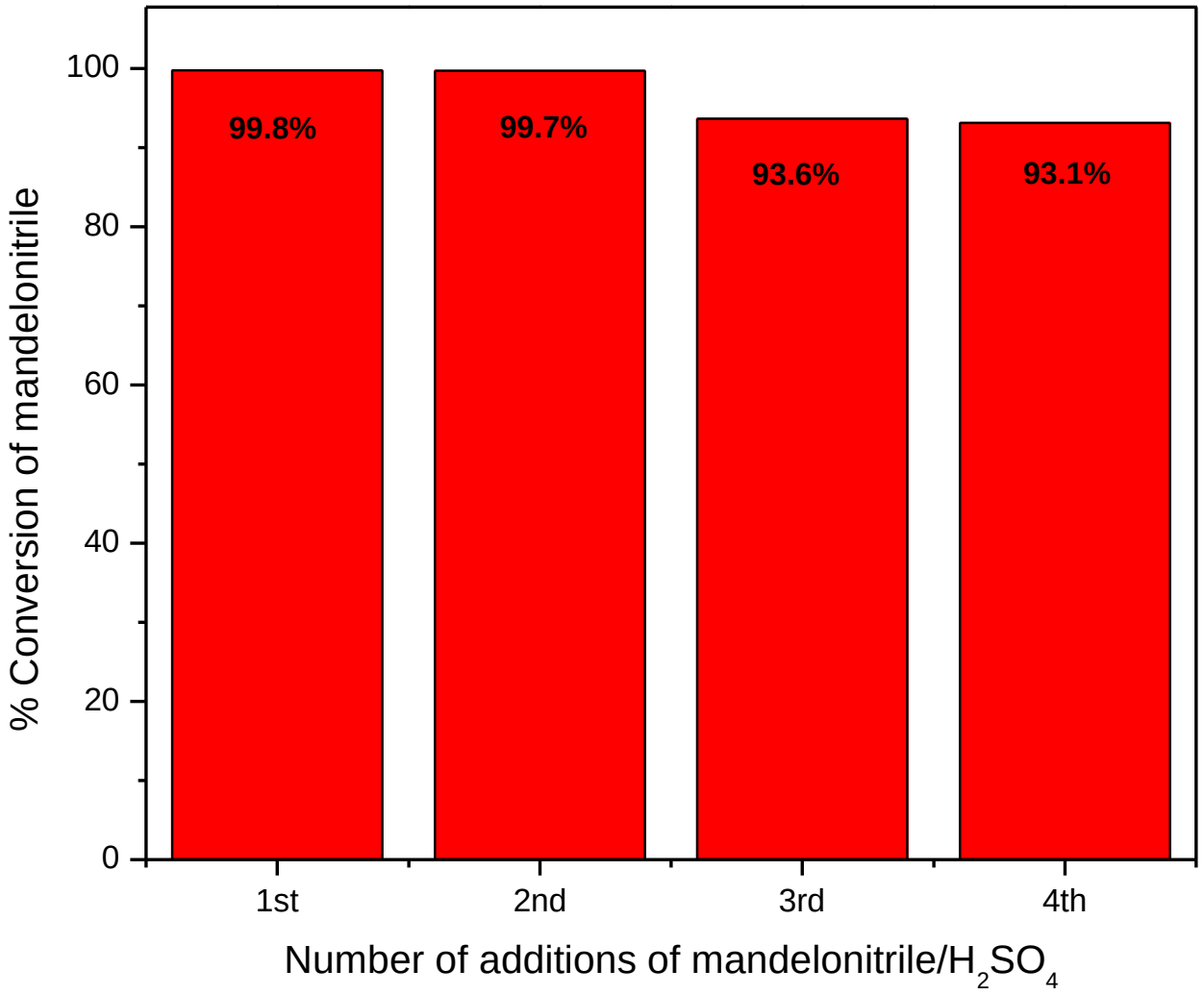

Figure 63. The change in conversion after repeat additions in the hydrogenation of mandelonitrile over annealed Pd/C.

3.5.7 Conclusions

Mandelonitrile hydrogenation was considered as a model for the industrial system by increasing the functionality by introducing the cyanohydrin group for the first time. Rather than providing straightforward results, problems arose whereby conversion could not be attained under the usual conditions employed for earlier systems. As a result of the studies into mandelonitrile, the following conclusions could be drawn:

- Mandelonitrile hydrogenation and 2-amino-1-phenylethanol hydrogenolysis to yield phenethylamine were shown to be non-facile under neutral conditions over a Pd/C catalyst.

- Through the use of co-adsorption studies with benzonitrile hydrogenation as a probe reaction, it was found that the hydroxyamine was most likely acting as a poison.

- The addition of equimolar amounts of sulphuric acid aided conversion by protonating the amine functionality in 2-amino-1-phenylethanol and thus preventing its strong adsorption (*i.e.* poisoning) on the catalyst. By removing the amine functionality from considerations of adsorption, the binding motif proposed for hydrogenolysis could be obtained via the hydroxyl and the reaction was able to proceed.

- Repeat additions of mandelonitrile/acid charges were used to replicate the fed-batch nature of the industrial system and yielded interesting results. Despite acid solving the problem of a “once-through” reaction, subsequent additions resulted in a cumulative poisoning of the system until, after the 4th addition, all activity was lost. To justify such an observation, it was suggested that both weakly and strongly bound imine intermediates were present on the catalyst surface. When weakly bound, intermediates were able to progress to the final product. However, strongly bound imines enabled an “alternative” reaction route whereby coupling of imine and amine products led to higher amine by-products. A surface effect, it can be seen that with each coupling reaction, the “footprint” of by-products greatly increases and thus dominate the catalyst surface, retarding hydrogenation activity.

- It was believed that high energy edge or corner sites of Pd were responsible for the strongly bound imine species and thus ultimately responsible for the cumulative poisoning effect. Therefore, an annealing pre-treatment was performed in an attempt to promote agglomeration of Pd particles to limit the amount of such high energy sites. It is noted that Pd particle size was shown to increase, and, despite a decrease in reaction rate, a repeat of the multiple additions experiment resulted in only a nominal decrease in conversion over the course of 4 additions. It is possible that such a method may be used to aid the industrial process, but further development is required.

3.6 Substituted-mandelonitriles: the effect of *para*-ring substituents on hydrogenation activity

With previous non-substituted substrates – *i.e.* mandelonitrile and benzonitrile – no observable imine intermediates were observed using various methods of analysis. The conclusion that was drawn from the experimental data was that no imine was observed because, as a surface species, it would react too quickly to desorb and be observed in the liquid phase.

In the case of benzonitrile, hydrogenation has been shown to be fast and complete (100% conversion, 100% selectivity to toluene). However, to justify why no imine (or its tautomer, an enamine) was observed, one must consider the electronic factors at play (see Scheme 23 below). For the enamine intermediate to form, disruption of the aromatic system is required. Clearly, such a loss in stable functionality appears unlikely. Therefore, the more reactive imine species (most likely to stay on catalyst) is the only route by which products can form, leading to a fast reaction and no observable intermediates.

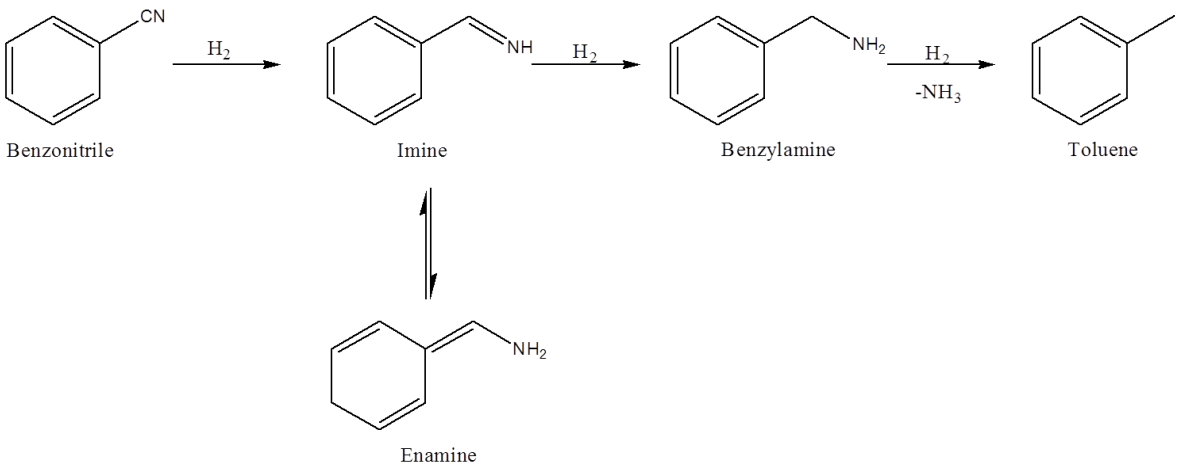

Scheme 23. Benzonitrile hydrogenation scheme showing that resonance stabilisation of the imine intermediate disrupts the aromaticity of the system, meaning it is unlikely to form. Consequently, it is believed that the imine species only exists as a short-lived, highly reactive surface species.

For mandelonitrile hydrogenation, where no activity was observed without the addition of an acid, the lack of imine observation was thought to be because of a lack of conjugation of such an intermediate. As Scheme 24 shows below, the enamine tautomer would be stable (by conjugation), but the presence of the acid is believed to drive the reaction forward. Therefore, the imine is thought to be unstable and the enamine simply has no time to form. The acid allows a way of achieving reaction, but limits the liquid phase availability of intermediates.

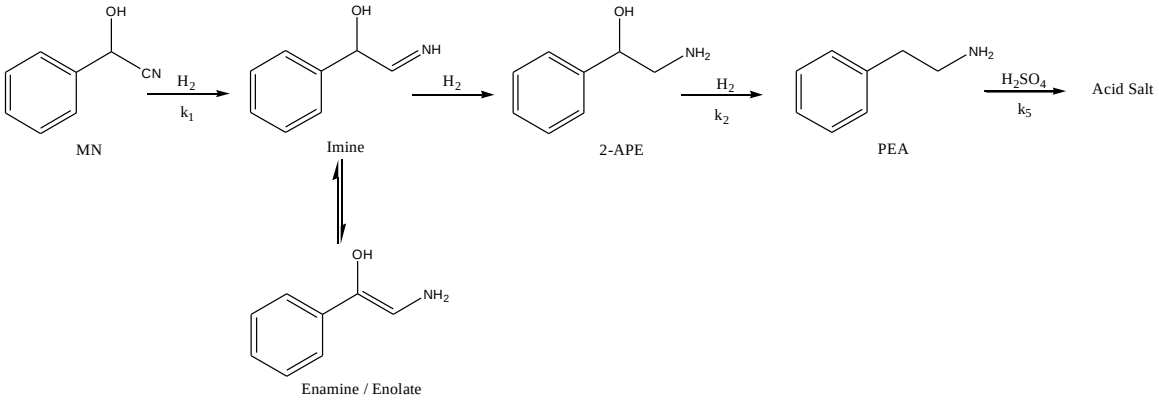

Scheme 24. Mandelonitrile hydrogenation scheme showing resonance stabilisation of the imine intermediate to form an enamine/enolate. However, under acidic conditions, the reaction is so fast (*i.e.* k_2 is large) that any intermediates formed are quickly converted and are consequently not observed in the liquid phase.

With the addition of an electron withdrawing group to the aromatic system, intermediate species may be stabilised by conjugation/resonance. An example is shown in Scheme 25. Previous studies have shown that such systems allow enamine observation by GCMS.[55] It is known that imine species are observable in the liquid phase in the industrial system (unspecified), and it was believed that ring substituents probably enable stabilisation of the intermediate. It was predicted therefore, that inclusion of such groups in the systems could lead to the observation of intermediates

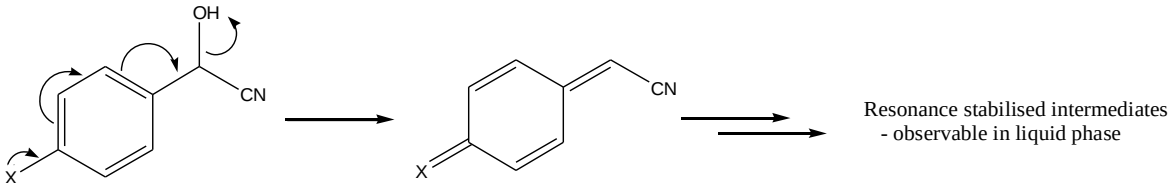

Scheme 25. Resonance stabilisation of substituted mandelonitrile type substrates. X represents an electron donating substituent group *para* to the cyanohydrin group.

There was therefore a need to stabilise any imine intermediates formed by either resonance or induction, or a combination of the two. Therefore, several substituted mandelonitrile substrates were used with *p*-substituents that had varying degrees of electron withdrawing/donating ability. By using such substrates, the reaction chemistry studied was also more closely linked to that of the actual process chemistry. The study of such model compounds again increased the complexity of the reaction chemistry. Additionally, through the use of a range of *p*-substituents and on comparison with a -H substituent (*i.e.* mandelonitrile), it was hoped that a Hammett-type relationship[118] could be established, allowing the prediction of reaction rate based solely upon substituent group.

3.6.1 Issues relevant to the hydrogenation of hydroxybenzyl cyanide (*p*-HO-$C_6H_5CH_2CN$)

Before any work was carried out on the more valuable substituted-mandelonitriles, the hydrogenation of hydroxybenzyl cyanide was considered since it was available cheaply and in large quantities. Forming the primary amine tyramine (*p*-HO-$C_6H_4CH_2CH_2NH_2$) via an intermediate imine, as shown in Scheme 26, hydroxybenzyl cyanide was expected to react in much the same way as its non-substituted counterpart, benzyl cyanide (which was hydrogenated as in Scheme 14, but with retention of the primary amine product by the catalyst/support).

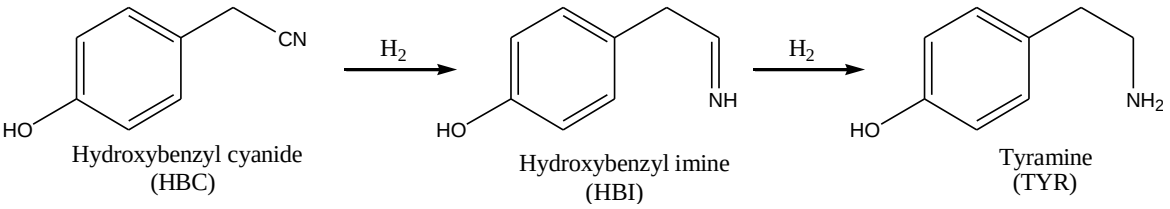

Hydroxybenzyl cyanide (HBC) — Hydroxybenzyl imine (HBI) — Tyramine (TYR)

Scheme 26. The hydrogenation of hydroxybenzyl cyanide via an imine intermediate to tyramine.

Hydroxybenzyl cyanide hydrogenation was first tested at high temperature (65 ^oC) to facilitate fast conversion, as was used for much of the other model compounds previously discussed. In addition to fast conversion, increased temperature (up to 100 ^oC) has been shown to increase selectivity to primary amine since desorption of the imine intermediate does not occur[55]. However, Figure 64 shows that the reaction was observed to be slow. Additionally, selectivity to the desired primary

amine tyramine was also poor at >5%. The other products formed were found to be the secondary and tertiary amines formed by the coupling of imine and amine species by the route shown in Scheme 27. No quantitative data could be obtained for these species since no analytical standards were available. However, work is currently underway at the academic centre to carry out a quantitative analysis of these (and other) reactions. No imines were identified in the liquid phase, suggesting that, as before, they were only present on the catalyst surface as highly reactive intermediates. Similarly, tyramine must have been retained by the catalyst/support system before being coupled to form higher amines. Neither being observed in the liquid phase suggests that the coupling reactions are catalyst mediated (rather than by any homogeneous route).

At extended sampling times; the reaction profile is consistent with catalyst corruption by amine products leading to a slow deactivation. Indeed, after extensive reaction time, conversion of hydroxybenzyl cyanide did not exceed 80%. It was assumed that retention of amine products via strong adsorption of the amine group could lead to such a scenario. As such, an acid additive (H_2SO_4) was used to protonate any amine products and thus prevent strong adsorption at the amine group, by the same route as that observed in protonating amine products in mandelonitrile hydrogenation. It was hoped that an acid additive would serve as a simple manner to prevent catalyst deactivation. In addition, as previously discussed, acid additives have been used extensively to control selectivity to primary amines[58-60] and so here, it would serve a dual purpose.

Figure 65 shows that upon addition of an acid, there was a remarkable change in product distribution. The desired primary amine, tyramine (salt), was observed as being the major product with a selectivity of *ca.* 75%. The secondary amine was again formed, despite addition of an acid and was found to have formed with *ca.* 25% selectivity. The amount of hydrogen consumed by the reaction was found to equate to the amount required to facilitate nitrile transformation to tyramine (salt) with the observed selectivity, plus the formation of the secondary amine formed by the coupling of hydroxybenzyl imine and tyramine.

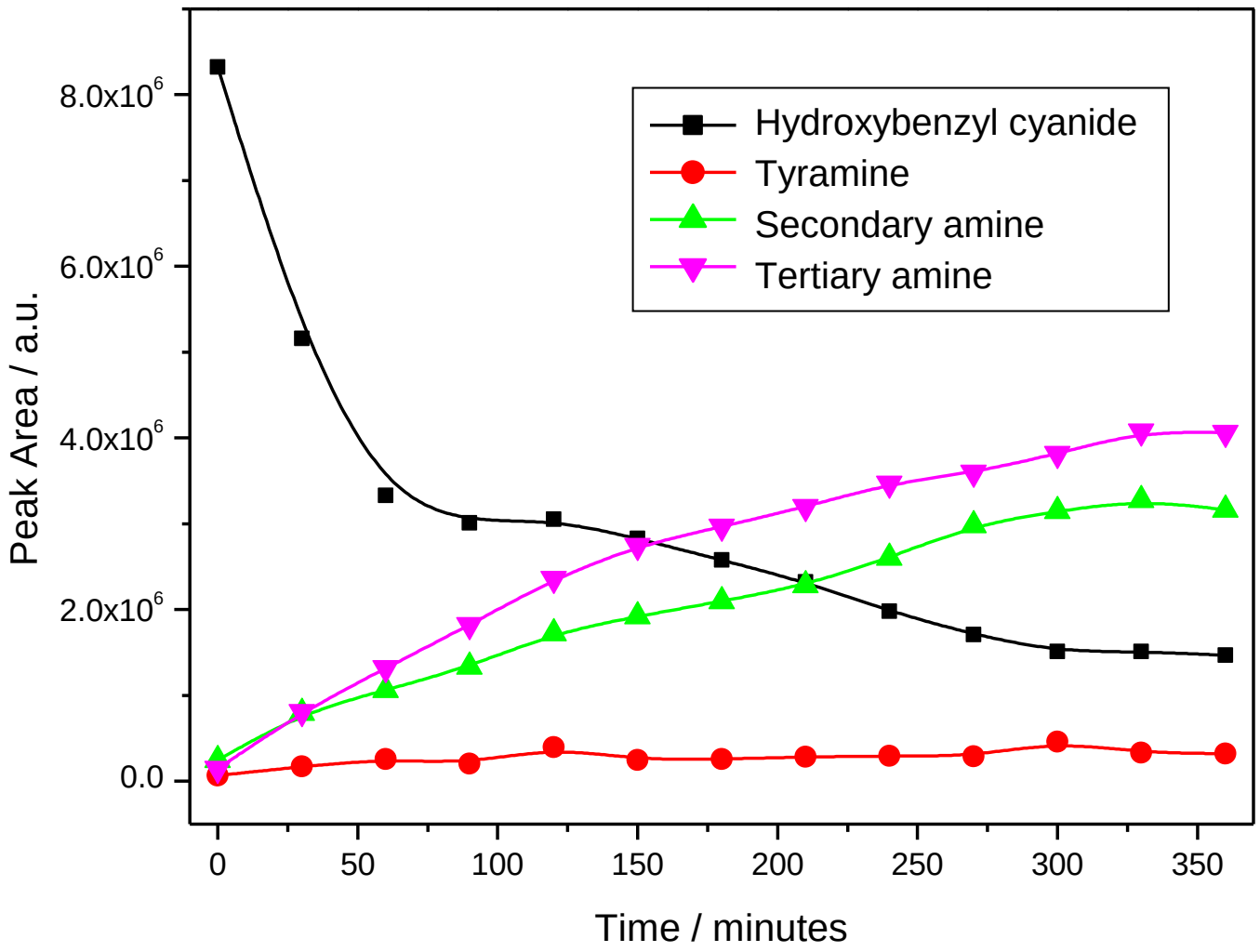

Figure 64. Reaction profile for the hydrogenation of hydroxybenzyl cyanide over 5% Pd/C, 0.02 moles of hydroxybenzyl cyanide, 4 bar hydrogen, 30°C.

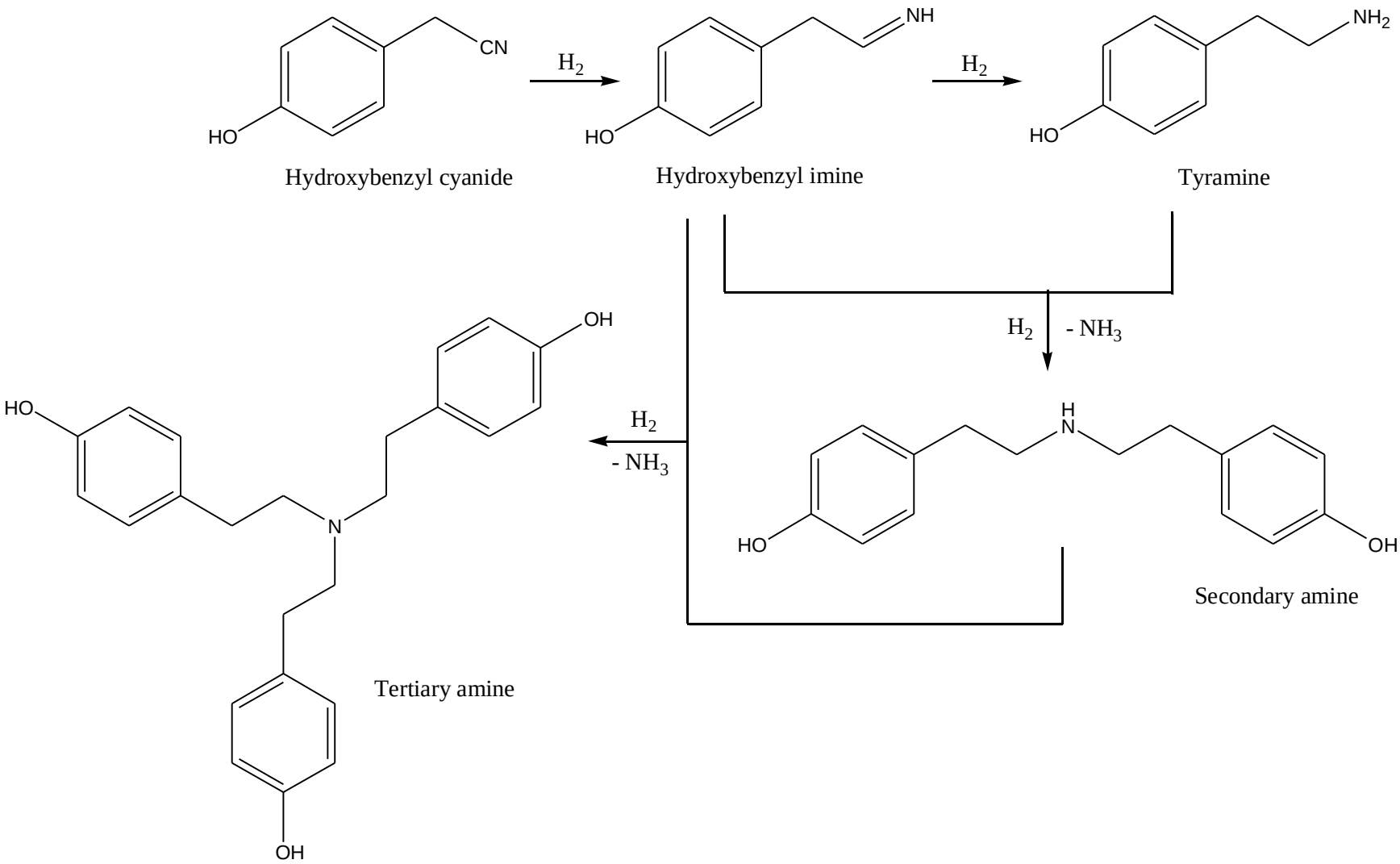

Scheme 27. Hydroxybenzyl cyanide hydrogenation over Pd/C showing the formation of secondary and tertiary amines due to the coupling of hydroxybenzyl imine and amine products.

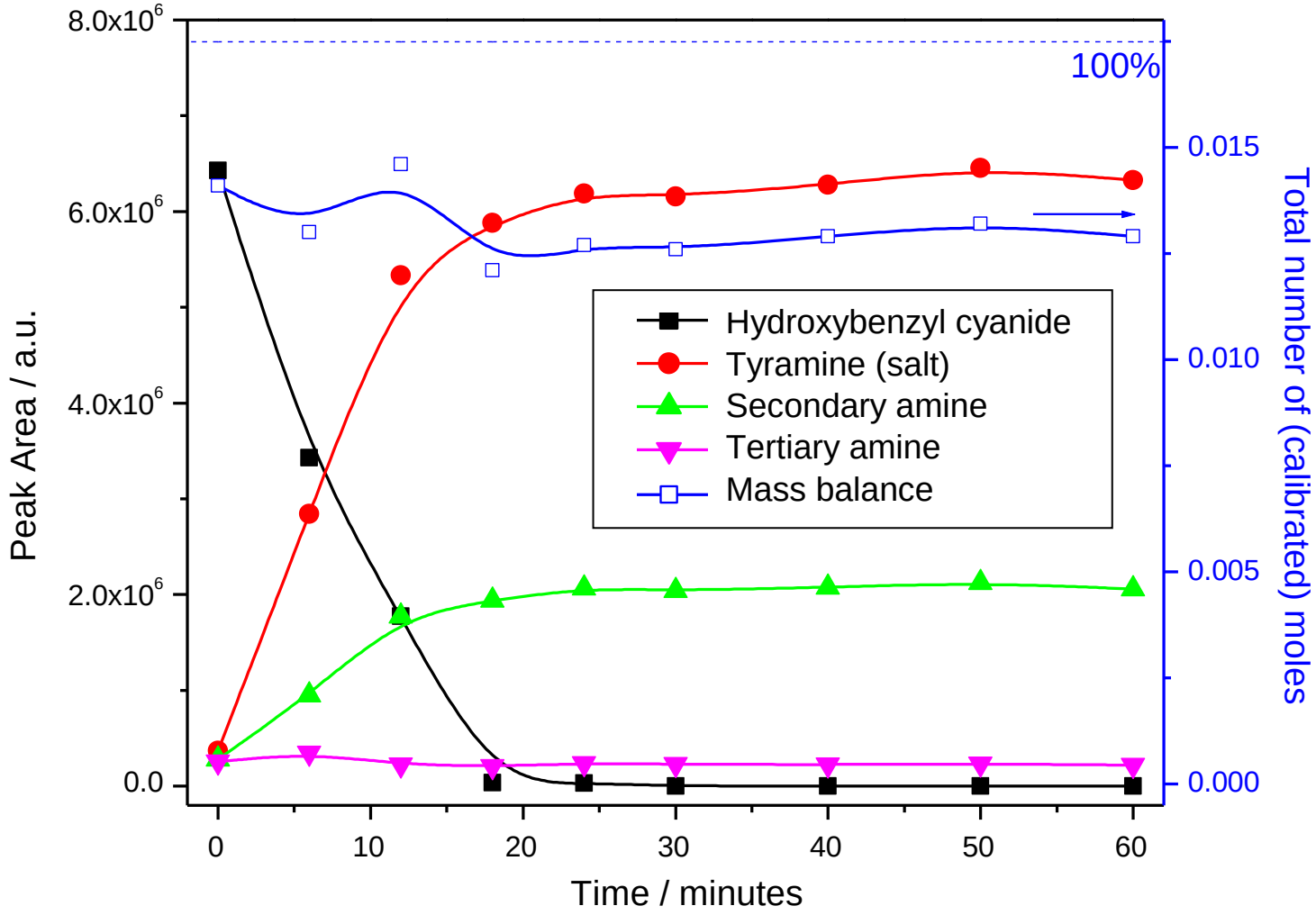

Figure 65. Reaction profile for the hydrogenation of hydroxybenzyl cyanide over 5% Pd/C, 0.02 moles of hydroxybenzyl cyanide, equimolar H_2SO_4, 4 bar hydrogen, 60°C.

On lowering reaction temperature, there was another change in product distribution and selectivity, suggesting that the problems previously described may have been temperature mediated. Figure 66 shows that here, tyramine (salt) was the sole product observed and that hydroxybenzyl cyanide was converted quickly in comparison to previous reactions (Figure 64 and Figure 65), and full conversion of the nitrile had taken place at around 6 minutes. Importantly, the intermediate observed in the reaction was found to be an imine (identified by NMR, diagnostic peak for β-carbon in ^{13}C found at 33.9 ppm, as indicated by DFT calculations[119]) and was observed as reaching a maximum concentration in the liquid phase at a time approximating to complete conversion of the nitrile. The mass balance for the reaction at this temperature fell and then recovered according to the presence of imine in the liquid phase and suggests that at least some of the intermediate was confined to the catalyst surface. Whereas no imine had been observed in previous reactions, under the conditions used here the imine was stable enough to be observed in the liquid phase due to the reduced temperature. It can also be concluded that imine/amine coupling to form higher amines is metal mediated, since in this case, no other products were observed at the lower temperature, despite both imine and primary amine being present in the liquid phase in the presence of acid (*i.e.* any homogenous route to secondary or tertiary amines can be discounted).

Since the hydrogenation of hydroxybenzyl cyanide provided such promising results, the conditions used here (low temperature of 30^{o}C in an acidic medium) were chosen as the ideal conditions for all other substituted substrates.

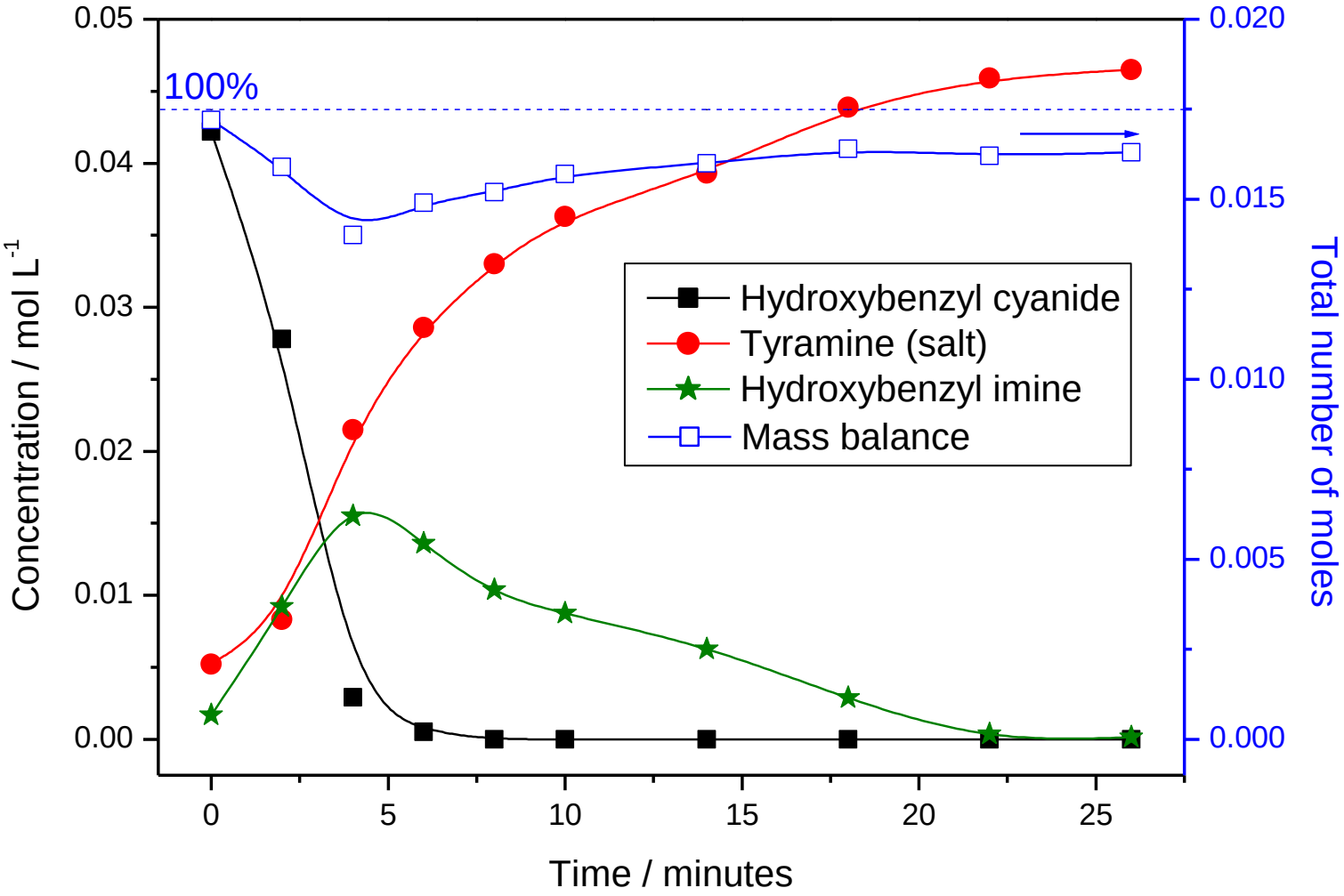

Figure 66. Reaction profile for the hydrogenation of hydroxybenzyl cyanide over 5% Pd/C, 0.02 moles of hydroxybenzyl cyanide, equimolar H_2SO_4, 4 bar hydrogen, 30°C.

The results for hydroxybenzyl cyanide hydrogenation allow further development of the catalyst model described in Section 3.3. The distinctive sites described for hydrogenation and hydrogenolysis remain unchanged. However, the effect of reaction temperature on product distribution is consistent with a dual-site hydrogenation model for the catalyst, shown schematically in Figure 67. Site I is responsible for hydrogen dissociation. Site II(a) is thought to be responsible for hydrogenation of the nitrile group. This site is believed to be any general palladium site and has a low activation barrier that allows hydrogenation to be facile, even at low temperatures (30^{o}C). Site II (b) however, is responsible for the coupling reaction that leads to secondary and tertiary amines. This site has a much higher activation barrier since it was found only to be accessible at increased temperature. Such a site confirms the high energy dependence for coupling reactions as proposed for mandelonitrile hydrogenation, where corner or edge sites were believed to be responsible for the cumulative poisoning effect in the repeat addition reactions. Site III (hydrogenolysis) has no role to play in the hydrogenation of this particular substrate, since it is not a cyanohydrin.

Section 3.5.6 has already shown that changes in catalyst morphology can lead to a dramatic improvement in catalyst lifetime. However, annealing of the catalyst did lead to a decrease in reaction rate, probably as a consequence of an increase in particle size and therefore, a decrease in dispersion. Rather than using any physical methods, the observation of a specialised high energy site means a more appropriate course of action could be to chemically treat the catalyst at the synthesis stage. It is hoped that a selective-poisoning strategy, as has been shown by Lennon *et al.*, may prevent coupling in other, more complex systems.[120,121] In a fine chemicals context this may help increase selectivity to primary amines, without the loss of any other functionality that could be compromised with the use of other, harsher catalysts, but also prevent a decrease in reaction rate as was observed after the annealing process.

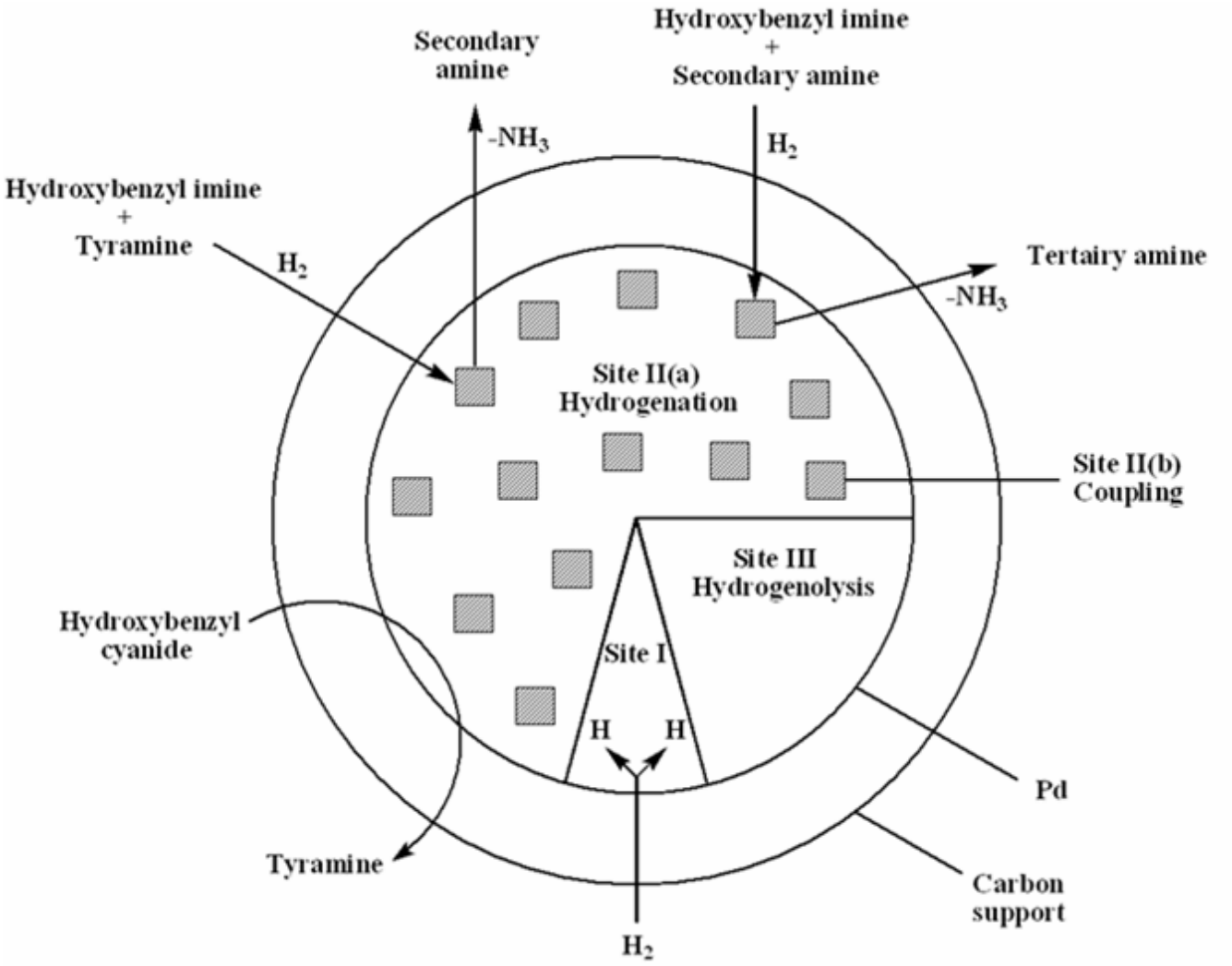

Figure 67. Suggested catalyst model for 5% Pd/C in the hydrogenation of aromatic nitriles, showing schematically that hydrogen dissociation (Site I), hydrogenation (Site II(a)), coupling (Site II(b)) and hydrogenolysis (Site III) occur on distinct sites.

3.6.2 The hydrogenation of 4-Methoxy-mandelonitrile (*p*-CH_3O-$C_6H_4CH(OH)CN$)

As with all substituted mandelonitrile-type substrates, the hydrogenation of methoxy-mandelonitrile to its corresponding primary amine can proceed via 2 distinct routes. Firstly, the reaction could proceed via a hydrogenolytic step resulting in the loss of hydroxyl group followed by nitrile hydrogenation. Secondly, the nitrile hydrogenation step could occur first, followed by hydrogenolysis of a hydroxyamine to the desired primary amine. Additionally, the intermediates of many of the substituted mandelonitrile reactions were found to be licensed materials unavailable for purchase. The Home Office were approached with regards the granting of a site license to handle these materials. However, after more than 18 months, the authorities had still not granted such a license, thereby preventing work on these compounds at the academic centre. Consequently, qualitative identification was carried out at the industrial centre by LCMS. However, due to time constraints, a quantitative analysis could not be obtained.

The reaction profile for the hydrogenation of methoxy-mandelonitrile (Figure 68) showed that the reaction proceeded solely via a hydroxyamine intermediate, as described in Scheme 28.

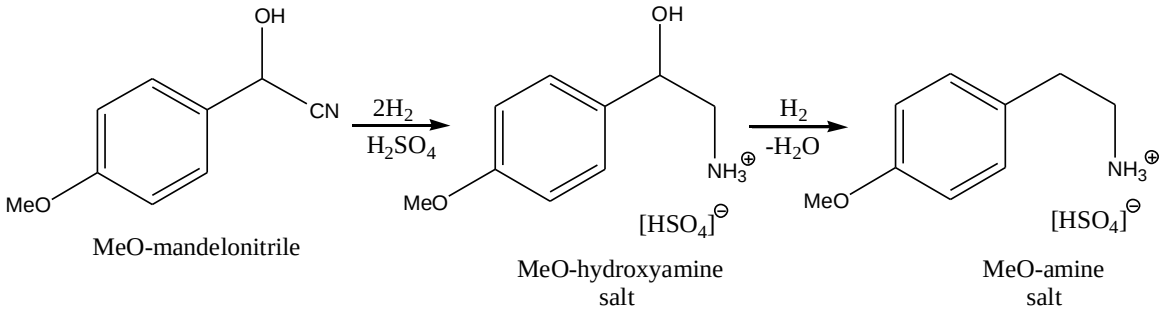

Scheme 28. The hydrogenation of methoxy-mandelonitrile.

Initial conversion of methoxy-mandelonitrile appeared fast and the desired methoxy-substituted primary amine (salt) was the sole product. However, catalyst deactivation proved to be a problem. It appears from the reaction profile that at extended sampling times (after *ca.* 100 minutes), little conversion of methoxy-mandelonitrile or methoxy-hydroxyamine took place. Previous studies on

mandelonitrile have shown that the intermediate hydroxyamine acted as a poison (Section 3.5.4). It is suggested therefore, that activity may be lost over time by the adsorption of methoxy-hydroxyamine on the catalyst, thus preventing complete conversion of nitrile.

No imine intermediate was observed in the liquid phase indicating that its presence was restricted to the catalyst surface as a reactive intermediate.

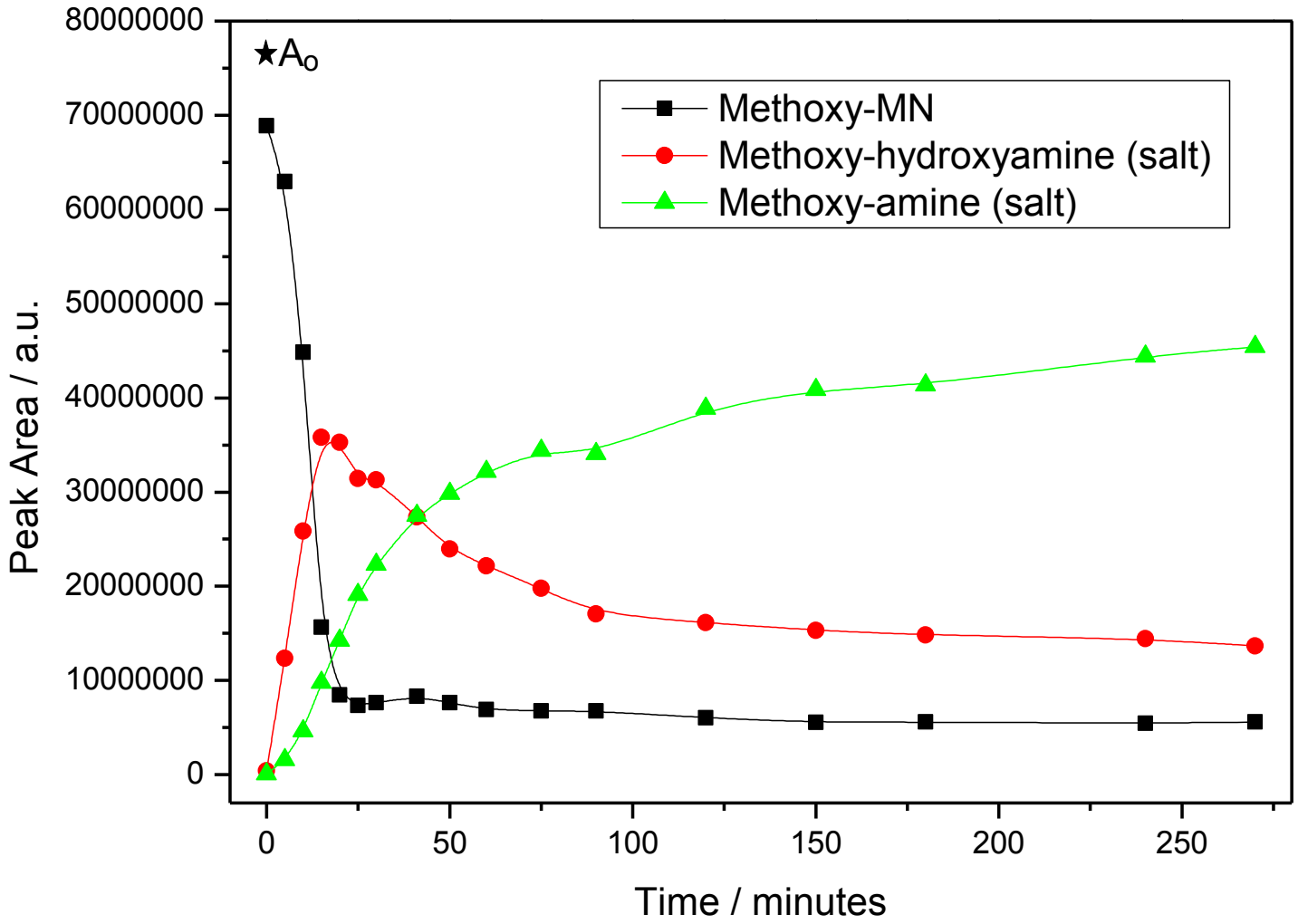

Figure 68. Reaction profile for the hydrogenation of methoxy-mandelonitrile over 5% Pd/C, 5 mmoles of methoxy-mandelonitrile, equimolar H_2SO_4, ambient pressure reactor, 60 mL min^{-1} H_2 flow, 30°C.

3.6.3 The hydrogenation of 4-Methyl-mandelonitrile (*p*-CH_3-$C_6H_4CH(OH)CN$)

Unlike for methoxy-mandelonitrile, Figure 69 shows that in the hydrogenation of methyl-mandelonitrile, full conversion of the starting material was observed in about 20 minutes reaction time. Most of the nitrile was found to be converted to the expected methyl-hydroxyamine (salt), whose maximum concentration coincided with complete conversion of the nitrile. The desired methyl-substituted amine (salt) was found to be the major product of the reaction and reached a level approximating to 90% of the mass balance. However, trace amounts of hydroxyamine intermediate remained at the end of sampling time, indicating that catalyst deactivation occurred.

Additionally, the reaction profile shows the presence of small amounts of methyl-benzyl cyanide (*p*-CH_3-$C_6H_4CH_2CN$). The presence of methyl-benzyl cyanide indicates that, despite being less favoured than the conventional route, that some of the methyl-mandelonitrile is hydrogenolysed first, before the nitrile is hydrogenated to the primary amine. This means that the reaction scheme (Scheme 29) for methyl-mandelonitrile must include methyl-benzyl cyanide, despite it being less favoured than the other route (where hydrogenation occurs first).

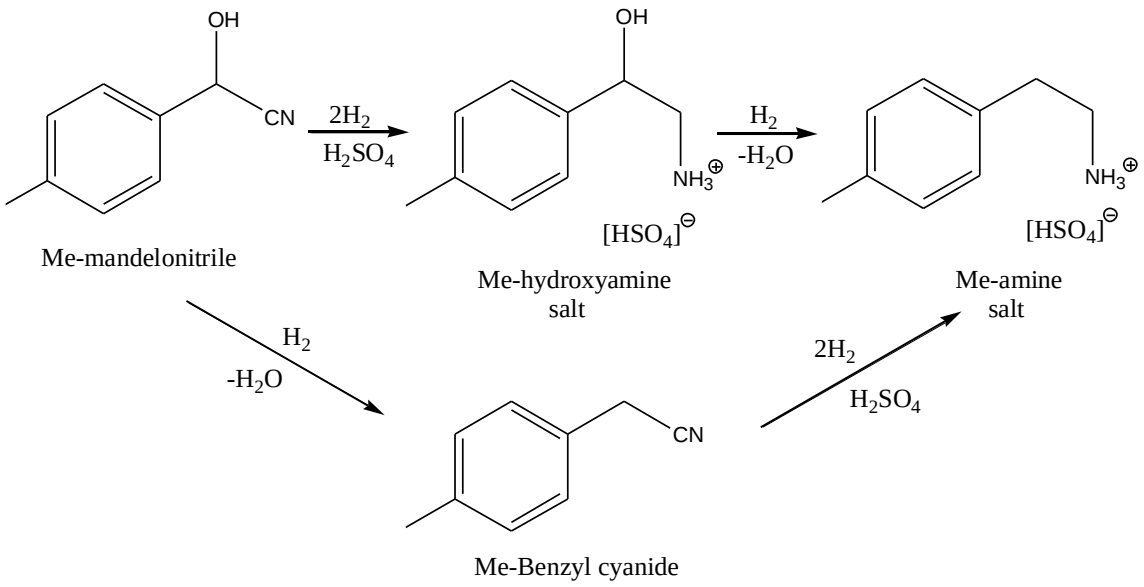

Scheme 29. The hydrogenation of methyl-mandelonitrile.

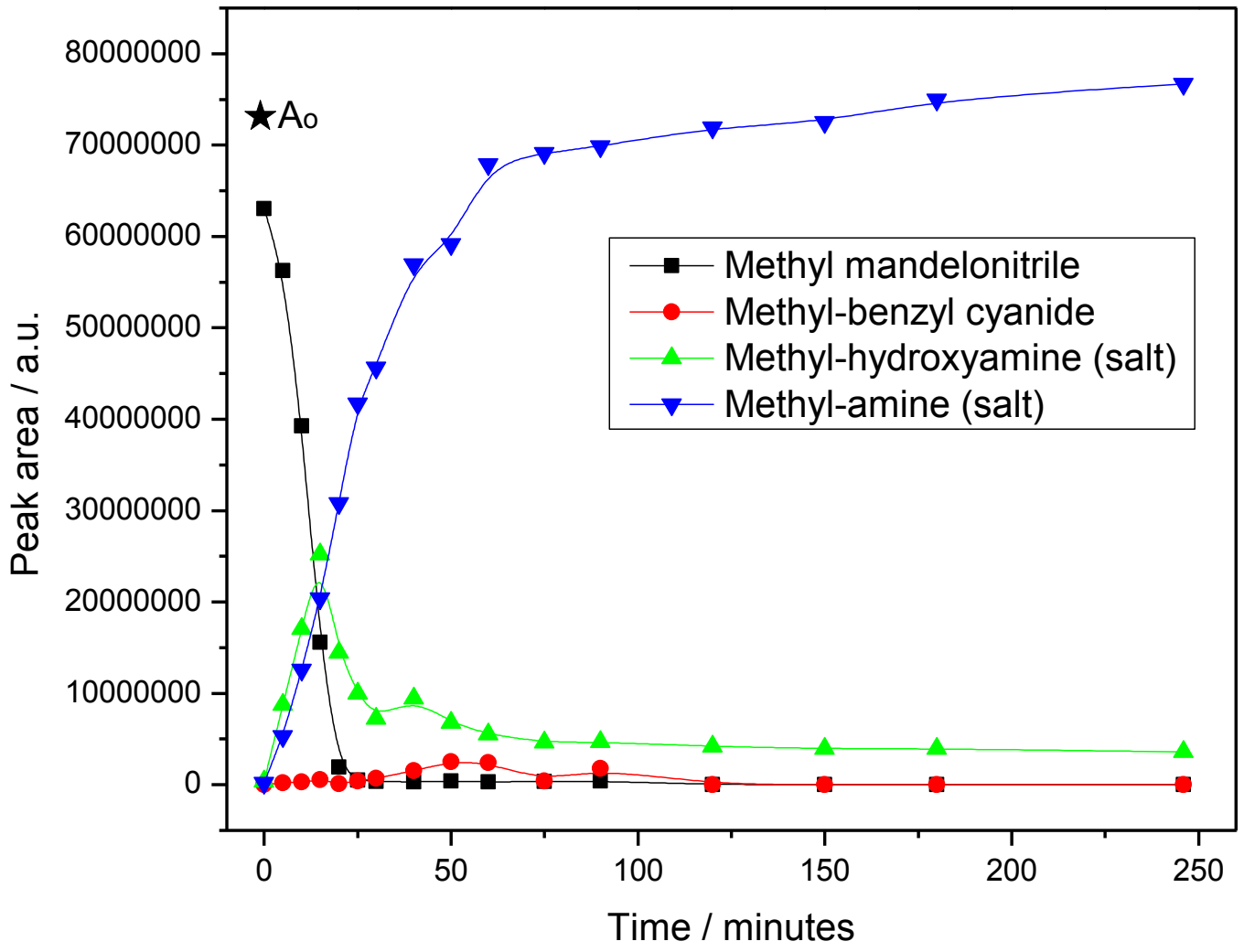

Figure 69. Reaction profile for the hydrogenation of methyl-mandelonitrile over 5% Pd/C, 5 mmoles of methyl-mandelonitrile, equimolar H_2SO_4, ambient pressure reactor, 60 mL min^{-1} H_2 flow, 30 ^oC.

3.6.4 The hydrogenation of 4-Chloro-mandelonitrile (*p*-Cl-$C_6H_4CH(OH)CN$)

The reaction profile for chloro-mandelonitrile (Figure 70) showed considerable similarity to that for methoxy-mandelonitrile Figure 68). The desired primary amine (salt) was found to be the sole product with the expected hydroxyamine (salt) formed as an intermediate upon initial conversion of chloro-mandelonitrile (as described in Scheme 30). As with all previous substituted mandelonitriles, maximum concentration of the hydroxyamine intermediate corresponded to a time approximating to maximum conversion of the starting material. Despite initially fast conversion, the catalyst showed signs of deactivation over time. Full conversion of the nitrile was not achieved after 6 hours and significant amounts of intermediate hydroxyamine were observed in the liquid phase after extended reaction times. Again, the fouling of the catalyst was attributed to retention of intermediate hydroxyamine.

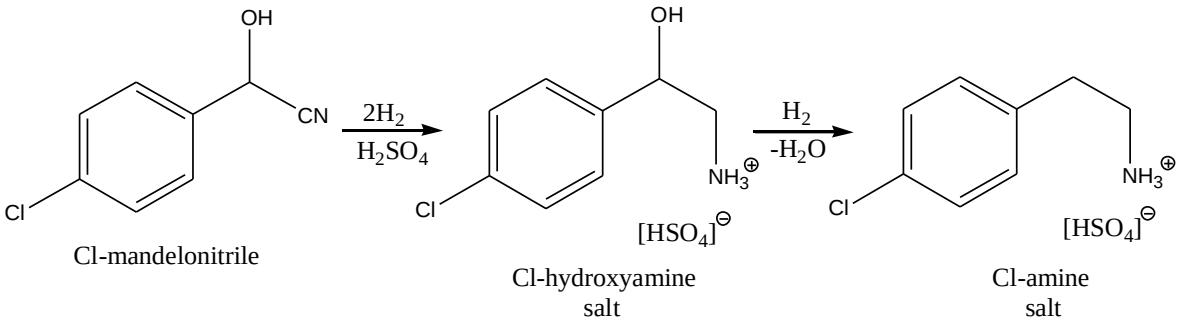

Scheme 30. The hydrogenation of chloro-mandelonitrile.

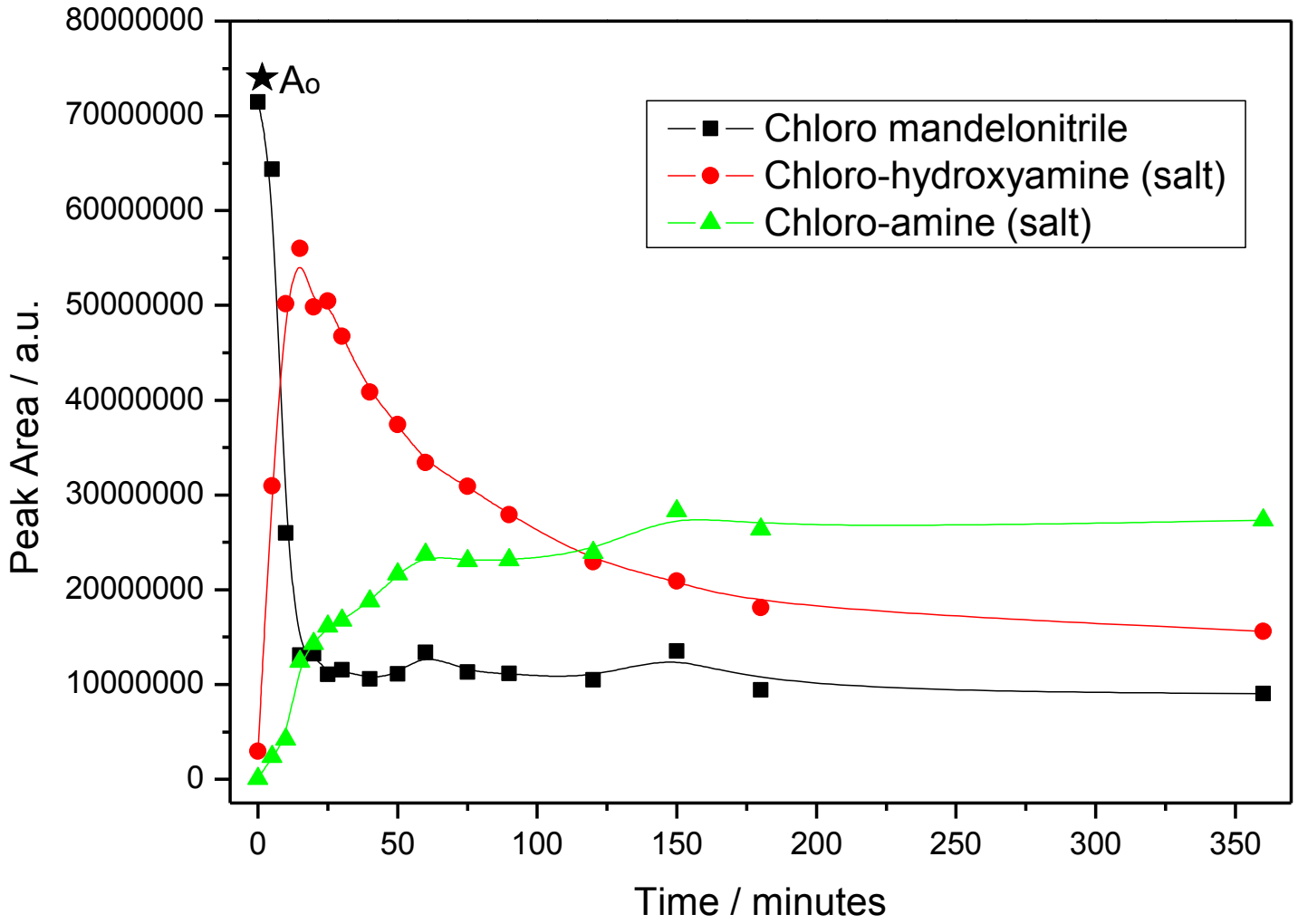

Figure 70. Reaction profile for the hydrogenation of chloro-mandelonitrile over 5% Pd/C, 5 mmoles of chloro-mandelonitrile, equimolar H_2SO_4, ambient pressure reactor, 60 mL min^{-1} H_2 flow, 30 ^oC.

3.6.5 The hydrogenation of 4-Hydroxy-mandelonitrile (*p*-HO-$C_6H_4CH(OH)CN$)

The hydrogenation of hydroxy-mandelonitrile was also found to proceed via hydroxyamine intermediate. However, the reaction profile was in stark contrast to the previous examples presented here. Rather than any deactivation issues, Figure 71 shows that hydroxy-mandelonitrile and all intermediates were fully converted giving the final products as the desired primary amine tyramine (salt) with selectivity of 84% and a secondary amine with selectivity of 16% (selectivities based on mass balance amounts).

For the first time when considering substituted-mandelonitriles type substrates, an imine intermediate was observed in the liquid phase (as confirmed by LCMS) and was shown to be octopamine imine (*p*-HO-$C_6H_4CH(OH)CH=NH$). The mass balance for the reaction was found to fall and recover with formation and conversion of the imine intermediate and was attributed to adsorbed imine. However, the decreased mass balance was larger than expected and could possibly have been as a result of retention of octopamine, which was present in lower than expected amounts (when compared to the reaction profiles for other substituted-mandelonitrile type substrates). Any mass imbalance in the latter stages of reaction was attributed to the presence of the non-calibrated secondary amine.

As is seen in Scheme 31, it is possible for two different secondary amines to form. LCMS analysis has shown that only the amine formed by coupling of octopamine-imine and octopamine was observed. This is probably due to the inability of tyramine to react at the amine centre, given that in the liquid phase it is only present as the hydrogen sulfate salt formed by reaction with sulphuric acid. Any secondary amine formed must, therefore, occur before octopamine interaction with the acid, thus allowing reaction of the amine group with the imine functionality of the intermediate. A small amounts of a methanol adduct of octopamine was also observed, but at insignificant concentrations and was attributed to a minor reaction pathway involving the solvent.

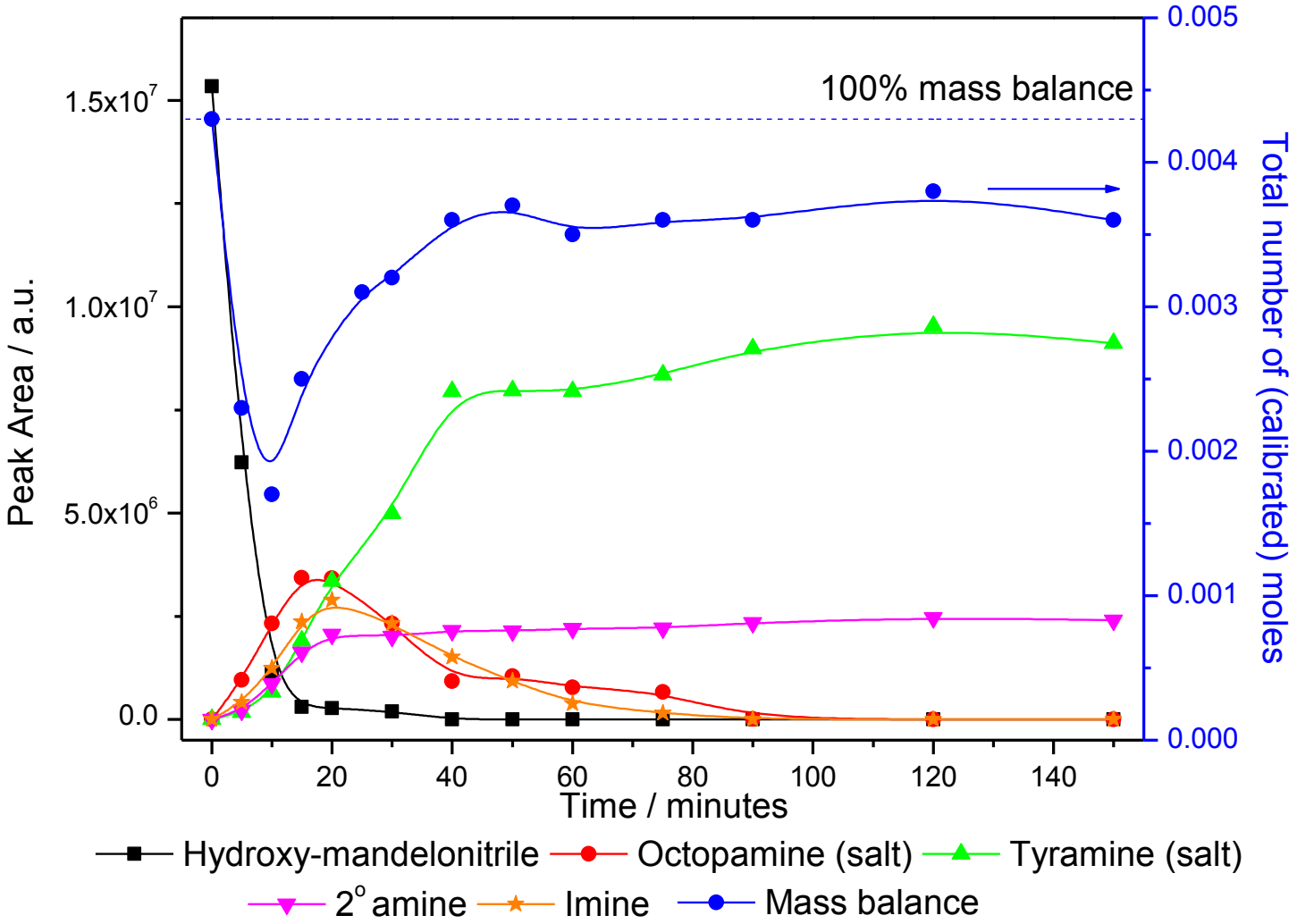

Figure 71. Reaction profile for the hydrogenation of hydroxy-mandelonitrile over 5% Pd/C, 5 mmoles of hydroxy-mandelonitrile, equimolar H_2SO_4, ambient pressure reactor, 60 mL min^{-1} H_2 flow, 30 ^oC.

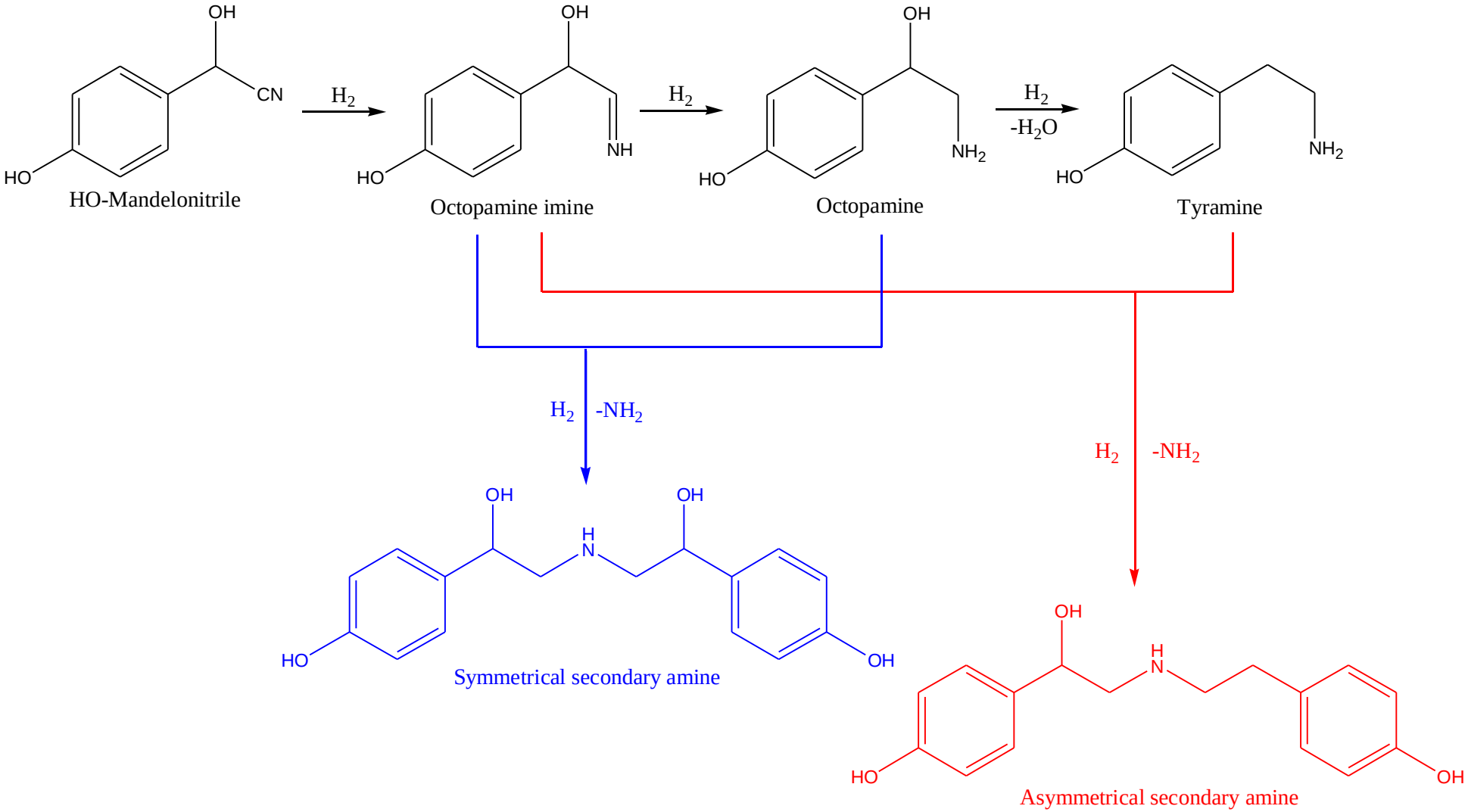

Scheme 31. The hydrogenation of hydroxy-mandelonitrile via intermediate octopamine to yield tyramine (salt). Two different coupling routes are possible: (i) coupling of imine and octopamine (blue) and (ii) coupling of imine and tyramine (red)

3.6.6 Discussion

Determination of the rate coefficients for each reaction using first order exponential decay fits in Origin (based on the consumption of starting material) was performed and the results presented in Table 8.

Table 8. Comparison of the reaction rates of various substituted mandelonitrile-type substrates as referenced against mandelonitrile.

Substrate	Electron withdrawing or donating?	Imine observed?	Higher amines observed?	R^2 (1^{st} order exponential decay fit)	Rate coefficient, k / x 10^{-3} s^{-1}
Mandelonitrile	N/A	No	No	0.98	1.64
Hydroxy-mandelonitrile	Donating[122]	Yes	Yes	0.99	3.44
Methoxy-mandelonitrile	Donating[122]	No	No	0.93	1.48
Methyl-mandelonitrile	Donating (mildly)[122]	No	No	0.93	1.48
Chloro-mandelonitrile	Withdrawing[123]	No	No	0.92	1.95

All four data sets seemed to fit reasonably well to a first order exponential decay. The rate coefficients show that hydroxy-mandelonitrile hydrogenation was the fastest of the reactions. The rate coefficients for all other hydrogenation reactions performed were comparable and approximated to half that of hydroxy-mandelonitrile.

An important observation is that the hydrogenation of hydroxy-mandelonitrile was the only reaction profile to show the presence of an imine. Rather, this reaction was the only one where the imine intermediate was stable enough to be observed in the liquid phase. In the case of hydroxy-mandelonitrile, the presence of a stable imine appears to be a requirement to produce any higher amines. For methoxy-, methyl- and chloro-mandelonitrile, because there were no stable imines observed (*i.e*. they existed only as reactive surface species with a short lifetime), selectivity to the desired primary amine was good for the substrate conversion observed. No

higher amines were observed because the imine intermediate did not exist for a sufficient time to react with any primary amine product. For hydroxy-mandelonitrile, the longer lifetime of the stabilised imine meant it had time to react with products, rather than simply being hydrogenated to an amine as in other reactions.

To justify this, one must consider the resonance and inductive effects. Scheme 32 shows that through a combination of resonance and induction, the imine intermediate can be stabilised in hydroxy-mandelonitrile hydrogenation. Route (a) shows that lone pair electrons form the hydroxy group can be moved through the molecule to give a stabilised imine. This would result in the loss of water and may go some way to explain why there appears to be lower levels of octopamine (salt) in the reaction profile (Figure 71) than was expected – since this form of stabilised imine would mean octopamine could not be formed.

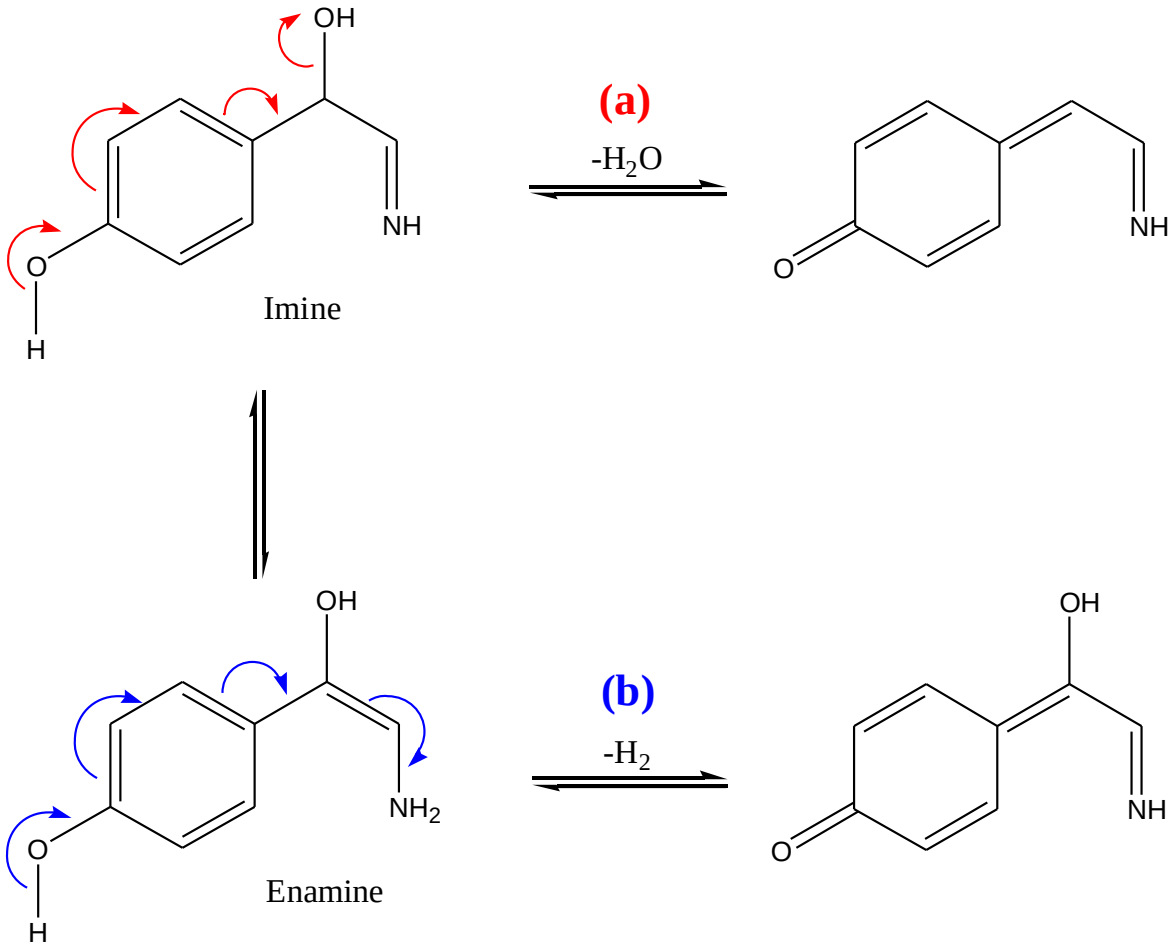

Scheme 32. Suggested resonance stabilisation of intermediates in hydroxy-mandelonitrile hydrogenation.

Route (b) shows how the enamine (tautomer of the imine) can also be resonance stabilised by donation of a lone pair from the hydroxyl group throughout the system. This route maintains conjugation throughout the molecule and also means that there is no loss of water and hence, octopamine is still a possible product.

With any of the other compounds tested here (methoxy-, methyl- and chloro-mandelonitrile), this type of stabilisation appears not to occur. It is because of the nature of the hydroxy group that the imine formed in the hydrogenation of hydroxy-mandelonitrile can be stabilised and is observable in the liquid phase. Hence, selectivity was reduced and a secondary amine was formed.

Finally, despite examining the hydrogenation of mandelonitrile, 4-methoxy-mandelonitrile, 4-methyl-mandelonitrile, 4-chloro-mandelonitrile and 4-hydroxy-mandelonitrile over Pd/C, due to differing reaction profiles, a Hammett-type analysis of the reaction system was thought to be unreliable and so was not pursued further.

3.6.7 Conclusions

- In terms of a global catalyst model, the hydrogenation of hydroxybenzyl cyanide has shown that a further sub-division of the hydrogenation site was required. Namely at low temperature (30 °C) the system possesses insufficient energy (kT) to surmount the barrier linked with the formation of higher amines. However, 60 °C is sufficient to surmount this barrier. The scenario can be encompassed within a model whereby the hydrogenation site identified earlier (Site II) is comprised of standard hydrogenation sites Site II (a) and higher energy sites responsible for by-product formation Site II (b).

- Methoxy-, methyl- and chloro-mandelonitrile hydrogenation reactions all lead to the eventual deactivation of the Pd/C catalyst used in these studies. Whilst initial reaction rates were broadly similar to that for mandelonitrile, the rate of hydrogenolysis of the relevant hydroxyamine intermediates was found to be on the whole slower. This suggests that the source of catalyst deactivation may be due to retention of hydroxyamine (however, the acid

additive should prevent such a scenario) or the formation and retention of higher amines, in much the same way as was observed in the mandelonitrile repeat addition experiments (over an unannealed catalyst).

- Hydroxy-mandelonitrile hydrogenation was the only substituted-mandelonitrile substrate studied where no deactivation issues were observed. Instead, the reaction rate was found to be approximately double that of all other mandelonitriles and the reaction was found to be complete after 60 minutes. However, despite an improvement in activity, selectivity was found to decrease as the result of the formation of a secondary amine by-product.

- Interestingly, only the hydroxy-substituted substrates led to the observation of imine intermediates in the liquid phase. It is believed that through resonance stabilisation due to the electron withdrawing effect of the hydroxyl group, imine intermediates are stable enough to desorb from the catalyst surface. However, whilst the observation coincided with the most active reactions, it may also be diagnostic of the formation of higher amines.

3.7 Reaction systems tested at the industrial centre

As an addition to the studies carried out in-house, a brief amount of time was spent at the industrial centre. Specifically, this time was used to concentrate on the industrial hydrogenation system (unspecified) over the industrial catalyst, but is not presented here. All reactions were carried out in the Syngenta Parr reactor as described in Section 2.1.4. This work is reported separately, not least as it allows comparisons between the academic and industrial protocols to be identified and considered.

To allow direct comparisons between the catalyst used in most of the studies discussed previously here and the industrial catalyst, the work-plan to be carried out was designed to use both 5% Pd/C, Aldrich (referred to as Glasgow University 1, or GU1) and the industrial 5% Pd/C (referred to as Syngenta 1, or S1). In addition to the process substrate, the other reaction systems studied were:

(i) As a benchmark, benzonitrile hydrogenation
(ii) Mandelonitrile hydrogenation with acid
(iii) 4-Hydroxy mandelonitrile hydrogenation with acid.

3.7.1 Benzonitrile hydrogenation

3.7.1.1 Benzonitrile over GU1

Benzonitrile hydrogenation was first carried out at ambient temperature (*ca.* 20 ^{o}C). and, even at reaction times of more than 6 hours, very little conversion of benzylamine to toluene was observed. The reaction was, therefore, repeated at higher temperature (60 ^{o}C) and the reaction profile is presented in Figure 72. The lowest temperature the reaction had been carried out at the academic centre was 30 ^{o}C (not presented in this study), and while hydrogenolysis was slow, toluene was observed in higher amounts than the reaction carried out at 20 ^{o}C at the industrial centre. One possibility for this observation is a restricted hydrogen supply within the Parr reactor. This issue will be considered further below.

Initial reactions used a larger concentration of substrate (*ca.* 0.2 mol L^{-1}) than is usual for reactions at GU to counter any rate increase as a consequence of the

higher-pressure Parr reactor (as opposed to the ambient pressure or Buchi reactor used previously). However, Figure 72 shows that a loss of catalyst activity was evident. Full conversion of nitrile occurs, but hydrogenolysis of benzylamine to toluene was limited and trace amounts of secondary amine – dibenzylamine – were observed ($C_6H_5CH_2$-NH-$CH_2C_6H_5$), as confirmed by GCMS. The presence of secondary amine fell over time suggesting that it was either converted to a tertiary amine (as evidenced by a loss in mass balance), or was broken down to yield benzylamine (appears unlikely given that mass balance does not recover). In previous studies presented in this project, no loss of activity and no higher amines were observed for the benzonitrile system. The rate of reaction (benzonitrile decay) was also observed to be much slower than is usual.

To counter the loss of activity, substrate concentration was reduced to levels used in previous studies discussed earlier (*ca.* 0.05 mol L^{-1}, as in Section 3.3). It was believed that the increased mass of substrate/products coupled with a slower rate was the cause of limited conversion. Figure 73 shows that the loss of activity is repeated over GU1. The initial rate of nitrile appears faster than the previous reaction (Figure 72). However, hydrogenolysis remains limited and toluene concentration looks to be steady towards the end of reaction sampling. Again, the formation and ultimate decay of secondary amine is repeated.

Two possible reasons for the difference in activity over GU1 at the industrial centre and the results discussed previously are thought to be either (i) a change in the catalyst or (ii) a difference in the reactors. Given that the catalyst used was the same sample/batch as that used throughout the project, it appears unlikely that changes in the catalyst were the cause.

It therefore seems more likely that some mass transfer limitation associated with the Parr reactor may be the central issue. Given that the ambient pressure and Buchi reactors produced comparable results with the same substrate and catalyst, but the Parr reactor shows a lower rate of hydrogenolysis (Figure 72), it is the latter reactor that is thought to be anomalous. It therefore appears that the hydrogenolysis process is retarded in the Parr reactor, and it is proposed that the gas/solution mixing properties are superior in the GU reactors. This attenuated supply of hydrogen to the catalyst surface then impedes the second stage process, which possesses the higher activation energy.

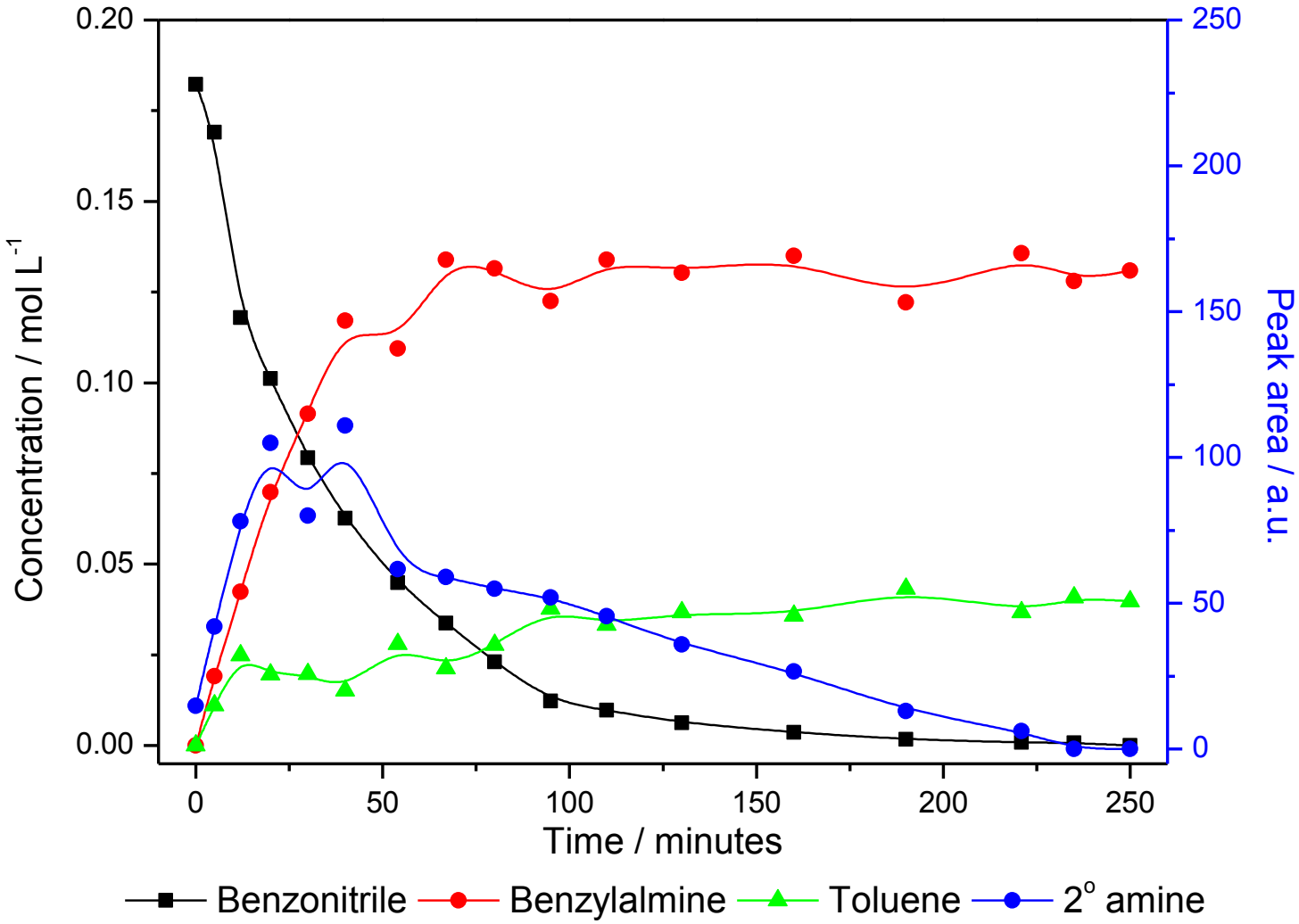

Figure 72. Reaction profile for the hydrogenation of benzonitrile over GU1 (5% Pd/C, Aldrich), *ca.* 15 mmoles of benzonitrile, Syngenta Parr reactor, 6 bar H_2, 60 ^{o}C (high concentration reaction of *ca.* 0.2 mol L^{-1}).

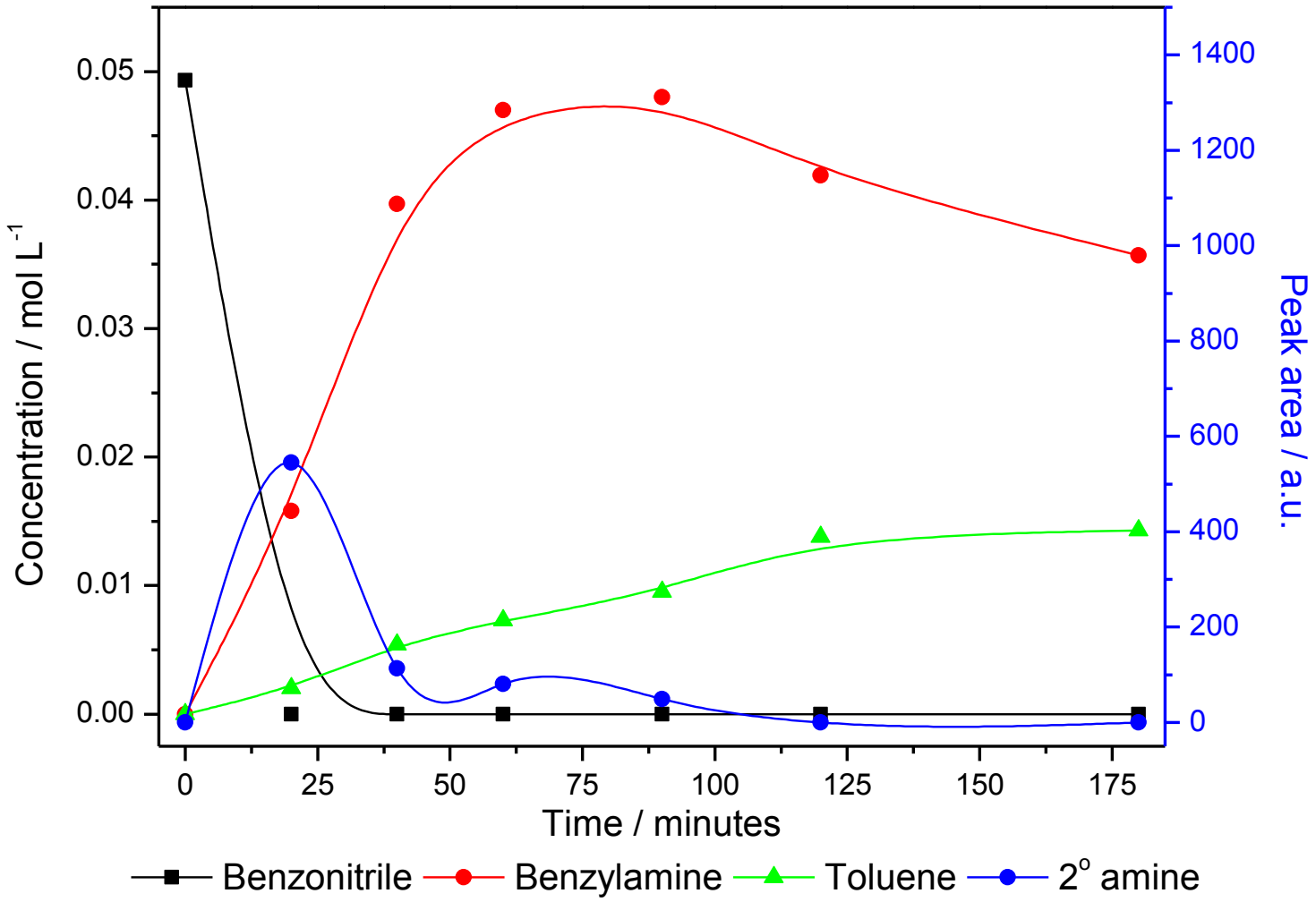

Figure 73. Reaction profile for the hydrogenation of benzonitrile over GU1 (5% Pd/C, Aldrich), *ca.* 4 mmoles of benzonitrile, Syngenta Parr reactor, 6 bar H_2, 60 ^{o}C (low concentration reaction of *ca.* 0.05 mol L^{-1}).

3.7.1.2 Benzonitrile over S1

Figure 74 shows that over S1, the reaction proceeded in a much more similar fashion to those results presented previously. Benzonitrile hydrogenation was found to be fast and full conversion was attained in around 50 minutes, at a time where maximum concentration of benzylamine was observed. No secondary amine was observed and toluene was found to be the only product of the reaction.

Now, the benzonitrile/S1/Parr combination (Figure 74) essentially replicates the trends seen for the benzonitrile/GU1/Buchi system (Figure 23), which initially indicates that the benzonitrile/GU1/Parr result (Figure 73) could be anomalous. However, these differences are thought to indicate some complexity in the reaction system, where the ultimate reaction profile is a convolution of differences between the two catalysts (GU1 and S1) and the hydrodynamics of the different reactor configurations.

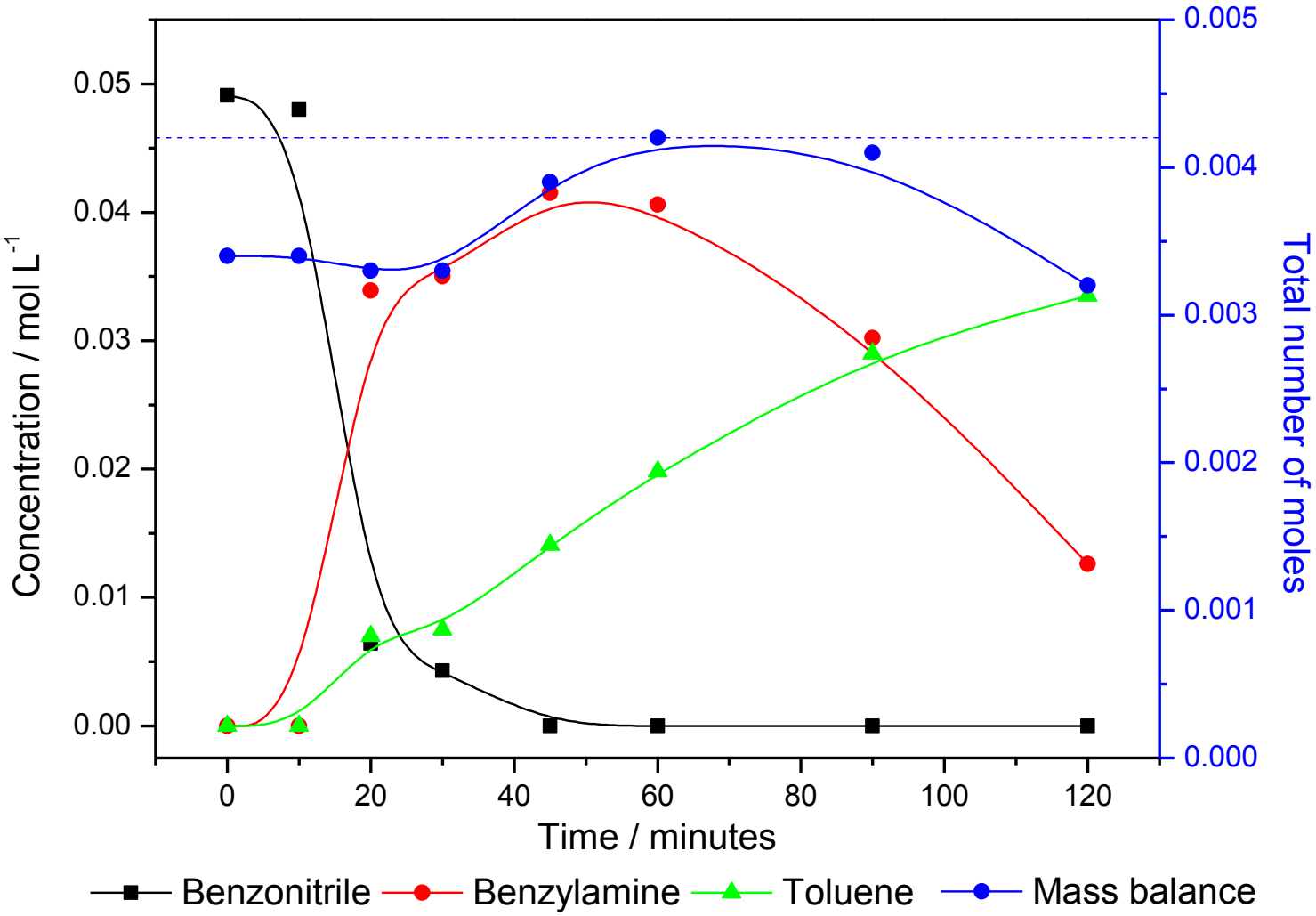

Figure 74. Reaction profile for the hydrogenation of benzonitrile over S1 (5% Pd/C, Syngenta), *ca.* 4 mmoles of benzonitrile, Syngenta Parr reactor, 6 bar H_2, 60 ^{o}C.

3.7.2 Mandelonitrile hydrogenation

3.7.2.1 Mandelonitrile over GU1

Again, the first reaction carried out on mandelonitrile (under acid conditions) used a larger-than-usual concentration of substrate (*ca.* 0.175 mol L^{-1}), which, as can be seen in Figure 75, resulted in a loss of catalyst activity. One would normally expect mandelonitrile hydrogenation to proceed with *ca.* 100% conversion and give *ca.* 100% selectivity to the primary amine phenethylamine (salt) in the presence of an acid.

As with benzonitrile hydrogenation, the reaction was repeated with lower substrate concentration (*ca.* 0.05 mol L^{-1}) and the reaction profile obtained is shown in Figure 76. Whilst the rate of hydrogenation and conversion of nitrile does not vary, hydrogenolysis of 2-amino-1-phenylethanol goes to (approaching) completion. As with benzylamine hydrogenolysis, it appears that an accumulation of 2-amino-1-phenylethanol (salt) may be responsible for the loss in activity. When its concentration is reduced, the catalyst is able to provide the necessary conversion. Despite a slower rate of hydrogenation and hydrogenolysis, the profile is similar to those discussed previously.

These trends are indicative of a reduced hydrogen supply within the Parr system compared to that experienced at the academic centre (in both the Buchi and ambient pressure reactors).

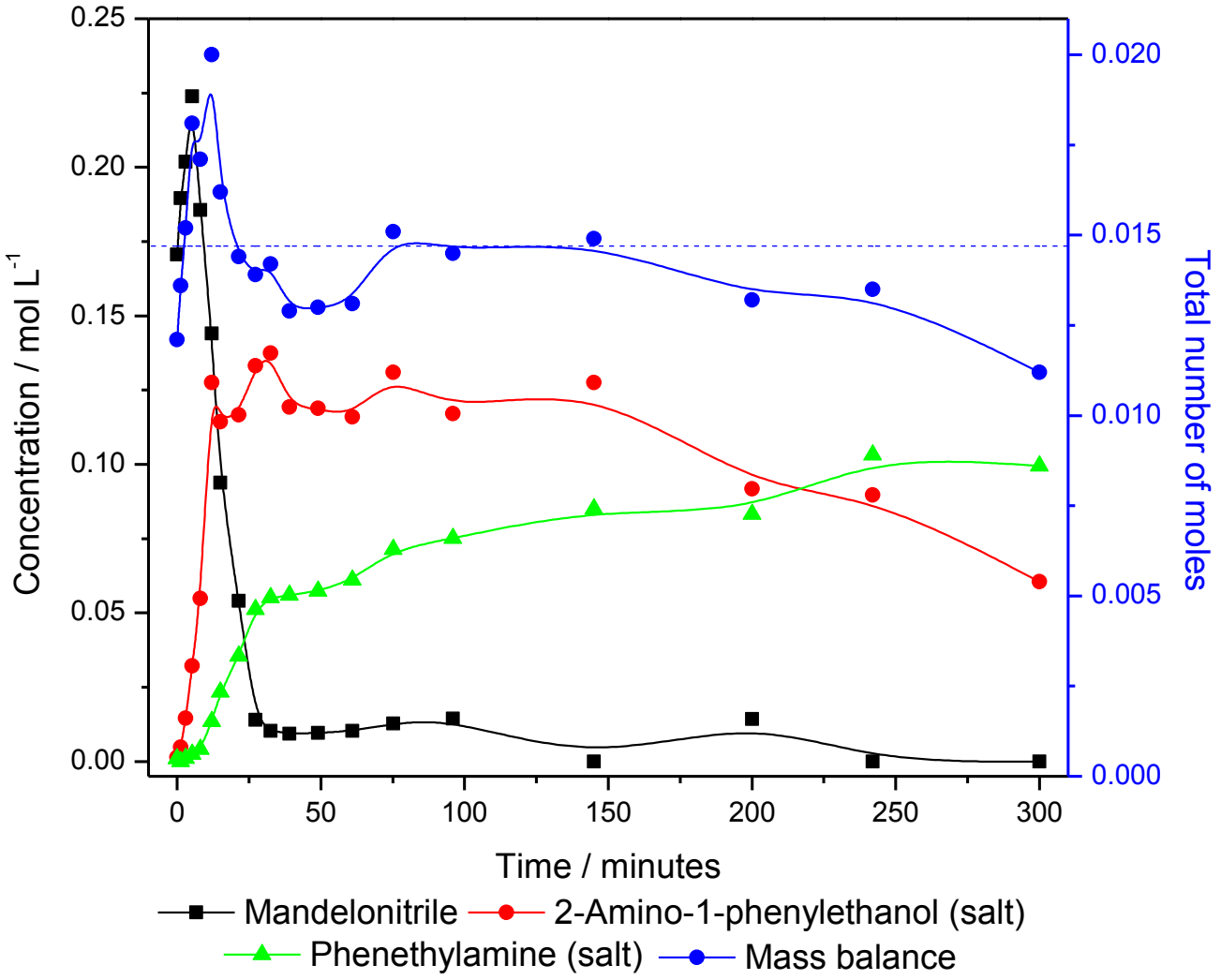

Figure 75. Reaction profile for the hydrogenation of mandelonitrile over GU1 (5% Pd/C, Aldrich), *ca.* 15 mmoles of mandelonitrile, equimolar H_2SO_4, Syngenta Parr reactor, 6 bar H_2, 20 ^{o}C (high concentration reaction of *ca.* 0.175 mol L^{-1}).

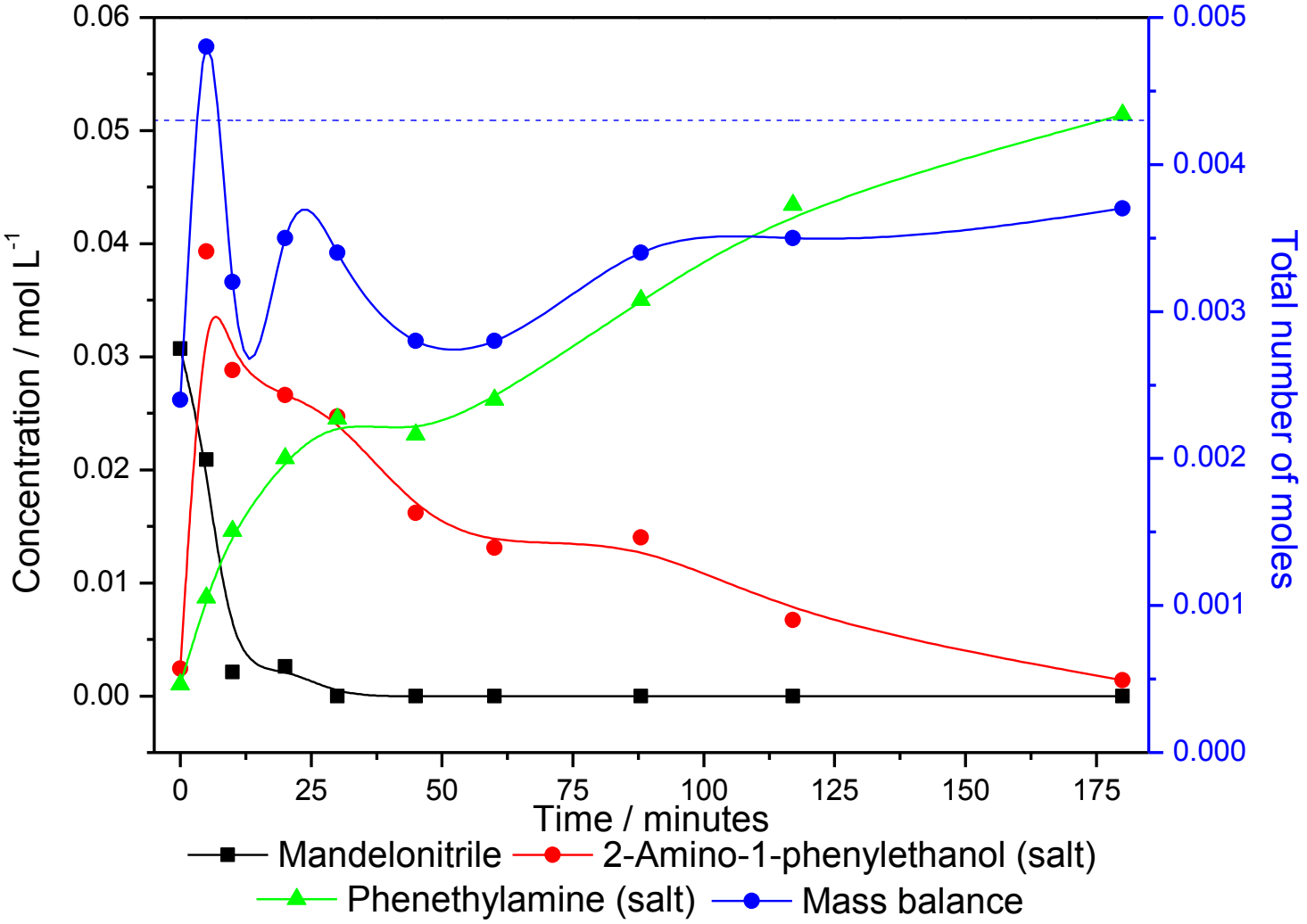

Figure 76. Reaction profile for the hydrogenation of mandelonitrile over GU1 (5% Pd/C, Aldrich), *ca.* 4 mmoles of mandelonitrile, equimolar H_2SO_4, Syngenta Parr reactor, 6 bar H_2, 20 ^oC (low concentration reaction of *ca.* 0.05 mol L^{-1}).

3.7.2.2 Mandelonitrile over S1

Figure 77 shows that when using S1, the reaction profile for mandelonitrile at the lower concentration of *ca.* 0.05 mol L^{-1} is much more similar to those previously discussed (Section 3.5). Nitrile hydrogenation is observed as fast (full conversion of nitrile in *ca.* 15 minutes), and hydrogenolysis of the intermediate hydroxyamine occurs much more readily than over GU1 in the Parr system. Phenethylamine (salt) is observed from the onset of reaction as the final product of the reaction.

However, as has been observed with some substituted mandelonitriles (and has been seen when larger quantities of substrates are used), 2-amino-1-phenylethanol (salt) concentration reaches a maximum, decays sharply, but then reaches a nearly constant value, suggesting a loss of activity. It is known that the intermediate hydroxyamine is responsible for catalyst poisoning in the absence of an acid additive and so it may be that not enough acid was used to counter the poisoning effect of the hydroxyamine.

Comparing Figure 76 and Figure 77, the profiles are broadly comparable. This suggests that S1 and GU1 behave similarly, indicating the testing of model compounds over GU1 at the academic centre as being directly applicable to the surface chemistry related to the actual industrial reaction.

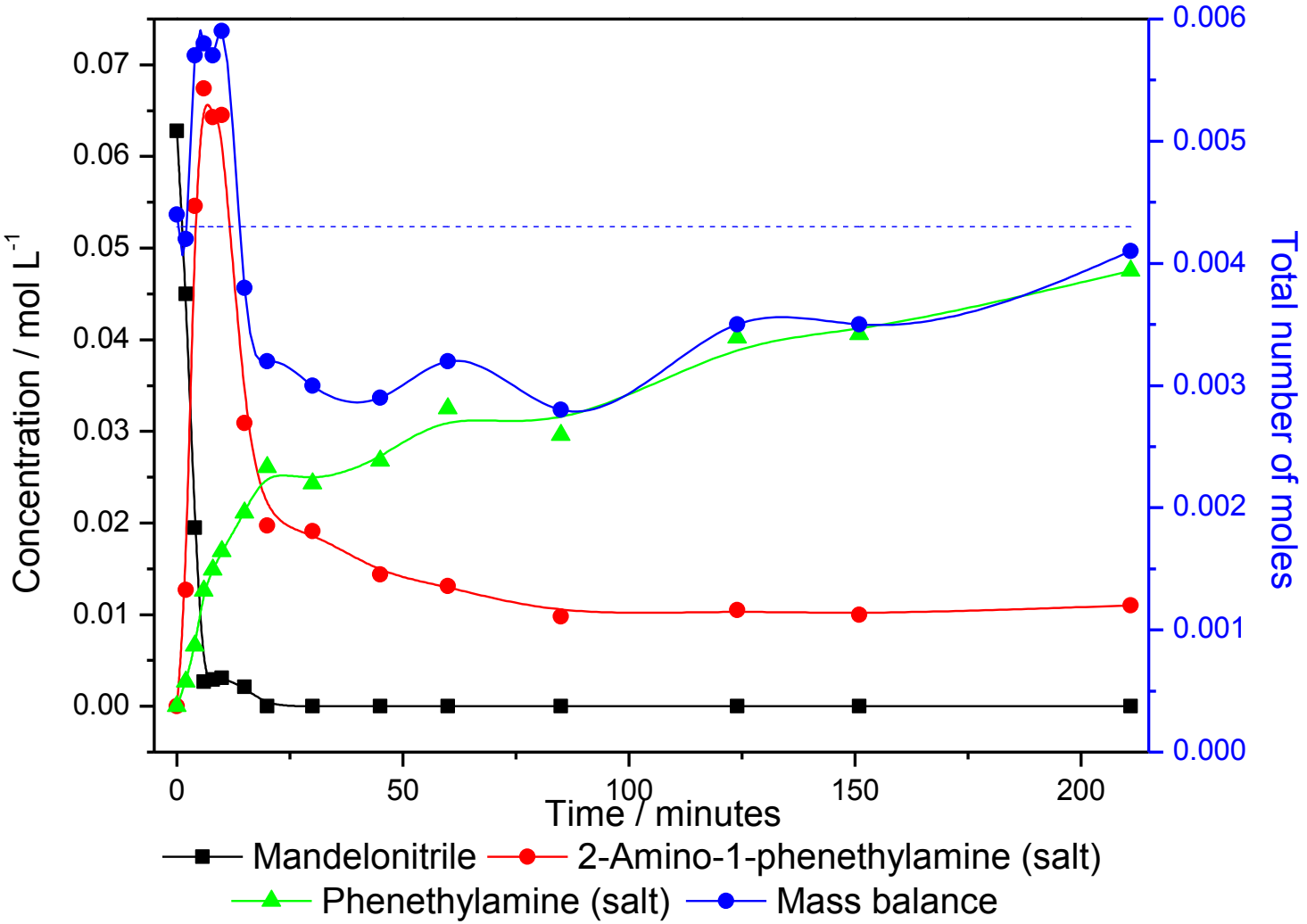

Figure 77. Reaction profile for the hydrogenation of mandelonitrile over S1 (5% Pd/C, Syngenta), *ca.* 4 mmoles of mandelonitrile, equimolar H_2SO_4, Syngenta Parr reactor, 6 bar H_2, 20 ^oC (low concentration reaction of *ca.* 0.05 mol L^{-1}).

3.7.3 Hydroxy-mandelonitrile hydrogenation over GU1 and S1, carried out at the industrial centre

Figure 78 shows the reaction profile for hydroxy-mandelonitrile hydrogenation over GU1. On close inspection, it can be seen that no hydroxybenzyl cyanide was observed and so it may be assumed that hydrogenation occurs first (as expected). The reaction proceeds via octopamine (salt) to produce tyramine (salt) as the major product, with selectivity of *ca.* 98%. A small amount of a secondary amine is also produced as a minor product (*ca.* 2% selectivity). Once again for hydroxy-mandelonitrile hydrogenation, octopamine-imine was formed as an intermediate and observed in the liquid phase. Whilst the profile is similar to that of previous studies (Section 3.6.5), selectivity to tyramine (salt) has improved somewhat from *ca.* 85% in those studies to *ca.* 98% here.

Over S1 the picture is rather simpler as is seen in the reaction profile in Figure 79. Again tyramine (salt) is the major product but, while selectivity is slightly lower than for GU1 at 90%, no higher amines were observed. The intermediate imine is observed in much lower amounts than over GU1 (note the difference in scale for the secondary y-axes). However, the catalyst appears to suffer from deactivation issues towards the end of sampling time, as evidenced by the constant concentration of octopamine after *ca.* 70 minutes. Thus, for this reaction, GU1 is producing a more favourable yield of product than the industrial catalyst (S1).

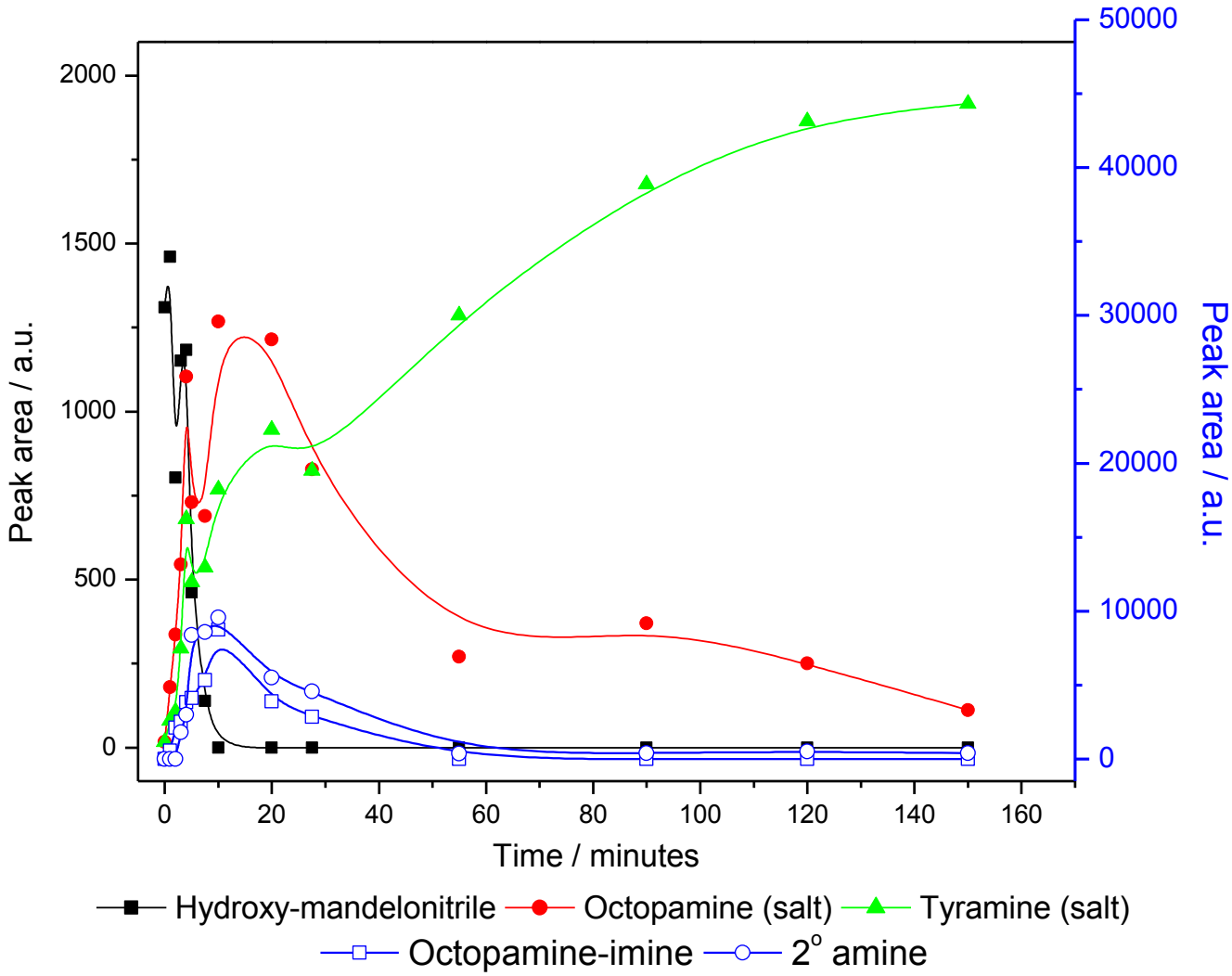

Figure 78. Reaction profile for the hydrogenation of hydroxy-mandelonitrile over GU1 (5% Pd/C, Aldrich), *ca.* 4 mmoles of hydroxy-mandelonitrile, equimolar H_2SO_4, Syngenta Parr reactor, 6 bar H_2, 20 °C. Components in blue are on the secondary axis.

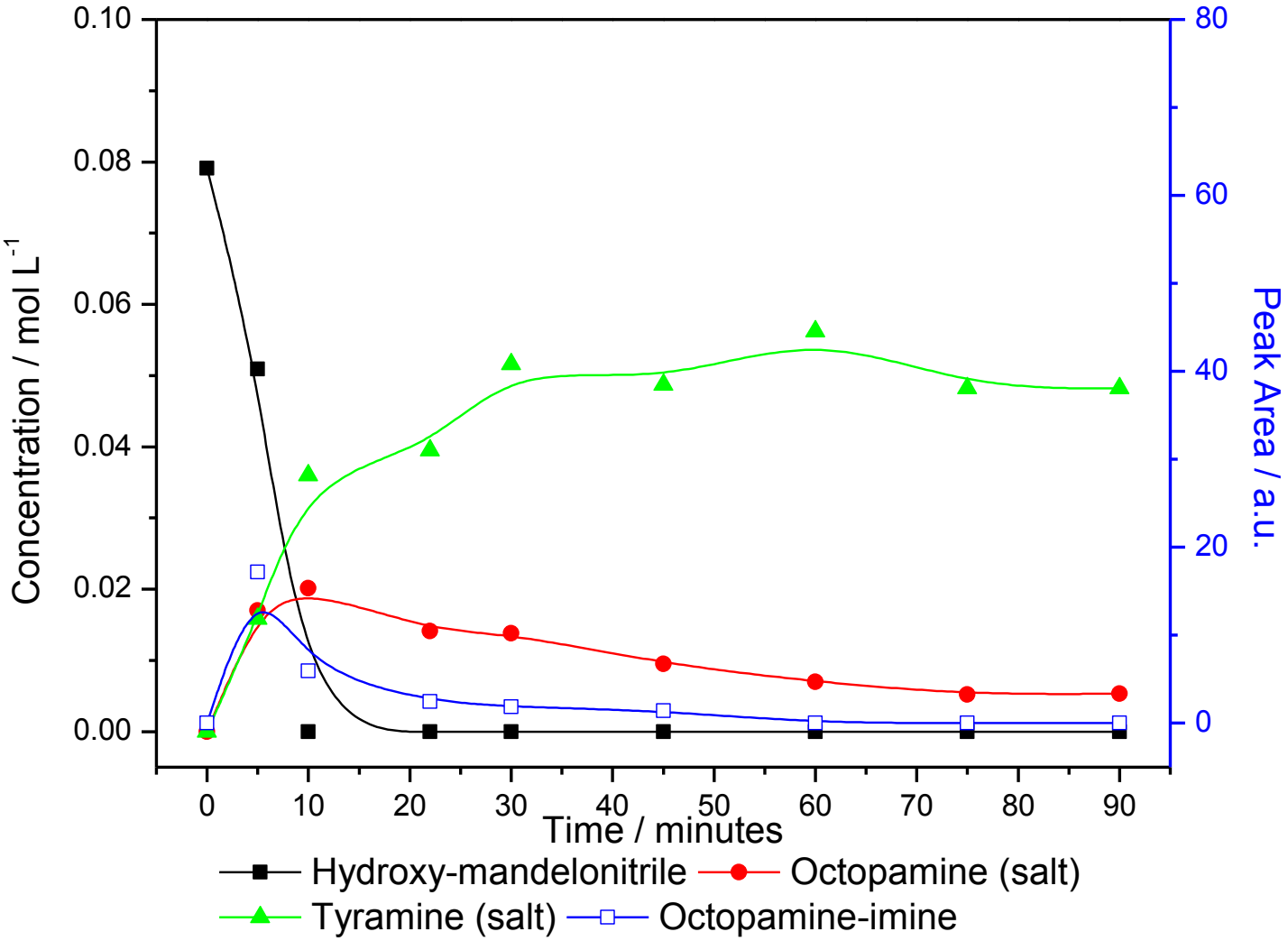

Figure 79. Reaction profile for the hydrogenation of hydroxy-mandelonitrile over S1 (5% Pd/C, Syngenta), *ca.* 4 mmoles of hydroxy-mandelonitrile, equimolar H_2SO_4, Syngenta Parr reactor, 6 bar H_2, 20 ^oC. Components in blue are on the secondary axis.

3.7.4 Conclusions

A series of reactions were carried out at the industrial centre using a Parr autoclave reactor to compare the reaction conditions and the catalyst used in the academic centre to those used in the industrial process.

- In the study for benzonitrile hydrogenation, the second stage hydrogenolysis proved difficult. Even at elevated temperature over GU1, hydrogenolysis was slow and the reaction profile showed signs of deactivation, suggesting some change in the catalyst activity. Over S1, the hydrogenation performed in a much more similar manner to the studies at the academic centre.

- For both benzonitrile and mandelonitrile hydrogenations, it was found that in more concentrated reactions, deactivation issues were more prevalent. This suggests that a cumulative poisoning effect (similar to that found in the mandelonitrile repeat additions experiment) may be at play, where the catalyst is “overloaded” with products, thereby limiting site availability. It is also possible that the higher concentrations of substrate exceed the available hydrogen supply, thereby facilitating catalyst deactivation. Variable concentration studies were not carried out at the academic centre.

- Both catalysts performed similarly for hydroxy-mandelonitrile hydrogenation, thereby showing that the 5% Pd/C (GU1) used was a good model for the industrial Pd/C catalyst.

Summarising the measurements undertaken at the industrial complex, it is apparent that catalyst deactivation can readily occur and that the academic data sets represent a favourable combination of substrate concentration and hydrodynamics. Enhanced hydrogen supply is desirable but the rate laws determined for benzonitrile hydrogenation suggest more is required beyond elevated hydrogen pressures. Comparable measurements between the Parr and Buchi reactors suggest more favourable mixing characteristics occur with the GU reactor. One possibility for the industrial reaction system would be to reduce the nitrile concentration and to use a catalyst modified in a similar fashion to the annealed Pd/C discussed in Section 3.5.6.

4 Final conclusions and future work

A series of model systems were used to probe the issues relevant to the hydrogenation of aromatic nitriles.

The hydrogenation of benzonitrile was chosen as the first model system because of its simple structure. However, the reaction proved to be rather more complex than expected. Hydrogenolysis was found to cause the loss of the desired benzylamine to yield the significantly less valuable toluene. Further investigations have shown that both hydrogenation and hydrogenolysis occur on distinct sites with varying kinetics and dependencies upon hydrogen pressure. The rate law for hydrogenation was found to be ambiguous, and suggested that the reaction may be on the verge of being limited by hydrogen supply. Such an observation is thought to be important in the industrial process, since a limited hydrogen supply may lead to an accumulation of semi-hydrogenated species (i.e. imine intermediates and hydroxyamines) that are thought to lead to catalyst deactivation.

Whilst hydrogenolysis was unexpected and unwanted in benzonitrile hydrogenation, the reaction is required if one is to yield a primary amine from the hydrogenation of cyanohydrins (*e.g.* mandelonitrile). Through various co-adsorption studies, it was shown that hydroxyamine intermediates formed in cyanohydrin hydrogenations were responsible for catalyst deactivation. One way around such a problem is to use an acid additive, that protonates the amine group of such species, thus preventing strong adsorption of the group. This method ensures that the proposed orientation required for hydrogenolysis can be attained, resulting in the loss of water to yield primary amine products.

However, in reactions designed to replicate the “fed-batch” nature of the industrial process, repeat additions of mandelonitrile and acid resulted in a dramatic loss in catalyst activity from one addition to the next, and a complete loss of conversion by the 4^{th} addition. It is suggested that the accumulation of strongly bound imine intermediates on high energy sites leads to coupling reactions and poisoning. The presence of high energy, so called “edge-sites”, was confirmed by varying the temperature of reaction in hydroxybenzyl cyanide hydrogenation studies.

Understanding what role an imine intermediate plays and the routes by which secondary and tertiary amines are formed in catalyst deactivation is one of the key problems in investigating cyanohydrin hydrogenation. It was always believed that an imine that was stable enough to desorb from the catalyst, and thus be observable in the liquid phase, was the route to many of the selectivity and deactivation issues that Syngenta observe in the industrial system. However, experimental results have shown that concept to be somewhat ambiguous.

The first issue was that no imines were observed in the majority of reactions performed. Because of this, no higher amines were observed and selectivity was always found to be good. Such systems included benzonitrile, benzyl cyanide and mandelonitrile hydrogenations, making it difficult to draw any conclusions about the role of an imine in such reactions. However, when one considered substituted mandelonitrile-type substrates, there was varying degrees of catalyst deactivation and reduced selectivity. Similarly, the presence of an imine in the liquid phase was dependent upon the substituent on the aromatic ring.

In the hydrogenation of hydroxy-mandelonitrile, the mass balance for the reaction was found to fall and recover with formation and conversion of the imine intermediate and was thus attributed to adsorbed imine. However, for all other *p*-substituted-mandelonitriles, no imine was observed and as such, no higher amines formed. Thus, from the experimental data presented here, the imine seems to have an ambiguous role:

(i) When no imine is observed, selectivity is good but catalyst deactivation is a problem in cyanohydrin hydrogenation.

(ii) When the imine is observed, as in the case of hydroxy-mandelonitrile, catalyst deactivation is not an issue. Indeed, conversion was found to be 100%. However, selectivity was significantly reduced despite a high yield of primary amine. However, hydroxybenzyl cyanide hydrogenation showed that even if the imine is observed, its presence does not necessarily lead to higher amines.

In summary, the presence of the imine in the liquid phase does not appear diagnostic of losses in selectivity or activity, but its role and the routes to deactivation are all ambiguous. In order to identify exactly which species are

responsible for loss of catalytic activity, there is a need to probe the interactions at the catalyst interface. While it was beyond the scope of this project, spectroscopic techniques to probe the catalyst surface, such as FTIR and INS spectroscopies, could be useful in identifying the exact nature of the poisons.

A possible solution to the problem of catalyst deactivation appears to be by limiting the number of high energy sites responsible for coupling reactions. Annealing of the Pd/C catalyst led to an increase in particle size and a change in particle shape that, despite a decrease in reaction rate, ensured that catalyst lifetime could be increased dramatically. This catalyst is in the process of being tested at the industrial centre, and its use should be extended to study its activity/lifetime in more complex reaction systems. Selective poisoning strategies could also be used during catalyst preparation to limit such sites.

5 Appendix 1 – FTIR tables of assignments

Table 9. FTIR assignments of gas phase benzonitrile.[124]

Wavenumber / cm^{-1}	Assignment
756	C-H bend
922	C-H bend
1026	C=C stretch
1070	C=C stretch
1446	C-C ring stretch
1455	C-C ring stretch
2238	CN stretch
3078	Symmetric C-H stretch (aromatic)
3088	Asymmetric C-H stretch (aromatic)

Table 10. FTIR assignments of gas phase benzylamine.[125]

Wavenumber / cm^{-1}	Assignment
803	Ring bending and stretching
850	Out of plane C-H stretch
906	NH_2 wag and CH_2 rock
1028	In plane C-H stretch
1387	C-C ring stretch
1451	C-C ring stretch
1497	C-C ring modes
1619	NH_2 scissoring
2903	C-H stretch (aliphatic)
3040	Symmetric C-H stretch (aromatic)
3078	Asymmetric C-H stretch (aromatic)

Table 11. FTIR assignments of gas phase toluene.[117,118]

Wavenumber / cm^{-1}	Assignment
693	C-H bend
729	C-H bend
1031	C=C stretch
1075	C=C stretch
1388	Methyl symmetric deformation
1457	Methyl asymmetric deformation
1498	C-H bend
1615	C=C asymmetric stretch
2912	C-H stretch (aliphatic)
3040	Symmetric C-H stretch (aromatic)
3078	Asymmetric C-H stretch (aromatic)

Table 12. FTIR assignments of gas phase ammonia.[108]

Wavenumber / cm^{-1}	Assignment
950	N-H wag
1631	H-N-H scissor
3444	N-H asymmetric stretch

Table 13. FTIR assignments of gas phase ammonia-d_3.[108]

Wavenumber / cm^{-1}	Assignment
745	N-D wag
1191	D-N-D scissor
2564	N-D asymmetric stretch

Table 14. FTIR assignments of gas phase toluene-d_3.[114,117]

Wavenumber / cm^{-1}	Assignment
708	C-H bend
927	C-H bend
1025	C=C stretch
1497	C-H bend
2075	C-D stretch (aliphatic)
2138	C-D stretch (aliphatic)
1606	C=C stretch
3040	Symmetric C-H stretch (aromatic)
3080	Asymmetric C-H stretch (aromatic)

6 Bibliography

1 R. A. Santen, P. W. N. M. van Leuwen, and J. A. Moulijn, *Stud. Surf. Sci. Catal.*, 1999, **123**, 3.

2 A. D. McNaught and A. Wilkinson, *IUPAC compendium of chemical terminology (the "Gold Book")*, Blackwell Scientific Publications, Oxford, 1997.

3 S. Furusaki, J. Garside, and L. S. Fan, *The expanding word of chemical engineering*, Taylor and Francis, London, 2nd edn., 2002.

4 M. Bowker, *The basis and applications of heterogeneous catalysis*, Oxford University Press, New York, 1998.

5 R. L. Augustine, *Catalytic hydrogenation techniques and applications in organic synthesis*, E. Arnold, London, 1965.

6 M. Benaglia, *Recoverable and recyclable catalysts*, John Wiley and Sons, Ltd., Chichester, 2009.

7 D. Lennon, D. R. Kennedy, G. Webb, and S. D. Jackson, *Stud. Surf. Sci. Catal.*, 1999, **126**, 341.

8 D. R. Kennedy, G. Webb, S. D. Jackson, and D. Lennon, *App. Catal. A: Gen.*, 2004, **259**, 109.

9 D. R. Kennedy, B. Cullen, D. Lennon, G. Webb, P. R. Dennison, and S. D. Jackson, *Stud. Surf. Sci. Catal.*, 1999, **122**, 125.

10 D. Lennon, R. Marshall, G. Webb, and S. D. Jackson, *Stud. Surf. Sci. Catal.*, 2000, **130**, 245.

11 R. Marshall, G. Webb, S. D. Jackson, and D. Lennon, *J. Mol. Catal. A: Chem.*, 2005, **226**, 227.

12 J. A. Lopez-Sanchez and D. Lennon, *App. Catal. A: Gen.*, 2005, 291, 301.

13 D. S. Anderson, University of Glasgow, 1999.

14 D. S. Anderson, S. D. Jackson, D. Lennon, and G. Webb, *Catal. Org. React.*, 2005, **103**, 195.

15 I. T. Duncanson, I. W. Sutherland, B. Cullen, S. D. Jackson, and D. Lennon, *Catal. Lett.*, 2005, **103**, 196.

16 B. Cullen, PhD Thesis, University of Glasgow, 2001.

17 R. Leslie, PhD Thesis, University of Glasgow, 2001.

18 I. T. Duncanson, MSc Thesis, University of Glasgow, 2002.

19 I. Sutherland, MSci Thesis, University of Glasgow, 2002.

20 E. Gibson, MSCi Thesis, University of Glasgow, 2003.

21 D. McKay, MSci Thesis, University of Glasgow, 2004.

22 K. Galloway, MSci Thesis, University of Glasgow, 2005.

23 J. Callison, MSci Thesis, University of Glasgow, 2006.

24 T. O. Salmi, J. P. Mikkola, and J. P. Warna, *Chemical reaction engineering and reactor technology*, CRC Press, Taylor and Francis Group, FL, 2011.

25 I. S. Metcalfe, *Chemical Reaction Engineering: A First Course*, Oxford University Press, Oxford, 1997.

26 D. Lennon, in *Chem-4M Lecture Series*, University of Glasgow, 2008.

27 R. A. Sheldon and H. van Bekkum, *Fine chemicals through heterogeneous catalysis*, Wiley-VCH, Weinheim, 1996.

28 B. Cornils and W. A. Herrman, *Applied homogeneous catalysis with organometallic catalysis*, Wiley-VCH, Weinheim.

29 K. Drauz and H. Waldemann, *Enzyme catalysis in organic synthesis*, Wiley-VCH, Weinheim, 1995.

30 G. Ertl, H. Knozinger, and J. Weitkamp, *Handbook of heterogeneous catalysis*, Wiley-VCH, Weinheim, 1992.

31 J. M. Thomas and W. J. Thomas, *Principles and applications of heterogeneous catalysis*, Wiley-VCH, Weinheim, 1997.

32 R. L. Augustine, *Heterogeneous catalysis for the synthetic organic chemist*, Marcel Dekker Publishing, New York, 1996.

33 R. A. Sheldon and H. van Bekkum, *Fine chemicals through heterogeneous catalysis*, Wiley-VCH, Weinheim, 2nd edn., 2002.

34 J. Whittall, *Catalysts for Fine Chemical Synthesis, Volume 5, Regio- and Stereo-Controlled Oxidations and Reductions*, Wiley, New York, 2007.

35 H. U. Blaser, C. Malan, B. Pugin, F. Spindler, H. Steiner, and M. Studer, *Adv. Syn. Catal.*, 2003, **345**, 103.

36 H. U. Blaser, *Catal. Today*, 2000, **60**, 161.

37 R. A. Sheldon, *Chem. Int.*, 1992, 906.

38 I. Jaffe, M. Segal, and A. Efraty, *J. Organomet. Chem.*, 1985, **294**, 17.

39 R. J. Farrauto and C. H. Bartholomew, *Fundamentals of industrial catalytic processes*, Chapman and Hall, UK, 1997.

40 S. P. Bawane and S. B. Sawant, *Chem. Eng. J.*, 2004, **103**, 13.

41 A. Agrawal and P. G. Tratnyek, *Environ. Sci. Technol.*, 1995, **30**, 153.

42 S. Laval, W. Dayoub, L. Pehlivan, E. Metay, A. Favre-Reguillon, D. Delbrayelle, G. Mignani, and M. Lemaire, *Tet. Lett.*, 2011, **53**, 4072.

43 E. M. Dangerfield, C. H. Plunkett, A. L. Win-Mason, B. L. Stocker, and M. S. M. Timmer, *J. Org. Chem.*, 2010, **75**, 5470.

44 L. Hegedus and T. Mathe, *App. Catal. A: Gen.*, 2005, **296**, 209.

45 C. V. Rode, M. Arai, M. Shirai, and Y. Nishiyama, *App. Catal. A: Gen.*, 1997, **148**, 405.

46 G. C. Bond, *Platinum Metal Reviews*, 1964, **8**, 60.

47 A. Balandin, *Adv. Catal.*, 1969, **19**, 1.

48 G. C. Bond and P. B. Wells, *Adv. Catal.*, 1964, **15**, 171.

49 G. C. Bond, D. A. Dowden, and N. MacKenzie, *Trans. Farad. Soc.*, 1958, **54**, 1537.

50 N. W. Campbell, W. Anderson, and J. Gilmore, *J. Chem. Soc.*, 1940, 819.

51 X. D. Xu, H. Vonk, A. C. J. M. Vanderiet, A. Cybulski, A. Stankiewicz, and J. A. Moulijn, *Catal. Today*, 1996, **30**, 91.

52 C. Barnett, *Ind. Eng. Chem. Prod. Res. Dev.*, 1969, **9**, 145.

53 S. Nishimura, *Handbook of heterogeneous catalytic hydrogenation for organic synthesis*, John Wiley and Sons Inc., New York, 2001.

54 Y. Huang, V. Adeeva, and W. Sachtler, *App. Catal. A: Gen.*, 2000, **196**, 73.

55 Y. Huang and W. Sachtler, *App. Catal. A: Gen.*, 1999, **182**, 365.

56 J. Zhu, B. A. Price, J. Walker, and S. X. Zhao, *Tet. Lett.*, 2005, **46**, 2795.

57 Y. Huang and W. Sachtler, *J. Catal.*, 1999, **188**, 215.

58 T. S. Work, *J. Chem. Soc.*, 1942, 426.

59 W. H. Carothers and G. A. Jones, *J. Am. Chem. Soc.*, 1925, **47**, 3051.

60 M. Friefelder and Y. Hay Ng, *J. Pharm. Sci.*, 1965, **54**, 1204.

61 W. H. Hartung, *J. Am. Chem. Soc.*, 1928, **50**, 3370.

62 J. von Braun, G. Blessing, and F. Zobel, *Chemische Berichte*, 1923, **56B**, 1988.

63 R. Juday and H. Adkins, *J. Am. Chem. Soc.*, 1955, **77**, 4559.

64 I. Ortiz-Hernandez and C. Williams, *Langmuir*, 2007, **23**, 3172.

65 M. J. F. M. Verhaak, A. J. van Dillen, and J. W. Geus, *Catal. Lett.*, 1994, 26, 37.

66 A. R. McInroy, MSci Thesis, University of Glasgow, 2002.

67 Syngenta UK, *Products and Innovations website*.

68 P. Kukula, M. Studer, and H. U. Blaser, *Adv. Syn. Catal.*, 2004, **346**, 1487.

69 S. S. Zumdhal, *Chemical principles*, Houghton Mifflin Company, Boston, 2007.

70 G. C. Bond, *Heterogeneous Catalysis, Principals and Applications*, Oxford University Press, Oxford, 1982.

71 A. R. McFarlane, L. McMillan, I. P. Silverwood, N. G. Hamilton, D. Siegel, S. F. Parker, D. T. Lundie, and D. Lennon, *Catal. Today*, 2010, **155**, 206.

72 A. Braithwaite and F. J. Smith, *Chromatographic methods*, Springer, New York, 1996.

73 D. L. Pavia, G. M. Lampman, G. S. Kritz, and R. G. Engel, *Introduction to Organic Laboratory Techniques*, Thomson Brooks/Cole, Belmont, CA, 4th edn., 2006.

74 A. Braithwaite and F. J. Smith, *Chromatographic methods* , Springer, New York, 1996.

75 N. G. Hamilton, MSci Thesis, University of Glasgow, 2005.

76 I. G. McWiliam and Dewar R.A., *Nature*, 1958, **181**, 760.

77 L. R. Snyder, J. J. Kirkland, and J. W. Dolan, *Introduction to modern liquid chromatography*, John Wiley and Sons, Hoboken, 3rd edn., 2010.

78 D. A. Skoog, D. M. West, and F. J. Holler, *Fundamentals of analytical chemistry*, Saunders College Publications, Philadelphia, 1996.

79 J. Sherma, *High performance liquid chromatography in phytochemical analysis*, CRC Press, Taylor & Francis Group, Florida, 2010.

80 D. H. Williams and I. Flemming, *Spectroscopic methods in organic chemistry*, McGraw Hill, New York, 5th edn., 1995.

81 P. J. Hore, J. A. Jones, and S. Wimperis, *NMR: The toolkit*, Oxford University Press, Oxford, 2006.

82 R. Harris, *Nuclear magnetic resonance spectroscopy*, Pittman Books, London, 1983.

83 S. H. Smallcombe, S. L. Patt, and P. A. Keifer, *J. Magn. Reson. Ser. A*, 1995, **117**, 295.

84 S. Braun and S. Berger, *200 and more NMR experiments*, Wiley-VCH, Weinheim, 2nd edn., 2004.

85 P. R. Griffiths, *Chemical infrared Fourier transform spectroscopy*, John Wiley and Sons, London, 1975.

86 P. W. Atkins, *Physical chemistry*, Oxford University Press, Oxford, 6th edn., 1998.

87 N. B. Colthup and L. H. Daly, *Introduction to infrared and Raman spectroscopy*, Academic Press, New York, 1975.

88 The Royal Society of Chemistry Fine Chemicals and Medicinals Group, *Atomic Absorption Spectroscopy*, The Royal Society of Chemistry, London.

89 D. B. Williams and C. B. Carter, *Transmission electron microscopy: A textbook for materials science*, Springer, New York, 1996.

90 J. L. Lemaitre and O. G. Menon, *Characterisation of heterogeneous catalysts*, New York and Basel, New York, 1984.

91 H. L. Gruber and A. Hansen, *J. Catal.*, 1971, **20**, 92.

92 P. A. Serman, *J. Catal.*, 1972, **24**, 460.

93 J. J. F. Scholten and A. van Monfoort, *J. Catal.*, 1962, **1**, 85.

94 S. D. Jackson and N. J. Casey, *J.C.S. Farad. Trans.*, 1995, **91**, 3269.

95 H. Dropsch and M. Baerns, *App. Catal.*, 1997, **158**, 163.

96 G. C. Bond and P. B. Wells, *App. Catal.*, 1985, **18**, 221.

97 T. Lear, PhD Thesis, University of Glasgow, 2003.

98 D. Lennon, T. Lear, and N. G. Hamilton, *Catal. today*, 2007, **126**, 219.

99 L. McMillan, MSci Thesis, University of Glasgow, 2007.

100 A. A. Frost and R. G. Pearson, *Kinetics and Mechanism*, Wiley, New York, 1961.

101 K. Jarowicki and P. Kocienski, *J. Chem. Soc., Perkin Trans.*, 2000, **1**, 2495.

102 T. W. Greene and P. G. M. Wuts, *Protective Groups in Organic Synthesis*, John Wiley and Sons, 3rd edn., 1999.

103 J. J. W. Bakkera, A. G. van der Neut, M. T. Kreutzer, J. A. Moulijn, and F. Kapteijn, *J. Catal.*, 2000, **274**, 176.

104 H. Greenfield, *Ind. Eng. Chem. Prod. Res. Dev.*, 1967, **6**, 142.

105 B. Chen, U. Dingerdissen, J. G. E. Krauter, H. G. J. L. Rotgerink, K. Mobus, D. J. Ostgard, P. Panster, T. H. Riermeier, S. Seebald, T. Tacke, and H. Trauthwein, *App. Catal. A: Gen.*, 2005, **280**, 17.

106 C. Joly-Vuillemin, D. Gavroy, G. Cordier, De Bellefon C., and H. Delmas, *Chem. Eng. Sci.*, 1994, **49**, 4839.

107 P. J. Kocienski, *Protecting groups*, Thieme, New York, 2005.

108 T. H. Koops, T. Visser, and W. M. A. Smit, *J. Mol. Struct.*, 1983, **96**, 203.

109 S. F. Parker, ISIS Facility, RAL, *September* 2011.

110 V. V. Rozanov and O. V. Krylov, *Russ. Chem. Rev.*, 1997, **66**, 107.

111 D. Ball, *J. Chem. Educ.*, 1998, **75**, 917.

112 M. Beller and C. Bolm, *Transition metals for organic synthesis: Building blocks and fine chemicals*, 2nd edn., 2008.

113 M. Freifelder, *J. Am. Chem. Soc.*, 1960, **82**, 2386.

114 P. Kukula, V. Gabova, K. Koprivova, and P. Trtik, *Catal. Today*, 2007, **121**, 27.

115 J. M. Arai, Y. Takada, and Y. Nishiyama, *J. Phys. Chem.*, 1998, **102**, 1968.

116 T. Lear, R. Marshall, E. Gibson, T. Schutt, T. M. Klapotke, G. Rupprechte, H. Freund, J. Winfield, and D. Lennon, *Phys. Chem. Chem. Phys.*, 2005, **7**, 565.

117 S. Kishimoto, *J. Phys. Chem.*, 1973, **77**, 1719.

118 L. P. Hammett, *J. Am. Chem. Soc.*, 1937, **59**, 96.

119 M. J. Frisch *et al.*, Gaussian 03W, Gaussian Inc., Pittsburgh, PA, 2003.

120 A. R. McInroy, A. Uhl, T. Lear, T. M. Klapötke, S. Shaikhutdinov, S. Schauermann, G. Rupprechter, H. J. Freund, and D. Lennon, *J. Chem. Phys.*, 2011, **134**, 214704.

121 S. D. Jackson, S. Munro, P. Colman, and D. Lennon, *Langmuir*, 2000, **16**, 6519.

122 D. E. Levy, *Arrow pushing in organic chemistry: an easy approach to understanding reaction mechanisms* , John Wiley & Sons, Inc., Hoboken, 2008.

123 M. S. Singh, *Advanced organic chemistry: Reactions and mechanisms*, Dorling Kindersley (India) Pvt. Ltd., Delhi, 2007.

124 H. W. Wilson and J. E. Bloor, *Spectrochimica Acta*, 1965, **21**, 45.

125 S. M. Melikova, A. Koll, A. Karpfen, and P. Wolschann, *J. Mol. Struct.*, 2000, **523**, 223.

126 D. Dolphin and A. Wick, *Tabulation of Infrared Spectral Data*, John Wiley & Sons Inc., New York, 1977.

127 M. Tasumi, T. Urano, and M. Nakata, *J. Mol. Struct.*, 1986, **146**, 383.

"… and hello to Jason Isaacs"
Dr. K.